OUTCROP-BASED GAMMA-RAY
CHARACTERIZATION OF ARSENIC-BEARING
LITHOFACIES IN THE GARBER-WELLINGTON
FORMATION, CENTRAL OKLAHOMA AQUIFER
(COA), CLEVELAND COUNTY, OKLAHOMA

By

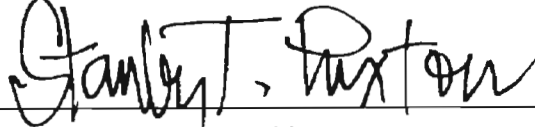GREGORY A GROMADZKI

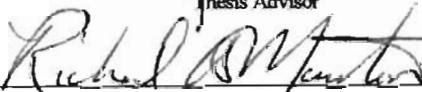Bachelor of Science

University of Maine

Orono, Maine

2002

Submitted to the Faculty of the
Graduate College of the
Oklahoma State University
in partial fulfillment of
the requirements for
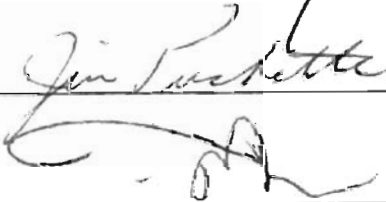the Degree of
MASTER OF SCIENCE
May, 2004

OUTCROP-BASED GAMMA-RAY

CHARACTERIZATION OF ARSENIC-BEARING

LITHOFACIES IN THE GARBER-WELLINGTON

FORMATION, CENTRAL OKLAHOMA AQUIFER
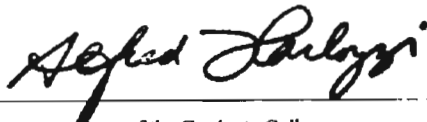
(COA), CLEVELAND COUNTY, OKLAHOMA

Thesis Approved:

_____

Thesis Advisor

_____

_____

_____

_____

Dean of the Graduate College

ii

ACKNOWLEDGEMENTS

TABLE OF CONTENTS

LIST OF FIGURES

LIST OF TABLES

CHAPTER I

INTRODUCTION

Problem Statement

The City of Norman uses surface water and ground water to meet the drinking

water demands of residential, commercial, and industrial users. In order to meet the

increasing demands for ground water, the city approved a 40-Year Strategic Water

Supply Plan (SWSP) that includes the development of 30 new ground water wells. The

recently finalized Environmental Protection Agency Arsenic Rule of 2001 lowers the

allowable arsenic standard from 50 micrograms per liter ($\mu g/L$) to 10 $\mu g/L$. Recent study

by CH2M HILL indicates that the City of Norman metropolitan area ground water

contains arsenic concentrations in excess of the new mandated maximum contaminant

level (MCL). As a result, the city's available ground water supply will be greatly reduced

unless practical solutions are developed and implemented. The excess concentration

commonly occurs in sandstone layers that are (1) just below the base of the confining

Hennessey Group, (2) near the base of the aquifer and (3) in areas where very old water

from long flow paths is moving up to discharge into streams (Smith et al., 2002).

If the city can isolate zones of arsenic-bearing water they may be able to produce

adequate amounts of water without drilling new wells or installing expensive treatment

equipment. Additionally, an understanding of arsenic distribution in the area based on

1

stratigraphy would improve chances of drilling and developing new wells that yield water within the safe drinking water standards. Results that emerge from this work have potential to be transferable to other aquifers and water-supply systems throughout the world.

Study Area

The Central Oklahoma Aquifer underlies about 3,000 square miles of central Oklahoma, including all or parts of Cleveland, Lincoln, Logan, Oklahoma, Payne, and Pottawatomie Countries (Fig. 1) (Christenson, 1998). Water from the aquifer is used extensively to meet the demands of residential, commercial, and industrial users. The largest city overlying the aquifer is Oklahoma City (year 2000 population 506,132). Other cities with year 2000 populations greater than 25,000 that heavily rely on the aquifer for at least part of their water supply include Norman (95,695), Edmond (68,315), Midwest City (54,088), and Moore (41,138). Land-surface elevations within the study area range from 800 feet to 1,400 feet (243 to 426 m) above sea level and generally are higher in the west. Most of the usable ground water is contained in the Permian geologic units, which include the Garber-Wellington Formation, and undivided rocks of the Chase, Council Grove and Admire Groups.

Objective & Approach

Past work by Mosier (1994) links arsenic in the Permian red beds of Oklahoma with shale, siltstone and finer-grained sandstones. As a consequence, arsenic concentrations in drinking water tend to be higher when the water is produced from finer-
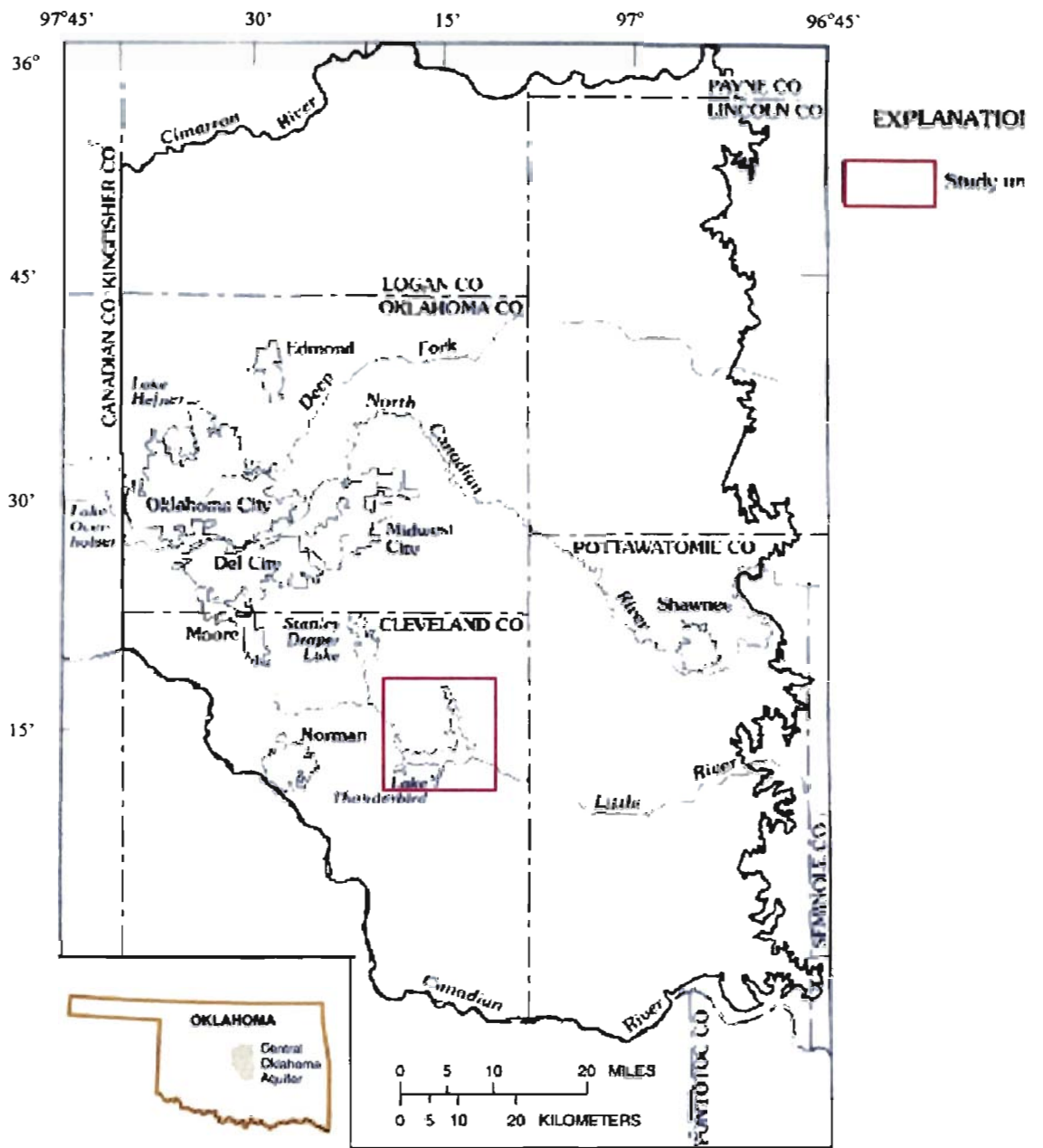
Figure 1. Geographic features of the study unit (modified after Christenson, 1998).

grained rocks than when water is produced from coarser-grained rocks (assuming sodium-bicarbonate water chemistry in both instances). This association between arsenic concentration and rock type therefore suggests that arsenic in the Permian rocks may vary with the depositional sedimentary environment. To date, however, the nature of the arsenic occurrence has not been systematically described relative to sedimentary lithofacies and depositional environments. In addition, important controls on the porosity (storativity) and permeability (hydraulic conductivity) of the Permian aquifer sandstones have not been described.

Approach:

1. Collect gamma-ray data and construct high-resolution vertical gamma-ray profiles for outcroppings of the Garber-Wellington Formation exposed in the Lake Thunderbird area of Cleveland County and surrounding regions. Gamma-ray measurements, which record the shaliness of the outcrops (K, U, and Th in the clays), can be used to classify the lithofacies, identify depositional environment, and assist in locating arsenic-prone intervals (assuming that, indeed, arsenic concentration varies with particle size of the sedimentary rock).

2. Perform textural analysis of the Permian sandstones (sieve analysis) strategically sampled from outcrops where the gamma-ray profiles were measured. These samples, once disaggregated and sieved, can provide supporting evidence for the notion that the gamma-ray response is sensitive to the grain size and clay content of the formations.

3. Establish the strength of statistical association among gamma-ray response, arsenic abundance, and lithofacies using whole rock chemistry and arsenic abundance data for subsurface wells (from USGS NOTS wells, 1990). Assuming these associations

yield significant relationships, recommend procedures by which gamma-ray response in outcrop and subsurface wells can be used to identify and quantify arsenic-prone lithofacies.

4. Calculate permeability for outcrop samples based on an established equation that uses textural data from sieve analysis. Based on these results, generate some vertical permeability profiles that can be compared with the gamma-ray profiles, lithofacies classes, and depositional environments. Summarize the comparisons and comment on the implications of the findings for a) locating the distribution of low-arsenic lithofacies in a well bore, and b) defining the permeability pathways in the aquifer system.

5. Provide study results and recommendations to Abbott (2004) for incorporation into his subsurface well log correlation and mapping study of the Garber-Wellington Formation stratigraphic interval. Also provide results to Kenney (2004) for use in her outcrop mapping of lithofacies and depositional environments in the Cleveland County area.

In the broader scheme, this thesis is one study among several theses (OSU) and government studies (USGS) being conducted in the City of Norman, Oklahoma area. The EPA in Ada, Oklahoma has funded this arsenic study. The ultimate purpose of the arsenic studies is to develop strategies and recommendations that could be used by municipalities to implement government mandated standards for allowable levels of arsenic in drinking water (<10 µg/L). The arsenic studies are designed to improve understanding about the habitat (environment) of arsenic within the context of the geology in the City of Norman, Oklahoma area. The OSU strategy is to evaluate whether or not the arsenic in the rocks varies with time (stratigraphy), with rock type (sand versus

5

shale, or lithofacies), or both. If arsenic levels are found to be lower in given stratigraphic intervals or in a certain lithofacies, the mapped geographic distribution of the deposits could be used to select new well locations. Additionally, certain intervals within wells could be selectively produced so that water originating in arsenic-prone layers does not enter the well bore and mix with water from the low arsenic intervals. In contrast to the OSU studies, the USGS studies are designed to address the engineering considerations and strategies required for selectively producing low-arsenic intervals within a well bore. The USGS is also conducting regional fluid flow modeling based on geological input from the OSU geology studies. These OSU/USGS studies are not designed to address other post-production engineering strategies for remediation of arsenic in drinking water, such as filtration or chemical treatment.

Geomorphology

The topography overlying the Central Oklahoma Aquifer is characterized by low, rolling hills in the eastern two-thirds of the study area where maximum local relief ranges from about 30 to 200 feet (9 to 60 m). The western third of the study area is characterized by flat plains with a relief of about 10 feet (3 m). The rolling hills in the east are underlain by lenticular beds of fine-grained, cross-bedded sandstone interbedded with siltstone and mudstone. These units represent the Garber-Wellington Formation, and the Chase, Council Grove, and Admire Groups (Christenson, 1998). The western plains are predominantly underlain by low-permeability, reddish-brown shale and mudstone of the Hennessey Group.

Stratigraphy

Stratigraphic units of the Central Oklahoma Aquifer include Quaternary alluvial and terrace deposits and Permian sedimentary rocks (Breit et al., 1990). These Permian rocks, beginning at the base include the undivided Admire Group, Council Grove, and Chase Group, Garber-Wellington Formation, and the Hennessey Group (Fig. 2A & B). The units dip to the west at about 50 ft/mi (9.47 m/km) and strike slightly west of north (Mosier and Bullock, 1988).

Permian Geologic Units

The Chase, Council Grove and Admire Groups are undifferentiated because they are lithologically similar within the study area. Rocks from these units are mostly red-brown to gray shales and orange-brown fine-grained, crossbedded sandstone that grades into arkosic sandstone and conglomerate towards the south (Mosier and Bullock, 1988; Christenson, Morton and Mesander, 1992). The combined thickness of these units ranges from 295 ft to 590 ft thick (90 to 180 m).

The Garber-Wellington Formation are stratigraphically above the undivided Admire Group, Council Grove, and Chase Group. The Garber-Wellington Formation is exposed in the central part of the study area. Their combined thickness ranges from 328 ft to 885 ft (100 to 270 m) (Mosier and Bullock, 1988; Christenson, Morton and Mesander, 1992). These units constitute the main water-bearing units of the Central Oklahoma Aquifer. Because their lithologies and water bearing characteristics are similar, they will be described together in this study. The units are a complex of lenticular beds of fine-grained sandstone with interbedded siltstone, mudstone, and small amounts of

7

System	Geologic Unit
Quaternary	Alluvium
	Terrace Deposits
Permian	
	El Reno Group
	Hennessey Group
	Garber Sandstone
	Wellington Formation
	Chase Group
	Council Grove Group
	Admire Group
Pennsylvanian	
	Vanoss Formation

Hennessey Group
Red-brown mudstone,
Siltstone and very fine-grained
sandstone

**Garber Sandstone and
Wellington Formation**
Lenticular beds of fine-grained
sandstone with interbedded
siltstone, mudstone and small
amounts of conglomerate

**Chase, Council Grove,
and Admire Groups**
Mudstone, fine-grained sandstone
and conglomerate

Figure 2A. Stratigraphic units of the Central Oklahoma Aquifer (Parkhurst et al., 1989).
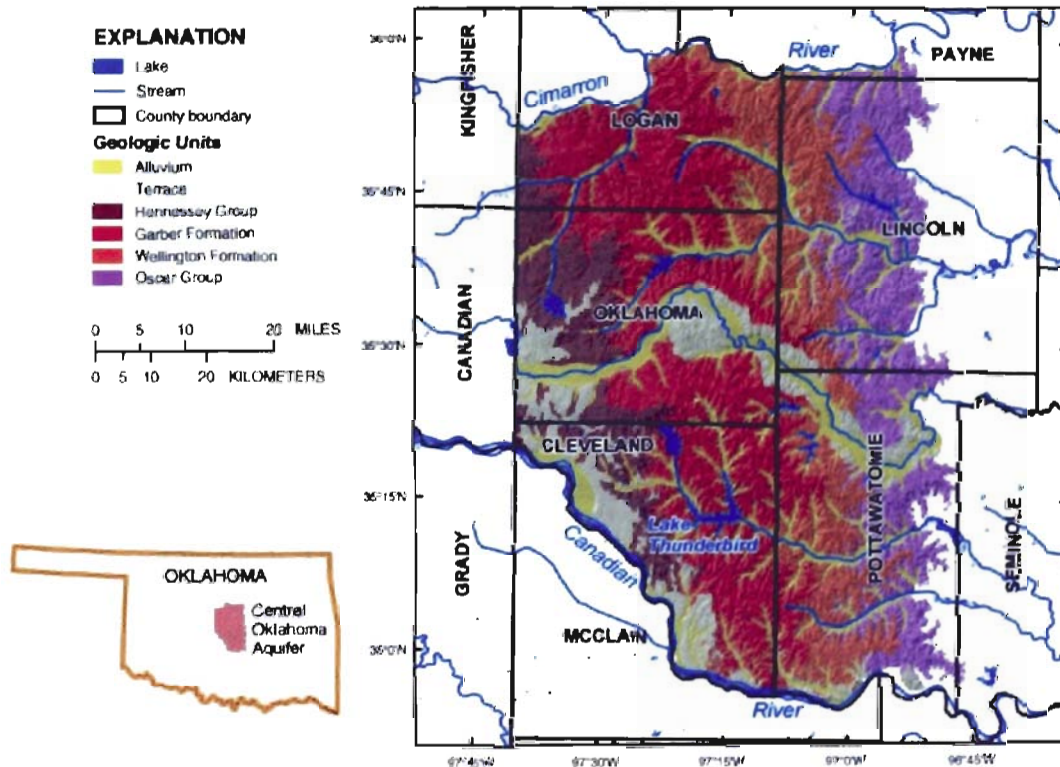
Figure 2B. Distribution of geologic units in the Central Oklahoma Aquifer (Jerrod Smith, 2004).

8

conglomerate. The amount of sandstone varies from 25 to 75 percent. The sandstone is very-fine to fine-grained, friable and locally cemented by either dolomite $(CaMg(CO_3)_2)$ or calcite $(CaCO_3)$.

The Hennessey Group is present in the western one-fourth of the study area where it ranges from 130 ft to 656 ft (40 to 200 m) in thickness, becoming thicker to the west and south. The Hennessey Group consists mainly of massive shale beds that range from a few centimeters to 10 ft (3.3 m) or more in thickness with less common layers of well-indurated siltstone and sandstone beds that similarly range from a few centimeters to about 10 ft (3.3 m) in thickness (Mosier and Bullock, 1988; Christenson, Morton and Mesander, 1992).

Quaternary Deposits

The Quaternary deposits of the study area include terrace deposits of one or more levels adjacent to and associated with the broad stream and river valleys. Three major rivers: the Cimarron River to the north, North Canadian River in the central part of the study area, and the Canadian River to the south have wide alluvium-filled valleys that cut across the area from west to east. Wind-blown sand accumulates on the northern side of major rivers due to the prevailing southerly winds forming large dunes (that are 6-10 m thick, Mosier and Bullock, 1988).

Structural History

The greatest period of mountain building in Oklahoma was in Pennsylvanian time. Flat-lying sedimentary rock layers in the southern half of the state were sharply

9

folded, tilted, and faulted; earlier formed igneous rock masses were pushed upwards and the three mountain chains, (Ouachita, Wichita and Arbuckle Mountains) were thrust high above surrounding seas. During uplift the land area in the present day Anadarko, Ardmore, and Arkoma Basins subsided (Fig. 3). The Arkoma Basin lies east of the study area, on the northern flank of the Ouachita Mountains. During late Pennsylvanian time the Arkoma Basin was filled with sediments from the Ouachita Mountains and was crosscut at several locations by east to west fluvial systems (Wylie, 1989). During Permian time the basin area uplifted because of continued uplift of the Ouachita Mountains and was eroded. The Ouachita Uplift and the Arkoma Basin area may have been a significant source of sediment to the units making up the Central Oklahoma Aquifer during Permian time (Johnson, 1989).

During early Permian time, the Anadarko Basin subsided slowly and shallow-marine cyclic limestones and shales were deposited in most of the basin. Along the eastern margin of the basin, the red beds of the Chase and Council Grove Groups in the study area were deposited in a continental environment that resulted from a general regression of normal marine waters. The Garber-Wellington Formation in the study area were deposited as a complex system of alluvial and deltaic sands and muds (Johnson, 1989). As the regression continued during middle Permian time, most of the basin was transformed into a hypersaline sea and a thick sequence of red beds and evaporates were deposited (Blaine Gypsum).

Post-Permian deposits in the study area were eroded during Jurassic, Cretaceous, and Tertiary epeirogenic uplifts. Little is known about post-Permian geologic history in

Legend:

- QUATERNARY
- TERTIARY
- CRETACEOUS
- JURASSIC
- TRIASSIC
- PERMIAN
- PENNSYLVANIAN
- MISSISSIPPIAN
- DEVONIAN-SILURIAN
- ORDOVICIAN
- CAMBRIAN Sedimentary
- CAMBRIAN Igneous
- PRECAMBRIAN Igneous

Anadarko Basin

Wichita Mts.

Hollis Basin

Ozark Uplift

Arkoma Basin

Ouachita Mts.

Tulsa

OKC

60 Miles
80 Km

A' — A

B' — B

HOLLIS BASIN   WICHITA MTS.   ANADARKO BASIN

OUACHITA MTS.   ARKOMA BASIN   OZARK UPLIFT

SEA LEVEL
10,000 FT.
20,000 FT.
30,000 FT.

Figure 3. Geologic provinces of Oklahoma (USGS, 1996c).

the area (Johnson, 1989). Quaternary alluvium and terrace sands were deposited and modern soils developed over the eroded surface of the early-late Permian rocks and the Quaternary alluvium and terrace.

Hydrology

The Central Oklahoma Aquifer consists of geologic units of Permian and Quaternary ages that yield substantial volumes of water to wells from an extensive, continuous ground water flow system in central Oklahoma (Christenson, Parkhurst and Breit, 1998). The aquifer can be divided into six geohydrologic zones on the basis of geohydrologic variations between confined or unconfined conditions, degree of mudstone interbedding and variations in major-ion chemistry with depth (Parkhurst, Christenson and Schlottmann, 1989). The six zones include: (1) the unconfined zone of the shallow (<300 ft) Garber-Wellington Formation; (2) the confined zone of the shallow Garber-Wellington; (3) the unconfined zone of the deeper (>300 ft) Garber-Wellington Formation; (4) the confined zone of the deeper Garber-Wellington Formation; (5) the shallow (<300 ft) Chase, Council Grove and Admire Groups, undivided; and (6) the deeper (>300 ft) Chase-Admire (Fig. 4) (Parkhurst, Christenson and Schlottmann, 1989).

Dominant water types in the aquifer range from calcium magnesium bicarbonate to sodium bicarbonate. Calcium-magnesium-bicarbonate water types are most common in shallow (<300 ft) unconfined zones and sand-rich parts of the aquifer. Sodium bicarbonate water is in the deep and confined zones of the aquifer (Parkhurst, Christenson and Schlottmann, 1989). The pH of water in the Permian part of the aquifer ranges from 6.0 to 9.5 (Schlottmann and Breit, 1992). The depth to the base of freshwater is greatest
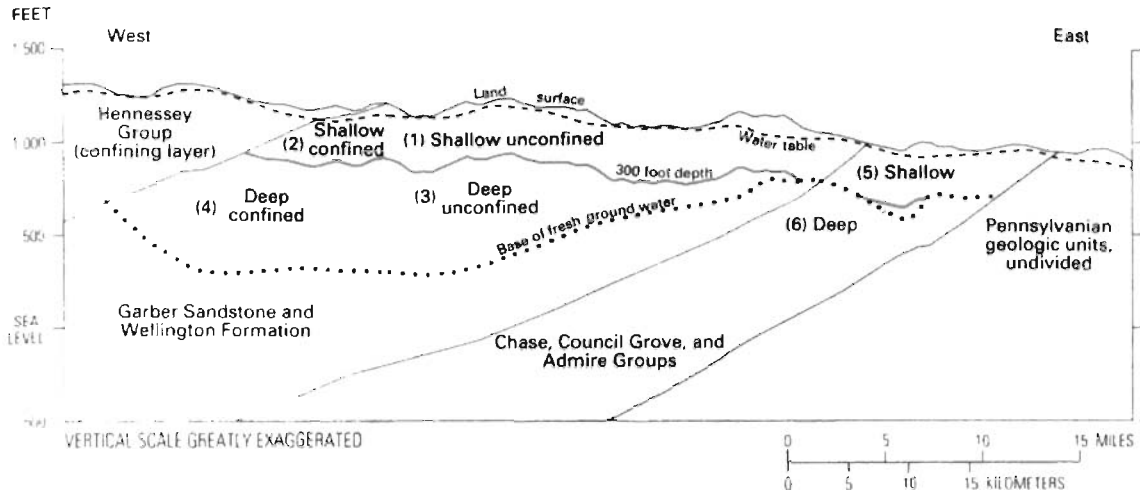
Figure 4. Geohydrologic cross-section along latitude 35°30' showing the six geohydrologic zones in the Central Oklahoma Aquifer (Parkhurst et al., 1989).

in the west-central part of the aquifer where freshwater is as deep as 1,000 feet (304 m) below land surface. Ground water in this flow system originates as recharge from precipitation 30-40 in (75-100 cm) at a rate of about 40 mm/y and discharges to streams and wells located throughout the region.

CHAPTER 2

LITERATURE REVIEW

The Central Oklahoma Aquifer is defined by a series of stratigraphic intervals (first described by Aurin et al., 1926) that produce substantial amounts of water from an extensive ground water flow system that occurs in Cleveland, Lincoln, Logan, Oklahoma, Payne and Pottawatomie Counties. The Central Oklahoma Aquifer is of great interest to water managers and to the public because it is a major source for water supplies in central Oklahoma and because it has several known and suspected water-quality problems. The U.S. Geological Survey (USGS) has completed several studies of the Central Oklahoma Aquifer as part of the National Water-Quality Assessment Program (NAWQA). The primary purpose of the NAWQA Program is to assess water quality for a large part of the Nation's water resources. A few (5) of the studies related to the Norman arsenic issue are discussed below.

In a recent study by CH2M HILL (Environmental Consulting Firm, Oklahoma City, June, 2002), 43 wells were analyzed, (the City of Norman owns 32 and University of Oklahoma (OU) owns 11). The average well can produce approximately 170 gallons per minute (gpm) while the combined system can produce about 10.3 million gallons per day (mgd). Based on the arsenic levels measured in the wells, 20 of the city's wells and all of OU's wells (for a total of 31) are impacted by the new federal standards. The

arsenic concentrations show significant variations ranging between 0.83 and 231 micrograms per liter ($\mu g/L$). The City of Norman average arsenic concentration is 22 $\mu g/L$, and University of Oklahoma average arsenic concentration is 35 $\mu g/L$. The overall average of the water wells owed by both the City of Norman and University of Oklahoma systems is 25 $\mu g/L$.

An understanding of some of the chemical controls on the mobility of arsenic is necessary to understand the reasons for the presence of arsenic in the Central Oklahoma aquifer. These finding are based on reports by Parkhurst et al., (1989), Parkhurst et al., (1992), and Schlottmann and Funkhouser (1991). Arsenic exists in many oxidation states in the natural environment including the As^{5+}, As^{3+}, As^{1+} and As^{3-} valences and rarely in elemental (neutral) form. Due to the various oxidation states, arsenic can form many natural inorganic and organic compounds. Varying pH (mainly owing to dissolution of carbonate cement and to ion exchange with clay minerals) and redox conditions mainly control the dominant aqueous species of arsenic.

Christenson (1998) conducted a ground water quality study of the Central Oklahoma Aquifer. The objectives of the study were to (1) describe regional ground water quality throughout the aquifer, (2) describe the major geochemical and geohydrologic processes operating in the aquifer, (3) identify the major factors affecting the ground water quality, and (4) describe the location, nature and causes of selected water-quality problems within the study unit. While the overall quality of water in the Central Oklahoma Aquifer is clean, water-quality problems occur in parts of the aquifer. Some of these problems were investigated, including concentrations of arsenic,

chromium, selenium, and uranium in excess of water-quality standards and the effect of urbanization on ground water quality.

Breit (1998) examined the diagenetic history of Permian rocks in the Central Oklahoma Aquifer. Variations in the chemical composition of water are largely a result of reactions between water and solid components of the aquifer, which began during sediment deposition in the Permian and continue with the circulation of modern dilute ground water. Breit (1998) found that detrital framework grains have been dissolved or altered, and authigenic minerals have precipitated and dissolved in response to changes in the composition of the pore water with time.

Mosier (1998) conducted a surficial and subsurface solid-phase geochemical characterization of materials from the area overlying the Central Oklahoma Aquifer to determine the abundances and distribution of chemical constituents. Knowledge and understanding of the sites and mechanisms for the mobilization of trace elements from the geologic materials into the ground water system were gained from the result of this study. The analytical results and partial dissolution studies indicate that the concentration of trace elements in ground water is affected by oxidation, adsorption-desorption and cation-exchange reactions at mineral surfaces.

CHAPTER 3

METHODOLOGY

Gamma Ray

Vertical gamma-ray profiles of outcrops were constructed from measurements taken using a portable gamma-ray spectrometer (Exploranium GR-320 Fig. 5). The natural radioactivity of sedimentary rocks can vary significantly, depending on the type of rock, the provenance of the sediment and the chemical maturity of the material. The Exploranium multi-spectral device provides a direct measurement at the surface of the outcrops, with no significant depth of penetration. This "at-surface" characteristic allows one to reliably relate the measured radioactivity contrasts to mapped bedrock, surficial geology and alterations associated with emplacement of mineral deposits. The GR-320 gamma-ray spectrometer is designed to detect and quantify gamma rays associated with potassium (^{40}K), uranium (^{238}U) and thorium (^{232}Th) and to accurately separate the signal into the respective gamma-ray energies for each element. The spectral capability distinguishes the Exploranium GR-320 spectrometer from other gamma-ray instruments (which measure total radioactivity).

Weathering of rocks commonly yields illite, which is a potassium-bearing clay. Also, uranium and thorium are present in trace quantities in most clay rich rocks. As the concentration of these different radioelements varies between different rock types, geologists can use the information provided by the gamma ray spectrometer to map the

Exploranium GR-320 Features

-256/512 channel operations: software selectable.
-One or two detector input: size range of 21 to 512 cu.ins.
-Automatic spectrum stabilization: internal or natural isotope
-8 regions of interest set from the keyboard.
-High linearity ADC with zero dead time.
-Choice of coincidence or anti-coincidence operation.
-Exposure rate mode for environmental data.
-Assay mode for geophysical data - %K, ppm eU, eTh.
-Input capability for GPS information with integrated data storage.
-717 full spectra or 4468 sets of ROI data in internal data storage.
-RS-232 serial digital output facilitates spectrum, ROI and GPS data output.
-Buffered output data for zero downtime during data transfer.
-Rechargeable or alkaline battery operation.
-Full remote control capability.
-User application programs supplied.
-Background, K, U and Th calibration using traceable test pads.
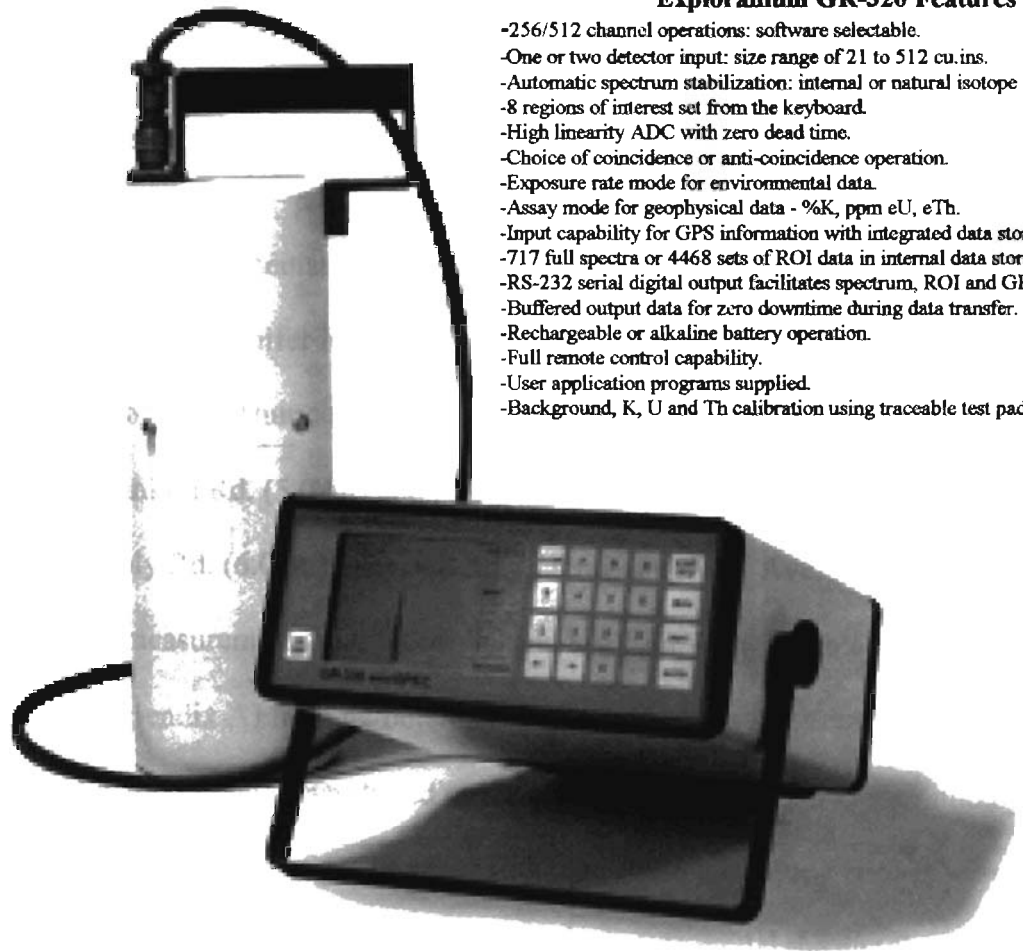
Figure 5. Portable gamma ray spectrometer (Exploranium GR-320 Manual).

lithology. The GR-320 is calibrated at the factory in order to accurately measure the concentrations of potassium (%), uranium (ppm) and thorium (ppm).

Outcrop Selection

In order to systematically describe the bedrock geology and major features of the Central Oklahoma aquifer in Cleveland County, six major transects were conducted in the vicinity of Lake Thunderbird (Fig. 6). The east-west transects include Alameda St. (5.0 mi), Franklin Rd. (5.0 mi) and Rock Creed Rd. (3.0 mi). The north-south transects include Peebly Rd. (6.0 mi), Newalla Rd. (3.0 mi) and 180th Ave. (3.0 mi). In total, 456 gamma-ray measurements were recorded and 368 samples were collected for grain size analysis (Appendix A) from 42 outcrops along the six transects in the study area.

Outcrop selection was based on relative sandstone bed thickness, lithological variability and presence of sedimentary structures. These selection criteria were pursued in order to capture the range of variations to adequately model the distribution of all sedimentary environments and lithofacies in our study area. For gamma ray measurements, spacing of between 10-15 in (25-38 cm) was commonly used for vertical outcrop profiles. This spacing was based on lithological contacts and logistical constraints related to the geometry or accessibility of exposure. When a more detailed profile was required for intervals of particular interests the spacing was reduced to 2-5 in (5-12 cm). The sampling time for each measurement was 60 seconds.

In preparation for each gamma ray measurement, the rock surface was smoothed or planed-off so that the contact area between the outcrop and the detector was maximized. Once the surface was ready, the detector was placed in contact with a planer
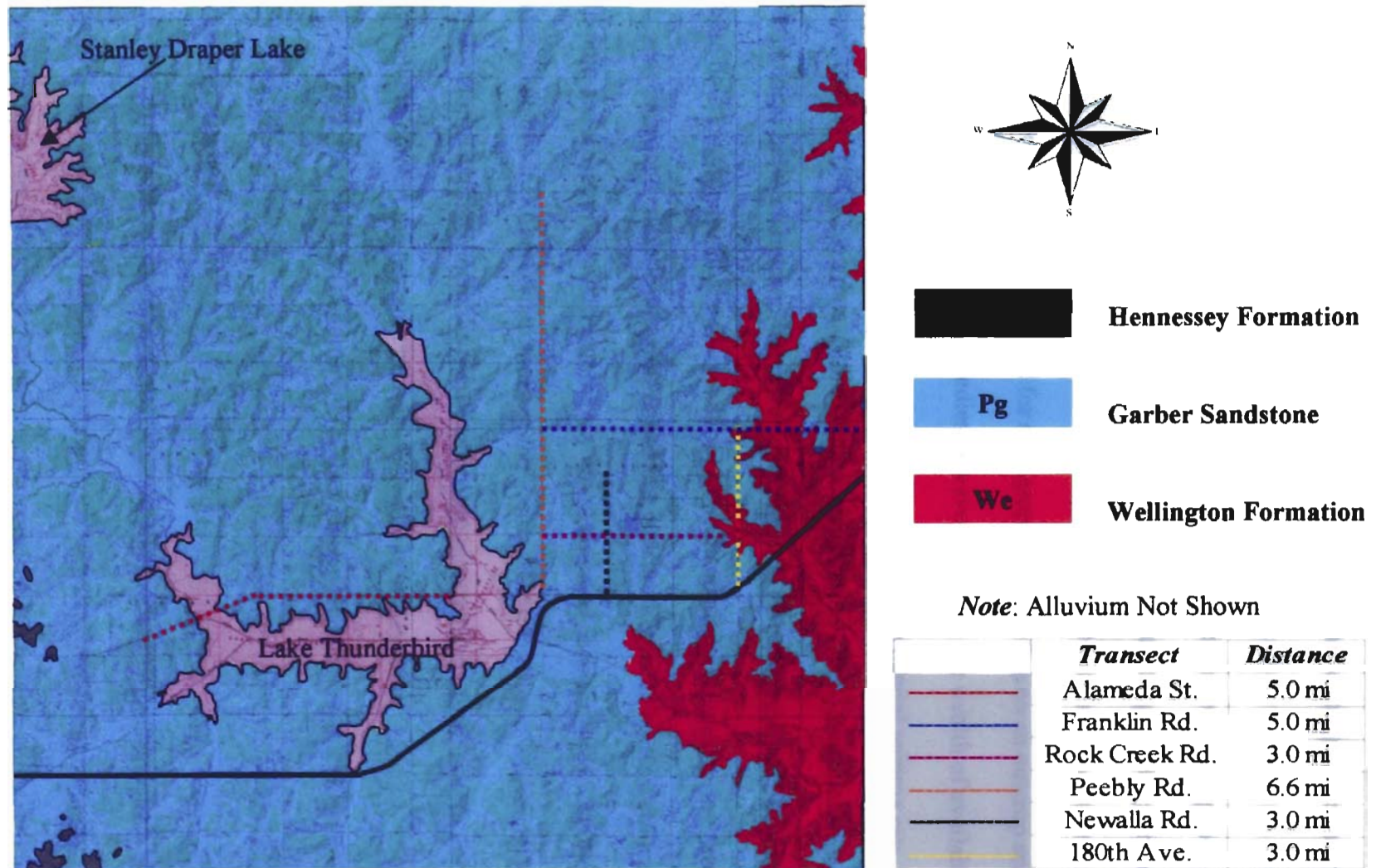
Figure 6. Location of the six major transects conducted in the vicinity of Lake Thunderbird, Cleveland County, Oklahoma.

rock surface and held stationary until the measurement was recorded. The sampled diameter of rock is 6.56 ft (2 m) with the main contribution to the gamma ray reading being the 1.64 ft (0.5 m) diameter around the detector.

Gamma-ray data generated using a hand-help spectrometer on exposed strata provide an invaluable source of data for improved understanding and interpretation of subsurface well log information. A portable gamma ray spectrometer unit provides high-resolution results that can be used for stratigraphic correlation on an outcrop scale. The particular advantage of outcrop studies however, lies with the wealth of available sedimentological data that can be calibrated directly to the natural gamma ray spectrometry (NGS) log data. Collaboration with Abbott, (2004) indicates that differences between outcrop-based versus subsurface gamma-ray data collected with a bore hole logging device are the result of physical and chemical weathering processes.

In order to make our results consistent with well log data units, we converted K%, U-ppm and Th-ppm into API gamma ray units. This was accomplished with the assistance of Mr. Robert Klimentidis at the Exxon-Mobil Upstream Research Company in Houston, Texas. Klimentidis (personal communication) provided us with the necessary formula to convert the portable gamma ray readings to API units:

$$API = 8 \ (+/-) \ 2 \ x \ (U\text{-}ppm) + 4 \ (+/-1) \ x \ (Th\text{-}ppm) + 16 \ (+/-) \ 2 \ x \ (K \ wt\%). \quad Eq. \ \#1$$

Textural Analysis

To establish relationship between gamma-ray measurements and grain size, samples (368 total) were collected from the rock surface where the gamma ray measurements were obtained. Samples were numbered accordingly and stored in plastic

bags. In the lab, a 150-gram sample was weighed and then crushed using a mortar and rubber pestle in preparation for analysis. All samples except for a select few (calcite and iron cemented conglomerates) were disaggregated. Each sample was sieved through a set of thirty-three wire mesh sieves using a Ro-Tap machine. The sieves ranged in size from 1 to 400 according to the U.S. Standard Sieve number. This range is equivalent to -4.64 to 5.00 phi grain size (25.0 to 0.0380 mm). Each sample was sieved for approximately 12 minutes. Finally, the contents of each sieve were weighed to the nearest gram on an electronic balance.

The results from sieving were input to an Excel spreadsheet. The spreadsheet was coded to automatically calculate the weight percentages of the individual grain size fractions present in each sample. These weight percentages were summed to form a cumulative weight percentage curve that was then plotted against phi grain size to form a standard grain size cumulative curve. Using the cumulative curve, we were able to determine the graphic mean, the inclusive graphic standard deviation (Folk, 1974) for comparison to the gamma ray curves and to calculate permeability (Collins, 2001). The equation used to calculate the graphic mean according to Folk, (1974) is:

$$Mz = (\phi_{16} + \phi_{50} + \phi_{84})/3 \qquad\qquad Eq.\ \#2$$

The phi grain size was read from the cumulative curves at the 16th, 50th and 84th percentile. By reading the data from these intervals the central two thirds of the grain size distribution was described. This estimate of mean grain size is much superior to the median (d_{50}) because it is based on three points along the curve and provides a better description of the data. The inclusive graphic standard deviation equation used to calculate the standard deviation is:

23

$$\sigma_1 = [(\phi_{84} - \phi_{16})/4] + [(\phi_{95} - \phi_5)/6.6]$$ Eq. #3

For this equation the phi grain size was read at 5th, 16th, 84th and 95th percentile from each

of the curves and input into the above equation. The inclusive standard deviation is an

average of the standard deviation calculated from $\phi16$ and $\phi84$, and the standard

deviation calculated from $\phi5$ and $\phi95$. According to Folk, (1974), this is the best overall

measure of sorting because it includes 90% of the distribution and is sensitive to values at

the tails of the distribution. Samples were classified according to the following verbal

(Table. 1) classification scale from Folk (1974):

<0.35ϕ	very well-sorted	1.0 - 2.0ϕ	poorly sorted
0.35 - 0.50ϕ	well-sorted	2.0 - 4.0ϕ	very poorly sorted
0.50 - 0.71ϕ	moderately well-sorted	>4.0ϕ	extremely poorly sorted
0.71 - 1.0ϕ	moderately sorted		

Table 1. Measurements of sorting values for a large number of sediments have
suggested the following verbal classification scale for sorting (after Folk, 1974).

In addition to comparing texture to gamma-ray response, mean grain size and sorting

were used to calculate the permeability. Permeability is a measure of the ease with which

fluids can be transmitted through a porous medium. The role of grain size and sorting on

the permeability of the Garber-Wellington Formation aquifer was calculated from an

equation generated by Collins, (2001). The equation was derived from experimental

results of Beard and Weyl, (1973) for unconsolidated sediments. Their work

demonstrates that high porosity sands are better sorted and lower porosity sands are more

poorly sorted. Permeability measurements obtained from their experiments indicate that

permeability varies more strongly with grain size than with sorting. High permeability sands are commonly coarser-grained and lower permeability sands are finer grained. Together, high porosity-high permeability sands are coarse grained and better sorted while low porosity-low permeability sands are more poorly sorted and finer-grained (based on experimental findings of Beard and Weyl, 1973). In the SI system, permeability has units of m^2, but for this study we will use units of Darcy. The conversion factor to the SI system is derived from one Beard and Weyl data (1darcy = $0.987 \times 10^{-12} m^2$). The equation used to calculate permeability is provided below (S_0 = sorting and ϕgs = phi grain size, see Collins, 2001 for discussion).

$$\text{Permeability} = 10^{\;6.16660 - .49463(S0) - 0.57248(\phi gs)} \qquad \text{Eq. \#4}$$

Thin-Section Analysis

Twenty-one standard thin sections were prepared by a commercial lab (Mineralogy, Inc. of Tulsa, Oklahoma). The thin sections were cut in a direction perpendicular to the lamination or bedding and stained for potassium feldspar. The goal of the thin section analysis was to obtain a close-up view of the mineralogical composition, porosity and to identify other micro-scale features that could be used to interpret the geological history of the sample.

Electron Microprobe Analysis (EM)

The EM analysis was conducted to establish the mineralogical and chemical composition of the rocks and to better document the habitat of arsenic. An electron microprobe (EMP) is a non-destructive method for determining the small-scale (~1µm) composition and distribution of elements in geological materials. The JEOL JXA-733

housed at OSU School of Geology was used for this study. The electron microprobe uses a high-energy focused electron beam to generate X-rays and electrons from the sample (Reed, 1995). The X-rays are characteristic of elements within a sample and can be generated from volumes as small as 3 μm (10^{-6}m) across. Each peak on X-ray spectrum represents an electron transition with a characteristic energy. Every element in a mineral has its own "fingerprint" of peaks so we can deduce which elements are present in the sample. Two types of X-ray spectrometers are used in the electron microprobe: the wavelength-dispersive spectrometer (WDS) and the energy-dispersive spectrometer (EDS) (Reed, 1995). The EDS measures all X-ray energies simultaneously, whereas the WDS is used for quantitative compositional analysis. The primary drawback of EDS is that it has poorer spectral resolution and is of limited value for quantitative analysis, especially for trace elements. The chemical composition is determined by comparing the intensity of X-rays from standards of known composition with those from unknown materials and correcting for the effects of absorption and fluorescence in the sample (Reed, 1995). The characteristic X-rays are captured by crystals. The OSU electron microprobe contains lithium fluoride (LIF), pentaerythritol (PET) and thallium acid phthalate (TAP) crystals. A detector is used to measure the characteristic X-rays.

Analyses of Naturally Occurring Trace Substances (NOTS)

The geochemical analyses of subsurface Permian rocks from eight-cored test wells in the Central Oklahoma aquifer was completed by Mosier et. al, (1990) as a pilot study of the U.S. Geological Survey's National Water-Quality Assessment (NAWQA) Program. These data were used to (1) evaluate the association between arsenic and

lithofacies, (2) calculate gamma-ray response and (3) to establish a relationship between gamma-ray response and arsenic content.

According to the NAWQA report, the cored material was split and sampled based on lithologic variations, (sandstone, mudstone, siltstone, etc.) and on visible diagenetic variations such as color, reduction spots, degree of carbonate cement, iron enrichment, etc. Rock samples were crushed and pulverized to minus 0.15 mm with ceramic plates. The samples (542 total) were analyzed by an inductively coupled plasma-atomic emission spectrometric (ICP-AES) technique for 37 elements. The elements determined and their limits of detection are summarized in Table 2.

Element	Limit	Element	Limit	Element	Limit	Element	Limit
Al%	0.005	Au	8	Ga	4	Sc	2
Ca%	0.005	Ba	1	Ho	4	Sn	10
Fe%	0.005	Be	1	La	2	Sr	2
K%	0.05	Bi	10	Li	2	Ta	40
Mg%	0.005	Cd	2	Mn	10	Th	4
Na%	0.005	Ce	4	Mo	2	U	100
P%	0.005	Co	1	Nb	4	V	2
Ti%	0.005	Cr	1	Nd	4	Y	2
Ag	2	Cu	1	Ni	2	Yb	1
As	10	Eu	2	Pd	4	Zn	2

Table 2. Lower limit of detection for ICP-AES analyses (microgram per gram)

Arsenic in the core samples was determined by hydride generation-atomic absorption spectroscopy (HG-AAS) (Crock and Lichte, 1982). Selenium was also determined by HG-AAS (Briggs and Crock, 1986; and Sanzolone and Chao, 1987). The limit of detection for both As and Se by this technique is 0.1 ppm. Uranium and thorium were measured using delayed neutron activation analysis (DNAA), which has limits of detection of 0.1 ppm for U and 1 ppm for Th (McKown and Millard, 1987). All analyses

27

were performed at the U.S. Geological Survey Laboratories in Lakewood, Colorado. Paul H. Briggs collected the ICP-AES data. James G. Cook, Kay R. Kennedy, and Eric P. Welsch were responsible for the HG-AAS data. Dave M. McKown and Robert B. Vaughn collected the DNAA data. The results and summarized analytical procedures were obtained from the USGS Open-File Report 90-456 by (Mosier E.L., 1990).

Statistical Analysis

Once the textural analysis and NOTS data were compiled, a large component of the data set was analyzed using Statistical Analysis System (SAS). Exploratory data analysis was conducting using univariate, bivariate and multivariate analysis. The SAS program helps to describe and summarize the Garber-Wellington Formation data so that the characteristics of the unit can be spatially generalized throughout the study area. SAS is also used to establish relationships among the many variables and to generate equations for the prediction of arsenic concentration relative to lithofacies.

CHAPTER 4

RESULTS & DISCUSSION

Part A-Gamma-Ray Interpretation

The recognition of characteristic gamma-ray well-log "shapes" and distinctive

vertical-profiles is a useful approach for conducting pattern correlation of well logs and

as an aid for interpreting depositional environments. In addition, the shape of the gamma

log curve is commonly used by well log interpreters as a means of describing down-hole

variations in grain size. In turn, these variations can be used to determine depositional

energy and infer depositional environments. The standard approach is to interpret bell

shaped gamma curves as a fining-upwards sequence (decreasing depositional energy) and

funnel shaped gamma curves as a coarsening-upward sequence (increasing depositional

energy) (Serra & Sulpice 1975). Log intervals deflecting to the left of the shale baseline

are considered sandstone; intervals deflecting to the right of the shale baseline are

considered mudstone.

Sandstone and mudstone proportions in well logs are commonly determined

systematically by selecting a "clean-sand" baseline on the gamma-ray log response. To

utilize this approach in this thesis, a clean sandstone baseline was determined from the

456 gamma ray measurements completed for the study. Based on inspection of a gamma

ray frequency distribution constructed with these measurements, a "clean-sand" baseline

was selected at 44 API (Fig. 7).

29
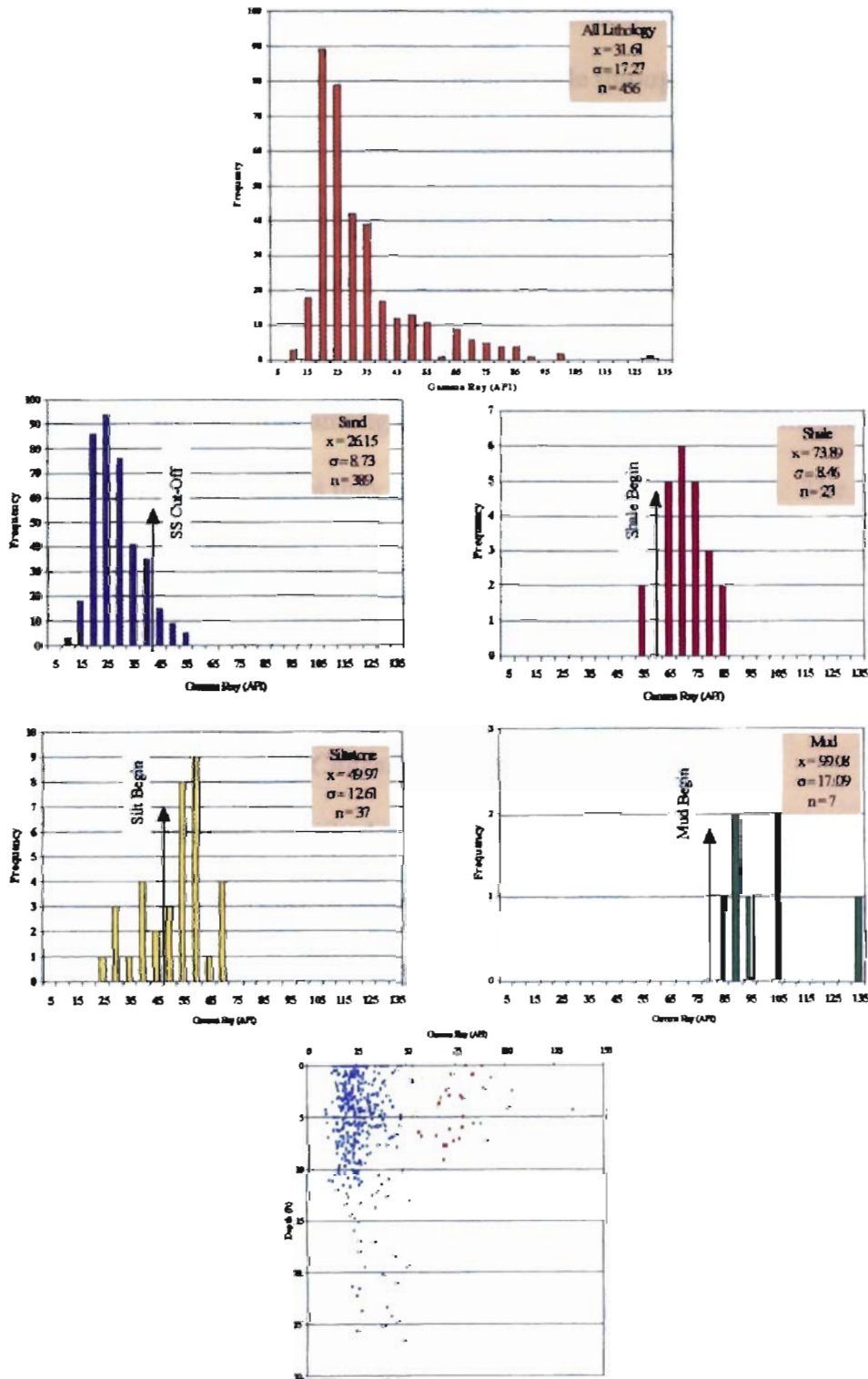
Figure 7. Gamma-ray frequency distribution by lithology and depth. Based on 456 gamma-ray measurements, a "clean-sand" baseline was quantitatively established at 44 API.

30

The success of using gamma ray logs as a fingerprint for geological interpretation depends on the distinctiveness of the vertical profile through a sandstone body and on our ability to interpret this profile in terms of depositional processes and environment. Channel-fill deposits are not laterally extensive relative to many other types of sedimentary deposits. This lack of continuity makes correlation of fluvial deposits over larger areas very difficult. Palaeosols however, may extend for tens of kilometers across a floodplain and are therefore among the most laterally extensive and mappable units within fluvial systems (unless they are eroded by younger channels). The purpose of the following outcrop classification and characterization is to identify gamma-ray fingerprints that can be used to reconstruct subsurface environments.

Outcrop Classification and Characterization

The 43 outcrops described along the six transects near Lake Thunderbird were grouped into lithofacies classes based on bedding styles, sedimentary structures and inferences about depositional environments. Eight separate lithofacies groups emerged from this exercise. We constructed vertical profiles of the outcrop classes exposed in the study area in order to compare gamma ray, lithofacies, grain size and calculated permeability. Five of the lithofacies group was analyzed using SAS so that inherent characteristics could be spatially generalized and compared/contrasted against the other lithofacies groups (Table. 3).

Group #1	Sandstone with stacked bar forms.					
Outcrops 25		n	Mean	Std. Dev	Minimum	Maximum
	API	255	27	14.30	9.20	134.40
	Grain Size (phi)	236	2.61	0.37	1.45	3.63
	Perm (D)	236	30	19.78	4.13	143.85
Group #2	Sandston with erosional base, but no internal sedimentary structure.					
Outcrops 8		n	Mean	Std. Dev	Minimum	Maximum
	API	93	34	16.77	16.00	89.20
	Grain Size (phi)	89	2.69	0.47	1.72	4.04
	Perm (D)	89	25	17.01	3.30	82.13
Group #3	Blocky cross-bedded sandstone with mud rip-up clasts.					
Outcrops 2		n	Mean	Std. Dev	Minimum	Maximum
	API	24	39	10.71	26.00	57.20
	Grain Size (phi)	14	2.39	0.45	1.71	2.92
	Perm (D)	14	38	23.96	17.16	87.23
Group #4	Horizontal to low-angle planar laminations					
Outcrops 6		n	Mean	Std. Dev	Minimum	Maximum
	API	85	34	17.41	10.40	83.60
	Grain Size (phi)	51	2.90	0.40	2.04	3.66
	Perm (D)	51	20	11.96	5.68	61.11
Group #5	Siltstone with interlaminated shale					
Outcrops 1		n	Mean	Std. Dev	Minimum	Maximum
	API	7	89	11.29	72.00	103.60
	Grain Size (phi)	4	3.45	0.06	3.39	3.54
	Perm (D)	4	5	1.07	3.72	6.31

Table 3. Summary statistics for five lithofacies. Statistical parameters could not be calculated for Groups # 6, 7 and 8 because the rocks could not be disaggregated.

Group #1 incorporates the largest number of outcrops (25). The group contains (1) stacked bar forms, (2) tabular and trough cross-bedded sandstone, (3) some with erosional bases, and sometimes having (4) mud clast rip-ups at the base (Fig. 8). A vertical section through a bar deposit exhibits a gradation from coarser material at the base to finer at the top, indicating fining upwards. The sandstone is moderately to well sorted and generally improves (fines) upwards. The gradational change in grain size vertically is interpreted to be a result of decrease in the flow velocity. Several outcrops show large-scale cross bedding at the base with mud clast rip-ups and smaller sets of cross-laminations near the top. The API vertical profile (Fig. 9) is consistent with clean sand (<44 API), suggesting most of the clays have been winnowed out of the system during deposition. The mean calculated permeability for this group is high (30 Darcies). There is no evidence in these outcrops for body fossils, tracks or root traces to suggest subaerial exposure. The sandstones are commonly poorly cemented and friable. Small amounts of red clay commonly bind the grains together. Rare cements include carbonate cement and less frequently sulfates (barite). At several locations, barite nodules are exposed in outcrop. The occurrence of barite is well recognized in the Oklahoma popular literature but an understanding of the genesis of these nodules requires additional studies.

Group #2 incorporates eight outcrops. This group contains sandstones that lack internal features, but which exhibit an erosional base (Fig. 10). The lack of sedimentary structures could be a sign of a rapid depositional event that failed to preserve internal structures and bedding features. This group may also be structureless because the grain size is so uniform. The truncation of underlying units suggests these sandstones are part
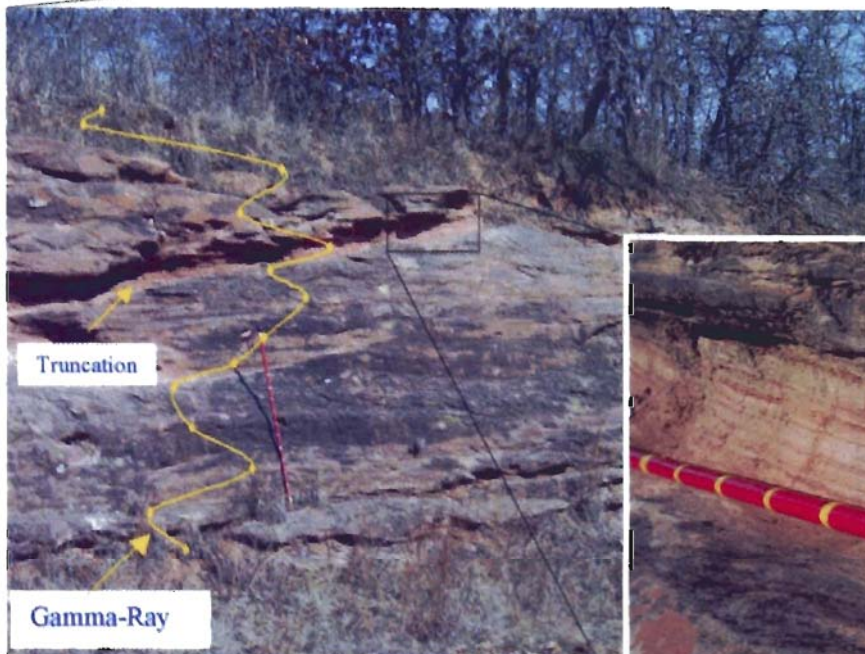
Labels within figure:
- Stacked Bars
- Truncation
- Gamma-Ray
- Truncational contact with underlying horizontal sand / silt stone laminations
- Alameda; Outcrop #7

Figure 8. Lithofacies Group #1 contains (1) stacked bar forms, (2) tabular and trough cross-bedded sandstone, (4) with an erosional base sometimes having (5) mud clast rip-ups. *Note*: Staff is 1.5 m in height, 10 cm increments.
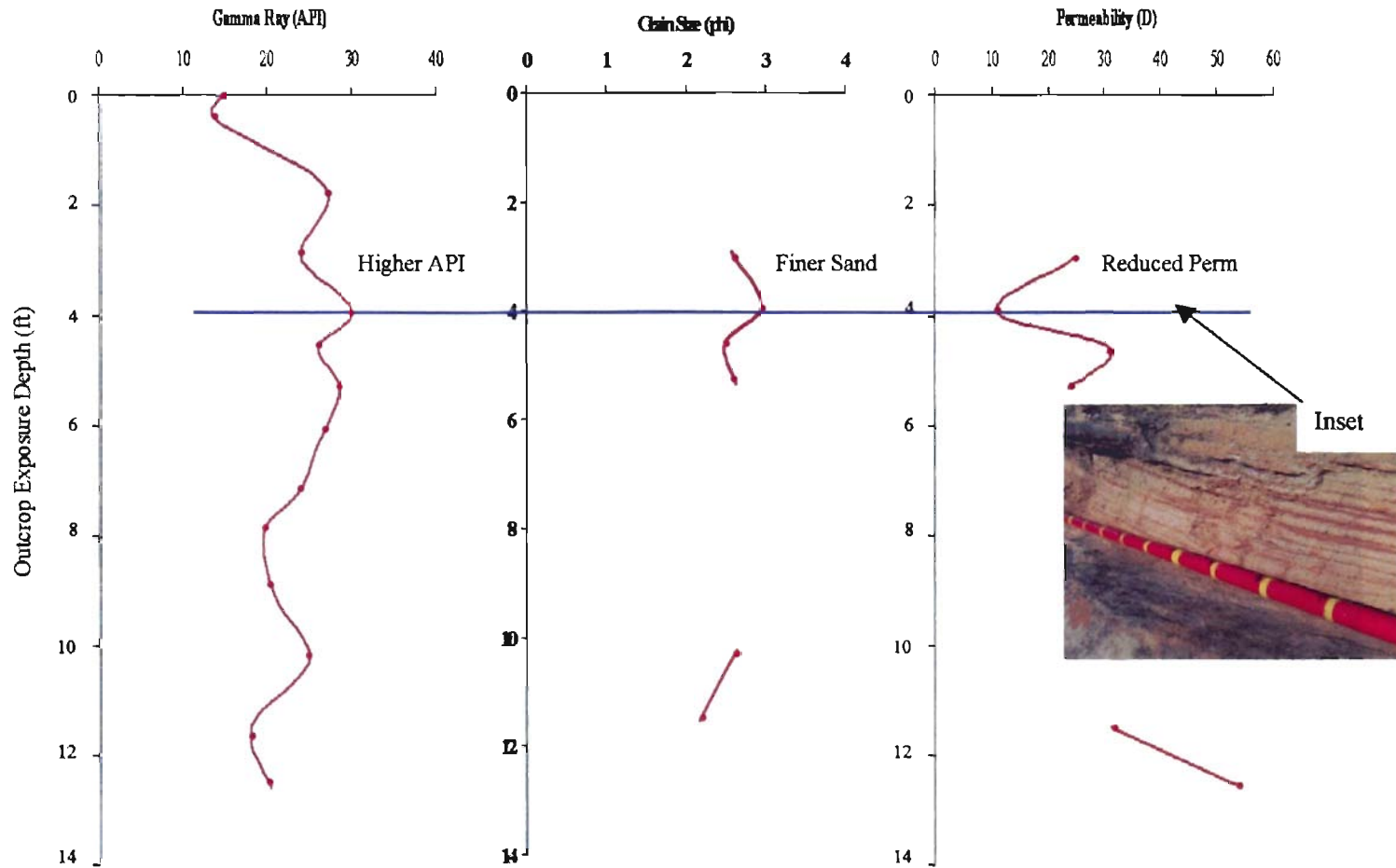
Figure 9. Vertical profile for Group #1, showing gamma-ray, lithofacies, grain size and calculated permeability.

Barite Nodules

Gamma-Ray

Susceptibility to Erosion
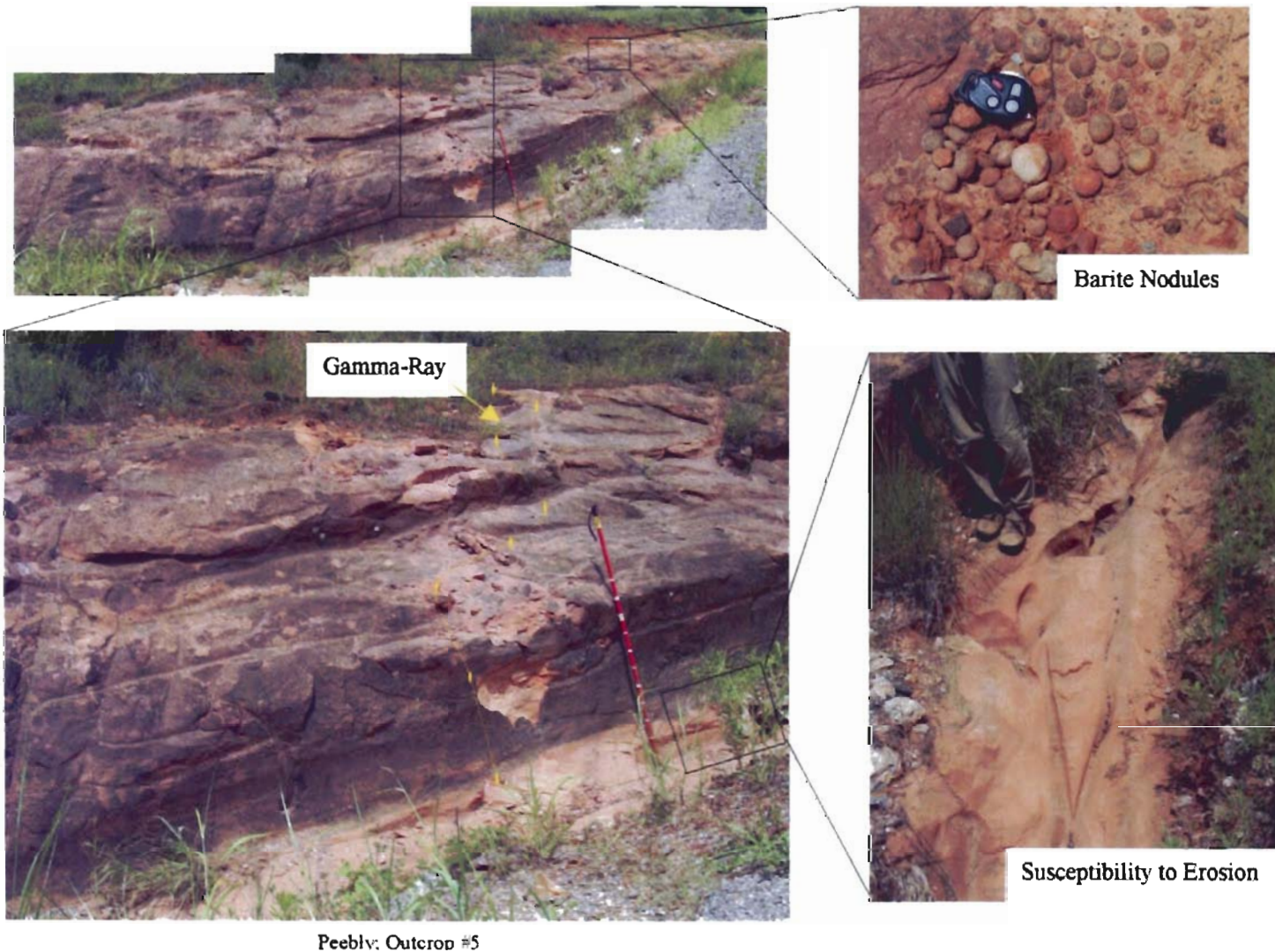
Figure 10. Lithofacies Group #2 contains sandstones that lack internal features, but which exhibit an erosional base. *Note*: This outcrop does not show an erosional base. *Note*: Staff is 1.5 m in height, 10 cm

of a channelized system similar to Group #1. Outcrops incorporated into this category were difficult to interpret because of road maintenance procedures by the highway department. This group has the same grain size as Group #1 but the slightly higher gamma ray suggests that the sandstone is muddier (Fig. 11).

Group #3 incorporates 2 outcrops. This group contains blocky cross-bedded sandstones with mud clast rip-up clasts (Fig. 12) at the base. The gradational change in grain size upwards is interpreted to be the result of decrease in flow velocity. Large-scale cross bedding occurs at the base with mud clast rip-ups and smaller sets of cross-lamination nearer the top. The unusual high gamma-ray average (39 API) is because of mud rip-up clasts found at the base of the unit, which would have a tendency to skew the API average to a higher value. This group contains the coarsest sized particles, thus the calculated permeability for this depositional setting is among the highest (38 Darcies) of all the lithofacies groups discussed (See profile Fig. 13). Because of modern subaerial weathering, rainwater has altered this outcrop by preferentially dissolving and enlarging the pore-spaces. In thin section, clay minerals with meniscus geometry (mechanically infiltrated) are present on detrital grain surfaces (Fig. 13 inset).

Group #4 incorporates six outcrops. This group contains sandstones with horizontal to low angle planar laminations (Fig. 14). These may be typical sheet wash events that originate away from the channel margin where the supply of sediment is low and the carrying capacity depends not only on the amount of water but also on the characteristics of the surface (roughness and gradient). The top surfaces of these laminations commonly contain parting laminations that can be used to measure current direction. The higher values in the API vertical profile (Fig. 15) suggest these are finer-
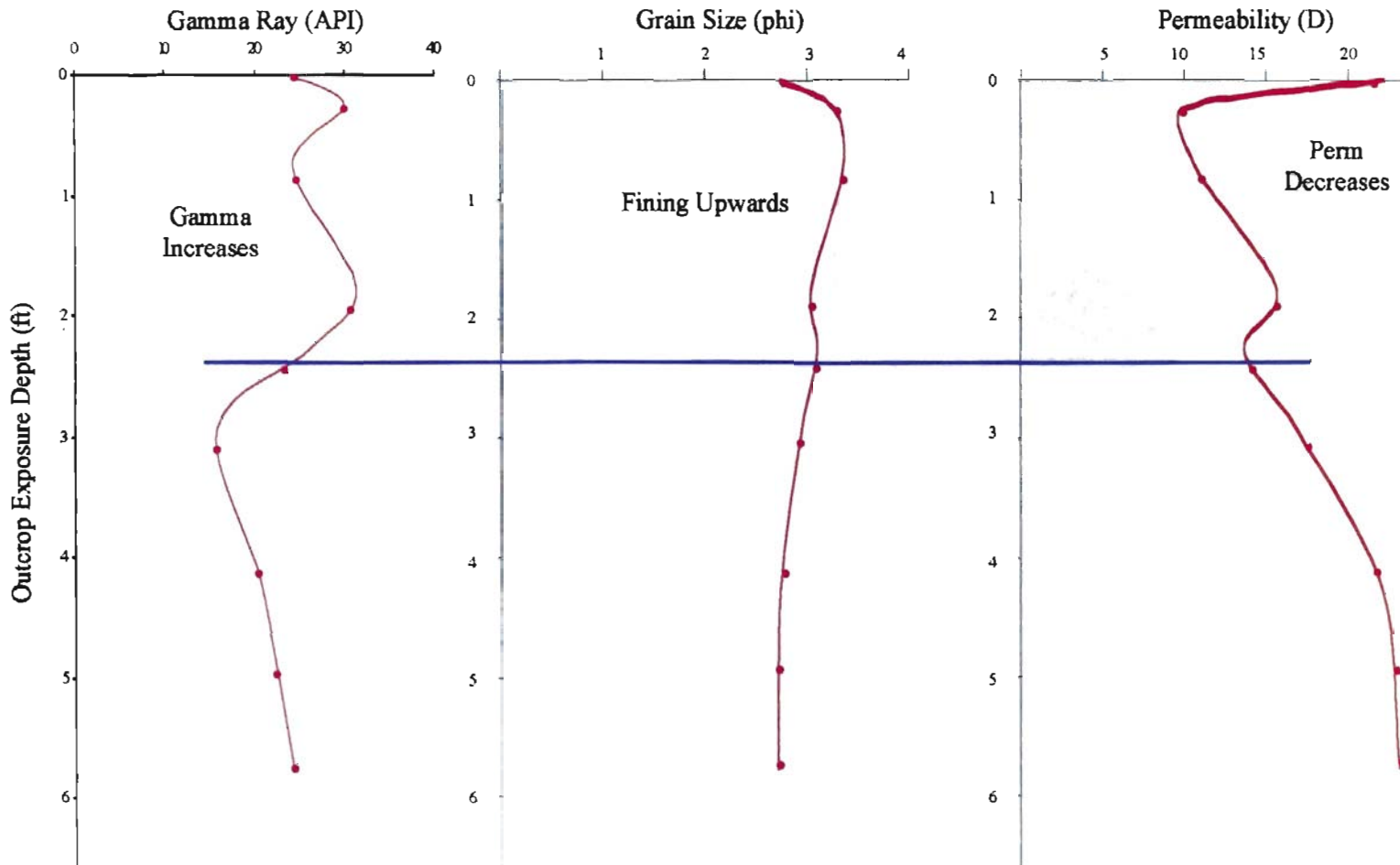
Figure 11. Vertical profile for Group #2, showing gamma-ray, lithofacies, grain size and calculated permeability.

Gamma-Ray
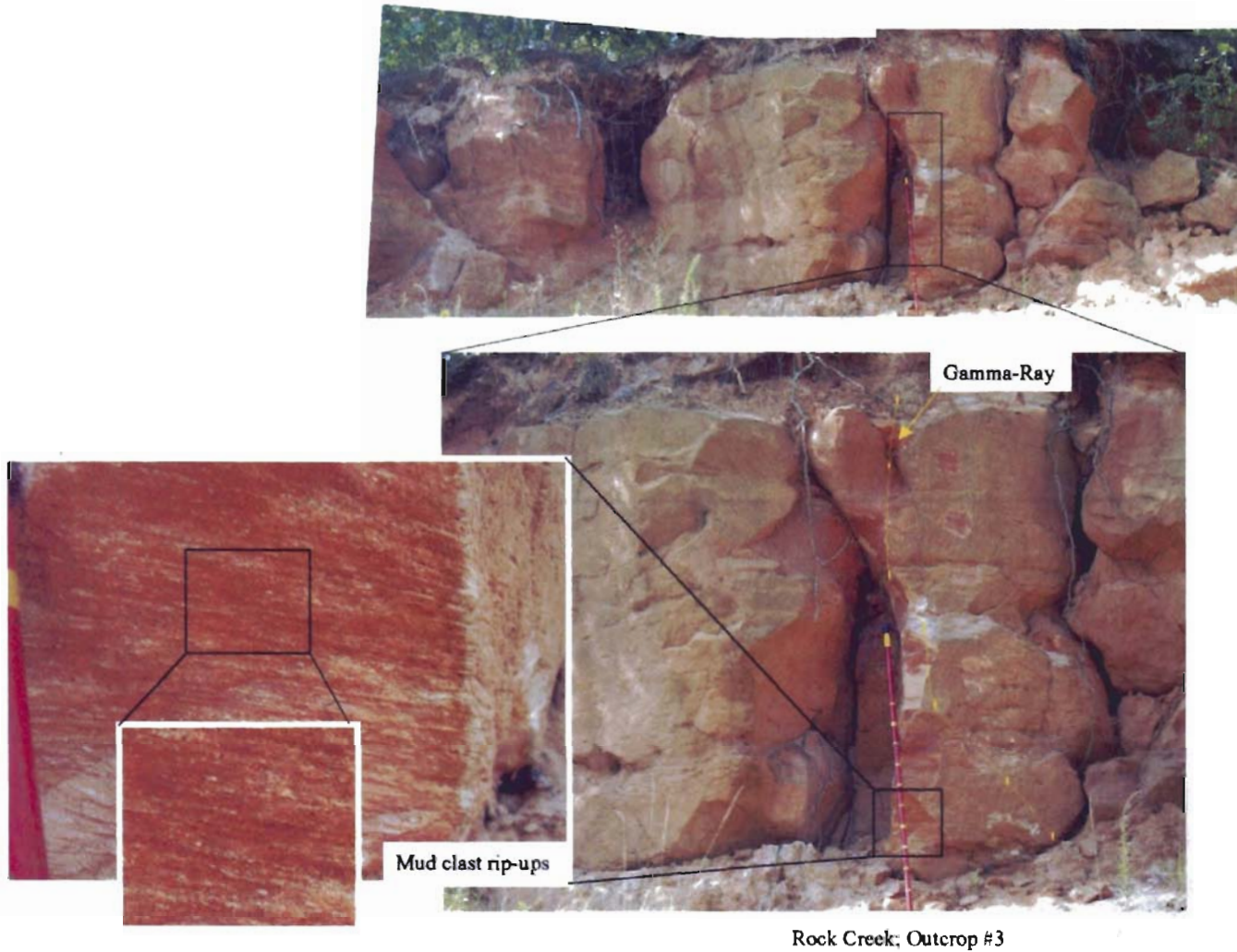
Mud clast rip-ups

Rock Creek; Outcrop #3

Figure 12. Lithofacies Group #3 contains blocky cross-bedded sandstones with mud clast rip-ups. *Note*: Staff is 1.5 m in height, 10 cm increments.

Group #3~Blocky Cross-Bedded Sandstone
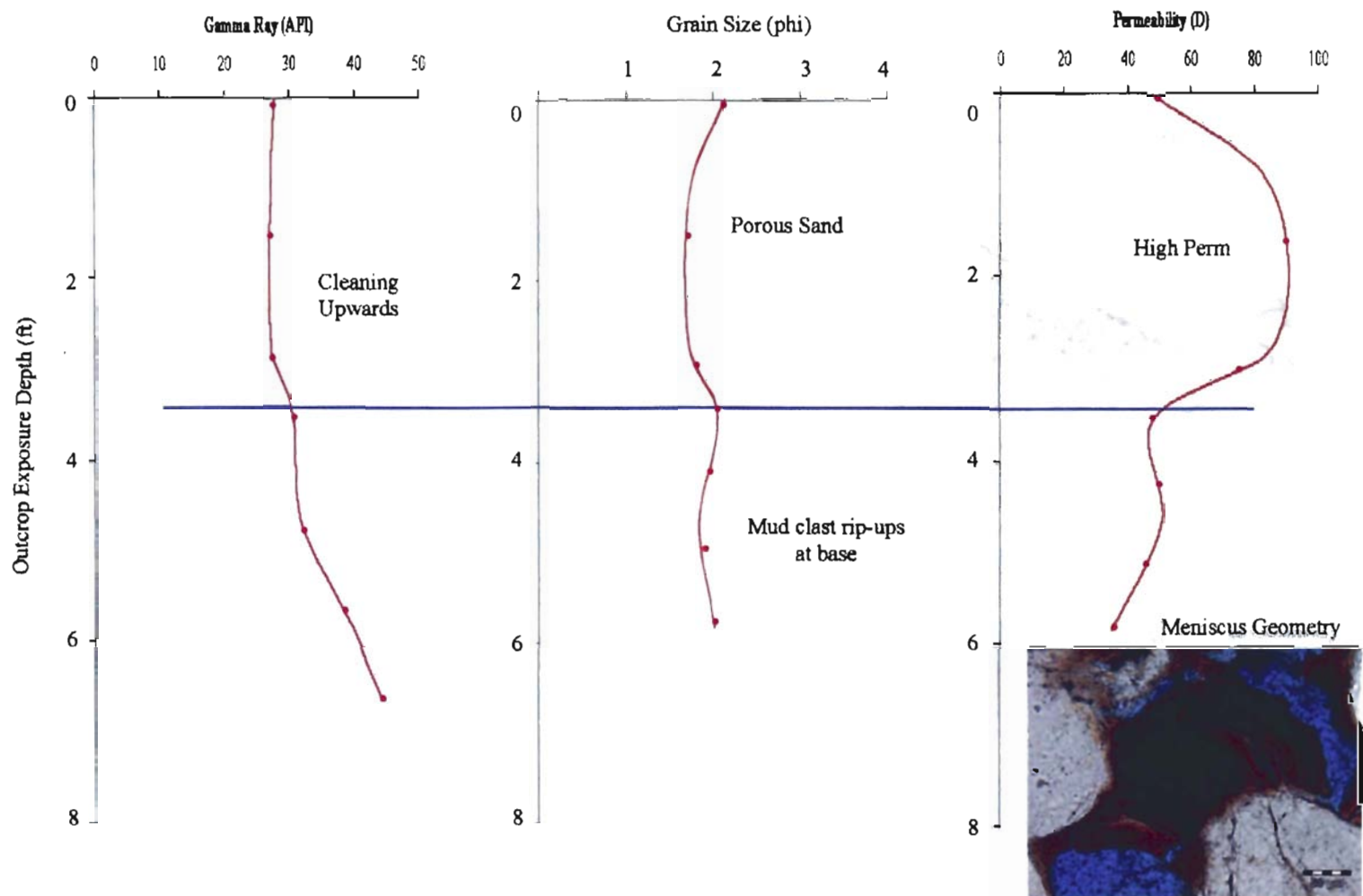
Figure 13. Vertical profile for Group #3, showing gamma-ray, lithofacies, grain size and calculated permeability.

40
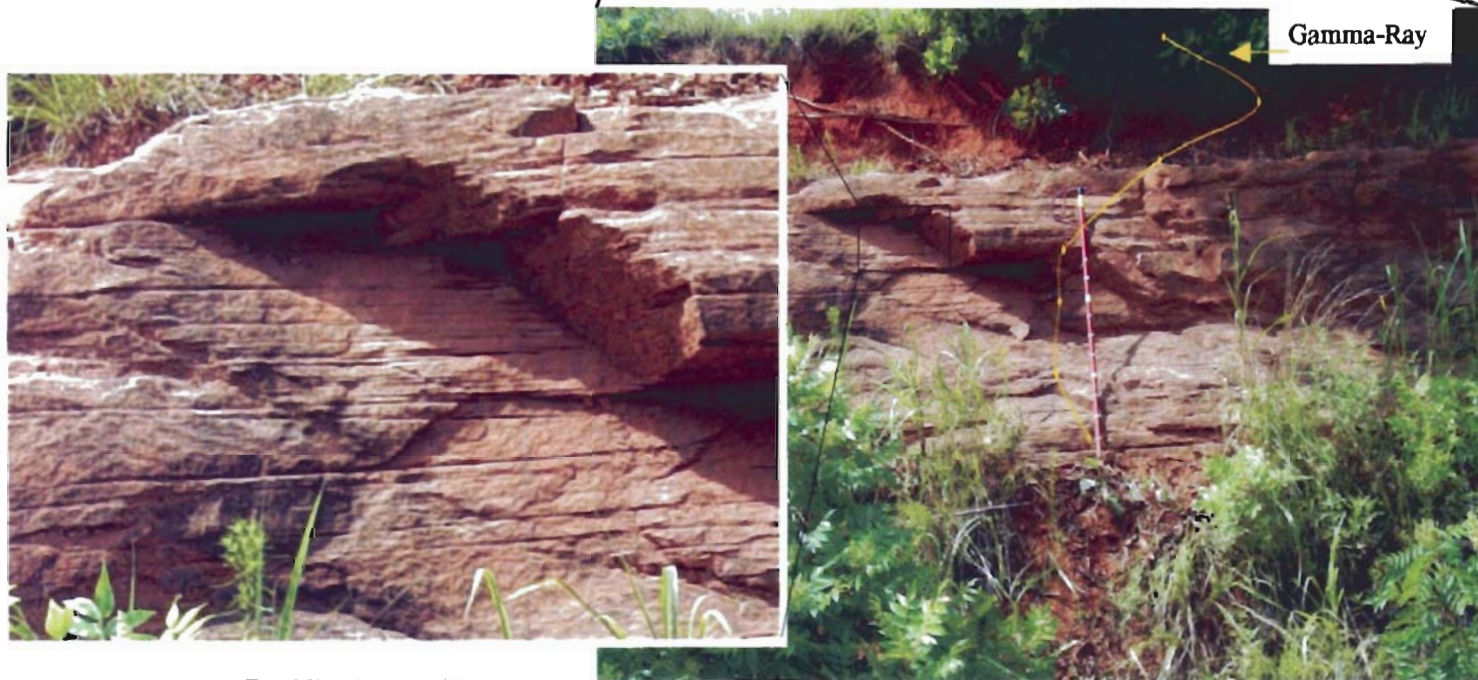
Franklin; Outcrop #5

Figure 14. Sandstone with horizontal to low-angle planar laminations, typical of Group #4. *Note*: Staff is 1.5 m in height.

Group #4~Horizontal to Low-Angle Planar Laminations
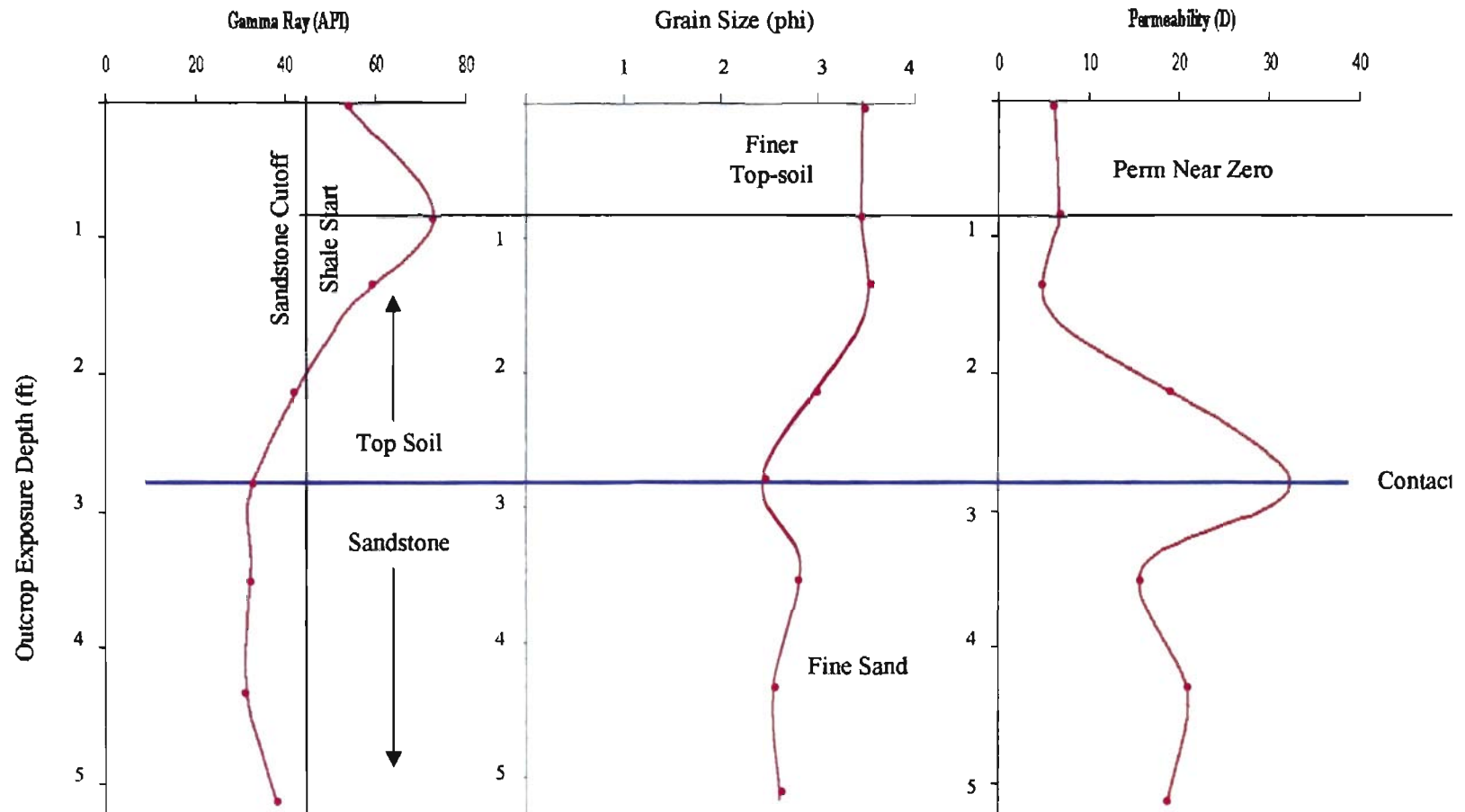
Figure 15. Vertical profile for Group #4, showing gamma-ray, lithofacies and calculated permeability.

grained sands (2.90 phi), thus the mean API value is slightly higher (33 API) and the calculated permeability is consequently reduced.

Group #5 incorporates only one outcrop. This group contains an interlaminated shale/siltstone that is blocky in appearance and without internal primary sedimentary structures (Fig. 16). The shales and siltstones of the Garber-Wellington Formation are highly susceptible to weathering and slaking. The shale has a strong tendency to break parallel to the bedding. Chemical reduction zones are common, probably the result of decay of present day organic material, such as roots. Naturally occurring radioactive elements tend to be found in greater abundance in mudstone and shales than any other sedimentary lithology, thus it is not surprising that the mean gamma ray value is considerably higher (89 API) relative to other lithofacies groups. Because of mechanical compaction during burial of the original silt and clay sediment, the porosity and permeability of this lithofacies group would be low (Fig. 17).

Group #6 is a mud-clast conglomerate that exhibits cross-bedding features (Fig. 18). The upper contact is gradational to sandstone while the lower contact is erosional, containing large pebble rip-up clasts. The conglomerate can be interpreted as a lag deposit formed by rapid water flow on a relatively flat surface during the first stages of a flash-flood event. Towards the base of the conglomerate, the unit contains small trough cross-bed (width maximum about 50 cm). These observations suggest that the conglomerates are intrabasinal. The clasts appear to be nodules of caliche (glaebules) and other "hardpan" zones eroded from the floodplain during a high-discharge precipitation event.

43

Top-soil

Gamma-Ray

Newalla; Outcrop #4

Figure 16. Interlaminated shale/siltstone that is blocky in appearance and without internal primary sedimentary structures, typical of Group #5. *Note*: The shales and siltstones of the Garber-Wellington are highly susceptible to weathering and slaking.

Group #5~Siltstone with Interlaminated Shale
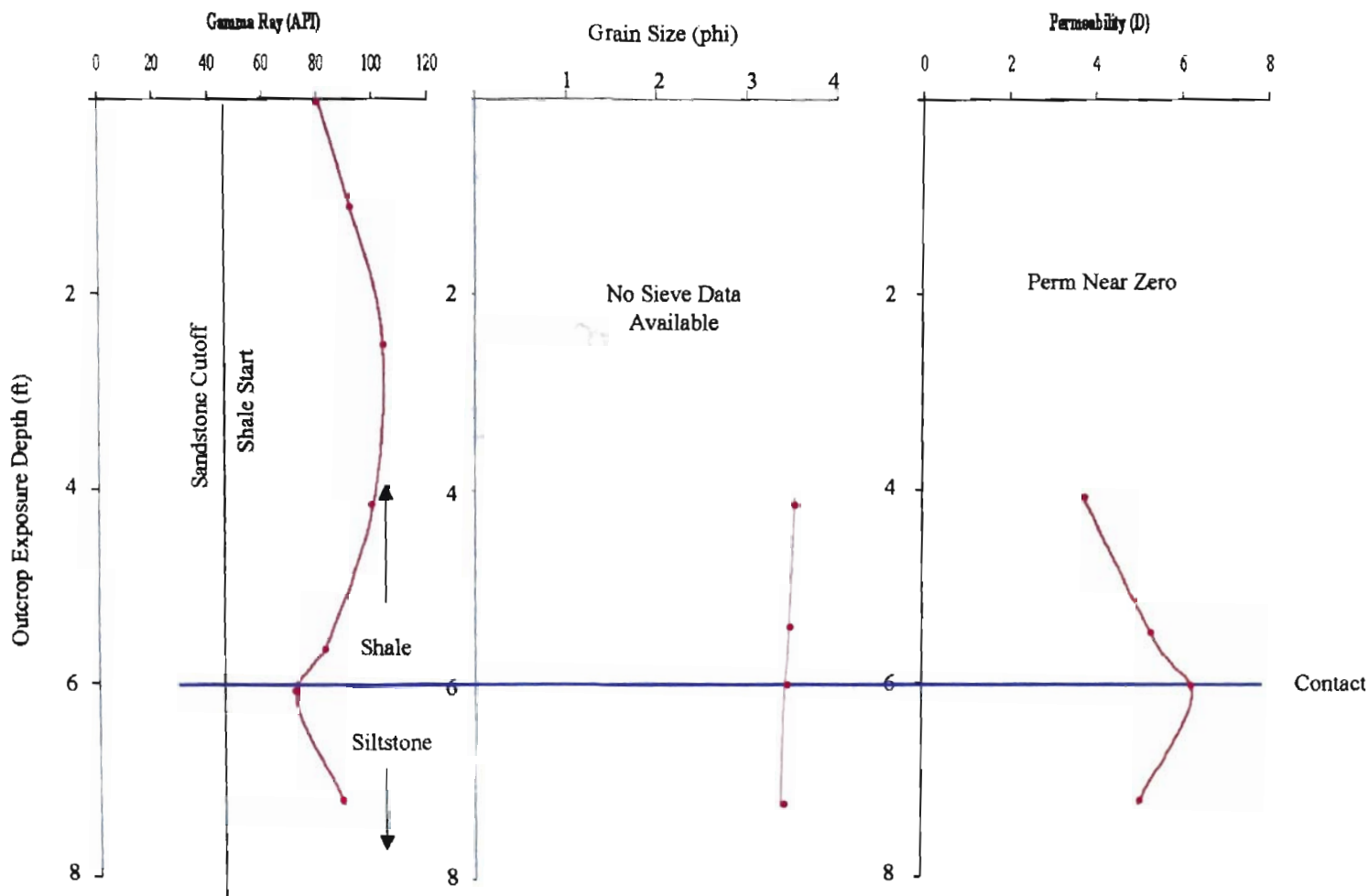
Figure 17. Vertical profile for Group #5, showing gamma-ray, lithofacies, grain size and calculated permeability.

Group #6~Mud-Clast Conglomerate
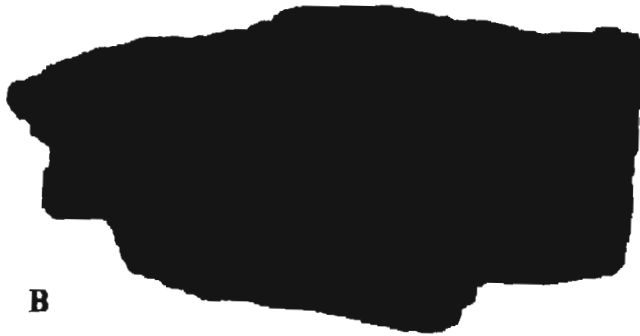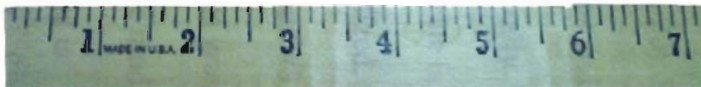
Figure 18. Mud-clast conglomerate that exhibits cross-bedding features. (A) Weathering profile, (B) close up of mud-clast conglomerate and (C) cross-bedding.

Group #7 lithofacies is present at only one outcrop. This lithofacies is a carbonate clast conglomerate (Fig. 19). This conglomerate exhibits horizontal planar laminations and is extremely well cemented with dolomite. No other examples of dolomitization of this magnitude have been found in the study area, thus we suggest that the dolomite originated in an isolated lake setting situated on the floodplain, adjacent to the river. Exposure of the water body in a seasonally arid environment may have promoted dolomite cementation. An alternative hypothesis is that the body of water was filled in by a flash flood event and became cemented. Because the sample could not be disaggregated in the lab, grain size and permeability calculations could not be determined. Since our conglomerate consists of mud-clasts cemented together with dolomite, it is not surprising to see a higher gamma ray value (36 API). The cement fills pore spaces between the grains. This diagenetic cement reduces the permeability. Rare sparry dolomite (Fig. 19) is the most abundant authigenic mineral throughout the aquifer.

Group #8 consists of an iron-cemented sandstone/conglomerate (Fig. 20). Several outcrops (4) show large-scale cross bedding at the base with mud clast rip-ups and smaller sets of cross-lamination nearer the top. The size of the particles generally decreased upwards as a result of decreased carrying capacity. The conglomerate is generally well cemented and when exposed to the atmosphere, becomes oxidized.

No statistical grain size results could be computed for Group #6, #7 and #8 because the conglomerate samples could not be disaggregated in the lab. Thus grain size, sorting and permeability could not be calculated. Thin-section analysis of one mud clast cross-bedded conglomerate (Group #6) indicates that the gravel-sized material is

Group #7~Carbonate Clast Conglomerate

Dolomite Crystals

200 µm
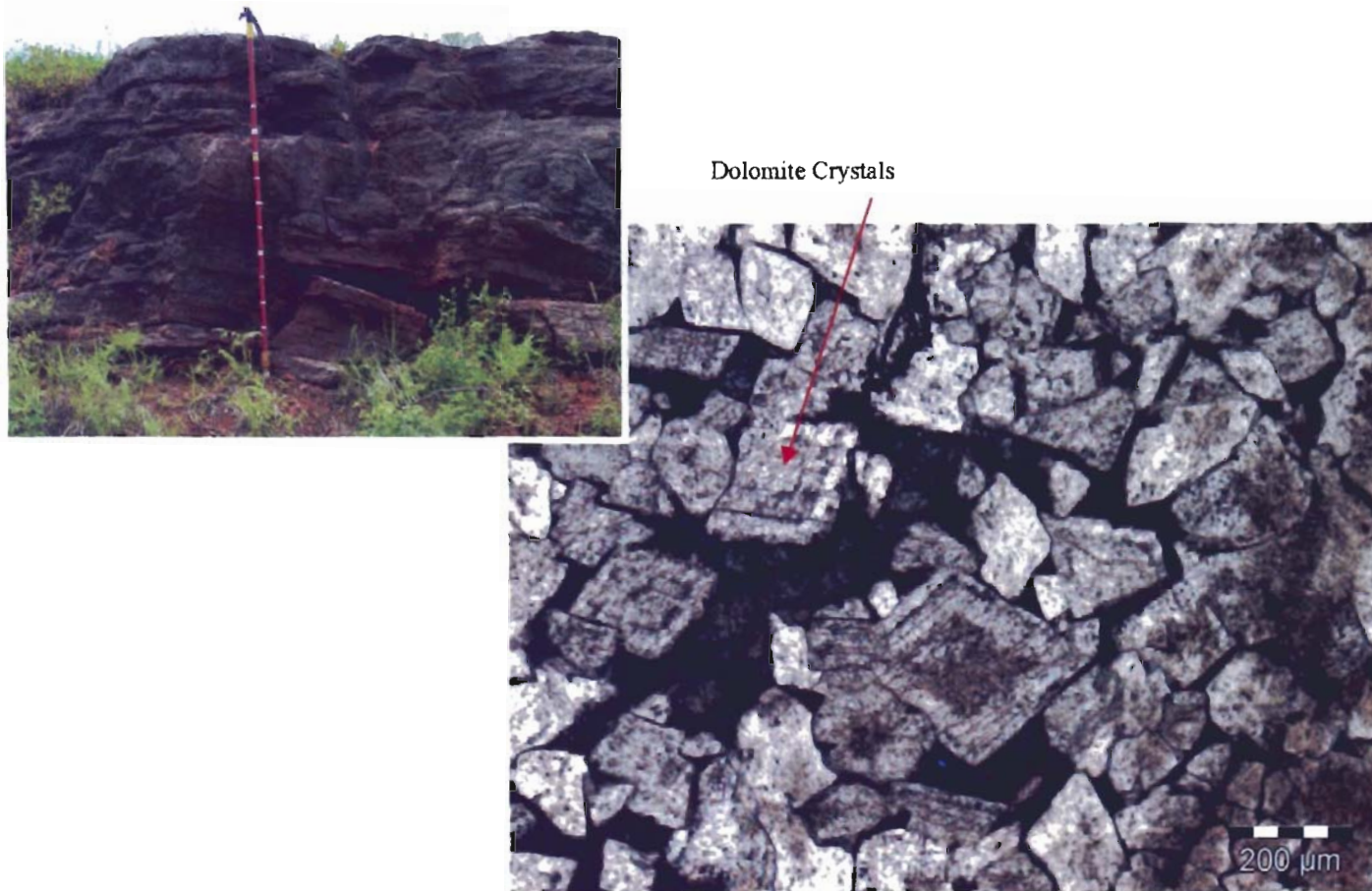
Figure 19. Carbonate clast conglomerate cemented together with dolomite, typical of Group #7.

Group #8~Iron-Cemented Sandstone/Conglomerate
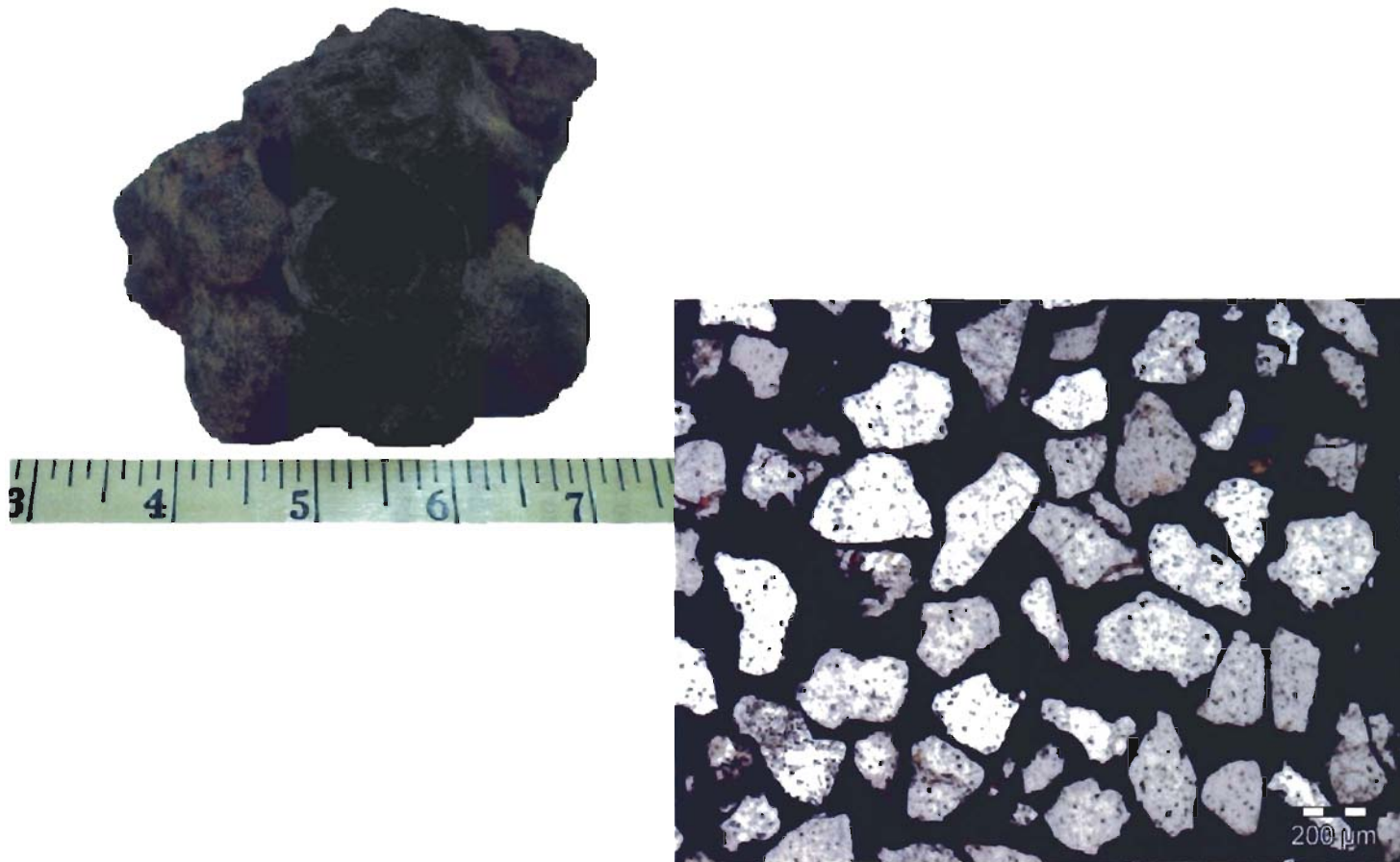
Figure 20. Iron-cemented sandstone/conglomerate, typical of Group #8. Photograph shows poikilotopic texture of quartz and Fe oxide (hematite) cement (black).

cemented together with carbonate and Fe oxide. The iron conglomerate (Group #8) is completely cemented by Fe oxide, thus permeability would be negligible. Additional outcrop data for each group discussed above may be found in Appendix B.

Subsurface Environments

Based on this work, subsurface gamma ray response in the Central Oklahoma Aquifer should include (1) bell-shaped and (2) blocky gamma-ray patterns characteristic of fluvial deposits. Traditionally, bell-shaped is generally considered a point bar deposit from a meandering river and a blocky response is considered to be a bar sand in a braided system. Traditional point bar deposits are not observed in these rocks. This may be because the banks of the river system were unstable and due to rapid lateral accretion, the sands had a tendency to be reworked as both transverse and longitudinal bars in the channel.

The horizontally laminated intervals (Group #4) may be difficult to detect on the gamma-ray well logs. We suspect these units occur a distance from the main channel where they may have formed sheetflow deposits on the floodplain. The relatively thin and well indurated conglomerates probably originated from the floodplain during a high-discharge event. These conglomerates may be associated with high resistivity kicks on the gamma-ray well logs.

Part B-Subsurface Permian Solid Phase Geochemical Data

The U.S. Geological Survey (USGS) completed geochemical studies of solid-phase geologic materials collected from the Central Oklahoma Aquifer study area in 1990. These geochemical studies were done as part of the National Water-Quality Assessment (NAWQA) Program of the USGS. In-order to conduct the study, the USGS drilled and cored eight test holes (Fig. 21) and performed a geochemical analysis on 549 rock samples from the cores. Samples collected were analyzed by the USGS for 37 different elements using an inductively coupled plasma-atomic emission spectroscopy (ICP-AES). Concentrations of arsenic were determined by hydride generation-atomic absorption spectroscopy because of better detection limits. Results from the USGS solid-phase geochemical study incorporated into this thesis can be found in Mosier et al. (1990).

We performed exploratory data analysis on the USGS geochemical data, with the hope of more precisely identifying and quantifying the habitat (environment) of arsenic in the subsurface rocks, In addition, because the geochemical data set contained measurements for K, U, and Th, the expected API gamma-ray response was calculated based on the equation discussed earlier in the thesis. (p. 22). The intent in performing this work was two-fold: (1) quantitatively establish the strength of association among lithofacies and arsenic occurrence and (2) to evaluate the utility of using subsurface gamma ray well logs as a means to identify arsenic prone intervals beneath City of Norman.
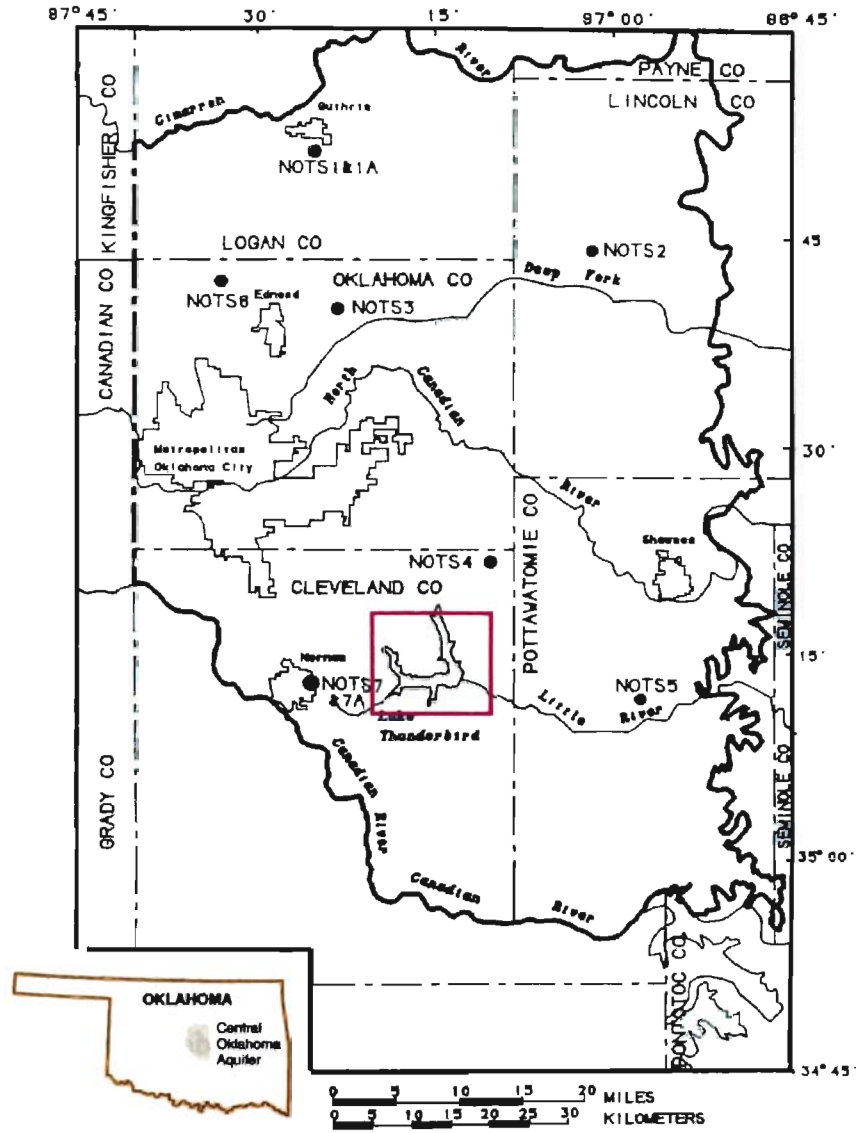
Figure 21. Location of NOTS test holes (modified from Mosier et al. 1990).

Seven of the test holes were drilled in areas where wells were known to yield ground water with high concentrations of arsenic, while test hole 4 was drilled in an area known to yield low concentrations of arsenic. Test holes 1A, 3, 4 & 6 intercepted the undifferentiated Garber-Wellington Formation in the unconfined, shallow (< 300 ft) portion of the aquifer. Test hole 6 penetrated the unconfined deeper (>300 ft) portion of the aquifer (Mosier, 1998). Test holes 2 & 5 intercepted the undifferentiated Chase, Council Grove, and Admire Groups in the unconfined, shallow parts of the aquifer. Test hole 7 was drilled to characterize the confining layer (Hennessey Group). Lastly, test hole 7A was drilled to study the arsenic in that part of the aquifer confined by the Fairmont Shale.

The USGS lithology classes were established by the USGS and are not totally comparable with the lithofacies groups discussed in outcrop classification and characterization (Part A) of thesis. The USGS strategy for selecting samples from the core for geochemical analysis was based on distinct changes in lithology, color and diagenetic cements. These data were subdivided on the basis of lithology according to Mosier (1994) in-order to describe observed geochemical variations. The distribution of the lithologic units in linear feet and in percentage of total core is summarized in Table 4.

Results from Analyzing the Geochemical Data Set

Significant statistical associations were discovered based on evaluation of frequency distributions and correlation coefficients for the data set. Many of the relationships are anticipated based on our knowledge of the rocks. The Permian red beds are mainly composed of quartz and aluminosilicate mineral phases. Aluminum (Al) for

NOTS	Sandstone	Mudstone	Conglomerate	Siltstone	Mixed	Total
1A	174.9	47.7	11.6	1.5	15.4	251.1
	69.7%	19.0%	4.6%	0.6%	6.1%	
2	140.9	104.8	3.8	10	2.5	262
	53.8%	40.0%	1.5%	3.8%	1.0%	
3	95.6	79.4	1.8	2.8	0	179
	53.2%	44.2%	1.00%	1.6%	0.0%	
4	191.8	67.6	0	1.5	8.9	269.8
	71.1%	24.5%	0.0%	0.5%	3.2%	
5	106	98.3	13	4.2	1.5	223
	47.5%	44.1%	5.8%	1.9%	0.7%	
6	367.2	85.6	22	24.5	14.8	514.1
	71.4%	16.7%	4.3%	4.8%	2.9%	
7	11.8	25.1	1.6	52.7	63.4	154.6
	7.6%	16.2%	1.0%	34.1%	41.0%	
7A	262.4	21.3	10.4	25.9	22.7	342.7
	76.6%	6.2%	3.0%	7.6%	6.6%	
Total	1350.6	529.8	64.2	123.1	129.2	2196.9
	61.5%	**24.1%**	**2.9%**	**5.6%**	**5.9%**	

Table 4A. Distribution of the lithologic units in linear feet and in percentage of each core.

Percentage by Lithology
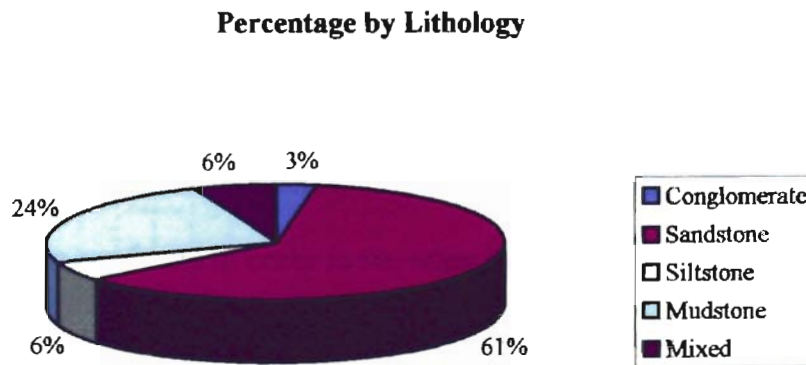
Table 4B. Distribution of lithologic units in percentage of total core.

example, found abundantly in red beds, increases systematically with the grain size in each lithology category. A summary of the USGS geochemical data grouped by lithology class is presented in Tables 5 and 6.

Other statistical associations have a direct bearing on the outcrop gamma-ray response and the occurrence and distribution of As. For instance, natural radioactive elements K, U, and Th occur in far greater abundance in the shales and mudstones than in the other lithologies (Figure 22). Consequently, the calculated gamma-ray response is much higher in these finer-grained lithofacies than in the coarser-grained lithofacies. In addition, univariate analysis shows that Fe and As are enriched in the finer-grained lithofacies (refer back Table 5 & 6). This observation has important implications for establishing a physical linkage between the sedimentary geology and the occurrence of As in the rocks via the use of the gamma ray logging tool. The approach and rationale are discussed below.

Frequency distributions grouped by lithofacies for Fe (Fig. 23) and As (Fig. 24) show that these two elements vary systematically with grain size of the sedimentary rocks. The finer-grained lithofacies (siltstone, clay, and mudstone) contain significantly more Fe and As than are found to occur in the other lithologies (conglomerate and sandstone). Based on the work of Breit et al. (1990) and Schlottmann et al. (1998) most of the Fe in the rock occurs as hematite; some of the Fe is associated with goethite and limonite. Other observations that suggest hematite is enriched in the finer-grained lithofacies in the Garber-Wellington Formation include: (1) shale and mudstone interbedded with sandstone (in core or outcrop) are commonly redder in appearance than

Cong   1

Variable	N	Mean	Std. Dev	Min	Max
Al	31	3.26	1.59	1.80	8.00
Ca	31	7.11	3.84	0.50	13.00
Fe	31	2.45	1.57	0.46	6.00
K	31	0.68	0.36	0.24	1.70
Mg	31	4.15	2.13	0.20	7.40
Na	31	0.27	0.13	0.14	0.65
As	31	6.83	4.14	2.00	17.00
Th	31	6.98	2.31	4.00	13.60
U	31	2.42	1.20	0.94	7.34
API	31	58.26	18.80	36.92	110.96

SS   2

Variable	N	Mean	Std. Dev	Min	Max
Al	247	2.87	1.70	0.28	7.30
Ca	247	1.10	1.93	0.01	15.00
Fe	247	1.39	0.93	0.11	4.80
K	247	0.59	0.37	0.07	1.60
Mg	247	0.77	1.05	0.03	8.00
Na	247	0.24	0.19	0.01	0.83
As	247	3.62	1.94	0.40	7.70
Th	247	6.62	3.18	1.30	14.10
U	247	2.12	1.37	0.35	9.59
API	247	52.04	25.89	5.40	112.64

Mud/SS   3

Variable	N	Mean	Std. Dev	Min	Max
Al	7	6.08	0.90	4.90	7.30
Ca	7	1.48	1.29	0.14	3.40
Fe	7	3.34	0.71	2.70	4.70
K	7	1.19	0.11	0.95	1.30
Mg	7	1.35	0.82	0.14	2.50
Na	7	0.33	0.22	0.05	0.59
As	7	8.18	4.03	4.20	15.00
Th	7	10.54	1.76	7.32	13.20
U	7	2.59	0.30	2.19	3.17
API	7	82.03	6.58	70.88	90.56

Silt   4

Variable	N	Mean	Std. Dev	Min	Max
Al	34	5.87	1.33	3.50	8.30
Ca	34	2.12	2.28	0.09	11.00
Fe	34	3.08	0.91	1.10	4.90
K	34	1.41	0.41	0.54	2.30
Mg	34	1.95	1.49	0.29	7.70
Na	34	0.63	0.24	0.08	1.10
As	34	7.57	2.90	3.10	15.00
Th	34	10.48	2.60	3.10	15.60
U	34	2.87	0.93	0.61	5.89
API	34	87.49	18.15	38.09	115.20

Table 5. Summary of the USGS geochemical data for major elements by lithology. Mean concentration of each element progressively increases from sandstone to clay. Fe and As are of interest in this study, thus are highlighted. *Note*: The USGS lithology classes were erected by the USGS and are not totally comparable with the lithofacies groups discussed in outcrop classification and characterization (Part A) of thesis. Outliers not incorporated into mean.

Mud/Silt 5

Variable	N	Mean	Std. Dev	Min	Max
Al	16	6.46	1.83	2.60	10.00
Ca	16	2.53	3.79	0.10	16.00
Fe	16	3.30	0.93	1.30	4.60
K	16	1.59	0.52	0.49	2.40
Mg	16	2.36	2.15	0.34	9.60
Na	16	0.61	0.23	0.27	0.97
As	16	8.46	2.73	3.50	14.00
Th	16	11.10	2.74	6.22	17.20
U	16	2.94	0.77	1.42	4.45
API	16	93.40	20.88	44.08	131.00

Mud 6

Variable	N	Mean	Std. Dev	Mini	Max
Al	104	7.95	1.17	3.60	9.90
Ca	104	1.68	1.65	0.11	8.60
Fe	104	4.22	0.86	0.90	5.70
K	104	1.50	0.33	0.92	2.60
Mg	104	1.89	0.94	0.54	5.00
Na	104	0.49	0.17	0.05	0.81
As	104	9.12	2.46	3.10	16.00
Th	104	12.93	2.02	7.14	17.30
U	104	3.25	0.71	1.66	5.91
API	104	101.91	14.11	57.04	136.16

Clay 7

Variable	N	Mean	Std. Dev	Min	Max
Al	5	8.00	1.08	6.80	9.50
Ca	5	0.90	1.01	0.21	2.60
Fe	5	4.46	0.69	3.60	5.40
K	5	1.76	0.40	1.20	2.20
Mg	5	1.20	0.62	0.85	2.30
Na	5	0.23	0.25	0.01	0.55
As	5	12.60	2.30	10.00	16.00
Th	5	14.04	1.67	11.90	16.40
U	5	2.84	0.23	2.64	3.25
API	5	107.10	9.92	97.92	122.88

Table 6. Summary of the USGS geochemical data for major elements by lithology. Mean concentration of each element progressively increases from sandstone to clay. Fe and As are of interest in this study, thus are highlighted. *Note*: The USGS lithology classes were erected by the USGS and are not totally comparable with the lithofacies groups discussed in outcrop classification and characterization (Part A) of thesis. Outliers not incorporated into mean.
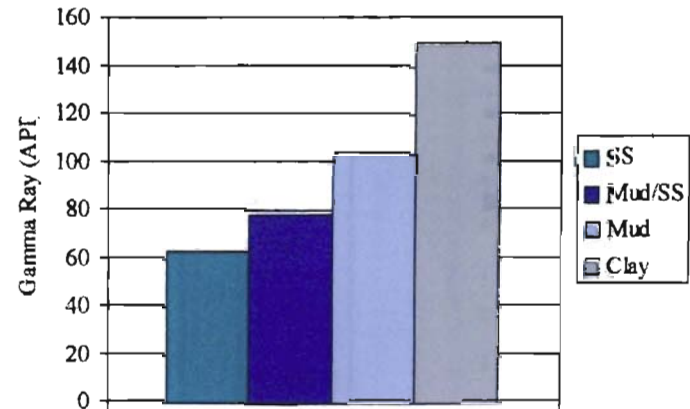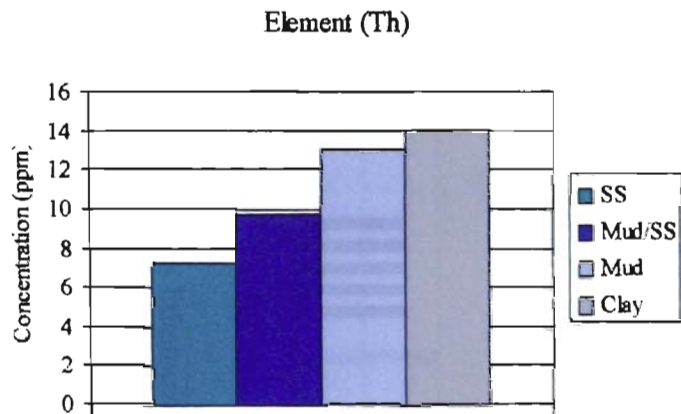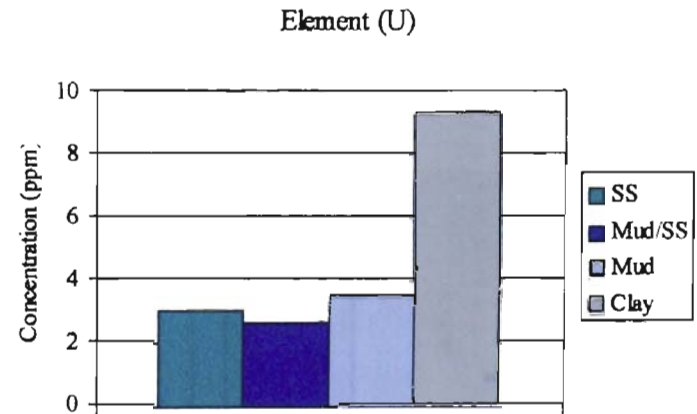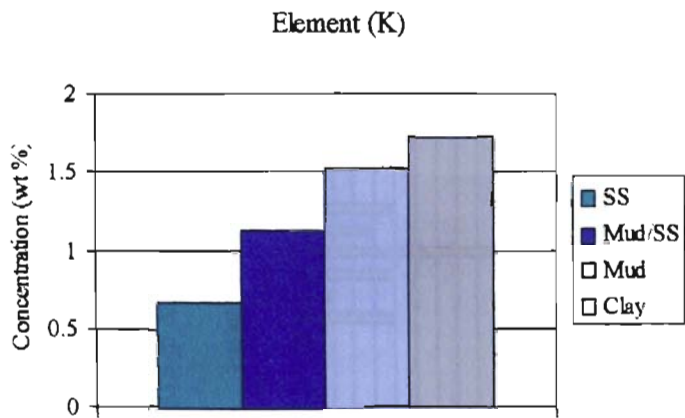
Figure 22. Natural radioactive elements K, U, and Th occur in far greater abundance in the shales and mudstones than in the other lithologies.
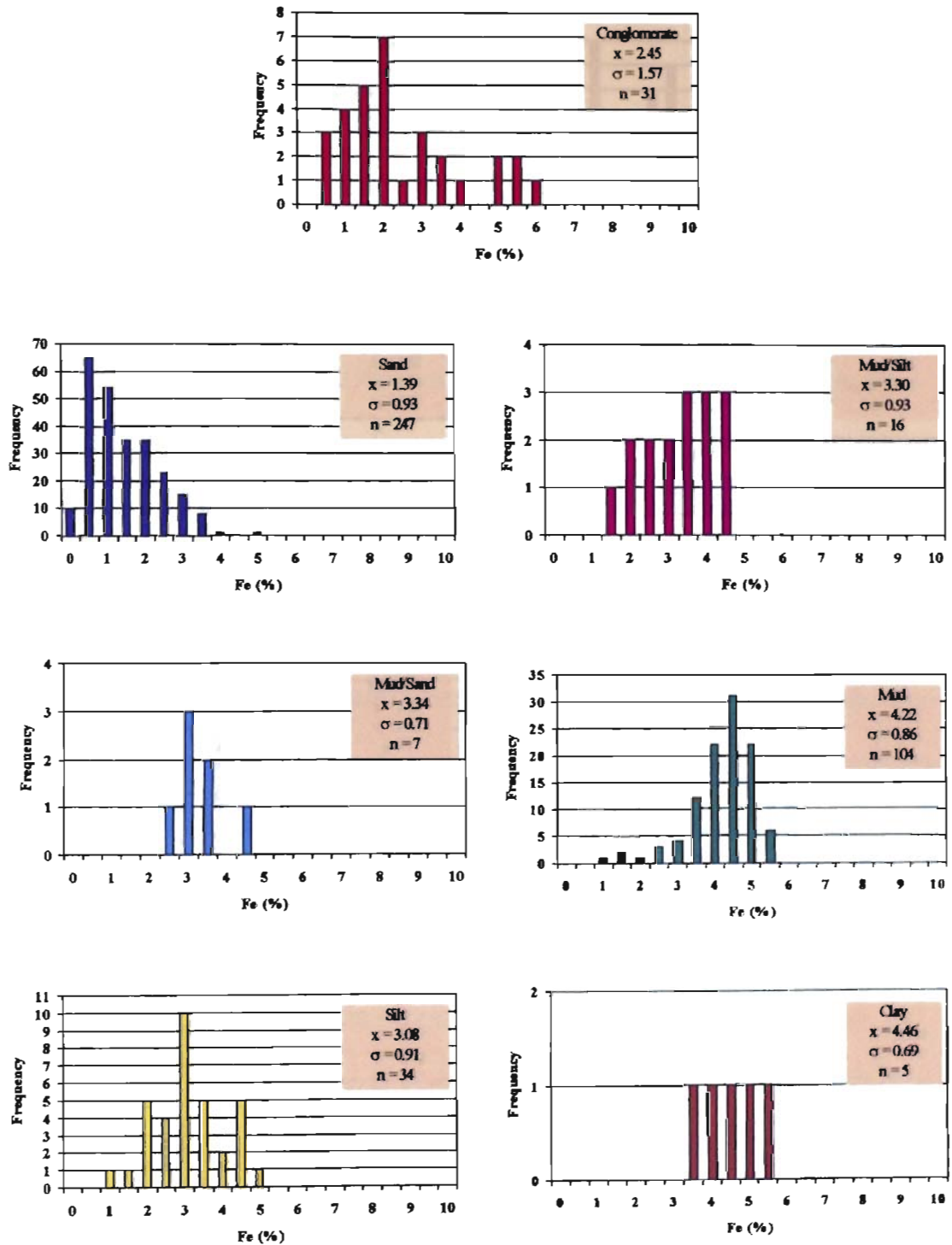
Figure 23. Frequency distribution for Fe subdivided by the USGS lithologic categories. Iron concentration (%) progressively increases from sandstone to clay stone. Outliers removed.
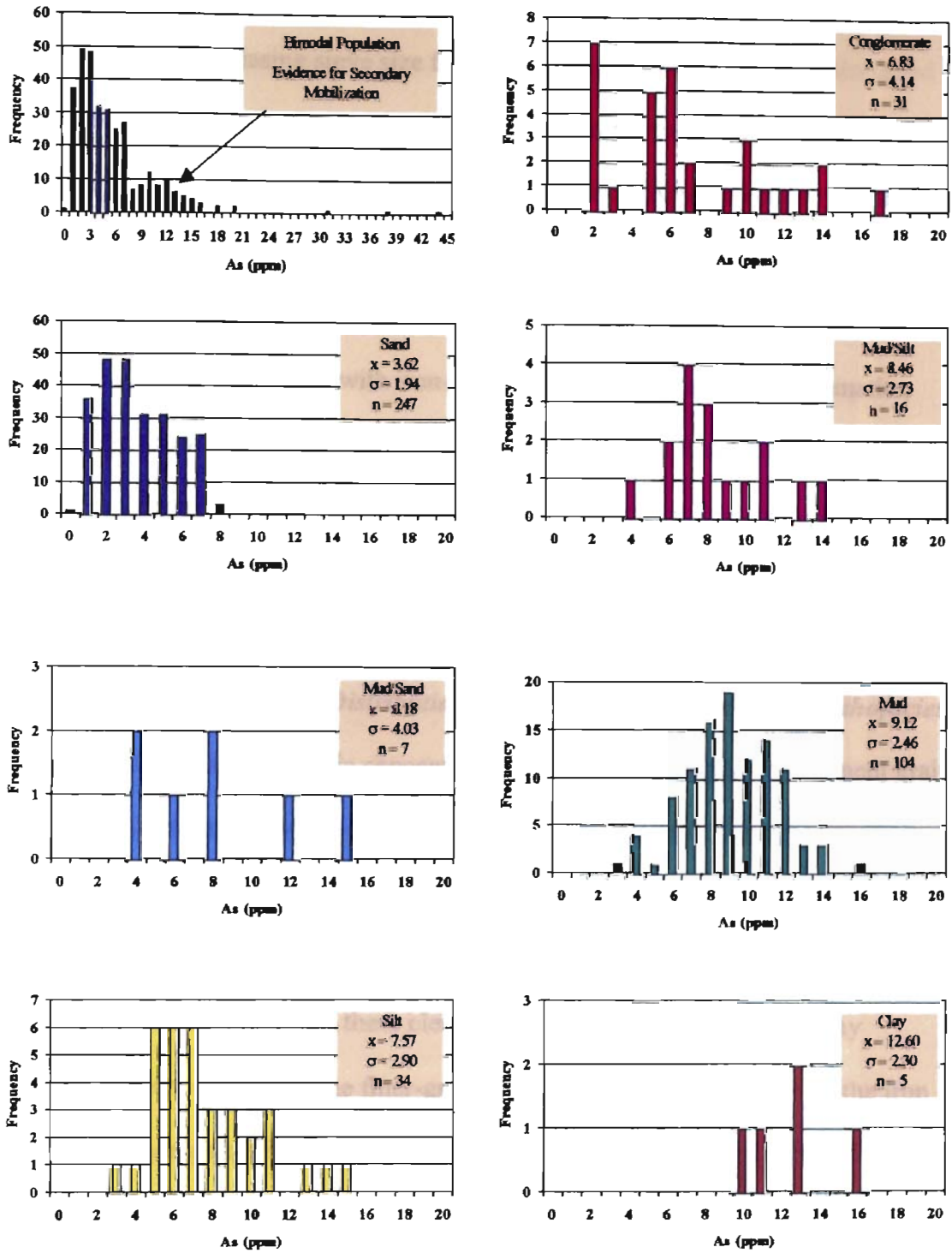
Figure 24. Frequency distribution for As subdivided by the USGS lithologic categories. Arsenic concentration (ppm) progressively increases from sandstone to clay stone. Outliers removed.

60

the adjacent sandstones and (2) sieve fractions of the disaggregated sandstones become redder in color with decreasing sieve size fraction.

As mentioned briefly above, arsenic abundance in the rocks varies strongly with the grain size and lithofacies as well (Figure 24 cited above). Arsenic concentrations are higher in the finer grained lithofacies than in the coarser grained lithofacies. We are not surprised by this finding; arsenic in sedimentary rocks is documented (Schlottmann et al, 1998) to be commonly associated with iron-bearing mineral phases (pyrite, hematite, goethite). In the Garber-Wellington Formation, we suggest that the As is adsorbed onto the fine-grained hematite that is disseminated throughout the Permian red beds of central Oklahoma.

Procedure for Mapping Arsenic Distribution in Subsurface Arsenic-prone Lithofacies

Because the iron and arsenic concentrations in the rocks vary with sediment grain size, the potential exists to develop an algorithm for the prediction of arsenic based on gamma-ray response. This predictive relationship, however, is one of association and not direct cause and effect. In other words, the gamma-ray response is a function of the U, K, and Th content of the rocks and these elements tend to be associated with clay minerals that are concentrated in the finer-grained lithofacies. By coincidence, the iron and the accompanying arsenic are also enriched in the finer-grained rocks by virtue of the association between adsorbed iron and the surfaces of the clay minerals. As a consequence, a quantitative relationship should exist between the gamma-ray response and the iron/arsenic content of the rocks. The gamma-ray response can be then be used to map arsenic occurrence in the subsurface Permian rocks of the City of Norman area.

The procedure and discussion for the establishment of a quantitative relationship between the gamma-ray response and the iron/arsenic content of the rocks is discussed below.

(1) Group the whole-rock geochemical analysis results by lithology; the USGS data set contains 542 iron (Fe) and arsenic (As) measurements distributed among seven lithologies (Mosier et al, 1990). These USGS lithologic subdivisions are based on the grain size of the rocks. Frequency distributions for these elements subdivided by the USGS lithologic categories are shown in Fig. 23 & 24.

(2) Evaluate the frequency distributions of iron and arsenic for each of the lithology groupings: The frequency distributions discussed above are relatively Gaussian in character when subdivided by lithology. Some of the distributions are slightly positively skewed. T-tests were used to identify statistically significant differences in iron and arsenic content between the lithology groups (Table 7 and 8). The difference between the means is too great to be a chance event (likelihood of <1 in 10,000). The data suggest that iron varies significantly between all lithologies except mud/silt vs silt ($p<0.43$) and clay vs. mud ($p<0.55$). Arsenic varies significantly between all lithologies except mud/silt vs. silt ($p<0.31$) and mud vs. mud/silt ($p<0.32$).

(3) Assuming a Gaussian or normal distribution for iron and arsenic, eliminate outliers in the data set for each of the lithologies: Data for each lithology class contains some significant outliers. We are uncertain as to why each of the lithology groups contains outliers. We suspect that some of the outliers are because of analytical

TESTING FOR DIFFERENCES IN LITHOLOGY

Lithology	Variable	Method	Variances	DF	t Value	Pr >[t]
SS vs Cong	Fe	Pooled	Equal	276	5.44	<.0001*
		Satterthwaite	Unequal	32.7	3.68	0.0008*
SS vs Mud/SS	Fe	Pooled	Equal	252	5.48	<.0001*
		Satterthwaite	Unequal	6.59	7.02	0.0003*
SS vs Silt	Fe	Pooled	Equal	279	9.94	<.0001*
		Satterthwaite	Unequal	43	10.09	<.0001*
SS vs Mud/Silt	Fe	Pooled	Equal	261	7.95	<.0001*
		Satterthwaite	Unequal	17	7.97	<.0001*
SS vs Mud	Fe	Pooled	Equal	349	26.49	<.0001*
		Satterthwaite	Unequal	207	27.3	<.0001*
Mud/Silt vs Silt	Fe	Pooled	Equal	48	0.79	0.4327ns
		Satterthwaite	Unequal	29	0.79	0.4381ns
Mud vs Mud/Silt	Fe	Pooled	Equal	118	3.91	0.0002*
		Satterthwaite	Unequal	19.2	3.71	0.0015*
Clay vs Mud	Fe	Pooled	Equal	107	0.59	0.5547ns
		Satterthwaite	Unequal	4.62	0.72	0.5048ns

* significant differences between population means.

ns - not significant, means between two populations are the same.

Hypothesis

H_o: $\mu 1 = \mu 2$ (means of the two groups are equal)

H_a: $\mu 1$ ne $\mu 2$ (means of the two groups are not equal)

Table 7. Testing for Fe differences between lithology groups.

TESTING FOR DIFFERENCES IN LITHOLOGY

	Variable	Method	Variances	DF	t Value	Pr >|t|
Lithology						
SS vs Cong	As	Pooled	Equal	276	7.36	<.0001*
		Satterthwaite	Unequal	31.7	4.25	0.0002*
SS vs Mud/SS	As	Pooled	Equal	252	5.9	<.0001*
		Satterthwaite	Unequal	6.08	2.98	0.0243*
SS vs Silt	As	Pooled	Equal	279	10.39	<.0001*
		Satterthwaite	Unequal	37.2	7.7	<.0001*
SS vs Mud/Silt	As	Pooled	Equal	261	9.4	<.0001*
		Satterthwaite	Unequal	16	6.97	<.0001*
SS vs Mud	As	Pooled	Equal	349	22.3	<.0001*
		Satterthwaite	Unequal	159	20.26	<.0001*
Mud/Silt vs Silt	As	Pooled	Equal	48	1.02	0.3106ns
		Satterthwaite	Unequal	31.2	1.05	0.3028ns
Mud vs Mud/Silt	As	Pooled	Equal	118	0.98	0.3284ns
		Satterthwaite	Unequal	18.9	0.91	0.3750ns
Clay vs Mud	As	Pooled	Equal	107	3.09	0.0025*
		Satterthwaite	Unequal	4.45	3.29	0.0258*

* significant differences between population means.

ns - not significant, means between two populations are the same.

Hypothesis
H_o: $\mu1 = \mu2$ (means of the two groups are equal)

H_a: $\mu1$ ne $\mu2$ (means of the two groups are not equal)

Table 8. Testing for As differences between lithology groups.

error/procedures and/or incorrect grouping of the rocks into lithology classes. The USGS grouping of samples into lithology classes was performed on the basis of visual appearance and not actual grain size measurement. We also know that some iron (and perhaps arsenic) has been chemically remobilized after deposition (chemically transported post-depositionally). For instance, iron precipitated as a concretion would yield a spot chemical analysis that would be elevated in iron relative to the background geochemistry of the host rocks.

For the purpose of this exercise, and assuming normal distributions for each of the lithology classes, we eliminated samples from the data set that were greater than and less than two standard deviations about the mean. Assuming normal distributions, this would conserve 95% of the data in each lithology population. We eliminated the outliers from the data sets because data on the tails of distributions can unduly influence statistical relationships. As a result of this treatment, 98 outliers from a population of 549 samples were eliminated from the data set (Table 9). This number of outliers, about 18% of the total population, is greater than expected and suggests that the iron and arsenic populations within some or each of the lithologies are not single homogeneous populations. A total of twenty-seven outliers would have been expected to occur if each of the populations were perfectly normally distributed. A scatter plot (Fig. 25) of iron versus arsenic has been constructed to illustrate the differences between the outliers and the remaining samples (all lithologies grouped into one population). This plot suggests that the outliers are slightly enriched in arsenic relative to the remaining population. The sandstone population in particular appears to contain a large number of significant outliers. We suggest that some of the iron (and perhaps arsenic) has been secondarily

Lithology	# Outliers	Percentage
Cong	11	11
SS	73	74
Silt	3	3
Mud/SS	3	3
Mud/Silt	2	2
Mud	5	5
Clay	1	1
Total	98	100

Table 9A. Number and percentage of samples removed from each lithology group.
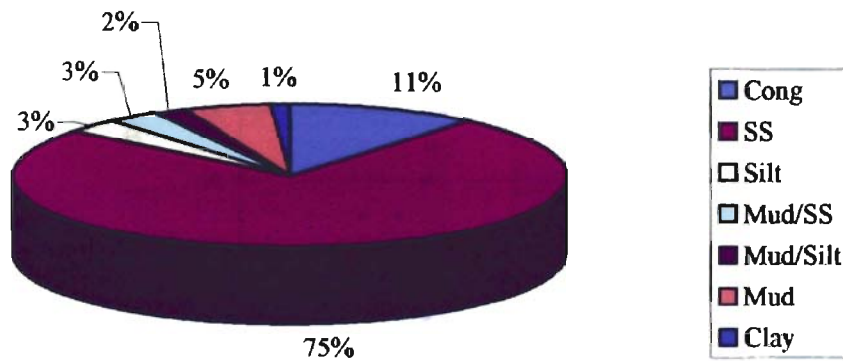
Table 9B. Pie-diagram illustrating percentage of outliers removed from each lithology.
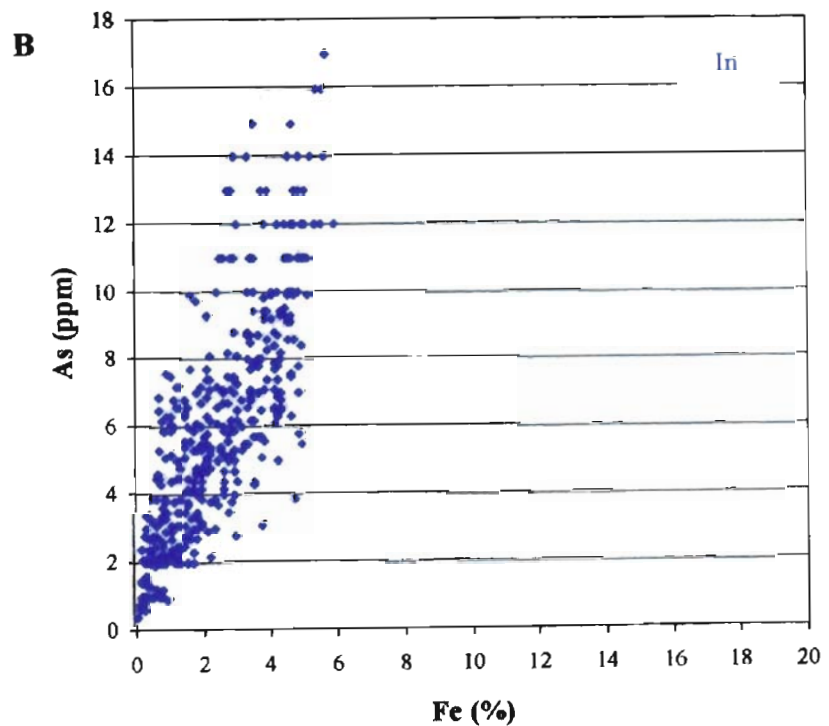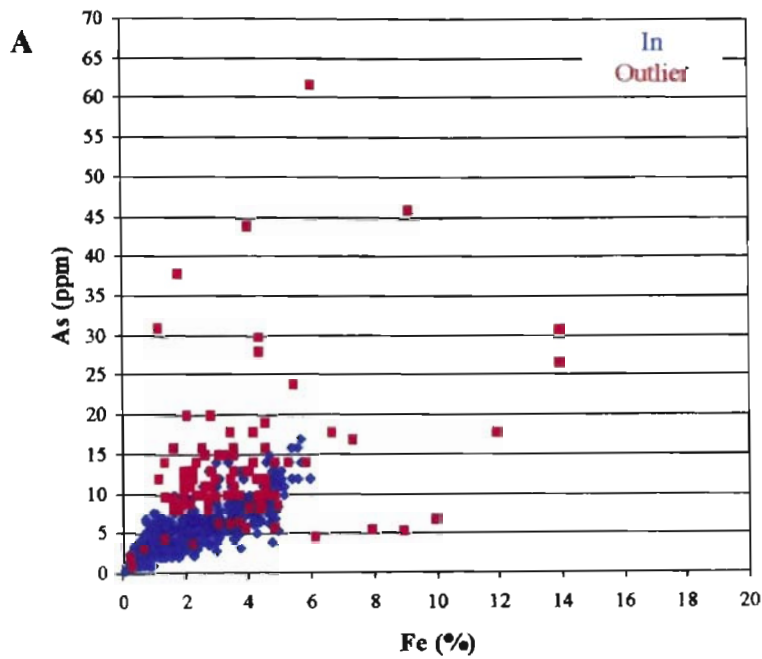
Figure 25. (A)-Fe versus As scatter plot illustrating the differences between outliers and the remaining population. (B)- Fe versus As scatter plot illustrating only the remaining population.

mobilized as indicated by the bimodal distribution. The conglomerate population also contains some outliers. This likely results because the conglomerates are extremely heterogeneous in terms of lithoclast types. The conglomerates are also difficult to sample for chemical analysis because of the range in particle sizes, matrix, and cements.

(4) Establish the strength of association between calculated gamma-ray response (API units) and the measured iron content of the rocks: The linear relationship between iron (Fe) versus gamma-ray (API) is shown in Figure 26. The r-value for this association is 0.78. This r-value translates to an r-square value of 0.62, which implies that 62% of the variation in iron can be attributed to the regression of iron content on gamma ray. Though statistically significant, this finding suggests that 38% of the variation in iron content in the rocks is independent of gamma-ray.

(5) Quantitatively establish the strength of association between the estimated iron content from above (step 4) and arsenic: The linear relationship between iron (Fe) versus arsenic (As) is shown in Figure 27. The r-value for this association is 0.80. This r-value translates to an r-square value of 0.64, which implies that 64% of the variation in arsenic can be attributed to the regression of arsenic content on iron. Though statistically significant, this finding suggests that 36% of the variation in arsenic content in the rocks is independent of iron.

(6) Use above relationship to identify combination of arsenic prone lithofacies beneath City of Norman on the basis of gamma ray logs: The calculated equation for iron (Fe) versus gamma ray (API) shown graphical in Figure 26 is:

(a) estimate iron content from gamma ray via

$$Fe = 0.04(API) \hspace{3cm} Eq. \#5$$

Geochemistry of NOTS
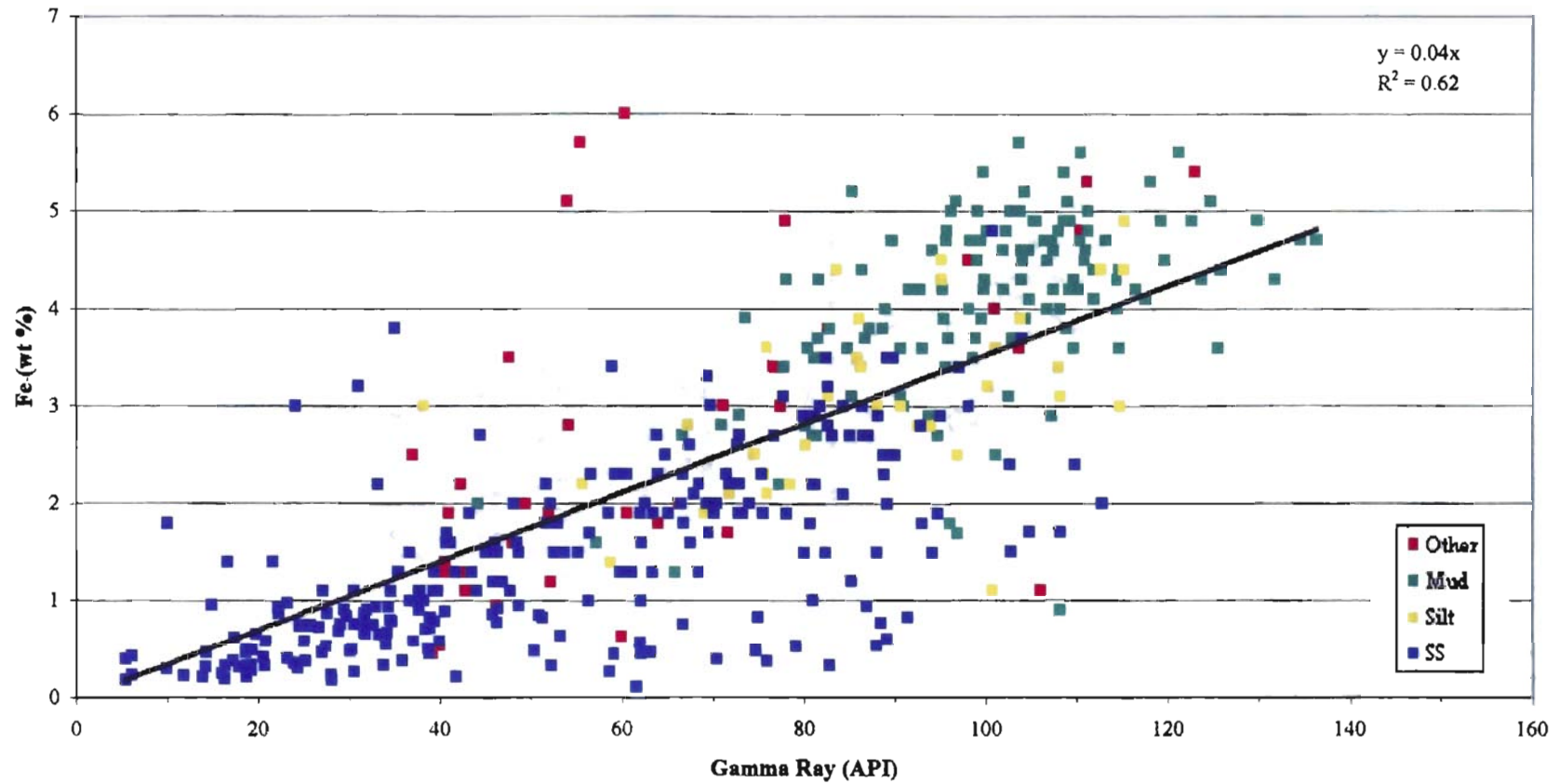
Figure 26. The iron (Fe) and gamma-ray (API) graphical representation (scatter plot).
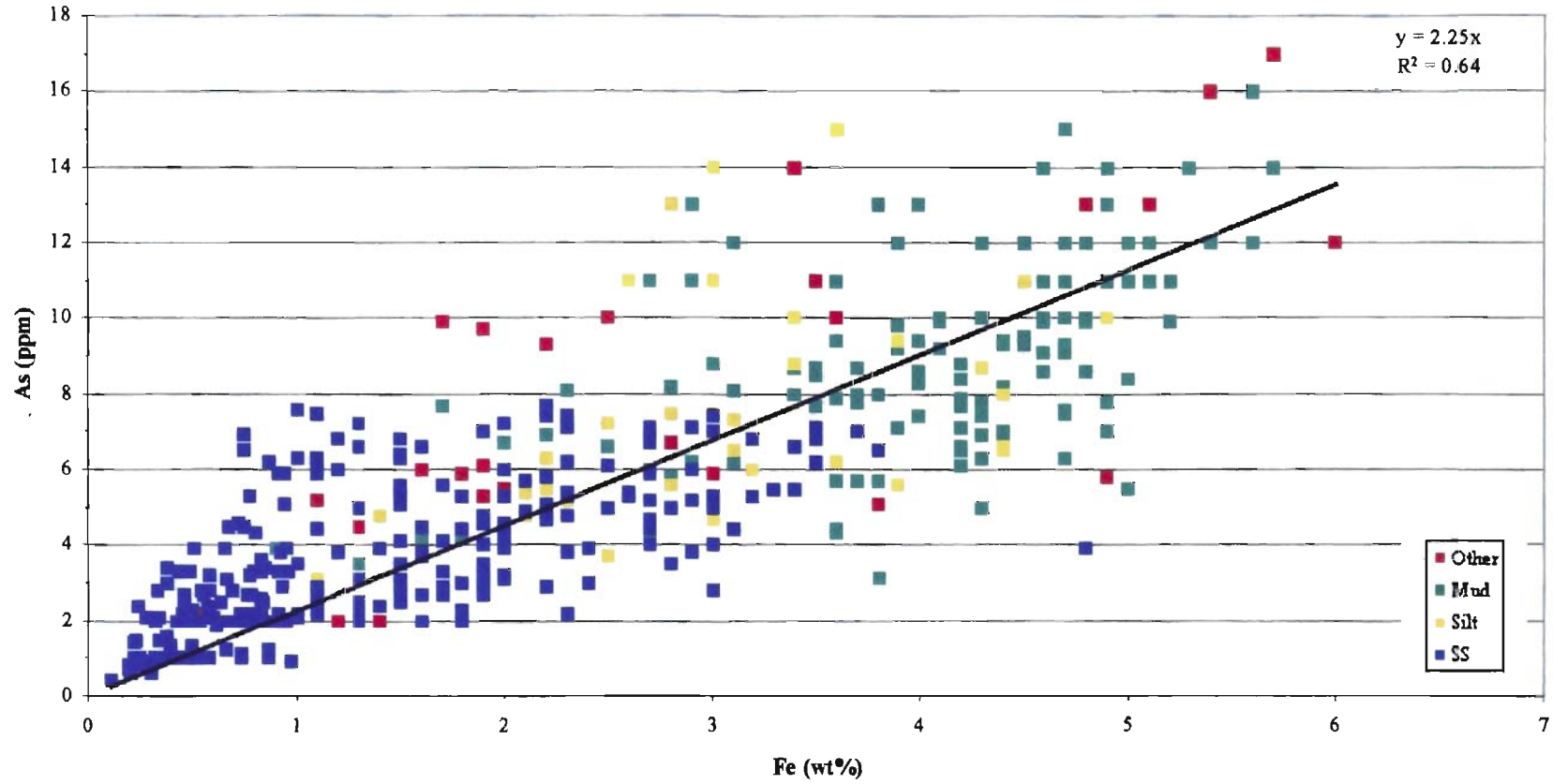
Figure 27. The iron (Fe) and arsenic (As) graphical representation (scatter plot).

The calculated equation for iron (Fe) versus arsenic (As) shown graphical in Figure 27 is:

(b) estimate the As content through association with Fe via

$$As = 2.25(Fe)$$ Eq.#6

Based on this work, Abbott (2004) can calculate potential arsenic concentrations in the subsurface relative to isopleth and lithofacies beneath Norman area. In turn, the mapped distribution of arsenic could be used by the city to select new drill-well locations. Additionally, certain lithofacies within the well could be selectively produced so that the water originating in arsenic-prone lithofacies (such as mudstone) does not enter the well bore and mix with water from the lower arsenic lithofacies (sandstone).

Gamma-Ray Association and Discussion

The gamma-ray relationship with sediment grain size and sorting as illustrated in outcrop classification and characterization Part A (vertical profiles) of the thesis and further illustrated by Figure 28 and 29 most likely reflects (1) the physical association of fine-grained hematite (and the accompanying arsenic) with clay mineral surfaces through adsorption of the iron-oxide complex to the clay mineral surfaces, or (2) presence in the rocks of hematite with associated arsenic that is finely disseminated throughout the groundmass of the finer-grained rocks, independent of the clay minerals. Regardless of the details of the physical relationship of the arsenic to the host rock, the variation of iron and arsenic with sediment grain size implies that the bulk of the iron and arsenic elements are most likely associated with detrital components of the sedimentary rocks and are not chemical precipitates. This conclusion is warranted based on an understanding of the permeability of sandstones and shales. On the basis of first principles, rates of

71

Grain Size Association
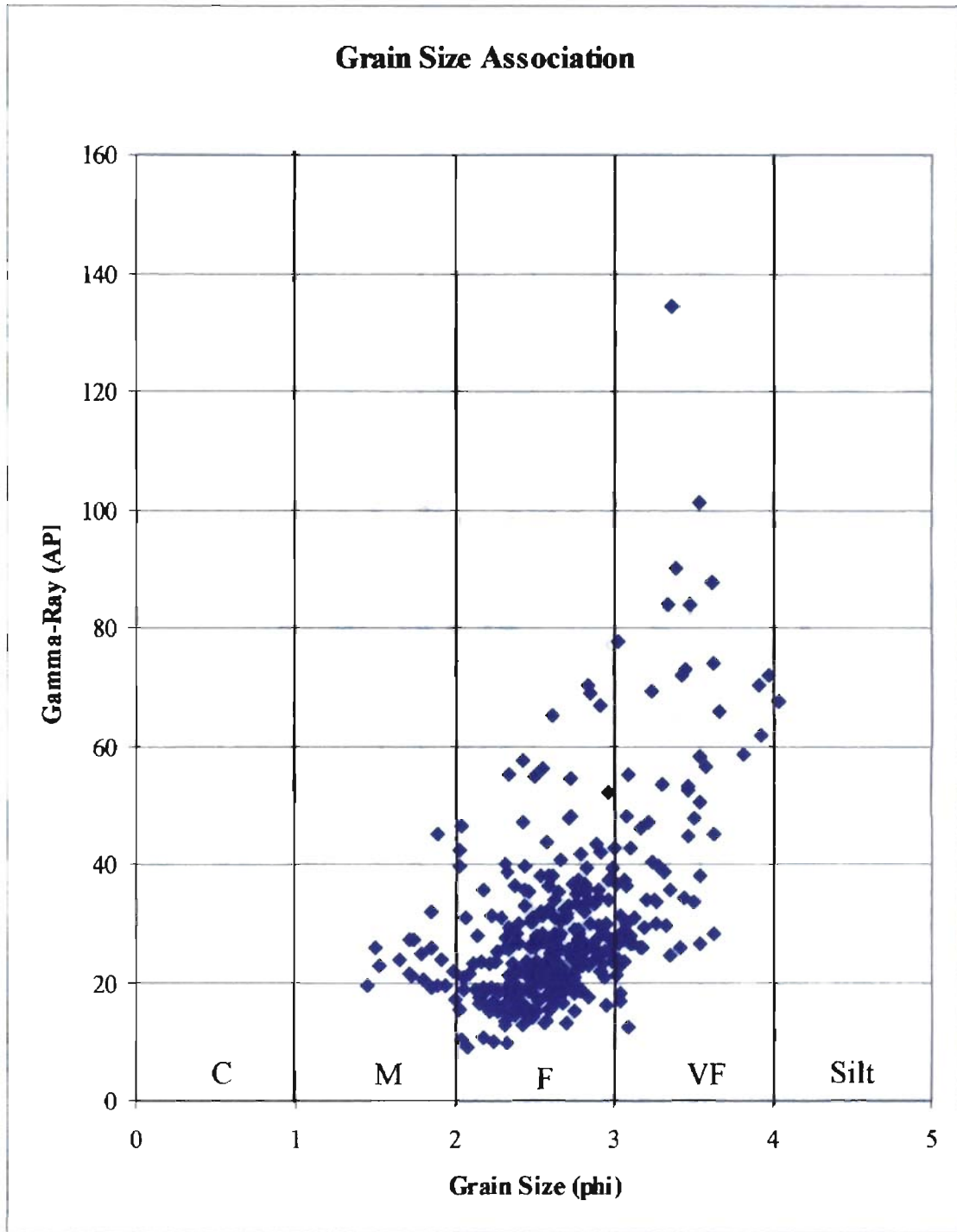
Grain Size Range	C	M	F	VF	Silt
Phi Avg	n/a	1.77	2.56	3.30	4.04
API Avg	n/a	24.32	25.99	44.85	67.60

Figure 28. Gamma-ray (API) relationship with grain size (phi). Gamma-ray progressively increases with the fining of the grain size. *Note*: The large clustering of data points between 2.00 and 3.00 phi represents 75% of our population.
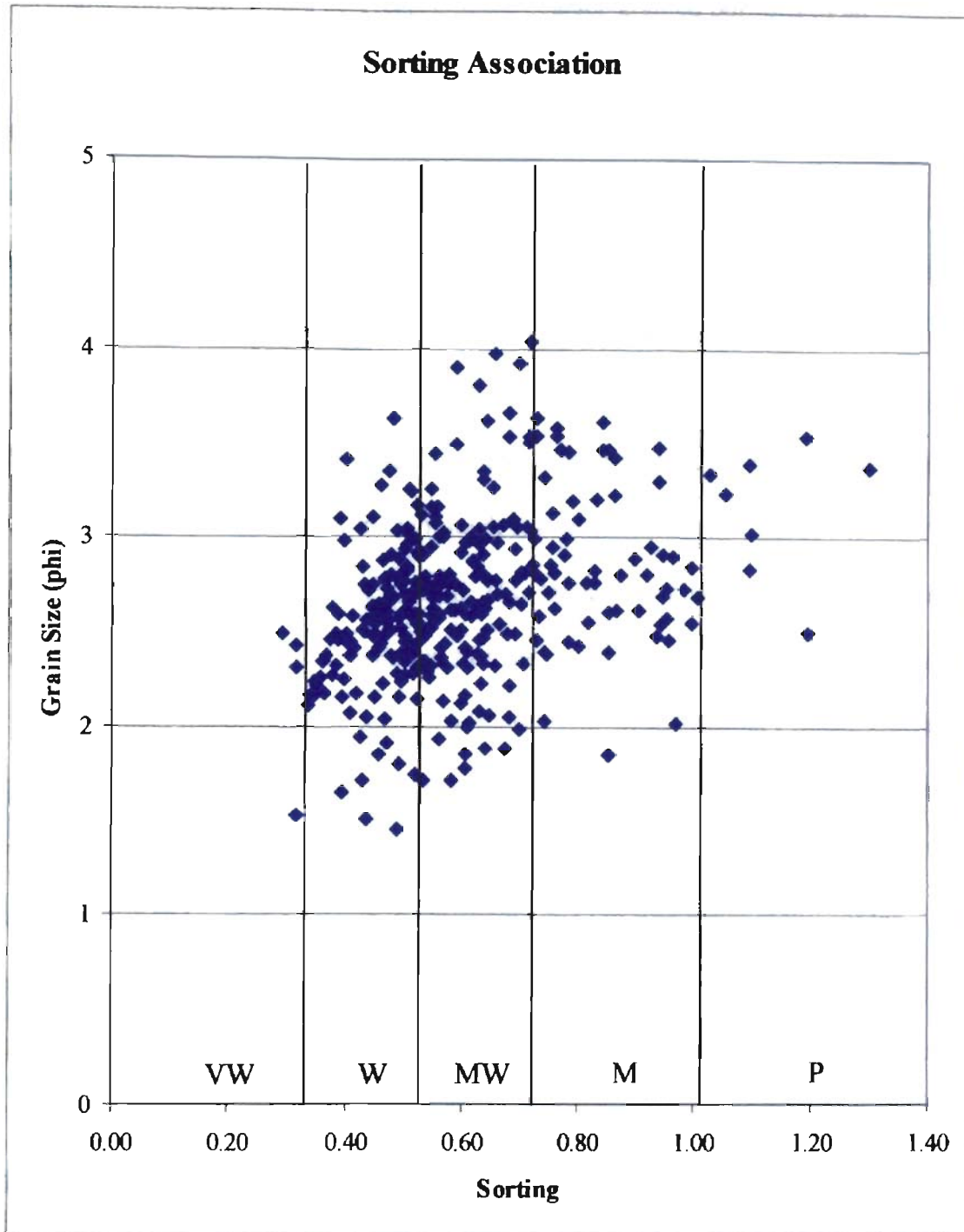
Sorting Range	VW	W	MW	M	P
Phi Avg	2.40	2.50	2.68	2.89	3.08
Sorting	0.31	0.44	0.59	0.81	1.11

Figure 29. Grain size (phi) relationship with sorting. Running water has a tendency to create well-sorted sediments, which have high porosity.

intergranular fluid flow would be greatest in the coarser-grained portions of an interbedded sandstone and shale sequence. This is because the coarser-grained sediments have larger pore throats (spaces between the framework grains) for the transmission of fluid relative to the smaller pore-throats that are present in finer-grained sandstones. Intergranular fluid flow would be even more retarded in the siltstones and shales, where, in addition to small pore throats, surface tension and capillary forces within the pore network would diminish the rate of fluid movement. Should the iron and arsenic be chemical precipitates, one would expect to find a greater volume of these elements in the portions of the section that are coarser grained; less iron and arsenic would occur in the portions of the section that are finer grained. This scenario is just the opposite of what we find in the rocks, supporting the argument that the iron and arsenic are associated with the detrital or primary depositional processes of these Permian sedimentary rocks. During high discharge events, the Permian rivers of the study area must have contained abundant red silt and clay in suspension, similar to the red waters that occur in the modern Cimarron River and Canadian River in Oklahoma and the Red River at the border between Oklahoma and Texas.

Though the bulk of the iron and arsenic appears to be associated with the detrital portions of the sedimentary rocks, some of the iron (and perhaps arsenic) has been secondarily mobilized (chemically mobilized after deposition, burial and/or uplift of the Permian sedimentary rocks). Rare evidence for secondary iron mobilization can be seen in some outcroppings. Some outcrops contain liesegang bands and iron concretions (Newalla Rd). A few outcrops outside of the Norman study area (near Edmond) contain relatively thick crusts of iron up to 2.5 cm in thickness. These crusts are also associated

74

with liesegang banding. In the Norman area, one vertical iron crust occurs along the east side of Newalla Road, Outcrop #7 (Fig. 30). To date, all of these diagenetic features have been found to occur in the sandstones and not in the conglomerates, siltstones or shales. Based on patterns of the liesegang bands within some sandstones, the source of diagenetic iron appears to be internal to the sandstones and/or from the immediately adjacent siltstones and shales. As a rule of thumb, a green rind of chemical iron reduction is commonly observed immediately below the contact between red channelized sandstone beds and the underlying siltstone/mudstone. The green rind occurs in the siltstone/mudstone and not in the sandstone. The green rind, which indicates that some iron has been chemically reduced, is evidence for the availability of mobile iron (reduced iron in the 2^+ state which is soluble versus iron in the 3^+ oxidized state, which is insoluble except at very low pH).

Iron/hematite precipitation

Newalla; Outcrop #7

Figure 30. Rare evidence for secondary mobilization.

XRD and Electron Microprobe Analysis (EMA)

The intent of performing this analysis was to document the mineralogical and chemical composition of the rocks and to better document the habitat of the arsenic. To more precisely determine the whole-rock chemistry, a rock sample was sent-out to the ConocoPhillips Laboratory in Bartlesville for XRD analysis. Results indicate that our rock sample is composed mostly of illite, smectite, quartz, K-spar and hematite (Fig. 31).

According to Mosier, (1990) geochemical analysis of solid-phase materials in the Central Oklahoma Aquifer indicates that the NOTS Core 7A-36 at a depth of 350.6-350.7 ft is a mudstone that contains an elevated arsenic concentration 62 ppm. A sample from this interval was selected in order to evaluate the habitat of the arsenic in this sample and establish arsenic mineralogical associations.

Two different regions within the mudstone (Fig. 32) were selected for analysis based on the variation in grain size within the sample. A back-scattered image (BSI) was taken of each region and the mineralogy was selectively identified with a petrographic microscope prior to analysis. Some common minerals identified were: quartz, muscovite, dolomite, FeAl-silicates (clay group) and zircon. Once the samples were carbon coated, an energy-dispersive spectrometer (EDS) was used to map the concentration of the eight most commonly forming rock elements: Aluminum (Al), Calcium (Ca), Iron (Fe), Potassium (K), Magnesium (Mg), Manganese (Mn), Sodium (Na) and Silica (Si). These element maps are shown in Fig. 33 and 34.

Quartz (Si) are clay matrix (Al) abundant in the mudstone. These clays form the groundmass of the sample. The sample also contains fragments of quartz, silt, calcite and

-
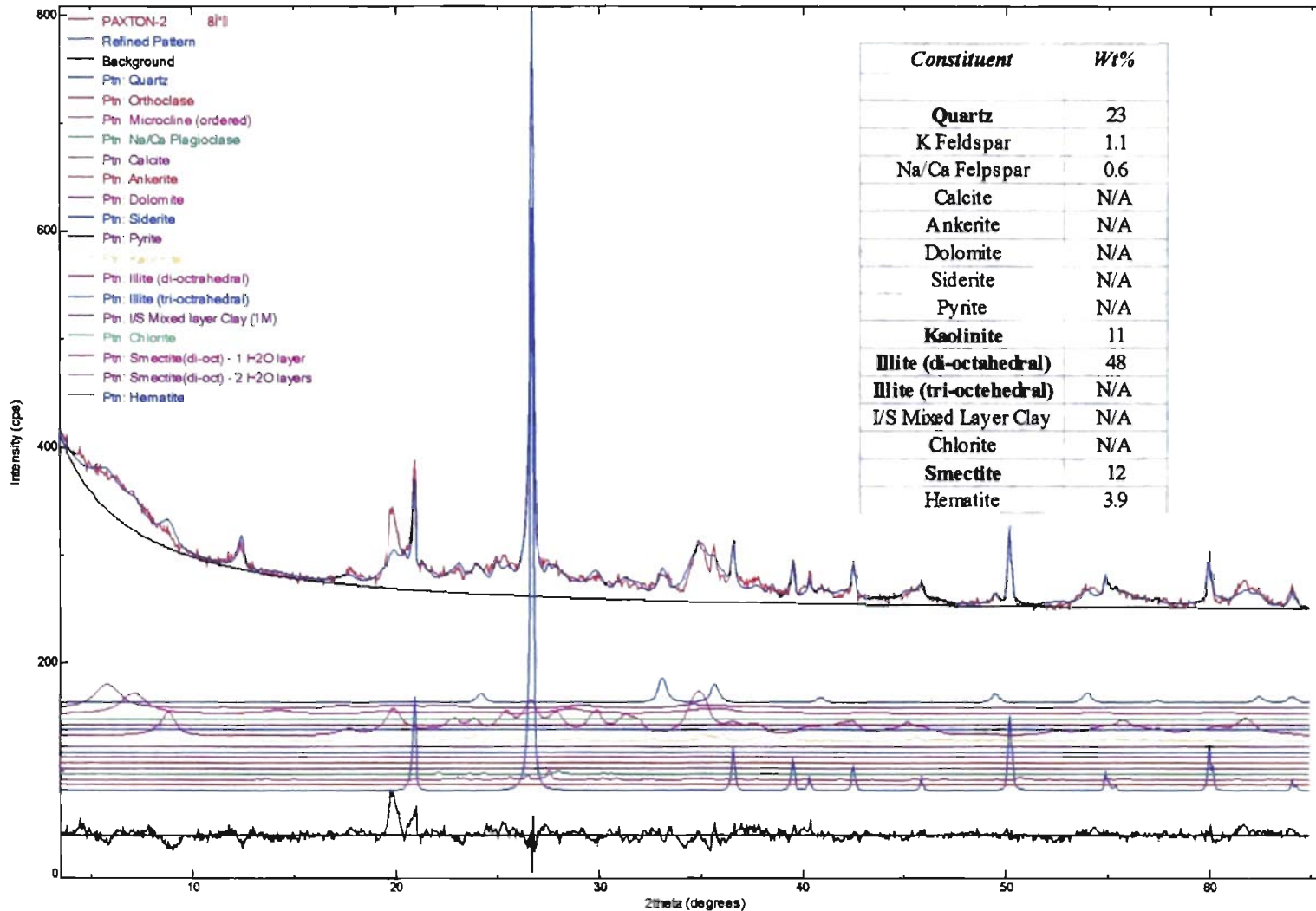
Figure 31. XRD results for a Permian mudstone sample from adjacent to I-35, near Edmond, OK. The mudstone is composed of the clays kaolinite, illite and smectite.

Constituent	Wt%
Quartz	23
K Feldspar	1.1
Na/Ca Felpspar	0.6
Calcite	N/A
Ankerite	N/A
Dolomite	N/A
Siderite	N/A
Pyrite	N/A
Kaolinite	11
Illite (di-octahedral)	48
Illite (tri-octehedral)	N/A
I/S Mixed Layer Clay	N/A
Chlorite	N/A
Smectite	12
Hematite	3.9
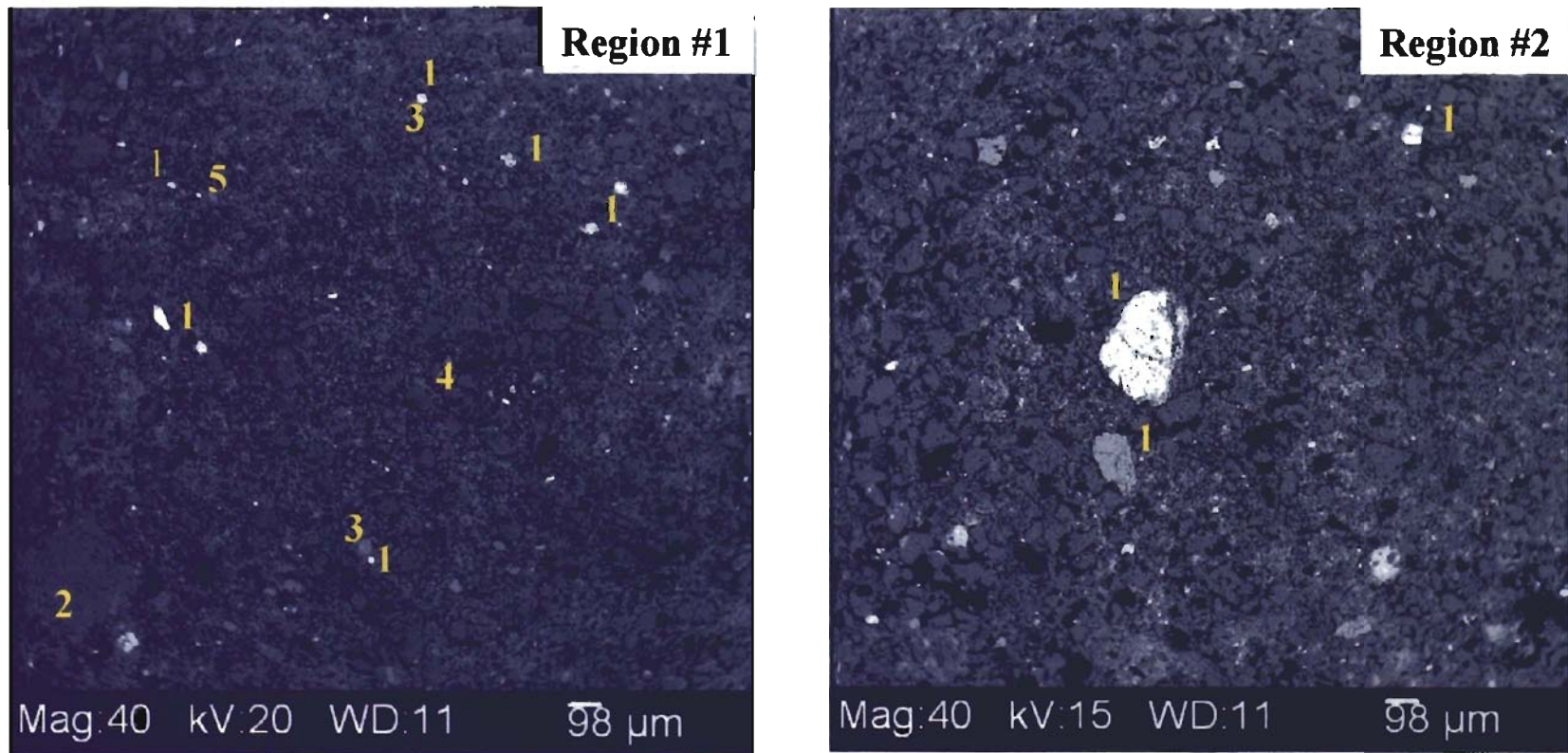
Figure 32. Regions selected for the electron microprobe analysis. The mineralogical constituents are (1) FeAl-silicate (clay), (2) dolomite, (3) muscovite, (4) quartz and (5) zircon.
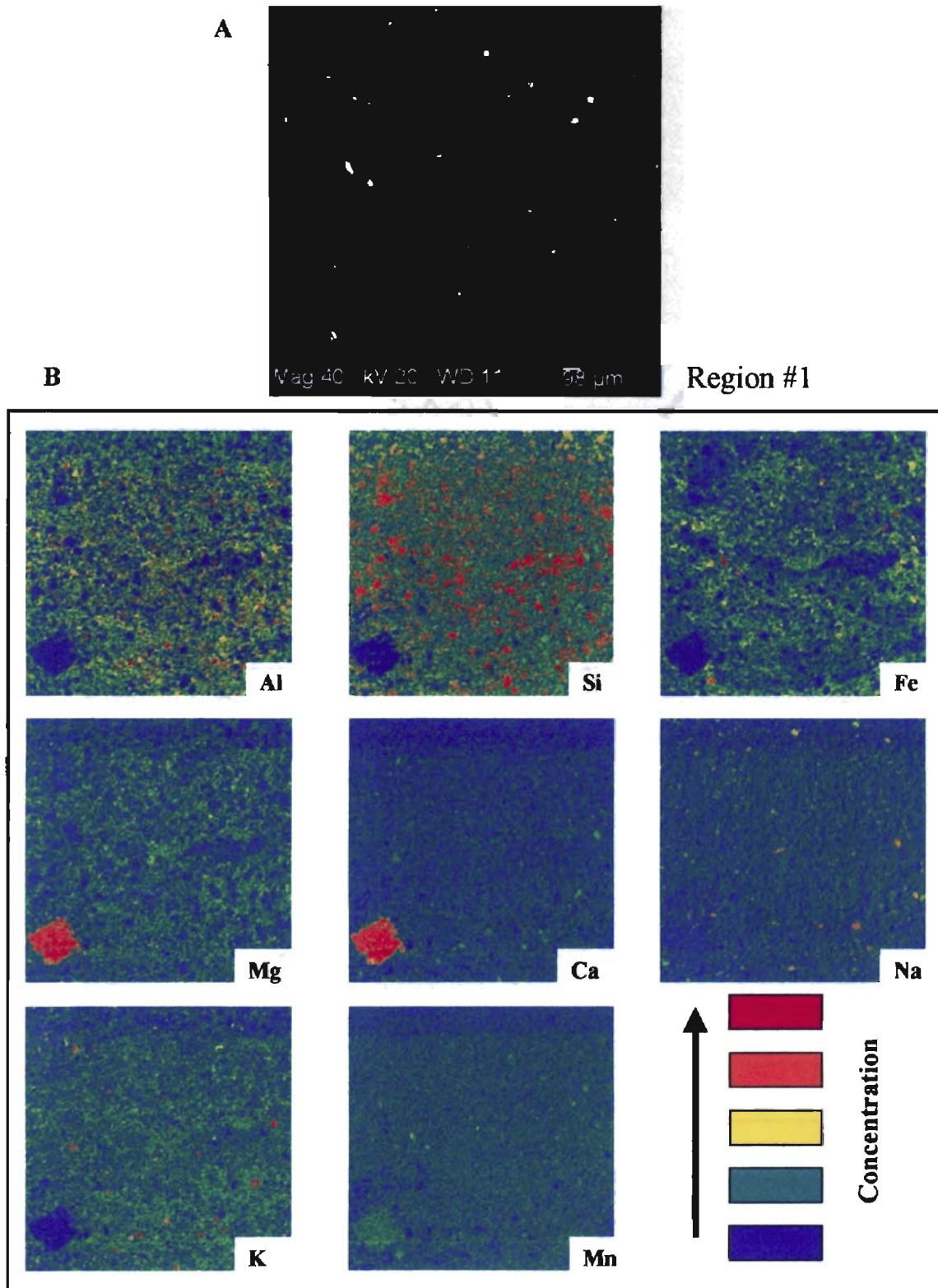
Figure 33. (A) Electron microprobe image of Region #1 and (B) element map showing the concentration of the eight most commonly forming rock elements in Region #1.
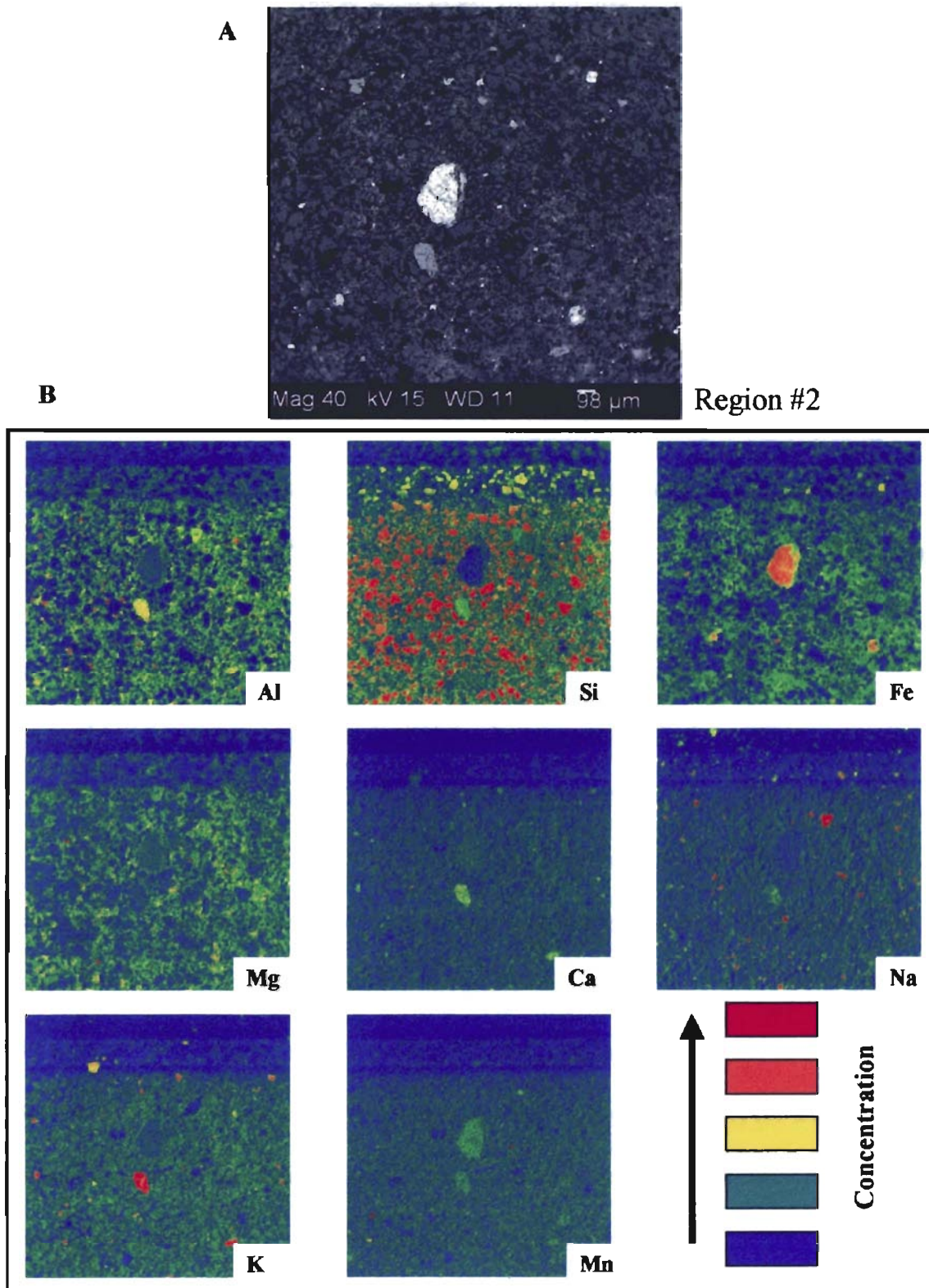
Figure 34. (A) Electron microprobe image of Region #2 and (B) element map showing the concentration of the eight most commonly forming rock elements in Region #2.

dolomite. Notice how each quartz grain in the element map (Fig. 35) is surrounded (coated) by elevated concentration of aluminum, which occurs mostly in the clays. (*Note*: There is some Al in the feldspar).

Iron (Fe) and Magnesium (Mg) are found to co-exist together in the mudstone. A 3-D element concentration map of Fe-Mg is shown in Figure 36.

Another elemental association established by microprobe work is the one between calcium (Ca) and sodium (Na). Previous work by Parkhurst, Christenson, and Breit (1996) indicated that elevated arsenic concentrations depend on several complex geologic and geochemical conditions, including dissolution of dolomite and exchange of the resulting dissolved Ca and Mg cations for Na cations on mixed-layer illite-smectite clays. This association is of significance because clay minerals, which are abundant in mudstone, control cation exchange in the aquifer. These changes and the presence of dissolved oxygen causes arsenic to be oxidized to more soluble forms (inorganic arsenate; As^{5+}). A 3-D element concentration map of Ca-Na is presented in Figure 37.

One of the drawbacks of EDS is that it has poor spectral resolution and is of limited value for quantitative analysis, especially for trace elements. Each peak on the spectrum represents a transition with a characteristic energy. Unfortunately the arsenic (105.010 nA°) and magnesium (107.360 nA°) peak overlapped. In order to resolve this problem, we turned to the wavelength-dispersive spectrometer (WDS) for a quantitative compositional analysis to differentiate between the two energy peaks. We conducted a transect (200 μm) across the sample using an accelerated voltage set at 20 nA (Fig. 38). No measurable amounts of arsenic were detected, which indicates that the amount must
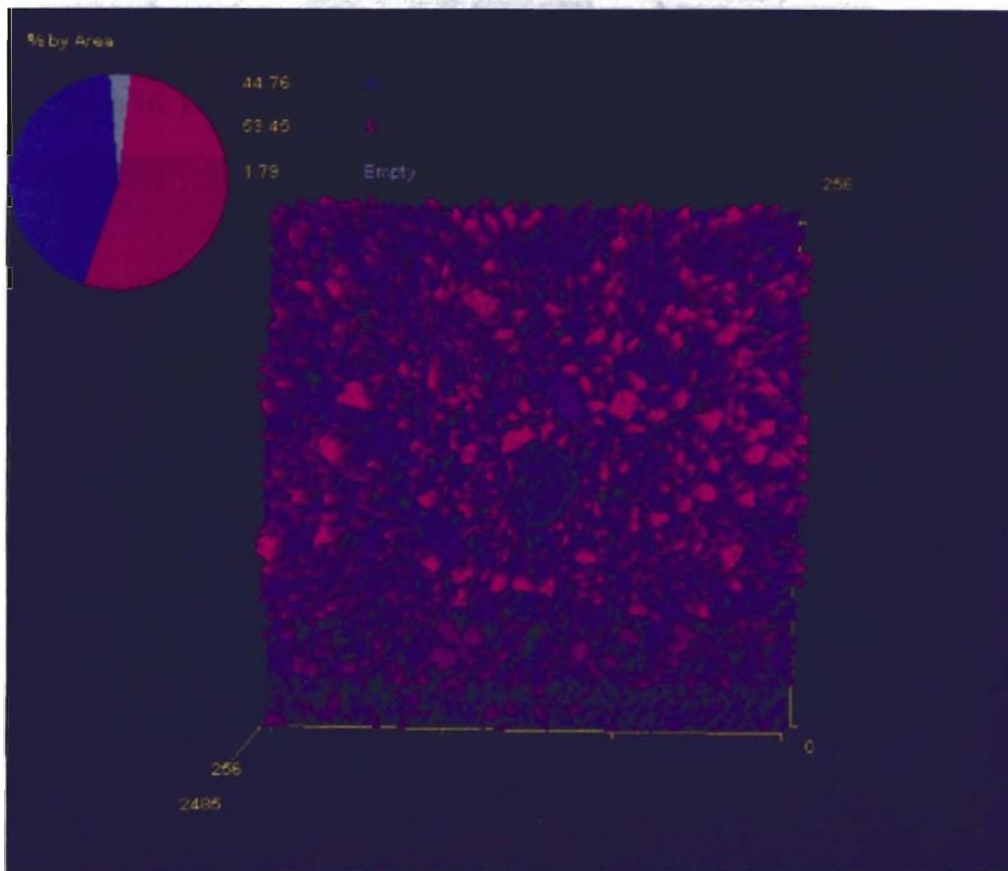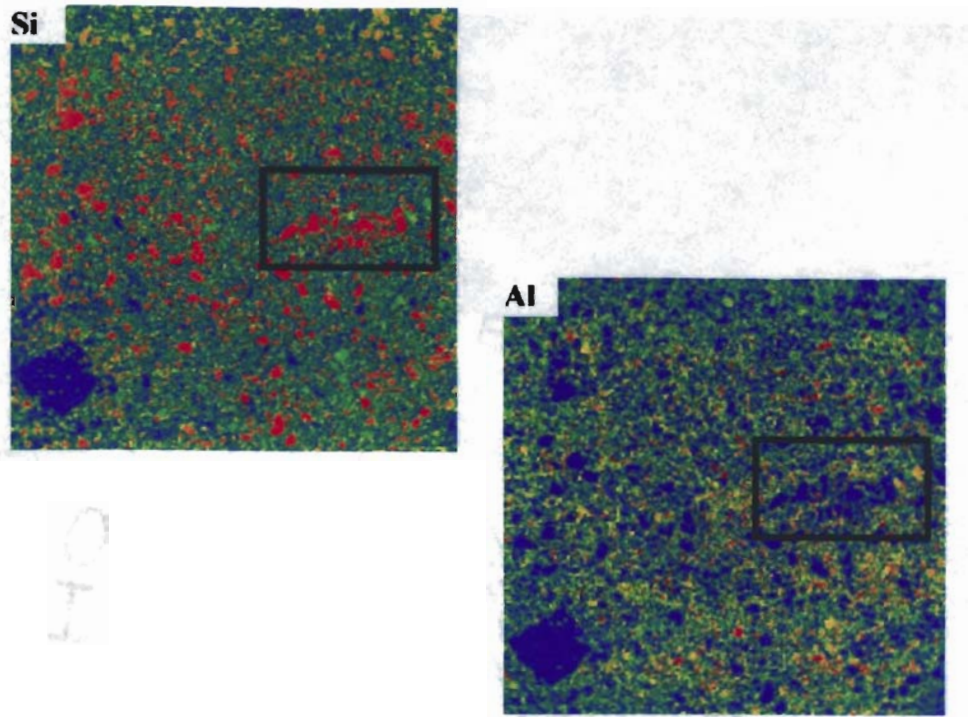
Figure 35. The major detrital constituents of this Permian mudstone are quartz and clay. Quartz grains are surrounded/coated by elevated concentrations of aluminum (clay).
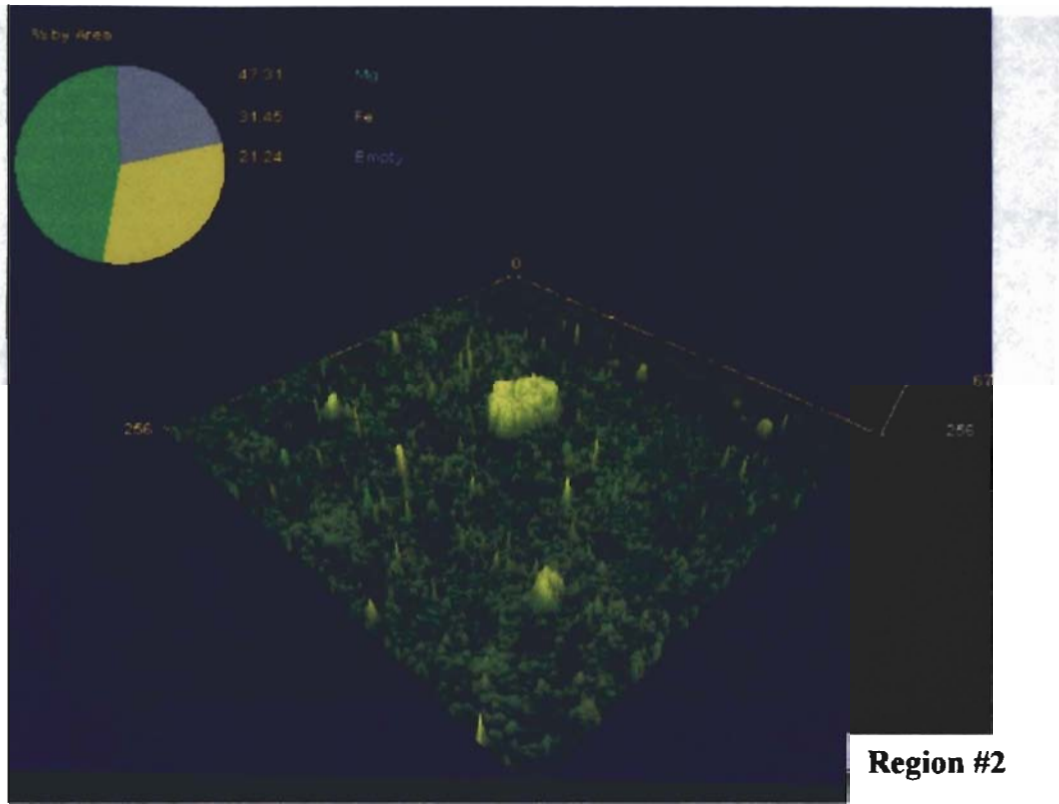
Figure 36. Element map of Fe and Mg co-existing together in the mudstone.
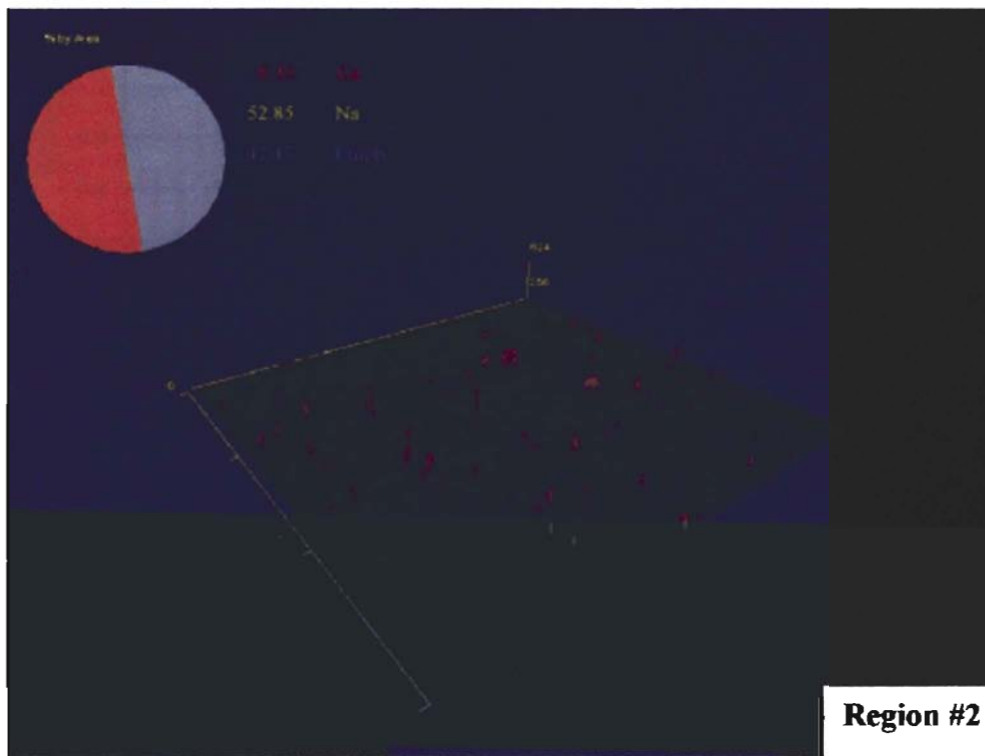
Figure 37. Element map of Ca and Na. Clay minerals, which are abundant in Na control cation exchange in the aquifer.
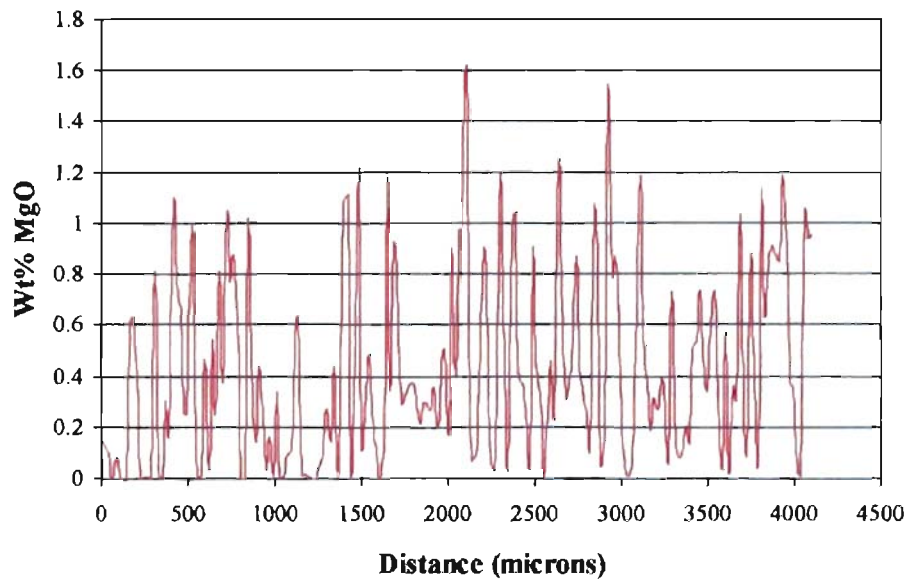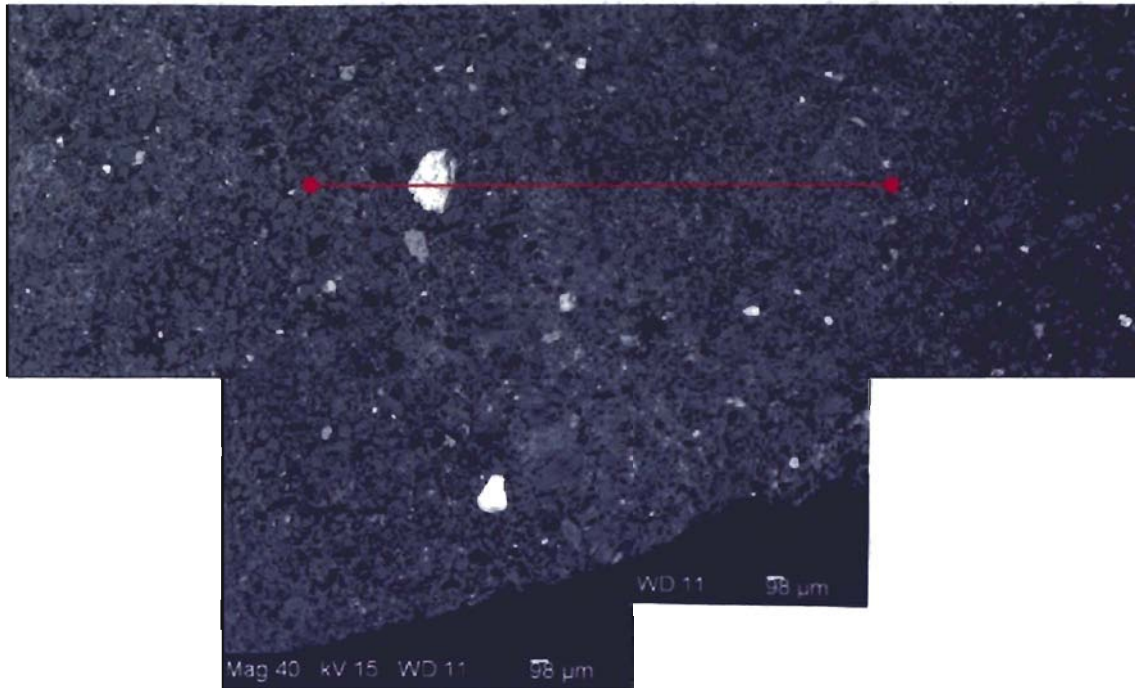
Figure 38. Transect (200 μm) across using the wavelength-dispersive spectrometer for a quantitative compositional analysis.

be below the detectable limit of the instrument. Quantitative results from this analysis can be found in Appendix C.

During the course of our study, the City of Norman re-opened one of its contaminated water wells for water sampling by the EPA/USGS. The scale (Fe precipitated crust) bailed from the well was brought back to the lab for analysis. Thin-section images indicate isopachous bands of iron precipitation occurred in the well bore. We conducted a quantitative compositional transect (100 μm) across the sample with an accelerated voltage set at 15 nA (Fig. 39) using the wavelength-dispersive spectrometer (WDS). Again, results from this analysis found no measurable amounts of arsenic, which indicates that the amount may be below our detectable limit. Quantitative results from this analysis can be found in Appendix D.

Impact of Microorganisms

Studies conducted by USGS Water Resources have shown that microorganisms can affect the redox chemistry of arsenic compounds. Under reducing conditions, which are usually encountered in ground water, microorganisms can catalyze the reduction of As^{5+} to As^{3+} in energy-generating reactions. Other microorganisms cause the release of absorbed arsenic through reduction and dissolution of Fe^{3+} and Mn^{4+}; as in the case of our iron precipitated crust. Most of the absorbed arsenic has been released leaving behind the iron as the solid precipitate. These transformations result in an increase in soluble arsenic and could contribute to contamination of the ground water. The iron oxides on the aquifer surface release arsenic into solution and the dissolved arsenic molecules bond with molecules in the ground water. Information on the magnitude of these microbial
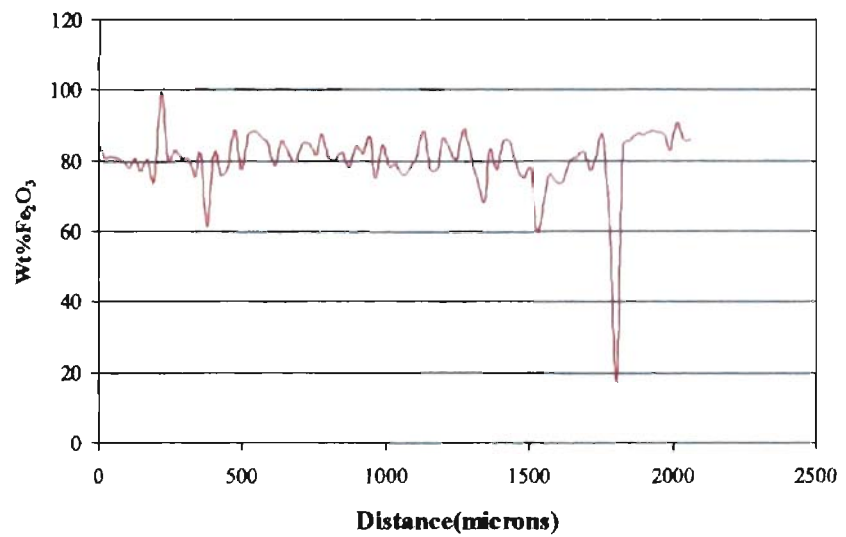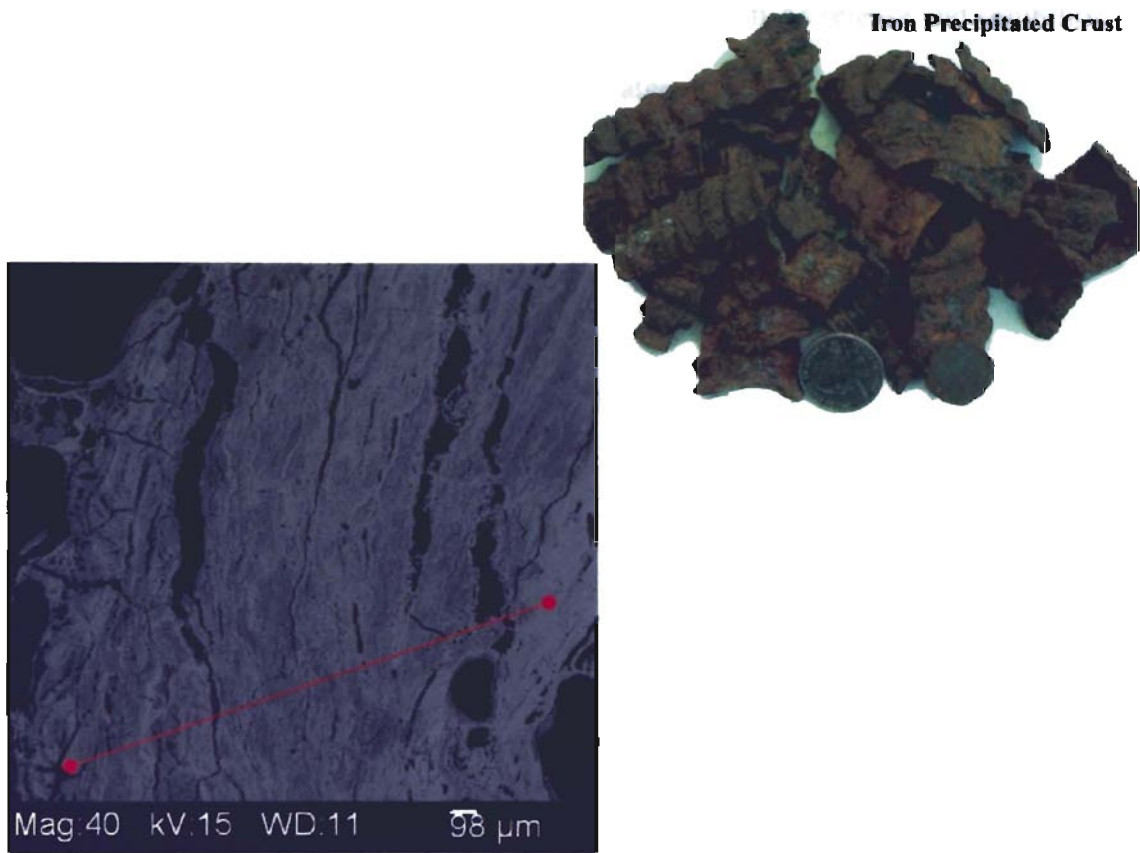
Figure 39. Transect (100 μm) across an iron crust using the wavelength-dispersive spectrometer for a quantitative compositional analysis.

processes in the ground water environment and their roles in As release and solubility is needed to improve As management options for water supplies.

CHAPTER 5

REGIONAL RECONNAISSANCE

Regional Reconnaissance of Lithofacies and Environments

In order to document how the sedimentary geology of other portions of the

Central Oklahoma Aquifer compares to outcrops in the Cleveland County area, our team

conducted reconnaissance surveys of the surrounding counties. Surveying nearby

counties was important in order to establish an inventory of lithofacies and associations

for use in determining the base-line against which to interpret well log response curves.

Interpretation of Garber-Wellington Formation well logs is central to the work of Abbott

(2004). To accomplish this, five additional outcrops were added to the inventory from

Cleveland County in order to have a larger range of lithofacies and vertical profiles. The

additional locations include (1) behind the Panera Bread Company in Edmond, (2) behind

the National Cowboy and Western Heritage Museum in Oklahoma City, (3) between the

assisted living centers on McElroy Road in Stillwater, (4) West Lakeview Road near the

west end of Lake Carl Blackwell and (5) along the north side of US 77 near Skeleton

Creek, north of Guthrie.

The Panera Bread Company outcrop (Fig. 40) was of particular interest to our

team because it contains a series of thin ripple-laminated bed sets encased in mudstones.

Because the ripple-laminated interval is adjacent to a trough-cross bedded sandstone with

an erosional base that also appears to be channelized, we interpret the ripple-laminated

Crevasse-Splays
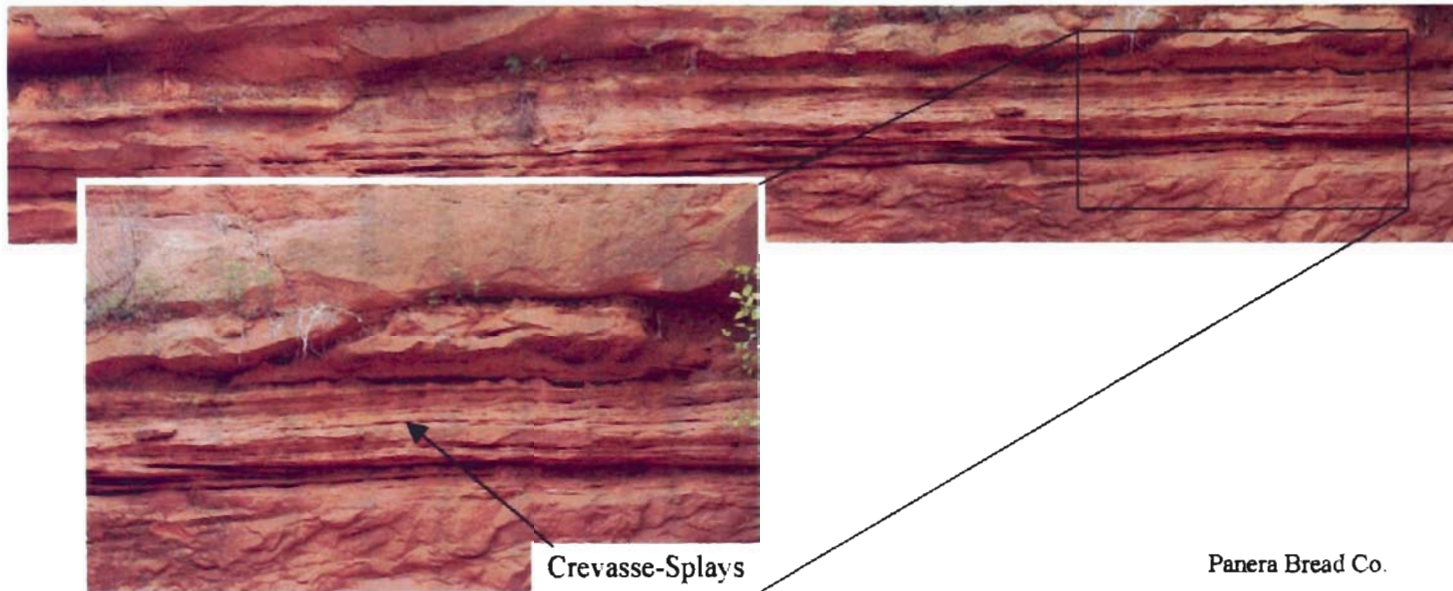
Panera Bread Co.

Figure 40. Panera Bread Co. reconnaissance outcrop indicating a crevasse-splay deposit.

bed sets to be crevasse splays. Crevasse splays form when fluvial discharge exceeds the capacity of a channel. Water flows over the leveed banks and out on to the floodplain where overbank or floodplain deposition can occur. In modern fluvial systems, the level of the bottom of the channel becomes raised by sedimentation in the channel and level of water at bank-full flow becomes higher than the floodplain level. When the levee breaks, water laden with sediment is carried out on to the floodplain to form a crevasse splay Nichols (1999) (see Fig. 41). The breach in the levee does not occur instantaneously but instead the opening develops as a gradually deepening and widening conduit for water to pass out on to the floodplain. Small-scale cross-bedding, climbing ripple laminations and some horizontal bedding are the main sedimentary features (Reineck and Singh, 1973). Muddy sediments generally cap crevasse splays. Ripple cross-laminations and minor planer laminated and massive bedding are typical sedimentary structures noted in crevasse splays.

The National Cowboy and Western Heritage Museum outcrop (Fig. 42) contains horizontally bedded fine sand alternating with laminated mud layers with some indication of roots. A mud-flake conglomerate forms a resistant layer between the lower and upper sequence. Based on these observations, we interpret the horizontally bedded fine sand alternating with laminated mud layers as floodplain (basin) deposits. Floodplain deposits accumulate adjacent to fluvial channels where fine-grained sediments have settled down from suspension in water derived from overbank flows. The coarser sediments associated with the overbank flow are usually deposited on the levees and as crevasse splays. The extent and development of floodplain deposits is mainly controlled by the
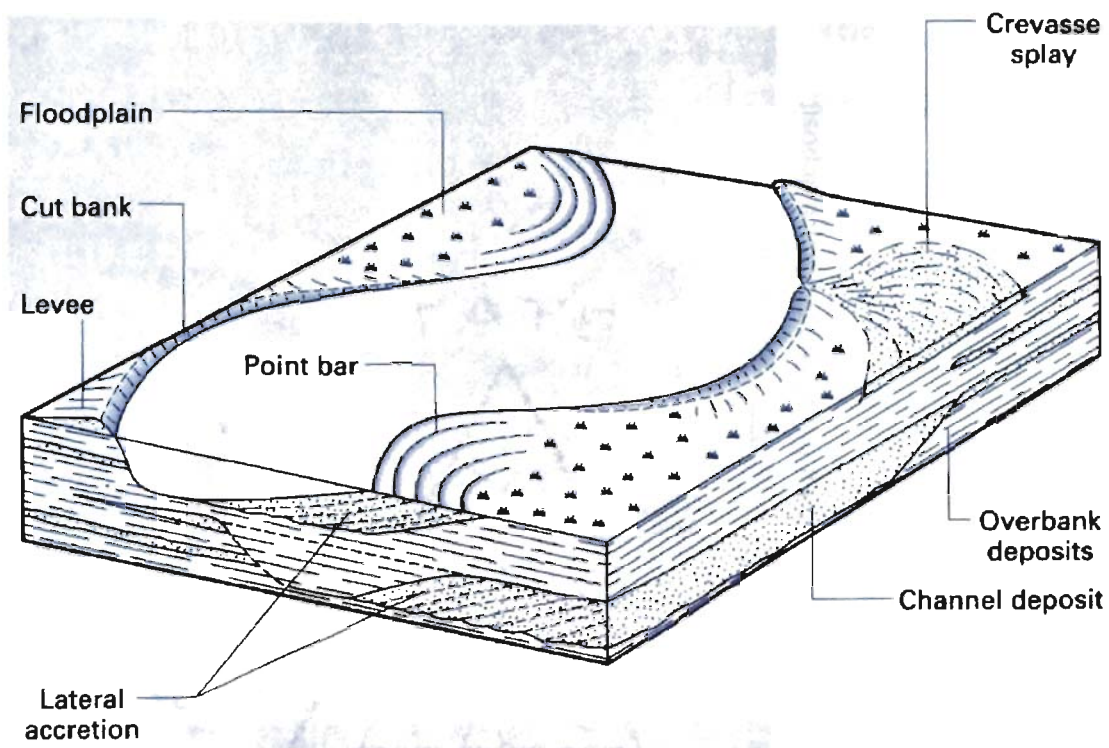
Figure 41. When the levee breaks, water laden with sediment is carried out on to the floodplain to form a crevasse splay deposit (Nichols, 1999).
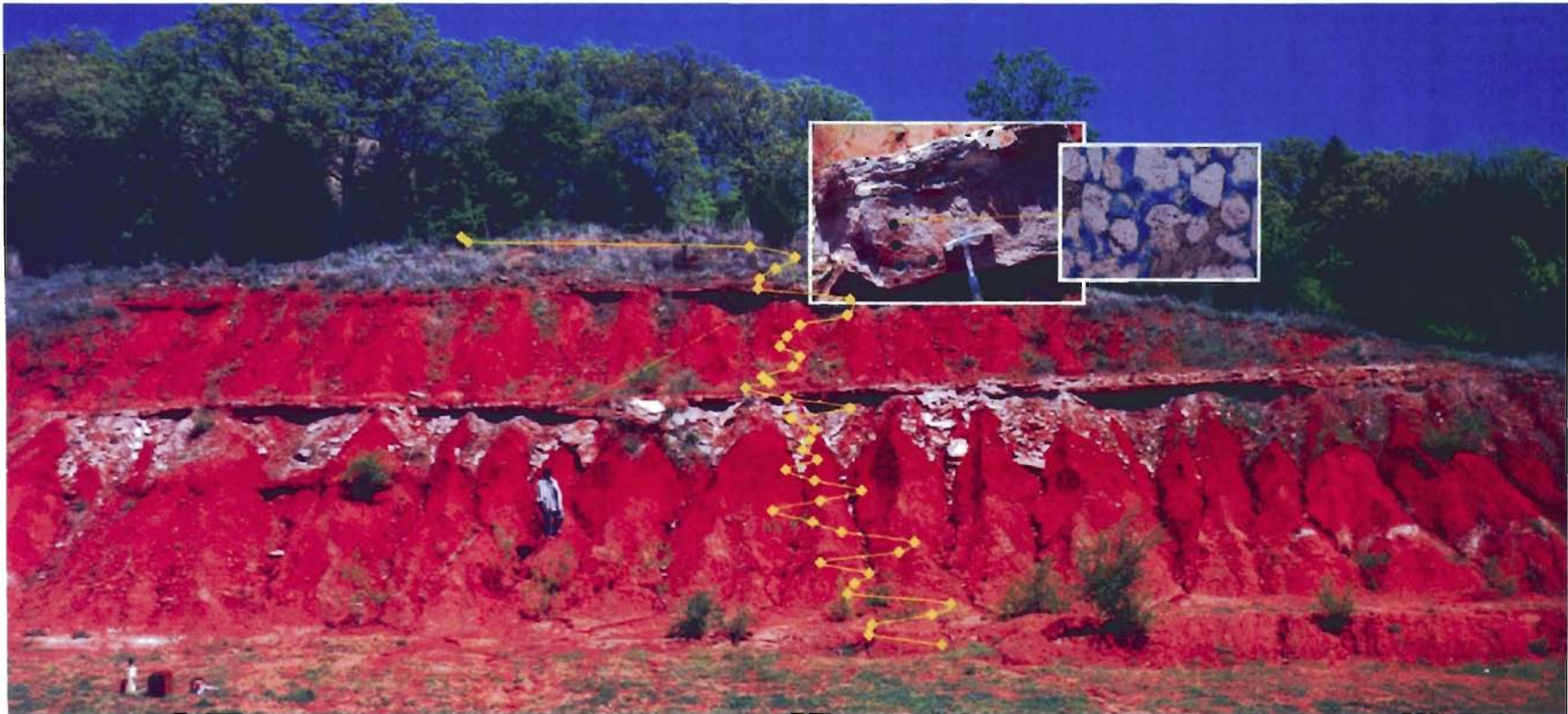
Figure 42. National Cowboy and Western Heritage Museum reconnaissance outcrop indicating a floodplain sequence deposit.

channel form and pattern. Braided streams with rapid rates of lateral migration inhibit the development of thick floodplain deposits like those found to occur in meandering systems. The section of Garber-Wellington Formation exposed at the National Cowboy and Western Heritage Museum may be a series of floodplain deposits. Thick floodplain deposits can be produced if streams become more or less fixed (or entrenched) in their position, so that long periods are available for deposition of fine sediments in the floodplain (Reineck and Singh., 1973).

Another example of a floodplain deposit that contains shallow channelized sandstone is evident on McElroy Road (Fig. 43) in Stillwater. Here the fine-grained floodplain mudstone is overlain by 1.5 m of ripple-laminated fine-grained sandstone, a thin interval of rippled siltstone, and 40 cm of horizontally laminated plane beds with parting lineations visible on the bedding surfaces. A thin (40 cm) laterally accreting sandstone unit that exhibits trough cross-bedding truncates the laminated plane beds.

West Lakeview Road (Fig. 44) was another of our sites; this outcrop contains stacked blocky sandstones with ripple-laminated surfaces. The sandstone is thickest in the center and gradually thins to the west as indicated by more mudstone abundance (channel margin facies). The sandstone body sits on a mudstone unit as if the channelized sandstone shifted on top of a former floodplain deposit. The mudstone contains oxidized traces of organic debris and slickensides caused by the loading of the overlying channelized sandstone deposit.

The sediments of floodplains undergo soil formation (pedogenic processes) and depending upon the climate, different types of soils are developed. Flood plain deposits

94
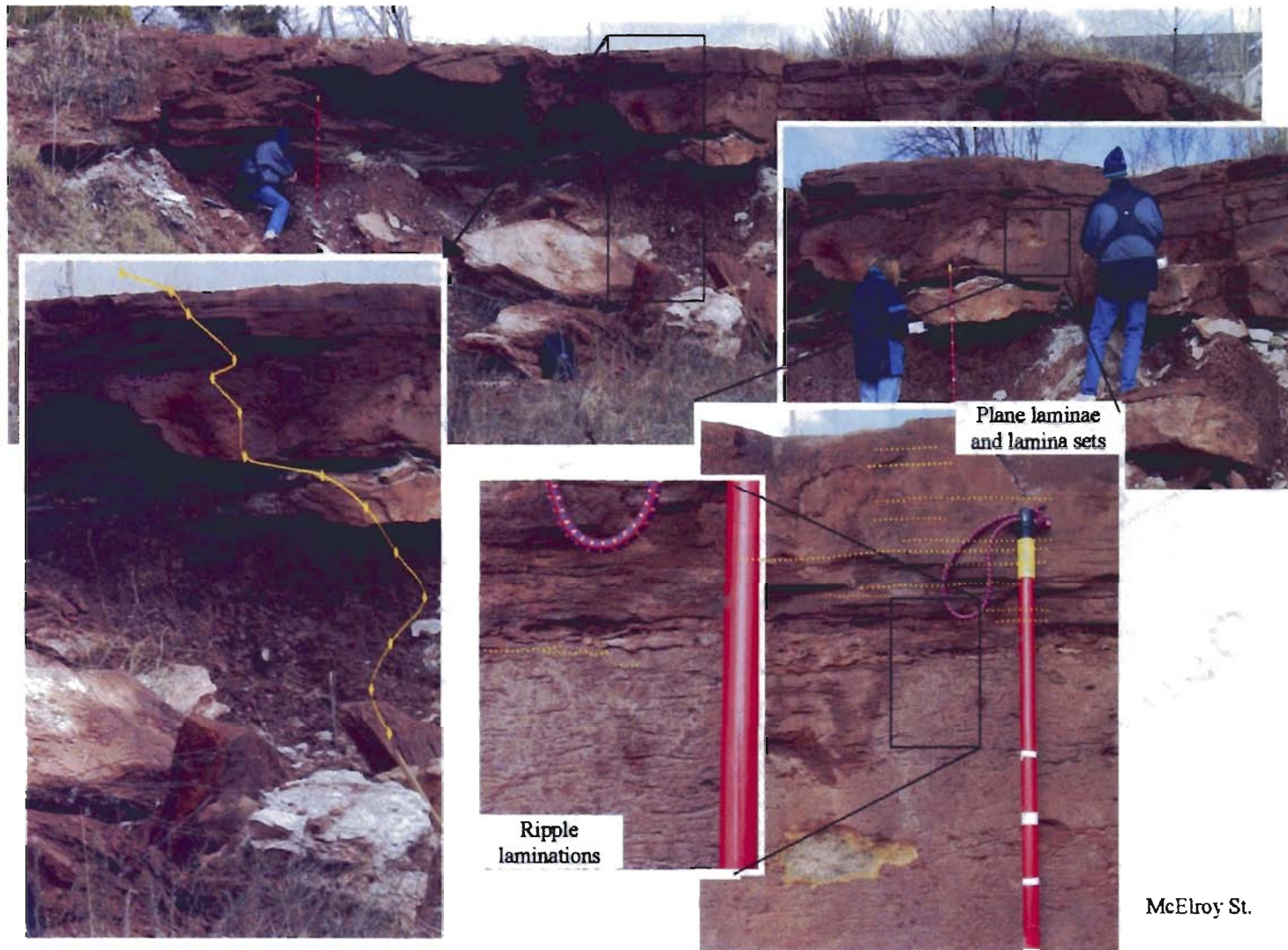
Figure 43. McElroy St reconnaissance outcrop indicating another floodplain deposit that contains some channelized sandstone.
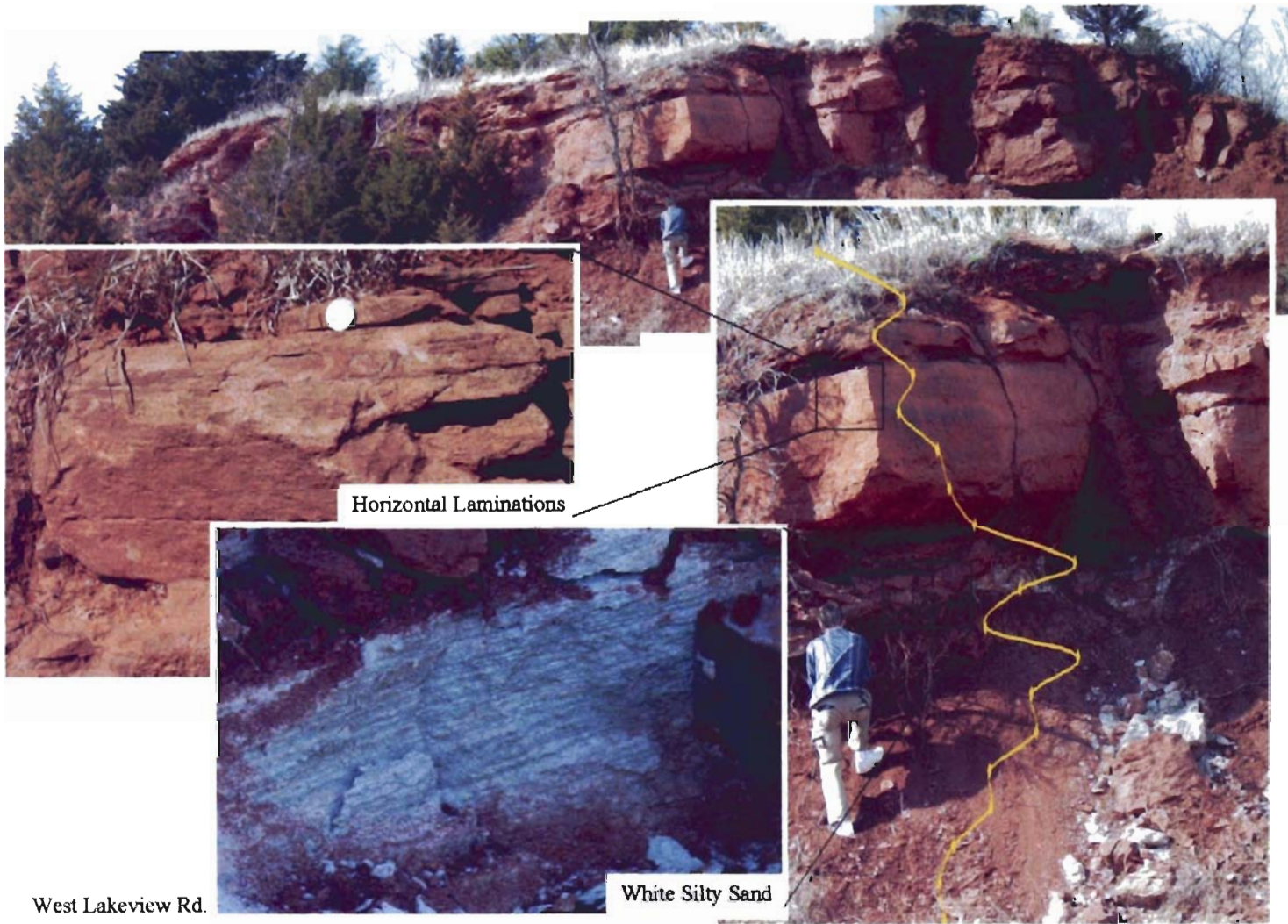
Figure 44. West Lakeview Rd. reconnaissance outcrop showing a channelized sandstone that has shifted on top of a former floodplain.

of semi-arid environments are characterized by negligible organic matter content, reddish coloration because of oxidizing conditions and the presence of calcium carbonate precipitated within the soil profile as calcrete, like the one found at Skeleton Creek (Fig. 45). The evaporation of water at the surface draws groundwater up into the soil profile. As the water evaporates, calcium carbonate dissolved in the groundwater is precipitated in the soil initially as root encrustations. These encrustations develop into small nodules called glaebules (Nichols, 1999). These glaebules grow and coalesce as precipitation continues.

Skeleton Creek (Guthrie)

Thick calcrete horizon

Evaporation at surface

Poorly developed soil profile

Carbonate glaebules

Groundwater drawn through soil

Coalesced glaebules and rhizoliths

Thick calcrete horizon

Well-developed soil profile
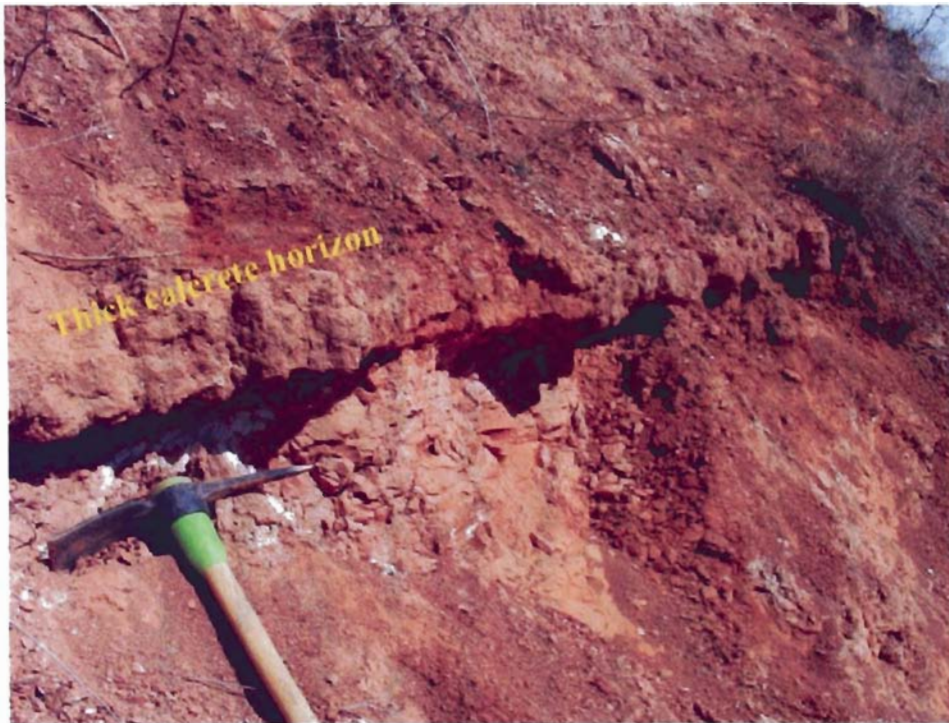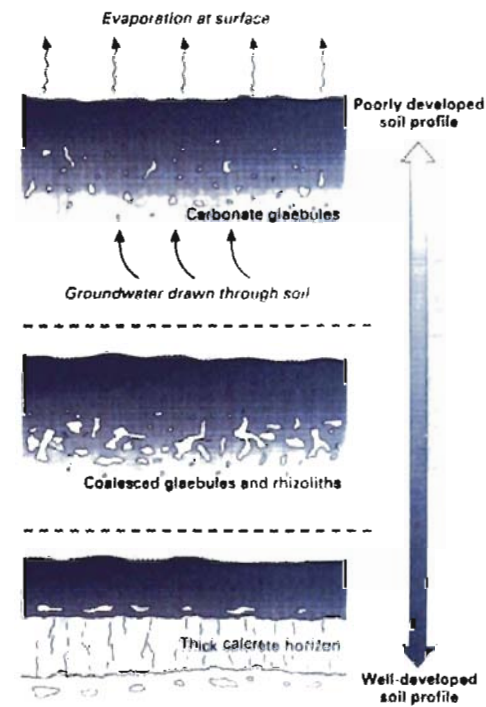
Carbonate Glaebules

Figure 45. Skeleton Creek reconnaissance outcrop showing the development of a soil profile with calcrete formation (Nichols, 1999).

CHAPTER 6

CONCLUSIONS

Purpose

Past work by Mosier (1994) suggests that arsenic in the Permian red beds of Oklahoma is associated with shale, siltstone, and finer-grained sandstones. As a consequence, arsenic concentrations in drinking water tend to be higher when the water is produced from finer-grained rocks than when water is produced from coarser-grained rocks. This association between arsenic concentration and rock type therefore suggests that arsenic in the Permian rocks may vary with the depositional sedimentary environment. The purpose of this thesis is to document and evaluate the habitat of the arsenic within the context of sedimentary lithofacies and depositional environments. This study will examine ways in which we can utilize outcrop-based high-resolution gamma-ray to characterize arsenic-bearing lithofacies. In addition, important controls on the porosity (storativity) and permeability (hydraulic conductivity) of the Permian aquifer sandstones have also been described in this thesis. Ultimately, through integration of on-going studies of Abbott (2004) and Kenney (2004), the projection of outcrop gamma-ray profiles and paleodepositional environment to the subsurface should help to further constrain the habitat (environment) of arsenic and better refine knowledge about regional permeability fairways in the aquifer.

Principal Findings / Contributions

Outcrop Classification and Characterization

The 43 outcrops described along the six transects near Lake Thunderbird were grouped into eight separate lithofacies classes based on bedding styles, sedimentary structures and inferences about depositional environments. We constructed vertical profiles for each class exposed in the study area in-order to compare gamma ray, lithofacies, grain size and calculated permeability. The vertical profiles are useful for assisting in the pattern correlation of subsurface well logs and as an aid for interpreting depositional environments. Based on gamma-ray and lithofacies classes, we observed evidence for a fluvial meandering/braided depositional setting in a semi-arid environment. This interpretation is based on (1) bell-shaped and (2) blocky gamma-ray patterns characteristic of fluvial deposits located adjacent to muddy floodplains. The floodplain mudstones contain evidence for soil formation.

1) Group #1 contains (1) stacked bar forms, (2) tabular and trough cross-bedded sandstone, (3) some with erosional bases, and sometimes having (4) mud clast rip-ups at the base. Vertical sections through these deposits exhibit a gradation from coarser material at the base to finer at the top, indicating a fining upwards grain size profile. An erosional base is a common feature of these channel forms, which are then filled by successive depositional events.

2) Group #2 contains sandstones that lack internal features, but exhibit an erosional base. The lack of sedimentary structures could be a sign of a rapid depositional event that failed to preserve internal structures and bedding features. The truncation of

100

underlying units suggests these sandstones are part of a channelized system similar to Group #1.

3) Group #3 contains blocky cross-bedded sandstones with mud rip-up clasts. Large-scale cross bedding occurs at the base with mud clast rip-ups and smaller sets of cross-lamination nearer the top. The unusual high gamma-ray readings for this group are the result of mud rip-up clasts found at the base of the unit, which would have a tendency to skew the API average to higher values.

4) Group #4 contains sandstones with horizontal to low angle planar laminations. These are interpreted to be sheet wash events that originate away from the channel margin where the supply of sediment is low and the carrying capacity depends not only on the amount of water but also on the characteristics of the surface topography. The top surfaces of these laminations commonly contain parting laminations that may be used to measure paleocurrent direction.

5) Group #5 contains an interlaminated shale/siltstone that appears blocky and without primary sedimentary structures. Naturally occurring radioactive elements tend to be found in greatest abundance in the mudstone and shale outcrops than any other sedimentary lithology, thus the mean API value is considerably higher (89 API). Because of mechanical compaction of the silt and clay in the siltstone/shale, the porosity and permeability of the rock type is very low.

6) Group #6 contains a mud-clast conglomerates that exhibits some cross-bedding features. The conglomerate can be interpreted as a channel lag deposit formed by rapid water flow on a relatively flat surface during the first stages of a flash-flood event. Observations suggest that the conglomerates are intrabasinal, being derived from erosion

and transportation of clasts from caliche and other "hardpan" zones that occurred on the floodplain.

7) Group #7 contains a carbonate clast conglomerate. This conglomerate exhibits horizontal planar laminations and is extremely well cemented with dolomite. The dolomite cement may have originated in a lake setting situated on the floodplain, adjacent to the river. Exposure of the water body in a seasonally arid environment may have promoted dolomite cementation. An alternative hypothesis is that the body of water was filled in by a flash flood event and became cemented.

8) Group #8 consists of an iron-cemented sandstone/conglomerate with large-scale cross bedding and mud clast rip-ups at the base. Smaller sets of cross-laminations occur near the top of the beds. The conglomerate is generally well cemented and when exposed to the atmosphere, becomes oxidized.

Geochemical Results

Past studies have shown that arsenic in sedimentary rocks is associated with iron-bearing mineral phases (pyrite, hematite, goethite). In the Garber-Wellington Formation, we suggest that the As is adsorbed onto the fine-grained hematite that is disseminated throughout the Permian red beds of central Oklahoma. Analysis and quantification of USGS geochemical data from the Central Oklahoma Aquifer confirms that As varies strongly with Fe and both are enriched in the finer-grained rocks. The relationships among Fe, As, and grain size are statistically significant and equations for the prediction of arsenic via a relationships to gamma ray have been developed. The relationships,

102

however, contain much scatter in the data. Some of the data scatter is probably because of secondary mobilization of iron and arsenic after burial of the Permian red beds.

Because the arsenic concentrations are higher in the finer grained lithofacies than in the coarser grained lithofacies, one may conclude that the arsenic in the rocks is detrital and inherited from the sediment source area. Should the iron and arsenic have been chemical precipitates, one would expect to find a greater volume of these elements in the portions of the section that are coarser grained; instead this scenario is just the opposite of what we find in the rocks, supporting the argument that the iron and arsenic are associated with the detrital or primary depositional processes of these Permian sedimentary rocks.

Implications

Natural occurrences of ground water with moderate (10 to 50 ug/L) to high (>50 ug/L) concentrations of arsenic are common throughout much of the Western United States. Knowledge of the geologic distribution of elevated concentrations is necessary for effective management of the nation's water resources. Additionally, better documentation of the geologic distribution of As may provide insight into the geochemical processes responsible for elevated concentrations in different hydrogeologic settings.

The principal findings in this thesis are as follows:

(1) Arsenic distribution varies strongly with lithofacies and not the internal stratigraphy of the Garber-Wellington Formation interval.

(2) Clay-rich lithofacies are found to be enriched in arsenic. Consequently, the mapped geologic distribution of these lithofacies could be used to select new drill-well locations.

(3) Because arsenic generally varies with lithology, intervals within wells could be selectively produced so that water originating in arsenic-prone lithofacies (mudstone) does not enter the well bore and mix with water from the low arsenic intervals (sandstone).

(4) Results from this study can be applied world wide provided that similar model conditions are met. The elevated arsenic concentrations depend on several complex geologic and geochemical conditions, including: (1) distribution of the elements in the solid phases, (2) redox conditions of the water, (3) changes in the water chemistry and (4) cation-exchange reactions. Provided that one is dealing with a sedimentary environment similar to the Garber-Wellington Formation, relative arsenic concentrations in the subsurface can be inferred from gamma-ray measurements.

Future Work

1) Detailed and extensive mapping of the Garber-Wellington Formation lithofacies and depositional environment outside of Cleveland County can be used to reconstruct a regional series of lithofacies and depositional environments that can be used to guide the exploration for low arsenic water throughout central Oklahoma.

2) A detailed study of the mineralogy and geochemistry of sandstones and shales within the context of the sedimentary geology could help to better constrain the habitat of

As in the rocks. At this point, we still do not understand the habitat of arsenic and where it is occurring in the Permian section (ie, with clay, iron or both).

REFERENCES

Abbott, B.N., (2004). Subsurface Well-Log Correlation of Arsenic-Bearing Lithofacies in the Permian Garber Sandstone and Wellington Formation, Central Oklahoma Aquifer (COA), Cleveland County, Oklahoma, Oklahoma State University unpublished M.S. Thesis.

Allen, J.R.L. (1974) Studies in Fluviatile Sedimentation: Implications for Pedogenic Carbonate Units, Lower Old Red Sandstone, Anglo-Welsh Outcrop. Geological Journal 9, 181-208.

Aurin, F. L., Officer, H.G., and Gould C.N., (1926) The Subdivisions of the Enid Formation: Bulletin American Association Petroleum Geologist., Vol. 10, No. 8 p. 786-99.

Beard, D.C. and Weyl, P.K. (1973). Influence of Texture on Porosity and Permeability of Unconsolidated Sand. AAPG Bulletin v.57, (No.2): 349-369 pp.

Breit, G.N., (1998). The Diagenetic History of Permian Rocks in the Central Oklahoma Aquifer: U.S. Geological Survey Water-Supply Paper 2357-A, p.45-70.

Breit, G.N., Rice, Cyndi, Esposito, Ken, and Schlottmann, J.L., (1990). Mineralogy and Petrography of Permian Rocks in the Central Oklahoma Aquifer: U.S. Geological Survey Open-File Report 90-678, 50 p.

Briggs, P.H., and Crock, J.G., (1986). Automated Determination of Total Selenium in Rocks, Soils and Plants: U.S. Geological Survey Open-File Report 86-40, 20 p.

CH2M HILL (2002) Arsenic Study for Ground Water Wells of Norman, Oklahoma and the University of Oklahoma.

Christenson, S.C., Morton, R.B., and Mesander, B.A., (1992). Hydrogeologic Maps of the Central Oklahoma Aquifer, Oklahoma: U.S. Geological Survey Hydrologic Investigations Atlas HA-724, 3 sheets.

Christenson, S.A., (1998). Ground-Water-Quality Assessment of the Central Oklahoma Aquifer: Summary of Investigations: U.S. Geological Survey Water-Supply Paper 2357-A, p. 1-44.

Christenson, S.A., Parkhurst, D.L., and Breit, G.N., (1998) Summary of Geochemical and Geohydrologic Investigations of the Central Oklahoma Aquifer: U.S. Geological Survey Water-Supply Paper 2357-A, p. 107-118.

Collins, Kelli. L., (2001). Permeability Pathways in the Canadian River Alluvium Adjacent to the Norman Landfill, Norman, Oklahoma, Oklahoma State University unpublished M.S. Thesis.

Crock, J.G., and Lichte, F.E., (1982). An Improved Method for the Determination of Trace Levels of Arsenic and antimony in Geologic materials by Automated Hydride Generation-Atomic Absorption Spectroscopy: Analytica Chemica Acta, v.144, p. 223-233.

Folk, Robert. L., (1974). Petrology of Sedimentary Rocks: Hemphill Publishing Company, Austin, Texas.

Hermance, J.R., (1999). A Mathematical Primer on Groundwater Flow: Prentice Hall, New Jersey, p. 10.

Johnson, Kenneth. S., (1989). Geologic evolution of the Anadarko Basin. In Anadarko Basin Symposium, 1988, ed K.S. Johnson. Oklahoma Geological Survey Circular 90: p. 3-12.

Johnson, Kenneth. S., (1998). Geology and Mineral Resources of Oklahoma: Oklahoma Geological Survey, Information Series #2.

Kenney, K., (2004). Outcrop-Based Lithofacies and Depositional Setting of Arsenic-Bearing Permian Red Beds in the Central Oklahoma Aquifer (COA), Cleveland County, Oklahoma, Oklahoma State University unpublished M.S. Thesis.

McKown, D.M., and Millard, H.T., Jr., (1987). Determination of Uranium and Thorium by Delayed Neutron Counting in Baedecker, P.A., ed., Methods for Geochemical Analysis: U.S. Geological Survey Bulletin 1770, p. I1-I12.

Mosier E.L., and Bullock J.H., J., (1988). Review of the General Geology and Solid-Phase Geochemical Studies in the Vicinity of the Central Oklahoma Aquifer: U.S. Geological Survey Circular 1019, 18 p.

Mosier, E.L., (1994). Geochemical Characterization of Solid-Phase Materials in the Central Oklahoma Aquifer: U.S. Geological Survey Water-Supply Paper 2357-A, p. 71-105

Mosier, E.L., Briggs, P.H., Crock, J.G., Kennedy, K.R., McKown, D.M., Vaughn, R.B., and Welsch, E.P., (1990). Analyses of Subsurface Permain Rock Samples from the Central Oklahoma Aquifer: U.S. Geological Survey Open-File Report 90-456, 64 p.

Nichols, G.J., (1999). Sedimentology and Stratigraphy. Blackwell Science Ltd; Osney Mead, Oxford, p. 117, 126.

Parkhurst, D.L. (1992). The Geochemical Evolution of Ground Waters in the Central Oklahoma Aquifer. *In* Ground Water Quality of the Central Oklahoma (Garber-Wellington) Aquifer Conference: Proceedings, February 20, 1992. Ed. S.C. Christenson and Lyn Carpenter. U.S. Geological Survey Open-File Report 92-116.

Parkhurst, D.L., Christenson, S.A., and Breit, G.N., (1996). Ground-Water Quality Assessment of the Central Oklahoma Aquifer-Geochemical and Geohydrologic Investigations: U.S. Geological Survey Water-Supply Paper 2357-C, p. 101.

Parkhurst, D.L., Christenson, S.C., and Schlottmann, J.L., (1989). Ground-water Quality Assessment of the Central Oklahoma aquifer, Oklahoma – Analysis of Available Water-Quality Data Through 1987: U.S. Geological Survey Open-File Report 88-728, 80 p.

Reed, S.J.B., (1995) Electron Probe Analysis. In: Microprobe Techniques in the Earth Sciences. In: Potts, P.J., Bowles, J.F.W., Reed, S.J.B. Cave, M.R. (Eds.) Microprobe Techniques in the Earth Sciences. Mineralogical Society Series, Kluwer Academic Publishers, Netherlands, p. 49-89.

Reineck, H.E., and Singh, I.B. (1973). Genesis of laminated sand and graded rhythmites in storm-sand layers of shelf mud. Sedimentology 18, p. 123-128.

Sanzolone, R.F., and Chao, T.T., (1987). Determination of Selenium in Thirty-Two Geochemical Reference Materials by Continuous-Flow Hydride Generation Atomic Absorption Spectrophotometry: Geostandards Newsletter, v. 11, p. 81-85.

Schlottmann, J. L., and Funkhouser, R.A., (1991). Chemical Analysis of Water Samples and Geophysical Logs from Cored Test Holes Drilled in the Central Oklahoma Aquifer, Oklahoma: U.S. Geological Survey Open-File Report 91-464.

Schlottmann, J.L., Mosier, E.L., and Breit., (1998). Arsenic, Chromium, Selenium and Uranium in the Central Oklahoma Aquifer: U.S. Geological Survey Water-Supply Paper 2357-A, p. 119-179.

Schlottmann,J.L., and Breit G.N., (1992). Mobilization of As and U in the Central Oklahoma Aquifer: Proceedings of the 7th International Symposium on Water-Rock Interaction, Park City Utah, 13-19 July 1992, A.A. Balkema, Rotterdam.

Serra, O. and Sulpice, L., (1975). Sedimentological Analysis of Shale-Sand Series from Well Logs. Transactions of the SPWLA 16th Annual Logging Symposium, paper W.

Smith, S. J. and Christenson, S. C., (2000) Public-Supply Well-Head Arsenic Remediation in Western Cleveland County, Oklahoma.

USGS, 1996c, Digital Surface Geology Maps of Oklahoma, USGS Open File Reports 96-373: Retrieved March, 2004 from http://ok.water.usgs.gov/gis/geology/index.html

Welch, Alan. H., Lico, Michael, S., and Hughes, Jennifer L., (1988). Arsenic in Ground Water of the Western United States. Groundwater 26, (No.3): p. 333-347.

Wylie, David. W., (1988). Arkoma Basin Overview: Shelf to Basin Geology and Resources of Pennsylvanian Strata. *In* The Arkoma Basin and Frontal Ouachita Mountains of Oklahoma, Ed. K.S. Johnson. Oklahoma Geological Survey Guidebook 25. p. 63-66.

APPENDIX A

TRANSECT DATA (Alameda St.)

Guide Number	Depth Interval (in)	Depth Interval (ft)	Total Count (ppm)	Potassium K (%)	Uranium U (ppm)	Thorium Th (ppm)	API
	Begin Transect (0.0 mi)						
	Intersection of 84th Ave and Alameda St.						
	Outcrop #1A (.6 mi)						
A1	0.0	0.00	7.9	0.7	0.7	5.2	37.60
A2	11.0	0.92	13.6	1.0	2.7	11.50	83.60
A3	19.0	1.58	8.1	0.7	0.5	5.7	38.00
A4	38.0	3.17	12.1	0.9	1.4	10.6	68.00
A5	48.0	4.00	11.6	0.8	1.3	10.7	66.00
A6	59.0	4.91	4.3	0.3	-0.2	2.6	13.60
A7	74.0	6.16	3.9	0.2	0.5	2.0	15.20
A8	89.0	7.41	4.3	0.2	0.4	3.0	18.40
A9	107.0	8.91	3.8	0.3	-0.3	3.8	17.60
A10	118.0	9.83	3.2	0.1	0.4	2.8	16.00
A11	124.0	10.33	4.1	0.4	0.1	2.9	18.80
A12	137.0	11.41	6.9	0.5	1.5	4.1	36.40
A13	151.0	12.58	7.1	0.4	1.4	5.5	39.60
A14	163.0	13.58	6.0	0.4	0.1	6.7	34.00
A15	172.0	14.33	5.4	0.4	0.1	3.6	21.60
A16	181.0	15.08	5.1	0.4	0.4	4.1	26.00
A17	191.0	15.91	5.3	0.3	0.3	4.1	23.60
A18	203.0	16.91	5.2	0.4	0.0	4.9	26.00
A19	221.0	18.41	8.4	0.6	1.4	5.7	43.60
A20	233.0	19.41	10.2	0.9	1.2	6.6	50.40
A21	242.0	20.16	8.5	0.8	0.4	5.5	38.00
A22	252.0	20.99	8.7	0.6	1.8	5.1	44.40
A23	258.0	21.49	5.7	0.3	0.3	4.8	26.40
A24	267.0	22.24	5.7	0.5	0.3	3.6	24.80
A25	280.0	23.32	8.0	0.6	0.4	6.9	40.40
A26	290.0	24.16	8.5	0.6	1.4	5.5	42.80
A27	302.5	25.20	8.0	0.5	0.7	6.1	38.00
A28							
A29	*Outcrop #1B (0 mi; 68 ft East of 1A)*						
A30							
A31	Depth Interval (in)	Depth Interval (ft)	Total Count (ppm)	Potassium K (%)	Uranium U (ppm)	Thorium Th (ppm)	*API*
A32							
A33	0.0	0.00	10.3	0.9	1.2	7.4	53.60
A34	15.0	1.25	11.0	0.8	1.4	8.4	57.60
A35	32.0	2.67	12.8	1.2	1.1	9.7	66.80
A36	43.0	3.58	12.5	1.1	1.3	10.0	68.00
A37	59.0	4.91	13.7	0.9	2.4	11.3	78.80
A38	72.0	6.00	13.7	1.2	1.3	12.2	78.40
A39	85.0	7.08	13.8	1.1	1.9	11.1	77.20
A40	100.0	8.33	6.7	0.6	0.7	4.2	32.00
A41	112.0	9.33	5.7	0.5	0.5	3.5	26.00
A42	130.0	10.83	4.4	0.3	0.3	3.3	20.40
A43	144.0	12.00	4.3	0.2	0.8	1.2	14.40

	Depth Interval (in)	Depth Interval (ft)	Total Count (ppm)	Potassium K (%)	Uranium U (ppm)	Thorium Th (ppm)	API
A44	160.0	13.33	4.0	0.2	0.5	2.9	18.80
A45	175.0	14.58	5.1	0.4	0.9	2.5	23.60
A46	191.0	15.91	7.8	0.6	1.1	6.1	42.80
A47	204.0	16.99	6.5	0.4	0.5	5.7	33.20
A48	216.0	17.99	5.9	0.5	0.5	3.5	26.00
A49	233.0	19.41	5.6	0.3	1.1	3.9	29.20
A50	246.0	20.49	7.0	0.6	0.4	6.0	36.80
A51	256.0	21.32	5.4	0.3	0.8	2.9	22.80
A52	266.0	22.16	4.9	0.2	0.9	3.7	25.20
A53	284.0	23.66	6.0	0.3	1.0	3.7	27.60
A54	297.0	24.74	8.9	0.6	1.6	5.7	45.20
A55	308.0	25.66	5.5	0.3	0.7	3.7	25.20
A56	319.0	26.57	8.9	0.7	1.0	7.3	48.40
A57							
A58	*Outcrop #2 (1.9 mi)*						
A59							
A60	**Depth**	**Depth**	**Total**	**Potassium**	**Uranium**	**Thorium**	
A61	**Interval (in)**	**Interval (ft)**	**Count (ppm)**	**K (%)**	**U (ppm)**	**Th (ppm)**	***API***
A62	0.0	0.00	6.0	0.4	0.8	3.3	26.00
A63	6.0	0.50	4.8	0.2	0.6	3.8	23.20
A64	18.0	1.50	4.6	0.3	0.0	3.6	19.20
A65	34.0	2.83	4.4	0.3	0.1	3.4	19.20
A66	48.0	4.00	4.3	0.3	0.2	2.6	16.80
A67	59.0	4.91	3.9	0.1	0.6	2.3	15.60
A68	71.0	5.91	3.9	0.0	0.8	3.0	18.40
A69	81.0	6.75	4.2	0.2	0.4	2.6	16.80
A70	91.0	7.58	3.9	0.3	0.0	2.6	15.20
A71	104.0	8.66	3.9	0.2	0.6	2.8	19.20
A72	111.0	9.25	4.4	0.3	0.5	3.1	21.20
A73							
A74	*Outcrop #3 (.5 mi)*						
A75							
A76	**Depth**	**Depth**	**Total**	**Potassium**	**Uranium**	**Thorium**	
A77	**Interval (in)**	**Interval (ft)**	**Count (ppm)**	**K (%)**	**U (ppm)**	**Th (ppm)**	***API***
A78	0.0	0.00	6.1	0.4	1.0	4.0	30.40
A79	10.0	0.83	6.1	0.3	0.4	5.1	28.40
A80	19.0	1.58	6.4	0.4	0.4	5.0	29.60
A81	28.0	2.33	6.2	0.4	0.3	4.3	26.00
A82	40.0	3.33	6.5	0.4	0.8	4.5	30.80
A83	55.0	4.58	6.7	0.4	0.6	5.5	33.20
A84	69.0	5.75	7.1	0.5	0.7	5.8	36.80
A85	84.0	7.00	7.9	0.5	1.2	6.0	41.60
A86	97.0	8.08	10.7	0.9	1.8	5.6	51.20
A87	105.0	8.75	10.0	0.5	1.5	8.3	53.20
A88	115.0	9.58	10.1	0.5	1.5	8.7	54.80
A89	125.0	10.41	8.6	0.6	1.4	8.0	52.80
A90	135.0	11.25	10.1	0.8	0.5	8.1	49.20
A91	145.0	12.08	10.3	0.7	1.2	9.1	57.20
A92	155.0	12.91	9.0	0.7	0.2	7.3	42.00
A93	165.0	13.74	10.6	0.9	1.4	7.7	56.40
A94	175.0	14.58	8.0	0.7	1.1	4.3	37.20

A95						
A96	*Outcrop #4 (.1 mi)*					
A97						
A98	**Depth**	**Depth**	**Total**	**Potassium**	**Uranium**	**Thorium**	
A99	**Interval (in)**	**Interval (ft)**	**Count (ppm)**	**K (%)**	**U (ppm)**	**Th (ppm)**	*API*
A100	0.0	0.00	5.2	0.3	1.4	3.5	30.00
A101	7.0	0.58	4.2	0.3	0.2	3.9	22.00
A102	16.0	1.33	4.1	0.2	0.9	2.7	21.20
A103	24.0	2.00	3.8	0.1	0.3	2.8	15.20
A104	37.0	3.08	3.8	0.2	0.4	2.2	15.20
A105	48.0	4.00	4.4	0.0	0.9	3.8	22.40
A106	65.0	5.41	4.5	0.3	-0.1	3.9	19.60
A107	75.0	6.25	3.9	0.2	0.0	2.5	13.20
A108	81.0	6.75	4.5	0.3	0.6	2.7	20.40
A109	91.0	7.58	4.8	0.3	0.3	3.7	22.00
A110	101.0	8.41	5.1	0.2	0.3	4.4	23.20
A111	111.0	9.25	5.4	0.3	1.0	2.7	23.60
A112	121.0	10.08	5.2	0.4	0.7	3.5	26.00
A113	131.0	10.91	7.7	0.6	0.6	6.5	40.40
A114							
A115	*Outcrop #5 (.5 mi)*						
A116							
A117	**Depth**	**Depth**	**Total**	**Potassium**	**Uranium**	**Thorium**	
A118	**Interval (in)**	**Interval (ft)**	**Count (ppm)**	**K (%)**	**U (ppm)**	**Th (ppm)**	*API*
A119	N/A	N/A	N/A	N/A	N/A	N/A	N/A
A120	0.0	0.00	6.9	0.5	0.4	6.4	36.80
A121	7.0	0.58	7.1	0.4	1.2	4.5	34.00
A122	17.0	1.42	6.9	0.5	1.2	4.0	33.60
A123	23.0	1.92	7.3	0.4	0.9	6.5	39.60
A124	31.0	2.58	6.4	0.4	1.0	5.3	35.60
A125	39.0	3.25	5.3	0.2	0.9	2.6	20.80
A126	49.0	4.08	6.0	0.4	0.4	4.4	27.20
A127							
A128	*Outcrop #6 (.4 mi)*						
A129							
A130	**Depth**	**Depth**	**Total**	**Potassium**	**Uranium**	**Thorium**	
A131	**Interval (in)**	**Interval (ft)**	**Count (ppm)**	**K (%)**	**U (ppm)**	**Th (ppm)**	*API*
A132	0.0	0.00	4.5	0.3	0.5	2.3	18.00
A133	5.0	0.42	3.8	0.2	0.2	2.5	14.80
A134	20.0	1.67	4.5	0.2	0.3	2.8	16.80
A135	37.0	3.08	4.3	0.2	0.7	2.8	20.00
A136	49.0	4.08	4.8	0.3	0.9	2.7	22.80
A137	59.0	4.91	4.0	0.3	0.5	2.6	19.20
A138	68.0	5.66	4.5	0.2	0.7	3.1	21.20
A139	76.0	6.33	4.5	0.2	0.7	3.0	20.80
A140	93.0	7.75	4.1	0.3	0.3	2.1	15.60
A141	105.0	8.75	4.6	0.1	1.0	2.4	19.20
A142	116.0	9.66	4.4	0.2	0.3	3.4	19.20
A143							
A144	*Outcrop #7 (.4 mi)*						

	Depth Interval (in)	Depth Interval (ft)	Total Count (ppm)	Potassium K (%)	Uranium U (ppm)	Thorium Th (ppm)	API
A145							
A146	Depth	Depth	Total	Potassium	Uranium	Thorium	
A147	Interval (in)	Interval (ft)	Count (ppm)	K (%)	U (ppm)	Th (ppm)	*API*
A148	0.0	0.00	4.5	0.3	-0.4	3.3	14.80
A149	5.0	0.42	4.1	0.2	-0.1	2.8	13.60
A150	20.0	1.67	4.3	0.3	0.9	3.7	26.80
A151	35.0	2.92	5.7	0.5	0.6	2.8	24.00
A152	47.0	3.92	6.4	0.5	0.0	5.5	30.00
A153	55.0	4.58	4.9	0.3	0.3	4.7	26.00
A154	64.0	5.33	5.0	0.3	0.3	5.3	28.40
A155	78.0	6.50	5.8	0.1	0.0	6.0	25.60
A156	87.0	7.25	5.0	0.4	-0.2	4.7	23.60
A157	95.0	7.91	4.5	0.3	0.3	3.1	19.60
A158	109.0	9.08	4.2	0.3	0.1	3.8	20.80
A159	123.0	10.25	4.8	0.3	1.0	3.0	24.80
A160	138.0	11.50	4.9	0.3	0.1	3.1	18.00
A161	151.0	12.58	4.3	0.3	0.2	3.5	20.40
A162							
A163	*Outcrop #8 (.3 mi)*						
A164							
A165	Depth	Depth	Total	Potassium	Uranium	Thorium	
A166	Interval (in)	Interval (ft)	Count (ppm)	K (%)	U (ppm)	Th (ppm)	*API*
A167	0.0	0.00	4.4	0.2	0.9	1.9	18.00
A168	6.0	0.50	4.1	0.1	0.8	2.8	19.20
A169	9.0	0.75	4.3	0.2	0.5	2.3	16.40
A170	22.0	1.83	6.4	0.4	0.3	6.6	35.20
A171	32.0	2.67	10.2	0.6	2.2	7.2	56.00
A172	41.0	3.42	6.7	0.4	1.2	5.5	38.00
A173	45.0	3.75	6.9	0.3	1.8	4.0	35.20
A174	54.0	4.50	6.7	0.4	0.7	5.0	32.00
A175	69.0	5.75	6.6	0.1	2.3	3.8	35.20
A176	84.0	7.00	6.0	0.3	1.3	3.7	30.00
A177	101.0	8.41	4.6	0.2	0.8	3.5	23.60
A178	112.0	9.33	5.6	0.2	0.7	5.1	29.20
	End of Transect (.3 mi)						
	Dead End (Marina)						
	Total Distance (5.0 mi)						

Guide Number	Sample #	F5	F16	F50	F84	F95	Avg Grain Size (phi)	Size	Std. Dev
A1	52	N/A	N/A	N/A	N/A	N/A	N/A	N/A	N/A
A2									
A3	51	1.58	2.05	2.58	3.15	3.85	2.59	F sand	0.62
A4									
A5	50	2.10	2.82	3.97	4.19	4.33	3.66	VF sand	0.68
A6	49	1.84	2.04	2.26	2.63	2.94	2.31	F sand	0.31
A7									
A8									
A9									
A10									
A11									
A12	48	1.30	1.88	2.36	2.87	3.83	2.37	F sand	0.63
A13									
A14									
A15									
A16									
A17									
A18									
A19	47	1.77	2.00	2.58	3.13	3.60	2.57	F sand	0.56
A20	46	1.90	2.70	3.74	4.16	4.30	3.53	VF sand	0.73
A21	45	1.83	2.90	3.64	4.08	4.60	3.54	VF sand	0.71
A22									
A23	44	2.07	2.69	2.94	3.46	4.02	3.03	VF sand	0.49
A24									
A25									
A26	43	1.97	2.54	3.04	3.72	4.55	3.10	VF sand	0.69
A27									
A28									
A29									
A30									
A31							Avg Grain Size (phi)		
A32	Sample #	F5	F16	F50	F84	F95	Size (phi)	Size	Std. Dev
A33									
A34									
A35									
A36	61	N/A	N/A	N/A	N/A	N/A	N/A	N/A	N/A
A37									
A38									
A39									
A40									
A41	60	1.93	2.11	2.53	3.15	3.63	2.60	F sand	0.52
A42									
A43									

	Sample #	F5	F16	F50	F84	F95	Avg Grain Size (phi)	Size	Std. Dev
A44	59	1.87	2.05	2.37	2.83	3.33	2.42	F sand	0.42
A45									
A46	58	1.92	2.50	2.95	3.55	4.24	3.00	VF sand	0.61
A47	57	2.26	2.40	2.84	3.38	3.70	2.87	F sand	0.46
A48									
A49									
A50	56	2.12	2.58	2.94	3.50	4.33	3.01	VF sand	0.56
A51									
A52									
A53	55	1.69	1.88	2.21	2.85	3.54	2.31	F sand	0.52
A54	54	2.00	3.10	3.65	4.12	4.56	3.62	VF sand	0.64
A55	53	2.05	2.28	2.80	3.74	4.20	2.94	F sand	0.69
A56									
A57									
A58									
A59									
A60							Avg Grain		
A61	Sample #	F5	F16	F50	F84	F95	Size (phi)	Size	Std. Dev
A62	42	1.90	2.31	2.92	3.36	4.24	2.86	F sand	0.62
A63	41	1.82	2.16	2.75	3.40	4.10	2.77	F sand	0.66
A64	40	1.50	1.86	2.24	2.90	3.51	2.33	F sand	0.56
A65	39	1.34	1.60	2.10	2.81	3.32	2.17	F sand	0.60
A66	38	1.44	1.80	2.18	2.75	3.14	2.24	F sand	0.50
A67	37	1.32	1.48	1.94	2.66	3.21	2.03	F sand	0.58
A68	36	1.45	1.88	2.19	2.75	3.31	2.27	F sand	0.50
A69	35	1.71	2.05	2.55	2.96	3.48	2.52	F sand	0.50
A70	34	1.95	2.11	2.50	2.86	3.24	2.49	F sand	0.38
A71	33	1.54	1.84	2.15	2.68	3.22	2.22	F sand	0.46
A72	32	1.69	1.98	2.27	2.86	3.54	2.37	F sand	0.50
A73									
A74									
A75									
A76							Avg Grain		
A77	Sample #	F5	F16	F50	F84	F95	Size (phi)	Size	Std. Dev
A78	84	1.09	1.46	2.58	3.40	4.05	2.48	F sand	0.93
A79	83	1.90	2.44	2.92	3.41	3.74	2.92	F sand	0.52
A80	82	1.85	2.48	2.83	3.40	3.84	2.90	F sand	0.53
A81	81	1.76	2.36	2.83	3.44	4.05	2.88	F sand	0.62
A82	80	2.00	2.34	2.76	2.36	3.90	2.49	F sand	0.29
A83	79	2.00	2.40	2.74	3.33	3.80	2.82	F sand	0.51
A84	78	2.00	2.32	2.68	3.20	3.66	2.73	F sand	0.47
A85	77	1.90	2.19	2.78	3.40	4.00	2.79	F sand	0.62
A86									
A87									
A88									
A89									
A90									
A91									
A92									
A93									
A94									

	Sample #	F5	F16	F50	F84	F95	Avg Grain Size (phi)	Size	Std. Dev
A95									
A96									
A97									
A98							**Avg Grain**		
A99	**Sample #**	**F5**	**F16**	**F50**	**F84**	**F95**	**Size (phi)**	**Size**	**Std. Dev**
A100	76	1.83	2.16	2.89	3.51	4.35	2.85	F sand	0.72
A101	75	1.79	2.05	2.54	2.95	3.45	2.51	F sand	0.48
A102									
A103									
A104									
A105									
A106	74	1.79	2.05	2.50	2.90	3.34	2.48	F sand	0.45
A107	73	1.89	2.14	2.60	2.95	3.42	2.56	F sand	0.43
A108	72	1.82	2.09	2.51	2.91	3.33	2.50	F sand	0.43
A109	71	1.95	2.23	2.64	3.05	3.68	2.64	F sand	0.47
A110									
A111									
A112	70	2.04	2.24	2.59	3.05	3.65	2.63	F sand	0.45
A113									
A114									
A115									
A116									
A117							**Avg Grain**		
A118	**Sample #**	**F5**	**F16**	**F50**	**F84**	**F95**	**Size (phi)**	**Size**	**Std. Dev**
A119	31	N/A	N/A	N/A	N/A	N/A	N/A	N/A	N/A
A120	30	2.07	2.38	2.75	3.29	3.82	2.81	F sand	0.49
A121	29	2.47	2.77	3.25	3.74	4.47	3.25	VF sand	0.55
A122	28	2.55	2.94	3.51	4.04	4.63	3.50	VF sand	0.59
A123	27	2.40	2.84	3.31	3.68	4.05	3.28	VF sand	0.46
A124	26	2.12	2.83	3.41	3.80	4.72	3.35	VF sand	0.64
A125	25	2.22	2.54	2.89	3.40	4.11	2.94	F sand	0.50
A126	24	1.85	2.35	3.08	3.74	4.24	3.06	VF sand	0.71
A127									
A128									
A129									
A130							**Avg Grain**		
A131	**Sample #**	**F5**	**F16**	**F50**	**F84**	**F95**	**Size (phi)**	**Size**	**Std. Dev**
A132	23	1.79	2.05	2.42	3.30	3.90	2.59	F sand	0.63
A133	22	1.77	2.02	2.33	2.95	3.68	2.43	F sand	0.52
A134	21	1.80	2.35	3.05	3.70	4.30	3.03	VF sand	0.72
A135	20	1.77	2.10	2.53	2.85	3.19	2.49	F sand	0.40
A136	19	1.81	2.14	2.58	2.91	3.50	2.54	F sand	0.45
A137	18	1.63	1.98	2.33	2.84	3.48	2.38	F sand	0.50
A138	17	1.80	2.14	2.59	3.15	3.76	2.63	F sand	0.55
A139	16	1.62	2.09	2.64	3.11	3.81	2.61	F sand	0.59
A140	15	1.77	2.00	2.27	2.85	3.31	2.37	F sand	0.45
A141	14	1.72	1.97	2.32	2.91	3.53	2.40	F sand	0.51
A142	13	1.58	1.95	2.34	3.10	3.83	2.46	F sand	0.63
A143									
A144									

117

	Sample #	F5	F16	F50	F84	F95	Avg Grain Size (phi)	Size	Std. Dev
A145									
A146							Avg Grain		
A147	Sample #	F5	F16	F50	F84	F95	Size (phi)	Size	Std. Dev
A148									
A149	69	2.03	2.20	2.56	2.97	4.00	2.58	F sand	0.49
A150									
A151	68	1.76	2.11	2.58	3.06	4.24	2.58	F sand	0.61
A152	67	1.65	2.14	2.82	3.90	4.83	2.95	F sand	0.92
A153	66	1.74	2.00	2.51	3.00	3.62	2.50	F sand	0.53
A154	65	1.95	2.14	2.49	3.25	4.24	2.63	F sand	0.62
A155									
A156	64	2.00	2.26	2.75	3.44	4.67	2.82	F sand	0.70
A157									
A158									
A159	63	2.02	2.28	2.65	2.95	3.41	2.63	F sand	0.38
A160	62	1.70	1.90	2.11	2.51	3.45	2.17	F sand	0.42
A161									
A162									
A163									
A164									
A165							Avg Grain		
A166	Sample #	F5	F16	F50	F84	F95	Size (phi)	Size	Std. Dev
A167	12	1.44	1.77	2.14	3.05	3.65	2.32	F sand	0.65
A168	11	1.47	1.84	2.32	3.21	4.02	2.46	F sand	0.73
A169	10	1.50	1.93	2.50	3.45	4.00	2.63	F sand	0.76
A170	9	1.70	2.06	2.60	3.30	3.84	2.65	F sand	0.63
A171	8	1.34	1.73	2.29	3.64	4.75	2.55	F sand	0.99
A172	7	1.37	1.77	2.31	3.55	4.64	2.54	F sand	0.94
A173	6	1.33	1.65	2.24	3.48	4.60	2.46	F sand	0.95
A174	5	1.37	1.80	2.36	3.55	4.75	2.57	F sand	0.95
A175	4	1.88	2.23	2.80	3.40	4.12	2.81	F sand	0.63
A176	3	1.40	1.86	2.24	3.10	4.24	2.40	F sand	0.74
A177	2	1.42	1.77	2.10	2.60	3.30	2.16	F sand	0.49
A178	1	1.35	1.75	2.20	3.06	3.83	2.34	F sand	0.70

Guide Number	Sorting	Perm (log)	Perm (md)	Perm (D)	Location
A1	N/A	N/A	N/A	N/A	Iron oxide crust
A2					Top soil (shaly)
A3	Mod well-sorted	4.40	24878	24.88	Sandstone unit
A4					Top of weathered shale/ss unit
A5	Mod well-sorted	3.75	5686	5.69	Base of weathered shale/ss unit
A6	Very well-sorted	4.71	51142	51.14	Top of massive red ss
A7					
A8					
A9					
A10					
A11					
A12	Mod well-sorted	4.52	32945	32.95	Middle of massive red ss
A13					
A14					
A15					
A16					
A17					
A18					
A19	Mod well-sorted	4.44	27444	27.44	Base of massive red ss
A20	Mod sorted	3.80	6360	6.36	Top of white ss w/ thin lamination
A21	Mod well-sorted	3.81	6405	6.40	Middle white ss w/ thin lamination
A22					Base white ss w/ thin lamination
A23	Well-sorted	4.21	16242	16.24	Top of white ss unit #2
A24					Middle of white ss unit #2
A25					White ss w/ thin laminations
A26	Mod well-sorted	4.07	11821	11.82	Base of white ss unit #1
A27					Orange top soil
A28					
A29					
A30					
A31					
A32	Sorting	Perm (log)	Perm (md)	Perm (D)	Location
A33					Orange top soil
A34					Purple top soil
A35					Shaly top soil
A36	N/A	N/A	N/A	N/A	Weathered iron oxide crust
A37					
A38					
A39					Weathered shale/ss Fe oxide crust
A40					Weathered shale/ss
A41	Mod well-sorted	4.44	27800	27.80	Top of massive red ss
A42					
A43					

	Sorting	Perm (log)	Perm (md)	Perm (D)	Location
A44	Well-sorted	4.60	39558	39.56	Massive red ss
A45					Massive red ss
A46	Mod well-sorted	4.17	14637	14.64	Erosional unit
A47	Well-sorted	4.31	20539	20.54	Middle of massive red ss
A48					
A49					Massive red ss
A50	Mod well-sorted	4.19	15344	15.34	Erosional unit
A51					Massive red ss
A52					
A53	Mod well-sorted	4.60	40148	40.15	Base of massive red ss
A54	Mod well-sorted	3.79	6228	6.23	Middle white ss w/ thin lamination
A55	Mod well-sorted	4.16	14516	14.52	Top of white ss unit #2
A56					Orange top soil
A57					
A58					
A59					
A60					
A61	**Sorting**	**Perm (log)**	**Perm (md)**	**Perm (D)**	**Location**
A62	Mod well-sorted	4.24	17466	17.47	Surface of orange ss
A63	Mod well-sorted	4.28	18907	18.91	Top of white ss
A64	Mod well-sorted	4.57	37288	37.29	Yellow ss
A65	Mod well-sorted	4.65	44290	44.29	Middle of dark orange ss
A66	Well-sorted	4.66	45442	45.44	Dark orange ss
A67	Mod well-sorted	4.74	54804	54.80	Base of dark orange ss
A68	Well-sorted	4.64	43469	43.47	Erosional unit
A69	Well-sorted	4.50	31533	31.53	Orange ss
A70	Well-sorted	4.57	37300	37.30	Orange ss
A71	Well-sorted	4.68	48307	48.31	White ss
A72	Well-sorted	4.58	38226	38.23	Base or red ss
A73					
A74					
A75					
A76					
A77	**Sorting**	**Perm (log)**	**Perm (md)**	**Perm (D)**	**Location**
A78	Mod sorted	4.31	20189	20.19	Orange top soil
A79	Mod well-sorted	4.26	17997	18.00	Surface of orange ss
A80	Mod well-sorted	4.26	18264	18.26	Top of white/pink ss
A81	Mod well-sorted	4.23	17163	17.16	White/pink ss
A82	Very well-sorted	4.62	41511	41.51	White/pink ss
A83	Mod well-sorted	4.32	20912	20.91	Colorful ss
A84	Well-sorted	4.39	24468	24.47	Colorful ss
A85	Mod well-sorted	4.28	19159	19.16	Base of white ss
A86					Top of shale/ss slope
A87					
A88					
A89					
A90					
A91					
A92					
A93					
A94					Base of shale/ss slope

	Sorting	Perm (log)	Perm (md)	Perm (D)	Location
A95					
A96					
A97					
A98					
A99	**Sorting**	**Perm (log)**	**Perm (md)**	**Perm (D)**	**Location**
A100	Mod sorted	4.20	15752	15.75	Surface of orange ss
A101	Well-sorted	4.51	32514	32.51	Top of white ss
A102					
A103					
A104					
A105					
A106	Well-sorted	4.54	34968	34.97	Middle of white ss
A107	Well-sorted	4.50	31939	31.94	White ss (leaching zone)
A108	Well-sorted	4.54	34588	34.59	Orange ss (leaching zone)
A109	Well-sorted	4.44	27810	27.81	Dark orange zone (leaching zone)
A110					
A111					
A112	Well-sorted	4.46	28978	28.98	Base of white ss
A113					Orange top soil
A114					
A115					
A116					
A117					
A118	**Sorting**	**Perm (log)**	**Perm (md)**	**Perm (D)**	**Location**
A119	N/A	N/A	N/A	N/A	Calcite nodules on surface
A120	Well-sorted	4.34	21685	21.68	Top of orange ss
A121	Mod well-sorted	4.05	11332	11.33	Surface pink ss w/ thin lamination
A122	Mod well-sorted	3.89	7815	7.81	Surface pink ss w/ thin lamination
A123	Well-sorted	4.08	12113	12.11	Surface pink ss w/ thin lamination
A124	Mod well-sorted	3.96	9034	9.03	Surface pink ss w/ thin lamination
A125	Well-sorted	4.25	17931	17.93	White ss
A126	Mod well-sorted	4.09	12182	12.18	Orange top soil
A127					
A128					
A129					
A130					
A131	**Sorting**	**Perm (log)**	**Perm (md)**	**Perm (D)**	**Location**
A132	Mod well-sorted	4.39	24613	24.61	Surface of white ss
A133	Mod well-sorted	4.54	34310	34.31	Top of white ss
A134	Mod sorted	4.10	12468	12.47	Middle of white ss
A135	Well-sorted	4.56	36312	36.31	
A136	Well-sorted	4.51	32264	32.26	Base of white ss
A137	Well-sorted	4.58	37774	37.77	Top of orange ss
A138	Mod well-sorted	4.41	25769	25.77	Middle of orange ss
A139	Mod well-sorted	4.40	25134	25.13	Erosional unit (weathered ss)
A140	Well-sorted	4.61	40494	40.49	Top of white ss
A141	Mod well-sorted	4.56	36372	36.37	Base of white ss
A142	Mod well-sorted	4.47	29212	29.21	Orange top soil
A143					
A144					

	Sorting	Perm (log)	Perm (md)	Perm (D)	Location
A145					
A146					
A147	**Sorting**	**Perm (log)**	**Perm (md)**	**Perm (D)**	**Location**
A148					Surface of red ss
A149	Well-sorted	4.47	29421	29.42	Top of orange ss
A150					
A151	Mod well-sorted	4.40	25372	25.37	Orange ss
A152	Mod sorted	4.04	10963	10.96	Top of erosional unit (shale & ss)
A153	Mod well-sorted	4.49	30828	30.83	Middle erosional unit (shale & ss)
A154	Mod well-sorted	4.37	23659	23.66	Base of erosional unit (shale & ss)
A155					
A156	Mod well-sorted	4.23	16908	16.91	Orange ss
A157					
A158					
A159	Well-sorted	4.50	31323	31.32	White ss (well-cemented)
A160	Well-sorted	4.74	54429	54.43	White ss w/ ripples & laminations
A161					Orange top soil
A162					
A163					
A164					
A165					
A166	**Sorting**	**Perm (log)**	**Perm (md)**	**Perm (D)**	**Location**
A167	Mod well-sorted	4.53	34240	34.24	Surface of orange ss (bar #3)
A168	Mod sorted	4.42	26284	26.28	Surface of orange ss (bar #2)
A169	Mod sorted	4.31	20303	20.30	Surface of orange ss (bar #1)
A170	Mod well-sorted	4.35	22589	22.59	Erosional unit (shale & ss)
A171	Mod sorted	4.23	17105	17.10	Erosional unit (shale)
A172	Mod sorted	4.27	18425	18.43	Surface of yellow ss
A173	Mod sorted	4.31	20363	20.36	Surface of white ss
A174	Mod sorted	4.25	17604	17.60	Pink ss
A175	Mod well-sorted	4.27	18424	18.42	White ss
A176	Mod sorted	4.45	27956	27.96	Orange ss
A177	Mod sorted	4.71	51100	51.10	Base of orange ss
A178	Mod well-sorted	4.50	31700	31.70	Orange top soil

APPENDIX A

TRANSECT DATA (Rock Creek Rd.)

Guide Number	Depth Interval (in)	Depth Interval (ft)	Total Count (ppm)	Potassium K (%)	Uranium U (ppm)	Thorium Th (ppm)	API
	Begin Transect (0.0 mi)						
	Intersection of Rock Creek Rd and Peebly Rd.						
	Outcrop #1 (1.1 mi)						
R1	0.0	0.00	8.1	0.6	0.7	6.4	40.80
R2	6.0	0.50	5.6	0.4	0.5	3.6	24.80
R3	11.0	0.92	5.6	0.3	1.1	3.1	26.00
R4	17.5	1.46	5.2	0.3	0.5	4.3	26.00
R5	34.5	2.87	6.8	0.4	1.3	4.7	35.60
R6	44.5	3.71	6.0	0.4	1.0	4.9	34.00
R7	50.5	4.21	6.7	0.4	1.1	5.1	35.60
R8	53.5	4.46	6.5	0.4	1.4	4.0	33.60
R9	59.5	4.96	6.2	0.5	0.1	5.0	28.80
R10	70.5	5.87	6.7	0.4	0.7	5.5	34.00
R11							
R12	*Outcrop #2A (.4 mi)*						
R13							
R14	**Depth**	**Depth**	**Total**	**Potassium**	**Uranium**	**Thorium**	
R15	Interval (in)	Interval (ft)	Count (ppm)	K (%)	U (ppm)	Th (ppm)	*API*
R16	0.0	0.00	5.6	0.3	0.5	4.9	28.40
R17	5.0	0.42	4.7	0.2	0.6	4.2	24.80
R18	22.0	1.83	4.0	0.2	0.4	2.1	14.80
R19	37.0	3.08	3.7	0.2	0.0	3.4	16.80
R20	55.0	4.58	3.2	0.1	0.0	2.0	9.60
R21	67.5	5.62	3.6	0.1	0.8	1.8	15.20
R22	75.5	6.29	3.5	0.2	0.0	3.1	15.60
R23	87.5	7.29	3.9	0.1	0.3	2.6	14.40
R24	101.5	8.45	4.0	0.1	0.8	2.6	18.40
R25							
R26	*Outcrop #2B (0 mi; 39 ft East of 2A)*						
R27							
R28	**Depth**	**Depth**	**Total**	**Potassium**	**Uranium**	**Thorium**	
R29	Interval (in)	Interval (ft)	Count (ppm)	K (%)	U (ppm)	Th (ppm)	*API*
R30	0.0	0.00	5.2	0.4	-0.2	3.6	19.20
R31	13.0	1.08	5.0	0.2	1.0	3.2	24.00
R32	26.0	2.17	4.7	0.2	0.6	3.8	23.20
R33	38.0	3.17	4.8	0.4	0.8	3.6	27.20
R34	49.0	4.08	5.6	0.4	0.6	3.7	26.00
R35	65.0	5.41	5.1	0.2	0.9	4.0	26.40
R36	77.0	6.41	4.7	0.2	0.6	3.0	20.00
R37	92.0	7.66	4.5	0.2	0.3	4.2	22.40
R38	100.0	8.33	4.8	0.3	0.6	2.8	20.80
R39	112.5	9.37	4.5	0.1	0.9	3.1	21.20
R40							
R41	*Outcrop #3 (1.0 mi)*						
R42							
R43	**Depth**	**Depth**	**Total**	**Potassium**	**Uranium**	**Thorium**	

124

	Interval (in)	Interval (ft)	Count (ppm)	K (%)	U (ppm)	Th (ppm)	*API*
R44							
R45	N/A	N/A	N/A	N/A	N/A	N/A	N/A
R46	0.0	0.00	6.4	0.6	0.5	3.6	28.00
R47	12.0	1.00	6.0	0.3	0.7	4.2	27.20
R48	32.0	2.67	5.5	0.4	0.3	4.6	27.20
R49	42.0	3.50	6.6	0.5	1.2	3.3	30.80
R50	56.0	4.66	7.2	0.5	1.1	3.8	32.00
R51	70.0	5.83	8.2	0.4	1.8	4.7	39.60
R52	80.0	6.66	8.9	0.6	0.8	7.1	44.40
R53							
R54	*Outcrop #4A (.2 mi)*						
R55							
R56	**Depth**	**Depth**	**Total**	**Potassium**	**Uranium**	**Thorium**	
R57	**Interval (in)**	**Interval (ft)**	**Count (ppm)**	**K (%)**	**U (ppm)**	**Th (ppm)**	*API*
R58	0	0.00	9.3	0.8	1.0	6.7	47.60
R59	8	0.67	9.4	0.8	0.8	6.0	43.20
R60	17.0	1.42	10.7	0.8	1.4	7.7	54.80
R61	32.0	2.67	6.4	0.5	0.8	4.9	34.00
R62	47.0	3.92	7.8	0.6	0.7	4.1	31.60
R63	60.0	5.00	6.7	0.4	0.6	4.3	28.40
R64	71.0	5.91	7.0	0.5	0.7	5.5	35.60
R65	83.0	6.91	8.6	0.5	1.9	4.8	42.40
R66	94.0	7.83	9.5	0.8	0.6	6.9	45.20
R67	100.0	8.33	10.0	0.6	1.5	8.4	55.20
R68	108.0	9.00	11.0	0.6	2.7	6.6	57.60
R69	121.0	10.08	8.9	0.5	1.8	6.4	48.00
R70							
R71	*Outcrop #4B (0 mi; 44 ft East of 4A)*						
R72							
R73	**Depth**	**Depth**	**Total**	**Potassium**	**Uranium**	**Thorium**	
R74	**Interval (in)**	**Interval (ft)**	**Count (ppm)**	**K (%)**	**U (ppm)**	**Th (ppm)**	*API*
R75	0.0	0.00	8.7	0.5	1.3	6.9	46.00
R76	5.0	0.42	8.5	0.7	0.7	7.0	44.80
R77	15.0	1.25	6.5	0.3	1.4	4.6	34.40
R78	21.0	1.75	4.5	0.4	0.1	3.1	19.60
R79	37.0	3.08	3.8	0.2	-0.2	4.3	18.80
R80	46.0	3.83	4.3	0.3	0.2	2.9	18.00
	End of Transect (.3 mi)						
	Intersection of Rock Creed Rd and Newalla Rd.						
	Total Distance (3.0 mi)						

125

Guide Number	Sample #	F5	F16	F50	F84	F95	Avg Grain Size (phi)	Size	Std. Dev
R1	10	1.92	2.17	2.65	3.17	3.62	2.66	F sand	0.51
R2	9	2.03	2.22	2.50	3.07	3.60	2.60	F sand	0.45
R3	8	2.20	2.62	3.20	3.67	4.14	3.16	VF sand	0.56
R4	7	1.60	2.09	2.44	2.90	3.35	2.48	F sand	0.47
R5	6	1.79	2.00	2.35	2.98	3.47	2.44	F sand	0.50
R6	5	2.14	2.45	2.95	3.48	3.78	2.96	F sand	0.51
R7	4	1.29	1.84	2.90	3.68	4.30	2.81	F sand	0.92
R8	3	2.14	2.82	3.28	3.67	4.10	3.26	VF sand	0.51
R9	2	2.00	2.38	3.14	3.65	4.20	3.06	VF sand	0.65
R10	1	2.05	2.33	2.83	3.36	3.69	2.84	F sand	0.51
R11									
R12									
R13									
R14							Avg Grain		
R15	Sample #	F5	F16	F50	F84	F95	Size (phi)	Size	Std. Dev
R16	19	2.40	3.25	3.61	4.03	4.28	3.63	VF sand	0.48
R17	18	2.02	2.25	2.57	3.08	3.60	2.63	F sand	0.45
R18	17	1.77	2.05	2.36	2.91	3.39	2.44	F sand	0.46
R19	16	1.45	1.97	2.33	2.87	3.36	2.39	F sand	0.51
R20	15	1.72	2.03	2.28	2.67	3.20	2.33	F sand	0.38
R21	14	1.67	1.99	2.22	2.59	3.18	2.27	F sand	0.38
R22	13	1.52	1.97	2.23	2.54	3.20	2.25	F sand	0.40
R23	12	1.68	2.05	2.31	2.66	3.05	2.34	F sand	0.36
R24	11	1.65	2.15	2.40	2.83	3.08	2.46	F sand	0.39
R25									
R26									
R27									
R28							Avg Grain		
R29	Sample #	F5	F16	F50	F84	F95	Size (phi)	Size	Std. Dev
R30	29	1.87	2.19	2.50	3.10	3.64	2.60	F sand	0.50
R31	28	2.00	2.28	2.78	3.25	3.68	2.77	F sand	0.50
R32	27	2.13	2.31	2.81	3.28	3.68	2.80	F sand	0.48
R33	26	2.17	2.47	2.98	3.53	3.85	2.99	F sand	0.52
R34	25	2.05	2.72	3.16	3.63	4.00	3.17	VF sand	0.52
R35	24	1.73	2.08	2.40	2.97	3.57	2.48	F sand	0.50
R36	23	1.98	2.30	2.80	3.16	3.50	2.75	F sand	0.45
R37	22	1.87	2.33	2.81	3.18	3.55	2.77	F sand	0.47
R38	21	2.00	2.28	2.76	3.13	3.50	2.72	F sand	0.44
R39	20	1.87	2.25	2.60	3.08	3.55	2.64	F sand	0.46
R40									
R41									
R42									
R43							Avg Grain		

R44	Sample #	F5	F16	F50	F84	F95	Size (phi)	Size	Std. Dev
R45	36	N/A	N/A	N/A	N/A	N/A	N/A	N/A	N/A
R46	35	1.32	1.54	2.15	2.72	3.10	2.14	F sand	0.56
R47	34	1.12	1.31	1.65	2.27	2.95	1.74	M sand	0.52
R48	33	1.22	1.32	1.60	2.23	3.23	1.72	M sand	0.53
R49	32	1.18	1.41	2.07	2.70	3.32	2.06	F sand	0.65
R50	31	0.60	1.12	1.76	2.67	3.66	1.85	M sand	0.85
R51	30	0.76	1.17	1.81	3.08	4.00	2.02	F sand	0.97
R52									
R53									
R54									
R55									
R56							Avg Grain		
R57	Sample #	F5	F16	F50	F84	F95	Size (phi)	Size	Std. Dev
R58	54	2.25	2.85	3.50	4.16	4.80	3.50	VF sand	0.71
R59	53	1.37	1.90	3.08	3.69	4.33	2.89	F sand	0.90
R60	52	1.22	1.41	2.02	4.06	4.74	2.50	F sand	1.20
R61	51	1.49	2.07	2.64	3.18	3.87	2.63	F sand	0.64
R62	50	1.72	2.13	2.65	3.31	4.12	2.70	F sand	0.66
R63	49	1.57	1.91	2.24	3.03	3.72	2.39	F sand	0.61
R64	48	1.47	1.88	2.16	2.50	2.85	2.18	F sand	0.36
R65	47	1.33	1.60	2.05	2.42	4.00	2.02	F sand	0.61
R66	46	1.24	1.38	1.78	2.50	3.84	1.89	M sand	0.67
R67	45	1.43	1.86	2.28	2.87	3.73	2.34	F sand	0.60
R68	44	1.47	1.90	2.38	2.98	3.68	2.42	F sand	0.60
R69	43	2.00	2.58	2.98	3.68	4.72	3.08	VF sand	0.69
R70									
R71									
R72									
R73							Avg Grain		
R74	Sample #	F5	F16	F50	F84	F95	Size (phi)	Size	Std. Dev
R75	42	2.05	2.73	3.11	3.63	4.17	3.16	VF sand	0.55
R76	41	1.52	2.83	3.50	4.05	4.58	3.46	VF sand	0.77
R77	40	1.42	1.91	3.00	3.79	4.65	2.90	VF sand	0.96
R78	39	1.33	1.49	2.02	2.32	2.78	1.94	M sand	0.43
R79	38	1.39	1.65	2.06	2.45	2.95	2.05	F sand	0.44
R80	37	1.47	1.82	2.15	2.49	2.96	2.15	F sand	0.39

Guide Number	Sorting	Perm (log)	Perm (md)	Perm (D)	Location
R1	Mod well-sorted	4.41	25753	25.75	White ss (bar surface)
R2	Well-sorted	4.48	30012	30.01	White ss (bar surface)
R3	Mod well-sorted	4.10	12602	12.60	White ss (bar surface)
R4	Well-sorted	4.54	34470	34.47	Orange/white ss (bar side)
R5	Mod well-sorted	4.54	34734	34.73	Orange ss (bar side)
R6	Mod well-sorted	4.24	17450	17.45	White ss (bar side)
R7	Mod sorted	4.13	13388	13.39	Erosional unit
R8	Mod well-sorted	4.07	11755	11.76	Top of white ss
R9	Mod well-sorted	4.11	13026	13.03	Middle of white ss
R10	Mod well-sorted	4.31	20440	20.44	Base of white ss
R11					
R12					
R13					
R14					
R15	Sorting	Perm (log)	Perm (md)	Perm (D)	Location
R16	Well-sorted	3.87	7433	7.43	Surface of orange/white ss
R17	Well-sorted	4.46	28709	28.71	Orange/white ss
R18	Well-sorted	4.56	36475	36.47	Orange/white ss
R19	Mod well-sorted	4.56	36639	36.64	Middle of orange/white ss
R20	Well-sorted	4.66	46193	46.19	Yellow ss
R21	Well-sorted	4.70	50306	50.31	Yellow ss
R22	Well-sorted	4.70	50587	50.59	White ss
R23	Well-sorted	4.67	46654	46.65	White ss
R24	Well-sorted	4.59	38640	38.64	Base of white ss
R25					
R26					
R27					
R28					
R29	Sorting	Perm (log)	Perm (md)	Perm (D)	Location
R30	Mod well-sorted	4.45	28502	28.50	Surface of orange ss
R31	Mod well-sorted	4.35	22645	22.65	Top of orange ss
R32	Well-sorted	4.35	22261	22.26	Base of orange ss
R33	Mod well-sorted	4.22	16443	16.44	White ss
R34	Mod well-sorted	4.11	12977	12.98	Middle of white ss
R35	Mod well-sorted	4.52	32884	32.88	White ss
R36	Well-sorted	4.39	24553	24.55	White ss
R37	Well-sorted	4.37	23330	23.33	White ss
R38	Well-sorted	4.41	25705	25.71	White ss
R39	Well-sorted	4.44	27849	27.85	Base of white ss
R40					
R41					
R42					
R43					

R44	Sorting	Perm (log)	Perm (md)	Perm (D)	Location
R45	N/A	N/A	N/A	N/A	Fe oxide rock
R46	Mod well-sorted	4.68	48315	48.32	Top of orange ss
R47	Mod well-sorted	4.93	85648	85.65	Orange ss
R48	Mod well-sorted	4.94	87232	87.23	Orange ss
R49	Mod well-sorted	4.69	48685	48.68	Orange ss
R50	Mod sorted	4.71	50876	50.88	Orange ss
R51	Mod sorted	4.55	35578	35.58	Base of orange ss
R52					Orange top soil
R53					
R54					
R55					
R56					
R57	Sorting	Perm (log)	Perm (md)	Perm (D)	Location
R58	Mod sorted	3.83	6728	6.73	Surface of white ss
R59	Mod sorted	4.09	12273	12.27	Base of white ss
R60	Poorly sorted	4.17	14649	14.65	Erosional unit
R61	Mod well-sorted	4.37	23193	23.19	Surface white/orange ss w/ ripples
R62	Mod well-sorted	4.32	20751	20.75	Top of white ss
R63	Mod well-sorted	4.52	32873	32.87	White ss
R64	Well-sorted	4.76	57346	57.35	White ss
R65	Mod well-sorted	4.73	53307	53.31	Orange/white ss
R66	Mod well-sorted	4.77	59316	59.32	Base of orange/white ss
R67	Mod well-sorted	4.55	35616	35.62	Thin bedded orange/white ss
R68	Mod well-sorted	4.50	31770	31.77	Thick bedded orange/white ss
R69	Mod well-sorted	4.08	12120	12.12	Surface of white ss
R70					
R71					
R72					
R73					
R74	Sorting	Perm (log)	Perm (md)	Perm (D)	Location
R75	Mod well-sorted	4.11	12862	12.86	Surface of white ss
R76	Mod sorted	3.83	6693	6.69	Pink ss
R77	Mod sorted	4.05	11268	11.27	Orange ss
R78	Well-sorted	4.86	72908	72.91	Orange/white ss
R79	Well-sorted	4.80	62412	62.41	Orange ss
R80	Well-sorted	4.76	57457	57.46	Base of orange ss

APPENDIX A

TRANSECT DATA (Franklin Rd.)

Guide Number	Depth Interval (in)	Depth Interval (ft)	Total Count (ppm)	Potassium K (%)	Uranium U (ppm)	Thorium Th (ppm)	API
	Begin Transect (0.0 mi)						
	Intersection of Franklin Rd and Peebly Rd.						
	Outcrop #1A (.1 mi)						
F1	0.0	0.00	6.4	0.3	1.2	5.0	34.40
F2	6.0	0.50	5.8	0.4	0.7	3.50	26.00
F3	15.0	1.25	5.9	0.4	1.1	3.2	28.00
F4	23.5	1.96	6.2	0.5	0.5	3.5	26.00
F5	30.5	2.54	5.0	0.4	0.6	2.9	22.80
F6	39.5	3.29	5.0	0.3	0.5	2.9	20.40
F7	49.5	4.12	5.1	0.3	0.8	3.1	23.60
F8							
F9	*Outcrop #1B (0 mi; 127 ft East of 1A)*						
F10							
F11	Depth Interval (in)	Depth Interval (ft)	Total Count (ppm)	Potassium K (%)	Uranium U (ppm)	Thorium Th (ppm)	*API*
F13	0.0	0.00	5.5	0.3	0.3	3.7	22.00
F14	8.0	0.67	5.8	0.3	1.1	3.7	28.40
F15	24.0	2.00	8.7	0.7	0.6	7.9	47.60
F16	39.0	3.25	5.6	0.3	0.6	5.2	30.40
F17	46.5	3.87	5.2	0.3	0.5	3.6	23.20
F18	59.5	4.96	5.2	0.2	1.0	4.3	28.40
F19	72.0	6.00	6.6	0.4	0.3	5.5	30.80
F20	78.0	6.50	5.2	0.3	0.5	3.8	24.00
F21	92.0	7.66	5.1	0.1	1.1	3.3	23.60
F22							
F23	*Outcrop #2 (.3 mi)*						
F24							
F25	Depth Interval (in)	Depth Interval (ft)	Total Count (ppm)	Potassium K (%)	Uranium U (ppm)	Thorium Th (ppm)	*API*
F27	0.0	0.00	5.7	0.4	0.4	4.2	26.40
F28	4.0	0.33	4.8	0.3	0.8	3.1	23.60
F29	12.0	1.00	4.6	0.3	0.5	3.4	22.40
F30	20.0	1.67	4.6	0.3	0.1	2.8	16.80
F31	28.5	2.37	4.5	0.4	0.1	2.7	18.00
F32	38.5	3.21	4.4	0.3	0.2	2.8	17.60
F33	49.5	4.12	4.9	0.3	0.2	2.8	17.60
F34							
F35	*Outcrop #3 (.6 mi)*						
F36							
F37	Depth Interval (in)	Depth Interval (ft)	Total Count (ppm)	Potassium K (%)	Uranium U (ppm)	Thorium Th (ppm)	*API*
F39	0.0	0.00	5.5	0.2	1.0	4.9	30.80
F40	10.0	0.83	3.9	0.2	0.1	2.9	15.60
F41	19.0	1.58	3.6	0.1	0.3	2.6	14.40
F42	24.0	2.00	4.1	0.1	0.7	2.9	18.80
F43	39.0	3.25	4.9	0.3	0.5	4.0	24.80

	Depth Interval (in)	Depth Interval (ft)	Total Count (ppm)	Potassium K (%)	Uranium U (ppm)	Thorium Th (ppm)	API
F44	44.0	3.67	5.1	0.3	0.7	3.2	23.20
F45	53.0	4.41	5.6	0.3	0.3	4.9	26.80
F46	61.0	5.08	6.2	0.2	0.8	5.8	32.80
F47	69.0	5.75	6.1	0.3	0.4	4.5	26.00
F48							
F49	*Outcrop #4 (1.5 mi)*						
F50							
F51	**Depth**	**Depth**	**Total**	**Potassium**	**Uranium**	**Thorium**	
F52	**Interval (in)**	**Interval (ft)**	**Count (ppm)**	**K (%)**	**U (ppm)**	**Th (ppm)**	***API***
F53	0	0.00	6.7	0.3	1.8	4.9	38.80
F54	11.0	0.92	4.3	0.2	0.5	3.0	19.20
F55	24.0	2.00	3.8	0.2	0.7	1.6	15.20
F56	34.0	2.83	4.5	0.2	0.8	2.4	19.20
F57	49.0	4.08	3.8	0.2	0.5	2.7	18.00
F58	59.0	4.91	4.1	0.2	0.4	2.3	15.60
F59	69.5	5.79	5.4	0.4	0.3	4.3	26.00
F60	76.5	6.37	5.6	0.3	1.2	4.0	30.40
F61	84.0	7.00	4.6	0.2	0.7	2.4	18.40
F62							
F63	*Outcrop #5 (.6 mi)*						
F64							
F65	**Depth**	**Depth**	**Total**	**Potassium**	**Uranium**	**Thorium**	
F66	**Interval (in)**	**Interval (ft)**	**Count (ppm)**	**K (%)**	**U (ppm)**	**Th (ppm)**	***API***
F67	0.0	0.00	10.2	0.7	1.7	7.1	53.20
F68	10.0	0.83	13.4	1.2	1.4	10.6	72.80
F69	19.0	1.58	9.7	0.7	1.0	8.3	52.40
F70	33.0	2.75	6.5	0.4	0.8	5.0	32.80
F71	41.0	3.42	6.6	0.4	0.4	5.6	32.00
F72	52.0	4.33	6.5	0.3	0.7	5.2	31.20
F73	62.0	5.16	6.7	0.3	1.1	6.1	38.00
F74							
F75	*Outcrop #6 (1.2 mi)*						
F76							
F77	**Depth**	**Depth**	**Total**	**Potassium**	**Uranium**	**Thorium**	
F78	**Interval (in)**	**Interval (ft)**	**Count (ppm)**	**K (%)**	**U (ppm)**	**Th (ppm)**	***API***
F79	0.0	0.00	4.8	0.4	0.2	3.2	20.80
F80	12.5	1.04	4.7	0.3	0.7	2.8	21.60
F81	27.5	2.29	5.8	0.5	0.6	3.8	28.00
F82	38.5	3.21	4.9	0.3	0.1	4.2	22.40
F83	52.5	4.37	5.4	0.4	0.7	3.6	26.40
F84	62.0	5.16	5.2	0.5	0.5	1.5	18.00
F85	72.0	6.00	4.8	0.4	0.0	2.9	18.00
F86	88.0	7.33	4.5	0.3	0.2	3.5	20.40
	End of Transect (.7 mi)						
	Intersection of 180th Ave and Fishmarket Rd.						
	Total Distance (5.0 mi)						

Guide Number	Sample #	F5	F16	F50	F84	F95	Avg Grain Size (phi)	Size	Std. Dev
F1	7	2.71	2.97	3.42	3.92	4.78	3.44	VF sand	0.55
F2	6	2.77	3.02	3.43	3.77	4.18	3.41	VF sand	0.40
F3	5	2.48	2.74	3.04	3.53	4.13	3.10	VF sand	0.45
F4	4	2.40	2.65	2.92	3.37	3.85	2.98	F sand	0.40
F5	3	2.25	2.57	2.95	3.60	4.70	3.04	VF sand	0.63
F6	2	2.03	2.22	2.50	2.97	3.77	2.56	F sand	0.45
F7	1	1.98	2.12	2.40	2.83	3.50	2.45	F sand	0.41
F8									
F9									
F10									
F11							Avg Grain		
F12	Sample #	F5	F16	F50	F84	F95	Size (phi)	Size	Std. Dev
F13	16	2.03	2.58	2.80	3.35	3.90	2.91	F sand	0.48
F14	15	2.00	2.22	2.75	3.34	3.86	2.77	F sand	0.56
F15	14	1.94	2.18	2.61	3.34	4.73	2.71	F sand	0.71
F16	13	1.92	2.10	2.57	3.33	4.12	2.67	F sand	0.64
F17	12	1.98	2.23	2.82	3.23	3.75	2.76	F sand	0.52
F18	11	2.00	2.16	2.47	3.03	3.67	2.55	F sand	0.47
F19	10	1.97	2.58	2.92	3.89	4.78	3.13	VF sand	0.75
F20	9	2.57	2.62	2.89	3.57	4.33	3.03	VF sand	0.50
F21	8	2.08	2.37	2.76	3.23	3.74	2.79	F sand	0.47
F22									
F23									
F24									
F25							Avg Grain		
F26	Sample #	F5	F16	F50	F84	F95	Size (phi)	Size	Std. Dev
F27	23	1.82	2.14	2.71	3.58	4.10	2.81	F sand	0.71
F28	22	1.90	2.20	2.81	3.57	4.61	2.86	F sand	0.75
F29	21	1.64	2.00	2.41	3.00	4.18	2.47	F sand	0.63
F30	20	1.67	2.07	2.64	3.26	3.75	2.66	F sand	0.61
F31	19	1.51	1.89	2.30	2.90	3.56	2.36	F sand	0.56
F32	18	1.79	2.10	2.55	3.10	3.75	2.58	F sand	0.55
F33	17	2.00	2.57	2.70	3.26	3.70	2.84	F sand	0.43
F34									
F35									
F36									
F37							Avg Grain		
F38	Sample #	F5	F16	F50	F84	F95	Size (phi)	Size	Std. Dev
F39	32	1.31	1.88	2.35	3.82	4.75	2.68	F sand	1.01
F40	31	1.41	1.85	2.19	2.83	3.35	2.29	F sand	0.54
F41	30	1.88	2.07	2.34	2.70	3.27	2.37	F sand	0.37
F42	29	1.75	1.99	2.23	2.57	3.14	2.26	F sand	0.36
F43	28	1.00	1.14	1.86	2.35	3.00	1.78	M sand	0.61

	Sample #	F5	F16	F50	F84	F95	Avg Grain Size (phi)	Size	Std. Dev
F44	27	1.53	1.84	2.09	2.41	2.82	2.11	F sand	0.34
F45	26	1.90	2.04	2.27	3.33	4.14	2.55	F sand	0.66
F46	25	1.40	2.00	2.73	3.40	4.02	2.71	F sand	0.75
F47	24	1.04	1.30	1.80	2.44	3.15	1.85	M sand	0.60
F48									
F49									
F50									
F51							Avg Grain		
F52	Sample #	F5	F16	F50	F84	F95	Size (phi)	Size	Std. Dev
F53	41	2.35	2.72	3.36	3.84	4.70	3.31	VF sand	0.64
F54	40	1.93	2.21	2.75	3.30	3.85	2.75	F sand	0.56
F55	39	1.90	2.17	2.77	3.30	3.90	2.75	F sand	0.59
F56	38	2.00	2.27	2.75	3.29	3.55	2.77	F sand	0.49
F57	37	1.52	1.92	2.36	2.97	3.50	2.42	F sand	0.56
F58	36	1.75	2.05	2.50	3.23	3.80	2.59	F sand	0.61
F59	35	1.66	2.06	2.58	3.30	4.23	2.65	F sand	0.70
F60	34	1.50	1.92	2.37	3.17	3.98	2.49	F sand	0.69
F61	33	1.41	1.82	2.20	3.15	4.13	2.39	F sand	0.74
F62									
F63									
F64									
F65							Avg Grain		
F66	Sample #	F5	F16	F50	F84	F95	Size (phi)	Size	Std. Dev
F67	56	1.93	2.65	3.50	4.24	4.85	3.46	VF sand	0.84
F68	55	1.77	2.73	3.58	4.04	4.78	3.45	VF sand	0.78
F69	54	1.90	2.65	3.51	4.24	4.89	3.47	VF sand	0.85
F70	53	1.56	1.93	2.36	3.03	3.50	2.44	F sand	0.57
F71	52	1.56	2.08	2.81	3.54	4.15	2.81	F sand	0.76
F72	51	1.32	1.83	2.43	3.40	4.12	2.55	F sand	0.82
F73	50	1.30	1.87	2.47	3.48	4.25	2.61	F sand	0.85
F74									
F75									
F76									
F77							Avg Grain		
F78	Sample #	F5	F16	F50	F84	F95	Size (phi)	Size	Std. Dev
F79	49	1.50	2.05	2.48	2.85	3.50	2.46	F sand	0.50
F80	48	1.83	2.10	2.53	3.00	3.78	2.54	F sand	0.52
F81	47	1.97	2.35	2.82	3.67	4.78	2.95	F sand	0.76
F82	46	2.00	2.30	2.65	3.07	3.90	2.67	F sand	0.43
F83	45	1.55	2.24	2.56	2.95	3.75	2.58	F sand	0.51
F84	44	1.73	2.13	2.60	3.14	4.00	2.62	F sand	0.60
F85	43	1.95	2.57	2.65	3.02	4.07	2.75	F sand	0.43
F86	42	1.75	2.10	2.51	2.85	3.48	2.49	F sand	0.45

Guide Number	Sorting	Perm (log)	Perm (md)	Perm (D)	Location
F1	Mod well-sorted	3.95	8842	8.84	Surface of white ss (bar)
F2	Well-sorted	4.04	10913	10.91	Top of light orange ss (bar)
F3	Well-sorted	4.19	15440	15.44	Middle of orange ss (bar)
F4	Well-sorted	4.28	19183	19.18	Base of orange ss (bar)
F5	Mod well-sorted	4.14	13655	13.65	Surface of red ss (bar)
F6	Well-sorted	4.50	31333	31.33	Erosional unit between 2 bars
F7	Well-sorted	4.58	38222	38.22	Base of red ss
F8					
F9					
F10					
F11					
F12	Sorting	Perm (log)	Perm (md)	Perm (D)	Location
F13	Well-sorted	4.29	19290	19.29	Surface of orange ss
F14	Mod well-sorted	4.32	21035	21.03	Base of orange ss
F15	Mod well-sorted	4.28	19171	19.17	Erosional unit (shale)
F16	Mod well-sorted	4.34	22030	22.03	Surface of purple ss (bar)
F17	Mod well-sorted	4.35	22400	22.40	Middle of purple ss (bar)
F18	Well-sorted	4.49	31055	31.05	Base of purple ss (bar)
F19	Mod sorted	4.02	10523	10.52	Ersosional unit
F20	Well-sorted	4.20	16015	16.01	Surface of red ss (bar)
F21	Well-sorted	4.36	22937	22.94	Base of red ss
F22					
F23					
F24					
F25					
F26	Sorting	Perm (log)	Perm (md)	Perm (D)	Location
F27	Mod well-sorted	4.23	16943	16.94	Surface of white ss (bar)
F28	Mod sorted	4.18	15024	15.02	Surface of white ss (bar)
F29	Mod well-sorted	4.46	28745	28.74	Dark orange/pink surface
F30	Mod well-sorted	4.36	23050	23.05	Dark yellow ss
F31	Mod well-sorted	4.56	35901	35.90	Dark orange ss
F32	Mod well-sorted	4.44	27362	27.36	Dark orange ss
F33	Well-sorted	4.35	22188	22.19	Base of dark orange ss
F34					
F35					
F36					
F37					
F38	Sorting	Perm (log)	Perm (md)	Perm (D)	Location
F39	Poorly sorted	4.15	14215	14.21	Brown top soil
F40	Mod well-sorted	4.61	40649	40.65	Surface of yellow ss
F41	Well-sorted	4.65	44437	44.44	Top of yellow ss
F42	Well-sorted	4.71	51879	51.88	Yellow ss w/ orange zones
F43	Mod well-sorted	4.87	73479	73.48	Yellow ss

	Sorting	Perm (log)	Perm (md)	Perm (D)	Location
F44	Very well-sorted	4.81	64505	64.51	Base of yellow ss
F45	Mod well-sorted	4.40	25194	25.19	Dark orange ss
F46	Mod sorted	4.27	18438	18.44	Dark orange ss
F47	Mod well-sorted	4.83	67658	67.66	Base of dark orange ss
F48					
F49					
F50					
F51					
F52	**Sorting**	**Perm (log)**	**Perm (md)**	**Perm (D)**	**Location**
F53	Mod well-sorted	3.98	9528	9.53	Orange ss
F54	Mod well-sorted	4.33	21463	21.46	Pink ss
F55	Mod well-sorted	4.32	21114	21.11	Pink ss
F56	Well-sorted	4.36	22832	22.83	Pink ss
F57	Mod well-sorted	4.52	33487	33.49	Pink ss
F58	Mod well-sorted	4.40	25259	25.26	Orange ss
F59	Mod well-sorted	4.33	21159	21.16	Orange ss
F60	Mod well-sorted	4.42	26461	26.46	Orange ss
F61	Mod sorted	4.45	28188	28.19	Brown ss
F62					
F63					
F64					
F65					
F66	**Sorting**	**Perm (log)**	**Perm (md)**	**Perm (D)**	**Location**
F67	Mod sorted	3.79	6144	6.14	Orange top soil
F68	Mod sorted	3.82	6668	6.67	Top soil w/ shale & ss
F69	Mod sorted	3.78	6044	6.04	Orange top soil
F70	Mod well-sorted	4.51	32235	32.24	Surface of dark orange ss
F71	Mod sorted	4.20	15969	15.97	Bands of multi-colored ss
F72	Mod sorted	4.32	20935	20.94	Bands of multi-colored ss
F73	Mod sorted	4.27	18800	18.80	Base of dark orange ss
F74					
F75					
F76					
F77					
F78	**Sorting**	**Perm (log)**	**Perm (md)**	**Perm (D)**	**Location**
F79	Well-sorted	4.53	33844	33.84	Thin surface of orange ss
F80	Mod well-sorted	4.47	29728	29.73	Top of orange ss
F81	Mod sorted	4.13	13362	13.36	Middle of orange ss
F82	Well-sorted	4.42	26216	26.22	Base of orange ss
F83	Mod well-sorted	4.46	28511	28.51	Surface of orange ss
F84	Mod well-sorted	4.39	24535	24.53	Middle of dark orange ss
F85	Well-sorted	4.40	25099	25.10	Dark orange ss
F86	Well-sorted	4.54	34725	34.72	Base of dark orange ss

APPENDIX A

TRANSECT DATA (Newalla Rd.)

.

Guide Number	Depth Interval (in)	Depth Interval (ft)	Total Count (ppm)	Potassium K (%)	Uranium U (ppm)	Thorium Th (ppm)	API
	Begin Transect (0.0 mi)						
	Intersection of Highway 9 and Newalla Rd.						
	Outcrop #1 (.8 mi)						
Guide Number	**Depth Interval (in)**	**Depth Interval (ft)**	**Total Count (ppm)**	**Potassium K (%)**	**Uranium U (ppm)**	**Thorium Th (ppm)**	**API**
N1	0.0	0.00	4.8	0.3	0.5	2.1	17.20
N2	9.0	0.75	4.8	0.3	0.6	2.50	19.60
N3	22.0	1.83	5.3	0.3	0.7	3.2	23.20
N4	37.0	3.08	4.8	0.3	0.2	4.2	23.20
N5	48.0	4.00	4.6	0.3	0.2	3.7	21.20
N6	59.0	4.91	5.0	0.2	0.9	3.5	24.40
N7	68.0	5.66	4.7	0.2	1.0	2.7	22.00
N8	81.0	6.75	4.2	0.2	0.5	2.7	18.00
N9	92.0	7.66	4.3	0.2	0.7	2.2	17.60
N10	105.0	8.75	5.1	0.3	0.3	4.0	23.20
N11	122.0	10.16	3.9	0.2	-0.2	3.5	15.60
N12	133.0	11.08	3.8	0.2	0.4	1.6	12.80
N13							
N14	*Outcrop #2 (.6 mi)*						
N15							
N16	**Depth Interval (in)**	**Depth Interval (ft)**	**Total Count (ppm)**	**Potassium K (%)**	**Uranium U (ppm)**	**Thorium Th (ppm)**	
N17							*API*
N18	0.0	0.00	4.8	0.3	0.1	3.6	20.00
N19	8.0	0.67	4.2	0.3	0.5	2.6	19.20
N20	20.0	1.67	5.1	0.4	0.1	3.6	21.60
N21	30.0	2.50	4.7	0.2	0.4	3.8	21.60
N22	43.0	3.58	4.4	0.3	0.5	2.6	19.20
N23	54.0	4.50	5.4	0.3	1.3	2.1	23.60
N24	67.0	5.58	5.4	0.3	0.5	4.2	25.60
N25	87.0	7.25	5.3	0.3	0.8	3.5	25.20
N26							
N27	*Outcrop #3 (.2 mi)*						
N28							
N29	**Depth Interval (in)**	**Depth Interval (ft)**	**Total Count (ppm)**	**Potassium K (%)**	**Uranium U (ppm)**	**Thorium Th (ppm)**	
N30							*API*
N31	0.0	0.00	16.4	1.6	1.1	13.5	88.40
N32	10.0	0.83	15.6	1.4	1.8	11.8	84.00
N33	27.0	2.25	15.4	1.2	1.9	13.7	89.20
N34	37.0	3.08	14.4	1.2	1.8	11.2	78.40
N35	43.0	3.58	12.4	0.9	1.8	9.5	66.80
N36	52.0	4.33	9.9	0.9	0.7	8.8	55.20
N37	57.0	4.75	8.8	0.6	1.6	6.2	47.20
N38	66.0	5.50	6.1	0.3	0.4	5.1	28.40
N39	75.0	6.25	5.6	0.3	0.9	4.0	28.00
N40							
N41	*Outcrop #4 (0 mi; 85 ft North of 3)*						
N42							
N43	**Depth**	**Depth**	**Total**	**Potassium**	**Uranium**	**Thorium**	

	Interval (in)	Interval (ft)	Count (ppm)	K (%)	U (ppm)	Th (ppm)	*API*
N44							
N45	0	0.00	14.8	1.2	1.8	11.7	80.40
N46	14.0	1.17	17.2	1.5	2.5	12.2	92.80
N47	29.0	2.42	19.2	1.8	2.3	14.1	103.60
N48	49.0	4.08	18.3	1.3	4.3	11.5	101.20
N49	67.0	5.58	15.3	1.2	1.0	14.2	84.00
N50	74.0	6.16	13.5	1.1	2.0	9.6	72.00
N51	87.0	7.25	16.2	1.1	3.8	10.5	90.00
N52							
N53	*Outcrop #5 (.1 mi)*						
N54							
N55	**Depth**	**Depth**	**Total**	**Potassium**	**Uranium**	**Thorium**	
N56	Interval (in)	Interval (ft)	Count (ppm)	K (%)	U (ppm)	Th (ppm)	*API*
N57	0	0.00	4.9	0.3	0.9	3.3	25.20
N58	10.0	0.83	5.0	0.2	1.1	2.9	23.60
N59	27.0	2.25	4.4	0.2	0.6	2.9	19.60
N60	40.0	3.33	4.2	0.2	0.5	2.7	18.00
N61	52.0	4.33	4.1	0.2	0.1	3.3	17.20
N62	66.0	5.50	3.3	0.2	0.0	1.7	10.00
N63							
N64	*Outcrop #6 (.5 mi)*						
N65							
N66	**Depth**	**Depth**	**Total**	**Potassium**	**Uranium**	**Thorium**	
N67	Interval (in)	Interval (ft)	Count (ppm)	K (%)	U (ppm)	Th (ppm)	*API*
N68	0	0.00	7.5	0.3	1.4	5.3	37.20
N69	7.0	0.58	7.0	0.4	1.5	3.9	34.00
N70	17.0	1.42	7.0	0.3	1.4	5.8	39.20
N71	26.0	2.17	7.3	0.3	1.9	4.3	37.20
N72	36.0	3.00	5.7	0.5	0.4	4.4	28.80
N73	50.0	4.17	5.7	0.3	0.8	5.2	32.00
N74	65.0	5.41	4.6	0.2	0.2	4.0	20.80
N75							
N76	*Outcrop #7 (0 mi; 197 ft North of 6)*						
N77							
N78	**Depth**	**Depth**	**Total**	**Potassium**	**Uranium**	**Thorium**	
N79	Interval (in)	Interval (ft)	Count (ppm)	K (%)	U (ppm)	Th (ppm)	*API*
N80	N/A	N/A	6.1	0.3	0.4	5.1	N/A
N81	0.0	0.00	5.1	0.4	0.0	3.9	22.00
N82	10.0	0.83	4.9	0.2	0.6	3.6	22.40
N83	16.0	1.33	4.6	0.1	0.5	4.0	21.60
N84	26.0	2.17	5.2	0.3	0.7	3.1	22.80
N85	31.0	2.58	4.8	0.3	0.5	2.6	19.20
N86	43.0	3.58	5.2	0.3	0.8	3.6	25.60
N87	54.0	4.50	5.9	0.5	0.1	3.9	24.40
N88	67.0	5.58	5.9	0.4	1.0	2.9	26.00
N89	85.0	7.08	5.8	0.4	0.9	2.6	24.00
N90	93	7.75	5.7	0.5	0.4	4.7	30.00
N91	109	9.08	6.2	0.3	0.3	4.8	26.40
N92							
N93							

N94	*Outcrop #8 (.4 mi)*					
N95						
N96	**Depth**	**Depth**	**Total**	**Potassium**	**Uranium**	**Thorium**	
N97	**Interval (in)**	**Interval (ft)**	**Count (ppm)**	**K (%)**	**U (ppm)**	**Th (ppm)**	***API***
N98	0	0.00	8.1	0.5	1.6	4.9	40.40
N99	9.0	0.75	7.2	0.3	1.6	4.7	36.40
N100	20.0	1.67	5.1	0.3	1.3	3.2	28.00
N101	28.0	2.33	3.8	0.2	0.3	2.5	15.60
N102	41.0	3.42	3.1	0.1	0.5	1.8	12.80
N103	50.0	4.17	3.2	0.2	0.2	1.1	9.20
N104	65.0	5.41	3.7	0.1	0.5	2.3	14.80
N105	74.0	6.16	3.8	0.2	0.0	2.5	13.20
N106	87.0	7.25	3.9	0.2	-0.1	3.5	16.40
N107	101.0	8.41	4.0	0.1	0.3	2.8	15.20
N108	115	9.58	4.0	0.3	0.2	2.5	16.40
N109	125	10.41	3.7	0.1	0.2	3.3	16.40
N110	132.0	11.00	3.2	0.2	0.2	1.5	10.80
	End of Transect (.3 mi)					
	Intersection of Newalla Rd and Franklin Rd.					
	Total Distance (3.0 mi)					

140

Guide Number	Sample #	F5	F16	F50	F84	F95	Avg Grain Size (phi)	Size	Std. Dev
N1	66	1.29	1.50	2.04	2.45	3.74	2.00	F sand	0.61
N2	65	1.27	1.45	1.96	2.40	3.40	1.94	M sand	0.56
N3	64	1.65	2.10	2.75	3.51	4.16	2.79	F sand	0.73
N4	63	1.32	1.66	2.16	2.82	3.90	2.21	F sand	0.68
N5	62	1.52	1.91	2.27	2.85	3.50	2.34	F sand	0.54
N6	61	1.86	2.35	2.85	3.51	4.14	2.90	F sand	0.64
N7	60	1.90	2.30	2.77	3.18	3.71	2.75	F sand	0.49
N8	59	1.68	2.13	2.60	3.06	3.60	2.60	F sand	0.52
N9	58	1.57	2.03	2.45	3.06	3.70	2.51	F sand	0.58
N10	57	1.54	2.11	2.60	3.25	4.15	2.65	F sand	0.68
N11	56	1.44	1.84	2.21	2.80	3.25	2.28	F sand	0.51
N12	55	1.48	1.88	2.24	2.83	3.44	2.32	VF sand	0.53
N13									
N14									
N15									
N16							Avg Grain		
N17	Sample #	F5	F16	F50	F84	F95	Size (phi)	Size	Std. Dev
N18	8	1.95	2.16	2.47	3.00	4.03	2.54	F sand	0.53
N19	7	1.60	1.94	2.45	3.06	3.64	2.48	F sand	0.59
N20	6	1.71	2.06	2.44	3.00	3.65	2.50	F sand	0.53
N21	5	1.96	2.26	2.58	2.95	3.38	2.60	F sand	0.39
N22	4	1.80	2.29	2.66	3.01	3.70	2.65	F sand	0.47
N23	3	1.89	2.19	2.59	2.97	3.31	2.58	F sand	0.41
N24	2	1.47	1.90	2.26	2.84	4.10	2.33	F sand	0.63
N25	1	1.35	1.81	2.25	2.71	3.45	2.26	F sand	0.54
N26									
N27									
N28									
N29							Avg Grain		
N30	Sample #	F5	F16	F50	F84	F95	Size (phi)	Size	Std. Dev
N31									
N32	13	1.31	2.20	3.58	4.24	4.72	3.34	VF sand	1.03
N33									
N34									
N35									
N36	12	1.29	2.30	3.24	3.74	4.20	3.09	VF sand	0.80
N37	11	1.74	2.35	3.28	4.02	4.66	3.22	VF sand	0.86
N38	10	1.94	2.18	2.65	3.15	3.70	2.66	F sand	0.51
N39	9	1.88	2.14	2.62	3.10	3.60	2.62	F sand	0.50
N40									
N41									
N42									
N43							Avg Grain		

N44	Sample #	F5	F16	F50	F84	F95	Size (phi)	Size	Std. Dev
N45									
N46									
N47									
N48	17	1.13	2.03	4.05	4.54	4.84	3.54	VF sand	1.19
N49	16	1.34	2.41	3.84	4.16	4.64	3.47	VF sand	0.94
N50	15	1.35	2.60	3.63	4.04	4.66	3.42	VF sand	0.86
N51	14	1.15	2.02	3.95	4.20	4.77	3.39	VF sand	1.09
N52									
N53									
N54									
N55							Avg Grain		
N56	Sample #	F5	F16	F50	F84	F95	Size (phi)	Size	Std. Dev
N57									
N58	22	1.70	1.98	2.20	2.57	3.07	2.25	F sand	0.36
N59	21	1.55	1.93	2.31	2.78	3.46	2.34	F sand	0.50
N60	20	1.77	1.98	2.29	2.84	3.51	2.37	F sand	0.48
N61	19	1.60	1.92	2.25	2.86	3.56	2.34	F sand	0.53
N62	18	1.75	1.96	2.20	2.56	3.05	2.24	F sand	0.35
N63									
N64									
N65									
N66							Avg Grain		
N67	Sample #	F5	F16	F50	F84	F95	Size (phi)	Size	Std. Dev
N68	29	2.00	2.40	3.05	3.74	4.20	3.06	VF sand	0.67
N69	28	1.80	2.39	3.20	4.02	4.60	3.20	VF sand	0.83
N70	27	2.04	2.38	2.95	3.65	4.15	2.99	F sand	0.64
N71	26	2.00	2.36	2.97	3.57	4.00	2.97	F sand	0.61
N72	25	1.97	2.24	2.67	3.34	3.95	2.75	F sand	0.58
N73	24	1.76	2.10	2.40	3.10	3.70	2.53	F sand	0.54
N74	23	1.80	2.21	2.55	3.29	3.80	2.68	F sand	0.57
N75									
N76									
N77									
N78							Avg Grain		
N79	Sample #	F5	F16	F50	F84	F95	Size (phi)	Size	Std. Dev
N80	41	N/A	N/A	N/A	N/A	N/A	N/A	N/A	N/A
N81	40	1.96	2.21	2.52	3.10	3.80	2.61	F sand	0.50
N82	39	2.01	2.20	2.45	3.04	3.74	2.56	F sand	0.47
N83	38	2.00	2.26	2.57	3.05	3.65	2.63	F sand	0.45
N84	37	2.04	2.27	2.73	3.52	4.10	2.84	F sand	0.62
N85	36	2.02	2.28	2.68	3.15	3.74	2.70	F sand	0.48
N86	35	2.00	2.27	2.64	3.23	4.00	2.71	F sand	0.54
N87	34	1.91	2.36	2.95	3.65	4.55	2.99	F sand	0.72
N88	33	1.87	2.38	2.95	3.58	4.24	2.97	F sand	0.66
N89	32	1.95	2.27	2.80	3.32	3.76	2.80	F sand	0.54
N90	31	2.10	2.58	3.04	3.62	4.04	3.08	VF sand	0.55
N91	30	2.22	2.64	3.05	3.65	4.05	3.11	VF sand	0.53
N92									
N93									

	Sample #	F5	F16	F50	F84	F95	Avg Grain Size (phi)	Size	Std. Dev
N94									
N95									
N96									
N97									
N98	54	2.24	2.78	3.28	3.67	4.15	3.24	VF sand	0.51
N99	53	2.00	2.54	3.07	3.60	4.20	3.07	VF sand	0.60
N100	52	2.19	2.44	3.05	3.59	4.03	3.03	VF sand	0.57
N101	51	1.95	2.20	2.54	3.05	3.55	2.60	F sand	0.45
N102	50	1.97	2.15	2.38	2.76	3.04	2.43	F sand	0.31
N103	49	1.37	1.71	2.08	2.43	2.87	2.07	F sand	0.41
N104	48	1.96	2.14	2.40	2.85	3.25	2.46	F sand	0.37
N105	47	1.84	2.06	2.37	2.88	3.19	2.44	F sand	0.41
N106	46	1.64	1.91	2.15	2.45	3.00	2.17	F sand	0.34
N107	45	1.70	1.93	2.17	2.54	3.00	2.21	F sand	0.35
N108	44	1.54	1.81	2.06	2.58	3.23	2.15	F sand	0.45
N109	43	1.46	1.90	2.25	2.79	4.00	2.31	F sand	0.61
N110	42	1.56	1.93	2.11	2.47	2.95	2.17	F sand	0.35

Guide Number	Sorting	Perm (log)	Perm (md)	Perm (D)	Location
N1	Mod well-sorted	4.74	55266	55.27	Surface of orange ss
N2	Mod well-sorted	4.80	63211	63.21	Top of orange ss
N3	Mod sorted	4.23	16936	16.94	White ss
N4	Mod well-sorted	4.58	38257	38.26	White ss
N5	Mod well-sorted	4.58	38059	38.06	White ss
N6	Mod well-sorted	4.21	16225	16.23	Middle of white ss
N7	Well-sorted	4.37	23325	23.32	White ss
N8	Mod well-sorted	4.44	27616	27.62	White ss
N9	Mod well-sorted	4.46	28891	28.89	White ss
N10	Mod well-sorted	4.33	21431	21.43	Base of white ss
N11	Mod well-sorted	4.63	42177	42.18	Surface of white ss (bar)
N12	Mod well-sorted	4.60	39445	39.44	Base of orange ss (bar)
N13					
N14					
N15					
N16					
N17	**Sorting**	**Perm (log)**	**Perm (md)**	**Perm (D)**	**Location**
N18	Mod well-sorted	4.47	29569	29.57	Surface of orange/white ss
N19	Mod well-sorted	4.47	29755	29.75	Top of white ss
N20	Mod well-sorted	4.49	31172	31.17	White ss
N21	Well-sorted	4.51	32234	32.23	White ss
N22	Well-sorted	4.44	27302	27.30	Middle of orange/white ss
N23	Well-sorted	4.50	31976	31.98	Orange ss
N24	Mod well-sorted	4.54	34472	34.47	Orange ss w/ laminations
N25	Mod well-sorted	4.63	42270	42.27	Base of orange ss
N26					
N27					
N28					
N29					
N30	**Sorting**	**Perm (log)**	**Perm (md)**	**Perm (D)**	**Location**
N31					Orange top soil w/shale
N32	Poorly sorted	3.77	5844	5.84	Purple ss w/shale
N33					Shaly slope
N34					Shaly slope
N35					Shaly slope
N36	Mod sorted	4.02	10461	10.46	Surface of pink ss
N37	Mod sorted	3.92	8313	8.31	Pink ss
N38	Mod well-sorted	4.41	25820	25.82	White ss
N39	Mod well-sorted	4.44	27484	27.48	Base of white ss
N40					
N41					
N42					
N43					

N44	Sorting	Perm (log)	Perm (md)	Perm (D)	Location
N45					Orange top soil w/ shale
N46					Shaly slope
N47					Shaly slope
N48	Poorly sorted	3.57	3729	3.73	Purple ss w/shale
N49	Mod sorted	3.74	5450	5.45	Purple ss
N50	Mod sorted	3.80	6319	6.32	Purple ss
N51	Poorly sorted	3.71	5070	5.07	Base of purple ss
N52					
N53					
N54					
N55					
N56	Sorting	Perm (log)	Perm (md)	Perm (D)	Location
N57					Slope of white ss
N58	Well-sorted	4.72	52831	52.83	Orange ss (bar side)
N59	Mod well-sorted	4.60	39696	39.70	Orange ss (bar side)
N60	Well-sorted	4.59	39181	39.18	White ss (bar surface)
N61	Mod well-sorted	4.58	38191	38.19	White ss (bar surface)
N62	Well-sorted	4.73	54029	54.03	Base of white ss
N63					
N64					
N65					
N66					
N67	Sorting	Perm (log)	Perm (md)	Perm (D)	Location
N68	Mod well-sorted	4.10	12657	12.66	Surface of gray ss
N69	Mod sorted	3.94	8737	8.74	Top of orange ss
N70	Mod well-sorted	4.16	14381	14.38	Orange ss
N71	Mod well-sorted	4.19	15443	15.44	Middle of orange ss
N72	Mod well-sorted	4.33	21275	21.27	Orange ss
N73	Mod well-sorted	4.47	29327	29.33	White/orange ss
N74	Mod well-sorted	4.37	23281	23.28	Base of white ss
N75					
N76					
N77					
N78					
N79	Sorting	Perm (log)	Perm (md)	Perm (D)	Location
N80	N/A	N/A	N/A	N/A	Fe oxide rock on fracture
N81	Mod well-sorted	4.44	27828	27.83	Surface of white ss
N82	Well-sorted	4.49	30593	30.59	Top of white ss
N83	Well-sorted	4.46	28943	28.94	Orange/white ss
N84	Mod well-sorted	4.25	17857	17.86	Orange/white ss
N85	Well-sorted	4.40	25264	25.26	Middle of orange/white ss
N86	Mod well-sorted	4.36	23156	23.16	Orange/white ss
N87	Mod sorted	4.12	13165	13.17	Orange/white ss
N88	Mod well-sorted	4.16	14465	14.47	Orange/white ss
N89	Mod well-sorted	4.32	20897	20.90	Orange/white ss
N90	Mod well-sorted	4.15	14105	14.10	Base of white/orange ss
N91	Mod well-sorted	4.14	13875	13.88	Base of erosional unit
N92					
N93					

	Sorting	Perm (log)	Perm (md)	Perm (D)	Location
N94					
N95					
N96					
N97	**Sorting**	**Perm (log)**	**Perm (md)**	**Perm (D)**	**Location**
N98	Mod well-sorted	4.08	11930	11.93	Surface of white ss
N99	Mod well-sorted	4.13	13587	13.59	Top of white ss
N100	Mod well-sorted	4.17	14921	14.92	White ss
N101	Well-sorted	4.48	29857	29.86	White ss
N102	Well-sorted	4.64	43637	43.64	White ss
N103	Well-sorted	4.80	62836	62.84	Middle of white ss
N104	Well-sorted	4.59	39077	39.08	White ss
N105	Well-sorted	4.59	38823	38.82	White ss
N106	Well-sorted	4.78	59651	59.65	White ss
N107	Well-sorted	4.75	55802	55.80	White ss
N108	Well-sorted	4.73	54187	54.19	Orange ss
N109	Mod well-sorted	4.56	36463	36.46	Orange ss
N110	Well-sorted	4.77	59343	59.34	Base of orange ss

APPENDIX A

TRANSECT DATA (Peebly Rd.)

Guide Number	Begin Transect (0.0 mi)						
	Intersection of Highway 9 and Peebly Rd.						
	Outcrop #1 (3 mi)						
Guide Number	Depth Interval (in)	Depth Interval (ft)	Total Count (ppm)	Potassium K (%)	Uranium U (ppm)	Thorium Th (ppm)	API
P1	0.0	0.00	4.2	0.1	0.7	4.1	23.60
P2	10.0	0.83	4.6	0.2	-0.2	4.6	20.00
P3	27.0	2.25	6.8	0.5	1.3	4.7	37.20
P4	38.0	3.17	9.0	0.6	1.8	6.0	48.00
P5	56.0	4.66	8.1	0.5	1.6	4.6	39.20
P6	67.0	5.58	5.1	0.3	0.7	3.0	22.40
P7	86.0	7.16	4.8	0.4	0.2	3.1	20.40
P8	97.0	8.08	4.9	0.3	-0.1	3.9	19.60
P9	111.0	9.25	5.5	0.5	0.4	4.0	27.20
P10	130.0	10.83	6.2	0.4	0.3	3.7	23.60
P11	134.0	11.16	5.7	0.4	0.2	4.8	27.20
P12	149.0	12.41	6.1	0.5	0.6	4.9	32.40
P13							
P14	Outcrop #2 (.7 mi)						
P15							
P16	Depth Interval (in)	Depth Interval (ft)	Total Count (ppm)	Potassium K (%)	Uranium U (ppm)	Thorium Th (ppm)	API
P17							
P18	0.0	0.00	7.5	0.5	1.5	4.5	38.00
P19	14.0	1.17	10.7	0.7	1.5	9.0	59.20
P20	34.0	2.83	7.8	0.7	0.7	5.8	40.00
P21	49.0	4.08	6.6	0.4	1.3	4.4	34.40
P22	52.0	4.33	5.4	0.4	0.2	4.9	27.60
P23	59.0	4.91	5.8	0.3	0.8	3.8	26.40
P24	69.0	5.75	5.5	0.5	0.6	3.7	27.60
P25	80.0	6.66	5.9	0.4	0.3	3.7	23.60
P26	92.0	7.66	7.5	0.5	0.6	6.8	40.00
P27							
P28	Outcrop #3 (1.8 mi)						
P29							
P30	Depth Interval (in)	Depth Interval (ft)	Total Count (ppm)	Potassium K (%)	Uranium U (ppm)	Thorium Th (ppm)	API
P31							
P32	0.0	0.00	6.7	0.3	0.9	4.3	29.20
P33	16.0	1.33	9.8	0.8	0.9	8.0	52.00
P34	24.0	2.00	12.5	0.9	1.9	9.3	66.80
P35	34.0	2.83	15.0	1.1	1.6	11.8	77.60
P36	51.0	4.25	21.0	1.9	4.1	17.8	134.40
P37	67.0	5.58	16.7	1.5	1.9	12.1	87.60
P38	77.0	6.41	10.7	0.8	1.6	7.7	56.40
P39	82.0	6.83	10.3	0.8	1.0	9.3	58.00
P40	87.0	7.25	12.5	0.9	3.2	8.5	74.00
P41	93.0	7.75	12.3	0.7	2.3	9.9	69.20
P42							
P43	Outcrop #4 (.3 mi)						

	Depth Interval (in)	Depth Interval (ft)	Total Count (ppm)	Potassium K (%)	Uranium U (ppm)	Thorium Th (ppm)	API
P44							
P45	Depth	Depth	Total	Potassium	Uranium	Thorium	
P46	Interval (in)	Interval (ft)	Count (ppm)	K (%)	U (ppm)	Th (ppm)	API
P47	0.0	0.00	6.3	0.1	0.8	6.2	32.80
P48	4.0	0.33	6.4	0.3	0.9	4.9	31.60
P49	40.0	3.33	7.4	0.2	1.1	7.7	42.80
P50	60.0	5.00	8.2	0.3	1.2	6.4	40.00
P51	65.0	5.41	6.3	0.3	0.9	4.4	29.60
P52	79.0	6.58	6.0	0.3	0.8	3.8	26.40
P53	96.0	8.00	5.9	0.4	0.1	4.0	23.20
P54	106.0	8.83	6.1	0.4	0.3	3.6	23.20
P55	113.0	9.41	5.6	0.2	0.8	3.8	24.80
P56	122.0	10.16	5.8	0.4	0.6	3.2	24.00
P57	138.0	11.50	5.7	0.5	0.3	3.9	26.00
P58							
P59	*Outcrop #5 (.2 mi)*						
P60							
P61	Depth	Depth	Total	Potassium	Uranium	Thorium	
P62	Interval (in)	Interval (ft)	Count (ppm)	K (%)	U (ppm)	Th (ppm)	API
P63	N/A	N/A	N/A	N/A	N/A	N/A	N/A
P64	0	0.00	5.4	0.3	0.7	3.4	24.00
P65	3.0	0.25	5.6	0.4	0.5	4.9	30.00
P66	9.0	0.75	5.3	0.4	0.7	3.1	24.40
P67	21.0	1.75	5.7	0.4	1.2	3.8	31.20
P68	27.0	2.25	5.7	0.4	0.3	4.4	26.40
P69	35.0	2.92	4.6	0.5	-0.3	2.6	16.00
P70	51.0	4.25	4.5	0.3	0.2	3.6	20.80
P71	69.0	5.75	5.1	0.4	0.2	4.1	24.40
P72							
P73	*Outcrop #6A (.6 mi)*						
P74							
P75	Depth	Depth	Total	Potassium	Uranium	Thorium	
P76	Interval (in)	Interval (ft)	Count (ppm)	K (%)	U (ppm)	Th (ppm)	API
P77	0.0	0.00	6.2	0.3	1.4	4.7	34.80
P78	12.0	1.00	4.9	0.3	0.2	3.9	22.00
P79	34.0	2.83	4.6	0.3	0.1	4.1	22.00
P80	52.0	4.33	8.0	0.5	0.4	6.6	37.60
P81	61.0	5.08	9.3	0.8	0.8	7.0	47.20
P82	69.0	5.75	10.1	0.8	0.9	6.6	46.40
P83	81.0	6.75	12.7	1.0	1.8	8.7	65.20
P84	93.0	7.75	13.0	1.2	1.6	9.6	70.40
P85	109.0	9.08	13.0	0.9	1.1	11.4	68.80
P86							
P87	*Outcrop #6B (0 mi; 515 ft South of 6A)*						
P88							
P89	Depth	Depth	Total	Potassium	Uranium	Thorium	
P90	Interval (in)	Interval (ft)	Count (ppm)	K (%)	U (ppm)	Th (ppm)	API
P91	0.0	0.00	4.5	0.2	0.8	2.6	20.00
P92	11.0	0.92	4.8	0.4	0.0	3.9	22.00
P93	21.0	1.75	5.2	0.4	0.1	3.1	19.60

P94	41.0	3.42	5.5	0.3	1.1	3.0	25.60
P95	57.0	4.75	7.2	0.4	1.4	4.9	37.20
P96	69.0	5.75	6.6	0.5	0.1	5.6	31.20
P97	82.0	6.83	8.2	0.3	2.0	5.7	43.60
P98	92.0	7.66	6.8	0.5	1.6	3.7	35.60
P99	102.0	8.50	6.3	0.3	0.6	5.2	30.40
P100	114.0	9.50	6.3	0.5	0.5	3.8	27.20
P101	124.0	10.33	5.6	0.4	0.8	3.1	25.20
P102	131.0	10.91	5.3	0.3	0.8	3.6	25.60
P103	146.0	12.16	7.1	0.5	1.5	3.7	34.80
P104	156.0	12.99	9.1	0.7	1.2	7.4	50.40
	End of Transect (.1 mi)					
	Intersection of Thunderbird Hills Rd and Peebly Rd.					
	Total Distance (6.6 mi)					

Guide Number	Sample #	F5	F16	F50	F84	F95	Avg Grain Size (phi)	Size	Std. Dev
P1	12	1.85	2.27	2.94	3.75	4.55	2.99	F sand	0.78
P2	11	1.72	2.05	2.59	3.13	3.64	2.59	F sand	0.56
P3	10	1.75	2.12	2.71	3.48	4.05	2.77	F sand	0.69
P4	9	1.65	2.18	2.85	3.13	3.50	2.72	F sand	0.52
P5	8	1.60	2.10	2.75	3.62	4.56	2.82	F sand	0.83
P6	7	1.88	2.20	2.60	3.02	3.63	2.61	F sand	0.47
P7	6	1.79	2.14	2.59	3.12	3.51	2.62	F sand	0.51
P8	5	1.90	2.18	2.69	3.28	4.05	2.72	F sand	0.60
P9	4	2.04	2.45	2.85	3.37	3.75	2.89	F sand	0.49
P10	3	1.90	2.49	3.00	3.68	4.51	3.06	VF sand	0.69
P11	2	1.75	2.14	2.72	3.48	4.11	2.78	F sand	0.69
P12	1	1.17	1.95	2.55	3.25	3.86	2.58	F sand	0.73
P13									
P14									
P15									
P16							Avg Grain		
P17	Sample #	F5	F16	F50	F84	F95	Size (phi)	Size	Std. Dev
P18	21	N/A	N/A	N/A	N/A	N/A	N/A	N/A	N/A
P19	20	N/A	N/A	N/A	N/A	N/A	N/A	N/A	N/A
P20	19	N/A	N/A	N/A	N/A	N/A	N/A	N/A	N/A
P21	18	N/A	N/A	N/A	N/A	N/A	N/A	N/A	N/A
P22	17	2.02	2.24	2.63	3.08	3.65	2.65	F sand	0.46
P23	16	1.77	2.09	2.27	2.76	3.35	2.37	F sand	0.41
P24	15	1.85	2.10	2.53	2.90	3.36	2.51	F sand	0.43
P25	14	1.76	2.08	2.50	2.95	3.46	2.51	F sand	0.48
P26	13	1.44	1.85	2.26	2.84	3.59	2.32	F sand	0.57
P27									
P28									
P29									
P30							Avg Grain		
P31	Sample #	F5	F16	F50	F84	F95	Size (phi)	Size	Std. Dev
P32	31	1.75	2.48	3.24	3.85	4.70	3.19	VF sand	0.79
P33	30	1.80	2.48	2.89	3.50	4.27	2.96	F sand	0.63
P34	29	1.42	2.25	2.87	3.60	4.30	2.91	F sand	0.77
P35	28	1.11	1.87	3.05	4.15	4.60	3.02	VF sand	1.10
P36	27	1.12	1.60	3.96	4.54	4.85	3.37	VF sand	1.30
P37	26	1.84	2.71	3.85	4.28	4.80	3.61	VF sand	0.84
P38	25	1.95	2.84	3.70	4.18	4.77	3.57	VF sand	0.76
P39	24	1.95	2.82	3.64	4.14	4.80	3.53	VF sand	0.76
P40	23	2.13	2.97	3.70	4.22	4.86	3.63	VF sand	0.73
P41	22	1.39	2.13	3.33	4.25	4.85	3.24	VF sand	1.05
P42									
P43									

	Sample #	F5	F16	F50	F84	F95	Avg Grain Size (phi)	Size	Std. Dev
P44									
P45							Avg Grain		
P46	Sample #	F5	F16	F50	F84	F95	Size (phi)	Size	Std. Dev
P47	42	N/A	N/A	N/A	N/A	N/A	N/A	N/A	N/A
P48	41	N/A	N/A	N/A	N/A	N/A	N/A	N/A	N/A
P49	40	N/A	N/A	N/A	N/A	N/A	N/A	N/A	N/A
P50	39	N/A	N/A	N/A	N/A	N/A	N/A	N/A	N/A
P51	38	2.08	2.70	3.21	4.05	4.75	3.32	VF sand	0.74
P52	37	2.13	2.96	3.55	4.09	4.75	3.53	VF sand	0.68
P53	36	2.45	2.63	2.95	3.54	3.75	3.04	VF sand	0.42
P54	35	2.13	2.48	2.86	3.45	4.00	2.93	F sand	0.53
P55	34	1.97	2.35	2.74	3.32	4.17	2.80	F sand	0.58
P56	33	1.87	2.29	2.70	3.40	3.73	2.80	F sand	0.56
P57	32	2.03	2.49	2.85	3.58	4.38	2.97	F sand	0.63
P58									
P59									
P60									
P61							Avg Grain		
P62	Sample #	F5	F16	F50	F84	F95	Size (phi)	Size	Std. Dev
P63	51	N/A	N/A	N/A	N/A	N/A	N/A	N/A	N/A
P64	50	2.00	2.28	2.67	3.27	4.00	2.74	F sand	0.55
P65	49	2.00	2.65	3.34	3.81	4.40	3.27	VF sand	0.65
P66	48	2.47	2.92	3.39	3.74	4.24	3.35	VF sand	0.47
P67	47	2.20	2.65	2.96	3.52	4.10	3.04	VF sand	0.51
P68	46	2.13	2.67	3.04	3.60	4.25	3.10	VF sand	0.55
P69	45	2.02	2.51	2.90	3.44	4.08	2.95	F sand	0.54
P70	44	1.97	2.23	2.68	3.34	3.70	2.75	F sand	0.54
P71	43	2.05	2.28	2.66	3.22	4.01	2.72	F sand	0.53
P72									
P73									
P74									
P75							Avg Grain		
P76	Sample #	F5	F16	F50	F84	F95	Size (phi)	Size	Std. Dev
P77	60	1.53	2.00	2.66	3.62	4.22	2.76	F sand	0.81
P78	59	1.81	2.05	2.38	2.82	3.55	2.42	F sand	0.46
P79	58	1.68	2.03	2.43	3.08	4.19	2.51	F sand	0.64
P80	57	1.90	2.44	2.94	3.55	4.09	2.98	F sand	0.61
P81	56	1.38	1.78	2.18	3.33	4.11	2.43	F sand	0.80
P82	55	1.29	1.48	1.87	2.75	4.08	2.03	M sand	0.74
P83	54	1.69	1.94	2.23	3.68	4.77	2.62	F sand	0.90
P84	53	1.15	1.82	2.55	4.13	4.57	2.83	F sand	1.10
P85	52	1.20	1.90	2.60	4.05	4.23	2.85	F sand	1.00
P86									
P87									
P88									
P89							Avg Grain		
P90	Sample #	F5	F16	F50	F84	F95	Size (phi)	Size	Std. Dev
P91	74	2.05	2.47	2.81	3.51	4.72	2.93	F sand	0.66
P92	73	1.55	2.11	2.70	3.25	4.31	2.69	F sand	0.70
P93	72	1.92	2.21	2.80	3.31	4.31	2.77	F sand	0.64

P94	71	1.76	2.09	2.69	3.30	4.24	2.69	F sand	0.68
P95	70	1.88	2.25	2.85	3.51	4.66	2.87	F sand	0.74
P96	69	1.95	2.40	2.86	3.36	3.85	2.87	F sand	0.53
P97	68	1.76	2.30	3.30	3.91	4.48	3.17	VF sand	0.81
P98	67	2.00	2.55	2.90	3.44	4.20	2.96	F sand	0.56
P99	66	2.35	2.84	3.35	3.69	4.35	3.29	VF sand	0.52
P100	65	1.76	2.66	3.18	3.70	4.30	3.18	VF sand	0.64
P101	64	1.62	1.95	2.30	2.75	4.00	2.33	F sand	0.56
P102	63	1.71	2.10	2.59	2.91	4.10	2.53	F sand	0.56
P103	62	1.44	1.84	2.44	3.05	4.05	2.44	F sand	0.70
P104	61	1.32	1.77	2.51	3.58	4.47	2.62	F sand	0.93

Guide Number	Sorting	Perm (log)	Perm (md)	Perm (D)	Location
P1	Mod sorted	4.09	12343	12.34	Surface of white/purple ss
P2	Mod well-sorted	4.43	26695	26.70	Top of white/purple ss
P3	Mod well-sorted	4.26	18209	18.21	Base white/purple ss w/ sh clasts
P4	Mod well-sorted	4.37	23623	23.62	Erosional unit (ss & sh)
P5	Mod sorted	4.16	14471	14.47	Erosional unit (ss)
P6	Well-sorted	4.46	28959	28.96	Surface of algamated channel ss
P7	Mod well-sorted	4.44	27449	27.45	Base of algamated channel ss
P8	Mod well-sorted	4.33	21588	21.59	Surface of orange ss w/ fore-sets
P9	Well-sorted	4.29	19508	19.51	Base of orange ss
P10	Mod well-sorted	4.09	12415	12.42	Erosional unit (ss)
P11	Mod well-sorted	4.25	17887	17.89	Surface of dark orange ss
P12	Mod sorted	4.35	22148	22.15	Base of dark orange ss
P13					
P14					
P15					
P16					
P17	Sorting	Perm (log)	Perm (md)	Perm (D)	Location
P18	N/A	N/A	N/A	N/A	Surface of black top-soil
P19	N/A	N/A	N/A	N/A	Top of dark orange top-soil
P20	N/A	N/A	N/A	N/A	Middle of dark orange top-soil
P21	N/A	N/A	N/A	N/A	Dark orange top-soil
P22	Well-sorted	4.44	27765	27.76	Surface of dark orange ss
P23	Well-sorted	4.63	42330	42.33	Top of dark orange ss
P24	Well-sorted	4.54	34481	34.48	Middle of dark orange ss
P25	Well-sorted	4.51	32711	32.71	Dark orange ss
P26	Mod well-sorted	4.58	37740	37.74	Base of dark orange ss
P27					
P28					
P29					
P30					
P31	Sorting	Perm (log)	Perm (md)	Perm (D)	Location
P32	Mod sorted	3.97	9330	9.33	Surface of purple/gray ss
P33	Mod well-sorted	4.18	15231	15.23	Thick bedded purple/gray ss
P34	Mod well-sorted	4.14	13798	13.80	Thin bedded purple/gray ss
P35	Poorly sorted	3.91	8172	8.17	C lay ss & sh
P36	Poorly sorted	3.62	4132	4.13	Clay
P37	Mod sorted	3.70	5036	5.04	Clay and ss
P38	Mod sorted	3.76	5806	5.81	Base of ss & sh
P39	Mod sorted	3.79	6124	6.12	Top of purple/gray ss
P40	Mod sorted	3.75	5615	5.61	Base of purple/gray ss
P41	Poorly sorted	3.81	6490	6.49	Base of dark red/brown top-soil
P42					
P43					

	Sorting	Perm (log)	Perm (md)	Perm (D)	Location
P44					
P45					
P46	**Sorting**	**Perm (log)**	**Perm (md)**	**Perm (D)**	**Location**
P47	N/A	N/A	N/A	N/A	Surface of iron oxide rock
P48	N/A	N/A	N/A	N/A	Top of iron oxide rock
P49	N/A	N/A	N/A	N/A	Middle of iron oxide rock
P50	N/A	N/A	N/A	N/A	Base of iron oxide rock
P51	Mod sorted	3.92	8297	8.30	Top of yellow ss
P52	Mod well-sorted	3.83	6726	6.73	Middle of yellow ss
P53	Well-sorted	4.24	17231	17.23	Base of white ss
P54	Mod well-sorted	4.25	17748	17.75	Erosional unit (ss)
P55	Mod well-sorted	4.30	19812	19.81	Top of yellow/pink ss
P56	Mod well-sorted	4.31	20366	20.37	Middle of pink ss
P57	Mod well-sorted	4.17	14911	14.91	Base of orange ss
P58					
P59					
P60					
P61					
P62	**Sorting**	**Perm (log)**	**Perm (md)**	**Perm (D)**	**Location**
P63	N/A	N/A	N/A	N/A	Calcite nodules
P64	Mod well-sorted	4.35	22166	22.17	Surface of orange ss
P65	Mod well-sorted	3.99	9844	9.84	Top of pink ss
P66	Well-sorted	4.03	10833	10.83	Middle of pink ss
P67	Mod well-sorted	4.19	15645	15.65	Base of dark brown ss
P68	Mod well-sorted	4.14	13681	13.68	Surface of pink ss
P69	Mod well-sorted	4.23	16920	16.92	Top of orange ss
P70	Mod well-sorted	4.35	22150	22.15	Middle of orange ss
P71	Mod well-sorted	4.37	23245	23.24	Base of orange ss
P72					
P73					
P74					
P75					
P76	**Sorting**	**Perm (log)**	**Perm (md)**	**Perm (D)**	**Location**
P77	Mod sorted	4.20	16019	16.02	Base of brown to-soil
P78	Well-sorted	4.58	37800	37.80	Top of yellow/orange ss
P79	Mod well-sorted	4.43	26904	26.90	Middle of yellow/orange ss
P80	Mod well-sorted	4.18	15175	15.18	Yellow/white ss
P81	Mod sorted	4.40	25073	25.07	Yellow/orange ss
P82	Mod sorted	4.66	45333	45.33	Base of yellow/orange ss
P83	Mod sorted	4.24	17483	17.48	Erosional unit (ss, sh, clay)
P84	Poorly sorted	4.02	10535	10.53	Erosional unit (ss, sh, clay)
P85	Poorly sorted	4.06	11537	11.54	Erosional unit (ss, sh, clay)
P86					
P87					
P88					
P89					
P90	**Sorting**	**Perm (log)**	**Perm (md)**	**Perm (D)**	**Location**
P91	Mod well-sorted	4.18	15154	15.15	Top of orange ss
P92	Mod well-sorted	4.30	19986	19.99	Orange ss (stacked bars)
P93	Mod well-sorted	4.28	19221	19.22	Orange ss (stacked bars)

P94	Mod well-sorted	4.31	20381	20.38	Orange ss (stacked bars)
P95	Mod sorted	4.18	15116	15.12	Base of orange ss
P96	Mod well-sorted	4.28	19080	19.08	Orange ss (stacked bars)
P97	Mod sorted	3.97	9309	9.31	Pink ss (stacked bars)
P98	Mod well-sorted	4.22	16414	16.41	Pink ss
P99	Mod well-sorted	4.05	11123	11.12	Pink ss
P100	Mod well-sorted	4.05	11147	11.15	Base of pink ss
P101	Mod well-sorted	4.57	37456	37.46	Red ss
P102	Mod well-sorted	4.46	28644	28.64	Red ss
P103	Mod well-sorted	4.44	27708	27.71	Base of red ss
P104	Mod sorted	4.23	16858	16.86	Erosional unit (ss, sh, clay)

APPENDIX A

TRANSECT DATA (180th Ave.)

	Begin Transect (0.0 mi)						
	Intersection of Highway 9 and 180th Ave.						
	Outcrop #1 (.2 mi)						
Guide Number	**Depth Interval (in)**	**Depth Interval (ft)**	**Total Count (ppm)**	**Potassium K (%)**	**Uranium U (ppm)**	**Thorium Th (ppm)**	**API**
A1	0.0	0.00	4.6	0.1	1.4	2.5	22.80
A2	9.5	0.79	5.5	0.3	1.1	3.1	26.00
A3	22.5	1.87	6.1	0.4	0.5	5.7	33.20
A4	32.5	2.71	5.8	0.3	1.3	3.9	30.80
A5	41.5	3.46	4.9	0.3	0.1	3.8	20.80
A6	44.5	3.71	4.7	0.3	0.3	3.3	20.40
A7	49.0	4.08	4.6	0.3	0.5	3.1	21.20
A8	54.5	4.54	4.5	0.3	0.5	2.7	19.60
A9	64.5	5.37	4.4	0.3	0.3	4.2	24.00
A10	73.5	6.12	4.2	0.2	-0.1	3.8	17.60
A11	82.2	6.85	5.1	0.4	0.0	3.9	22.00
A12	95.5	7.96	5.7	0.3	0.9	3.6	26.40
A13							
A14	*Outcrop #2 (.7 mi)*						
A15							
A16	**Depth Interval (in)**	**Depth Interval (ft)**	**Total Count (ppm)**	**Potassium K (%)**	**Uranium U (ppm)**	**Thorium Th (ppm)**	*API*
A17							
A18	0.0	0.00	4.0	0.1	0.7	2.8	18.40
A19	12.0	1.00	4.3	0.2	1.0	1.8	18.40
A20	32.0	2.67	4.8	0.1	0.9	2.9	20.40
A21	52.0	4.33	5.6	0.3	0.8	4.4	28.80
A22	73.0	6.08	5.3	0.2	1.3	3.1	26.00
A23	93.0	7.75	5.6	0.1	2.1	2.4	28.00
A24	105.0	8.75	4.6	0.3	1.0	2.6	23.20
A25	111.0	9.25	4.4	0.2	0.6	3.4	21.60
A26	120.0	10.00	4.9	0.3	0.7	3.1	22.80
A27	130.0	10.83	4.8	0.3	0.8	3.2	24.00
A28	137.0	11.41	5.0	0.2	1.2	3.3	26.00
A29	147.0	12.25	4.7	0.3	0.6	2.5	19.60
A30	159.0	13.24	5.5	0.4	0.9	3.1	26.00
A31							
A32	*Outcrop #3 (.4 mi)*						
A33							
A34	**Depth Interval (in)**	**Depth Interval (ft)**	**Total Count (ppm)**	**Potassium K (%)**	**Uranium U (ppm)**	**Thorium Th (ppm)**	*API*
A35							
A36	0.0	0.00	6.1	0.3	0.8	4.9	30.80
A37	18.0	1.50	9.8	0.6	2.0	7.2	54.40
A38	28.0	2.33	13.6	1.1	0.9	11.4	70.40
A39	34.0	2.83	13.0	0.7	2.3	10.6	72.00
A40	37.0	3.08	12.4	0.9	2.6	8.1	67.60
A41	40.0	3.33	7.6	0.4	1.6	5.7	42.00
A42	45.0	3.75	6.2	0.3	1.6	4.6	36.00
A43	57.0	4.75	7.0	0.3	1.2	5.5	36.40

	Depth Interval (in)	Depth Interval (ft)	Total Count (ppm)	Potassium K (%)	Uranium U (ppm)	Thorium Th (ppm)	API
A44	67.0	5.58	6.6	0.2	1.8	5.3	38.80
A45	71.0	5.91	7.4	0.4	0.8	4.9	32.40
A46							
A47	*Outcrop #4 (.1 mi)*						
A48							
A49	**Depth**	**Depth**	**Total**	**Potassium**	**Uranium**	**Thorium**	
A50	**Interval (in)**	**Interval (ft)**	**Count (ppm)**	**K (%)**	**U (ppm)**	**Th (ppm)**	***API***
A51	0.0	0.00	4.9	0.2	0.9	3.7	25.20
A52	20.0	1.67	7.1	0.4	0.8	6.3	38.00
A53	35.0	2.92	6.4	0.5	0.8	4.1	30.80
A54	47.0	3.92	8.5	0.4	1.5	6.2	43.20
A55	57.0	4.75	10.0	0.6	1.2	8.6	53.60
A56	61.0	5.08	11.7	0.9	1.0	9.0	58.40
A57	69.0	5.75	11.6	1.0	0.9	9.7	62.00
A58	75.5	6.29	7.1	0.4	1.5	5.3	39.60
A59	79.5	6.62	5.9	0.3	0.4	5.8	31.20
A60	88.5	7.37	5.0	0.3	0.7	3.9	26.00
A61	98.5	8.21	4.9	0.2	0.8	3.0	21.60
A62	108.5	9.04	4.7	0.3	0.2	3.2	19.20
A63	115.5	9.62	4.7	0.4	0.1	2.9	18.80
A64	126.5	10.54	6.4	0.3	1.0	5.7	35.60
A65							
A66	*Outcrop #5 (1.2 mi)*						
A67							
A68	**Depth**	**Depth**	**Total**	**Potassium**	**Uranium**	**Thorium**	
A69	**Interval (in)**	**Interval (ft)**	**Count (ppm)**	**K (%)**	**U (ppm)**	**Th (ppm)**	***API***
A70	0	0.00	3.1	0.1	0.3	2.3	13.20
A71	8.0	0.67	3.7	0.1	0.4	1.9	12.40
A72	21.0	1.75	4.0	0.3	0.1	3.1	18.00
A73	33.0	2.75	4.9	0.3	0.5	3.1	21.20
A74	45.5	3.79	3.6	0.2	0.4	2.4	16.00
A75	57.5	4.79	4.2	0.2	0.8	3.6	24.00
A76	67.0	5.58	3.5	0.1	0.8	2.6	18.40
A77	75.0	6.25	3.5	0.3	0.2	2.5	16.40
A78	82.5	6.87	3.0	0.1	0.6	1.0	10.40
A79	94.5	7.87	4.4	0.5	0.1	1.6	15.20
A80	112.5	9.37	4.5	0.4	0.8	2.2	21.60
A81	125.5	10.45	4.5	0.3	-0.1	2.5	14.00
A82	139.5	11.62	5.7	0.7	0.6	1.4	21.60
	End of Transect (.4 mi)						
	Intersection of 180th Ave and Franklin Rd.						
	Total Distance (3.0 mi)						

Guide Number	Sample #	F5	F16	F50	F84	F95	Avg Grain Size (phi)	Size	Std. Dev
A1	12	1.63	2.03	2.72	3.65	4.72	2.80	F sand	0.87
A2	11	1.69	2.03	2.69	3.58	4.58	2.77	F sand	0.83
A3	10	1.64	2.00	2.65	3.62	4.13	2.76	F sand	0.78
A4	9	1.52	1.95	2.23	2.67	3.55	2.28	F sand	0.49
A5	8	1.32	1.53	2.00	2.63	4.00	2.05	F sand	0.68
A6	7	1.28	1.40	1.76	2.24	3.13	1.80	M sand	0.49
A7	6	1.25	1.34	1.58	2.24	3.60	1.72	M sand	0.58
A8	5	1.27	1.40	1.76	2.50	3.66	1.89	M sand	0.64
A9	4	1.35	1.57	1.92	2.25	3.32	1.91	M sand	0.47
A10	3	1.53	1.81	2.03	2.60	3.66	2.15	F sand	0.52
A11	2	1.29	1.45	1.90	2.61	3.97	1.99	M sand	0.70
A12	1	1.31	1.71	2.19	3.30	4.31	2.40	F sand	0.85
A13									
A14									
A15									
A16							Avg Grain		
A17	Sample #	F5	F16	F50	F84	F95	Size (phi)	Size	Std. Dev
A18	25	1.88	2.16	2.76	3.48	4.33	2.80	F sand	0.70
A19	24	1.86	2.17	2.66	3.54	3.82	2.79	F sand	0.64
A20	23	1.80	2.15	2.65	3.28	3.63	2.69	F sand	0.56
A21	22	1.82	2.13	2.72	3.47	3.84	2.77	F sand	0.64
A22	21	1.75	2.06	2.60	3.25	3.90	2.64	F sand	0.62
A23	20	1.53	2.00	2.49	3.05	3.73	2.51	F sand	0.60
A24	19	1.75	2.00	2.25	2.83	3.54	2.36	F sand	0.48
A25	18	1.26	1.36	1.63	2.16	2.78	1.72	M sand	0.43
A26	17	1.22	1.31	1.52	1.74	2.60	1.52	M sand	0.32
A27	16	1.26	1.33	1.57	2.06	2.67	1.65	M sand	0.40
A28	15	1.04	1.26	1.50	1.75	3.10	1.50	M sand	0.43
A29	14	0.63	1.11	1.46	1.78	2.75	1.45	M sand	0.49
A30	13	1.36	1.81	2.75	3.64	4.62	2.73	F sand	0.95
A31									
A32									
A33									
A34							Avg Grain		
A35	Sample #	F5	F16	F50	F84	F95	Size (phi)	Size	Std. Dev
A36	35	1.43	1.87	2.49	3.50	4.45	2.62	F sand	0.87
A37	34	1.38	1.88	2.55	3.75	4.77	2.73	F sand	0.98
A38	33	2.23	3.50	3.93	4.29	4.83	3.91	VF sand	0.59
A39	32	2.35	3.43	3.96	4.52	4.88	3.97	VF sand	0.66
A40	31	2.48	3.37	4.00	4.75	4.93	4.04	Silt	0.72
A41	30	2.07	2.45	2.87	3.43	4.40	2.92	F sand	0.60
A42	29	2.08	2.34	2.82	3.33	3.78	2.83	F sand	0.51
A43	28	1.95	2.10	2.50	3.15	3.85	2.58	F sand	0.55

	Sample #	F5	F16	F50	F84	F95	Avg Grain Size (phi)	Size	Std. Dev
A44	27	1.65	1.93	2.24	2.81	3.80	2.33	F sand	0.55
A45	26	1.32	1.88	2.57	3.62	4.67	2.69	F sand	0.94
A46									
A47									
A48									
A49							Avg Grain		
A50	Sample #	F5	F16	F50	F84	F95	Size (phi)	Size	Std. Dev
A51	49	1.88	2.18	2.67	3.57	4.38	2.81	F sand	0.73
A52	48	1.71	2.08	2.56	3.20	3.70	2.61	F sand	0.58
A53	47	1.69	2.15	2.62	3.32	4.20	2.70	F sand	0.67
A54	46	2.25	2.57	2.85	3.26	4.58	2.89	F sand	0.53
A55	45	1.78	2.38	3.26	4.26	4.87	3.30	VF sand	0.94
A56	44	2.52	3.15	4.05	4.23	4.88	3.81	VF sand	0.63
A57	43	2.61	3.30	3.80	4.68	4.92	3.93	VF sand	0.70
A58	42	1.61	1.93	2.25	3.15	4.76	2.44	F sand	0.78
A59	41	1.43	1.78	2.13	2.76	3.97	2.22	F sand	0.63
A60	40	1.53	1.87	2.23	2.83	3.38	2.31	F sand	0.52
A61	39	1.32	1.58	1.97	2.71	3.61	2.09	F sand	0.63
A62	38	1.26	1.43	1.87	2.25	2.91	1.85	M sand	0.46
A63	37	1.34	1.63	2.07	2.66	3.57	2.12	F sand	0.60
A64	36	1.51	2.03	2.84	3.84	4.76	2.90	F sand	0.94
A65									
A66									
A67									
A68							Avg Grain		
A69	Sample #	F5	F16	F50	F84	F95	Size (phi)	Size	Std. Dev
A70	62	2.00	2.22	2.69	3.20	3.69	2.70	F sand	0.50
A71	61	2.40	2.75	3.05	3.48	3.77	3.09	VF sand	0.39
A72	60	2.37	2.65	2.95	3.52	4.27	3.04	VF sand	0.51
A73	59	2.15	2.55	2.95	3.52	4.25	3.01	VF sand	0.56
A74	58	1.94	2.10	2.41	2.80	3.45	2.44	F sand	0.40
A75	57	2.03	2.25	2.71	3.38	3.95	2.78	F sand	0.57
A76	56	2.00	2.20	2.65	3.20	3.75	2.68	F sand	0.52
A77	55	1.85	2.13	2.73	3.18	3.73	2.68	F sand	0.55
A78	54	1.34	1.64	1.99	2.50	3.00	2.04	F sand	0.47
A79	53	1.64	2.02	2.54	2.99	3.65	2.52	F sand	0.55
A80	52	1.38	1.84	2.34	2.96	3.66	2.38	F sand	0.63
A81	51	1.59	2.01	2.49	2.95	3.58	2.48	F sand	0.54
A82	50	1.37	1.91	2.46	3.10	3.87	2.49	F sand	0.68

Guide Number	Sorting	Perm (log)	Perm (md)	Perm (D)	Location
A1	Mod sorted	4.15	14183	14.18	Surface of white ss
A2	Mod sorted	4.19	15649	15.65	White ss
A3	Mod sorted	4.22	16654	16.65	Top of slope
A4	Well-sorted	4.64	43478	43.48	Slope on top of red ss
A5	Mod well-sorted	4.67	47232	47.23	Top of red ss
A6	Well-sorted	4.91	81963	81.96	
A7	Mod well-sorted	4.91	82134	82.13	
A8	Mod well-sorted	4.79	61856	61.86	
A9	Well-sorted	4.86	72365	72.36	
A10	Mod well-sorted	4.70	50160	50.16	
A11	Mod well-sorted	4.70	50697	50.70	Base of red ss
A12	Mod sorted	4.39	24615	24.62	Red unconsolidated ss
A13					
A14					
A15					
A16					
A17	**Sorting**	**Perm (log)**	**Perm (md)**	**Perm (D)**	**Location**
A18	Mod well-sorted	4.24	17251	17.25	Surface
A19	Mod well-sorted	4.27	18753	18.75	Top of slope
A20	Mod well-sorted	4.37	23326	23.33	
A21	Mod well-sorted	4.28	19135	19.14	
A22	Mod well-sorted	4.37	23382	23.38	
A23	Mod well-sorted	4.45	28382	28.38	Slope on top of yellow ss
A24	Well-sorted	4.60	39697	39.70	Top of dark yellow ss
A25	Well-sorted	4.99	97949	97.95	
A26	Very well-sorted	5.16	143856	143.86	
A27	Well-sorted	5.04	110703	110.70	
A28	Well-sorted	5.11	129120	129.12	
A29	Well-sorted	5.11	130248	130.25	Base of dark yellow ss
A30	Mod sorted	4.15	14165	14.16	Ditch
A31					
A32					
A33					
A34					
A35	**Sorting**	**Perm (log)**	**Perm (md)**	**Perm (D)**	**Location**
A36	Mod sorted	4.26	18147	18.15	Surface of gray top soil
A37	Mod sorted	4.14	13815	13.81	Orange top soil
A38	Mod well-sorted	3.66	4545	4.55	
A39	Mod well-sorted	3.59	3886	3.89	
A40	Mod sorted	3.52	3308	3.31	Slope of shale & clay
A41	Mod well-sorted	4.22	16637	16.64	Surface of pink ss
A42	Mod well-sorted	4.32	20733	20.73	Top of pink ss
A43	Mod well-sorted	4.44	27256	27.26	

	Sorting	Perm (log)	Perm (md)	Perm (D)	Location
A44	Mod well-sorted	4.58	38431	38.43	Base of pink ss
A45	Mod sorted	4.18	15150	15.15	Orange top soil
A46					
A47					
A48					
A49					
A50	**Sorting**	**Perm (log)**	**Perm (md)**	**Perm (D)**	**Location**
A51	Mod sorted	4.22	16619	16.62	Surface of gray top soil
A52	Mod well-sorted	4.40	25286	25.29	Gray top soil
A53	Mod well-sorted	4.31	20418	20.42	
A54	Mod well-sorted	4.27	18633	18.63	Orange top soil w/ reduction
A55	Mod sorted	3.83	6813	6.81	Top of slope
A56	Mod well-sorted	3.70	4955	4.95	
A57	Mod well-sorted	3.59	3935	3.93	Slope of shale & clay
A58	Mod sorted	4.40	25171	25.17	Surface of bar
A59	Mod well-sorted	4.60	40017	40.02	Top of bar
A60	Mod well-sorted	4.61	40440	40.44	
A61	Mod well-sorted	4.68	47937	47.94	Base of bar
A62	Well-sorted	4.90	79883	79.88	Surface of bar
A63	Mod well-sorted	4.68	47693	47.69	Base of bar
A64	Mod sorted	4.06	11405	11.41	Orange top soil
A65					
A66					
A67					
A68					
A69	**Sorting**	**Perm (log)**	**Perm (md)**	**Perm (D)**	**Location**
A70	Well-sorted	4.39	24613	24.61	Unconsolidated white ss (slope)
A71	Well-sorted	4.22	16703	16.70	Base of white ss
A72	Mod well-sorted	4.20	15714	15.71	Orange ss w/ thin laminations
A73	Mod well-sorted	4.19	15417	15.42	Orange ss w/ thick laminations
A74	Well-sorted	4.59	39078	39.08	
A75	Mod well-sorted	4.31	20487	20.49	Base of orange ss
A76	Mod well-sorted	4.40	24868	24.87	Top of white ss
A77	Mod well-sorted	4.38	24078	24.08	
A78	Well-sorted	4.79	61105	61.11	
A79	Mod well-sorted	4.48	29873	29.87	
A80	Mod well-sorted	4.51	32714	32.71	
A81	Mod well-sorted	4.50	31591	31.59	Base of white ss
A82	Mod well-sorted	4.43	26706	26.71	Orange top soil w/ gravel

APPENDIX B

Group #1~ Sandstone with Stacked Bar Forms

Outcrop #2
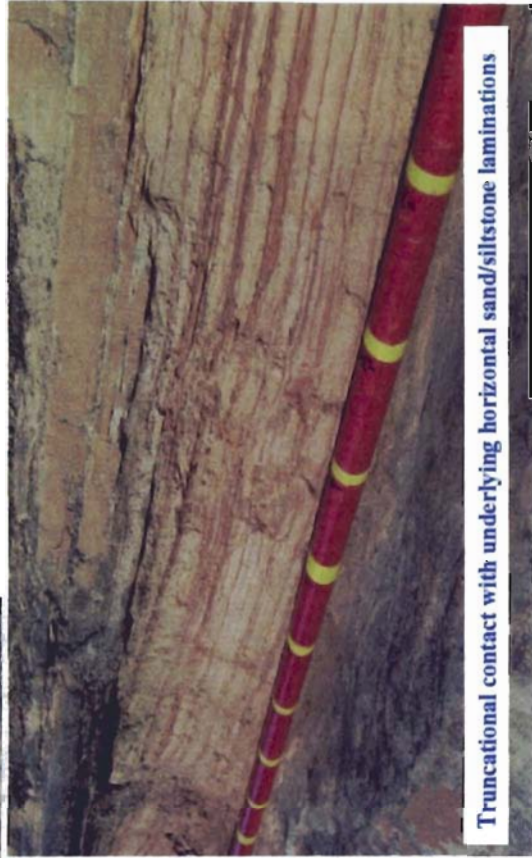
165

Truncational contact with underlying horizontal sand/siltstone laminations

Alameda; Outcrop #7

166

Erosional contact

Rock Creek Rd.

Outcrop #1

167

Outcrop #2A

Rock Creek Rd.

Outcrop #2B

Rock Creek Rd.

169

Outcrop #2A & B

170

Ripple Lamination

Rock Creek; Outcrop #4

171

Crevasse—splay

Beaver Creek Rd

Outcrop #4A

172

Rock Creek Rd

Outcrop #4B

173

Franklin: Outcrop #2

174

Franklin Rd

Outcrop #3

175

Outcrop #4

176

Franklin; Outcrop #6

177

Trough cross-bedding

Newzulla Rd.

Outcrop #1

178

Erosional contact with overlying shale sandstone

Newalla Rd

Outcrop #2

179

Concentrations of metals

Outcrop #2

Newalla Rd

Trough cross-bedding

Newalla Rd.

Outcrop #5

181

Outcrop #6

Newalla Rd.

182

Newalla Rd.
Outcrop #7

183

Hard hematite precipitate zone

Erosional contact, where Bird's eye shale sands form

Trace Fossils

Newalla: Outcrop #7

Erosional contact with underlying shale/sandstone

Newalla: Outcrop #8

185

Peebly; Outcrop #1

Cross-bedding
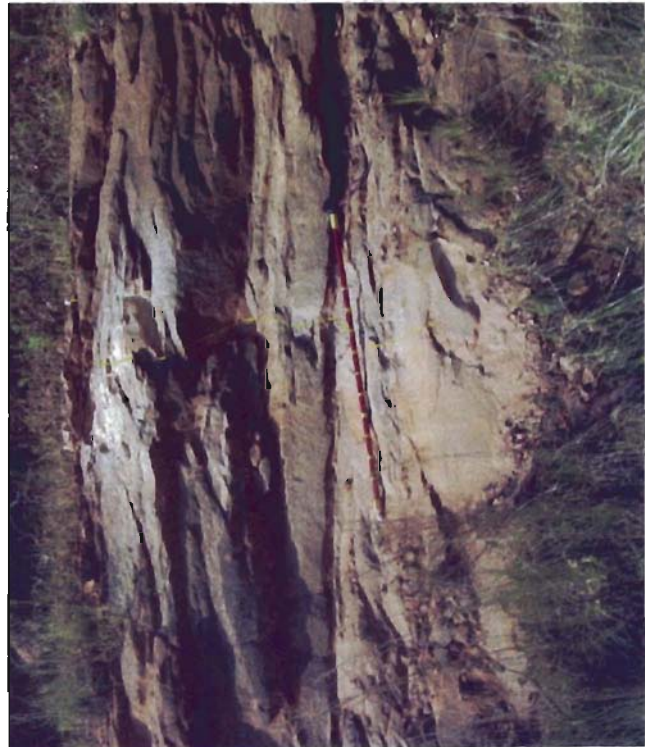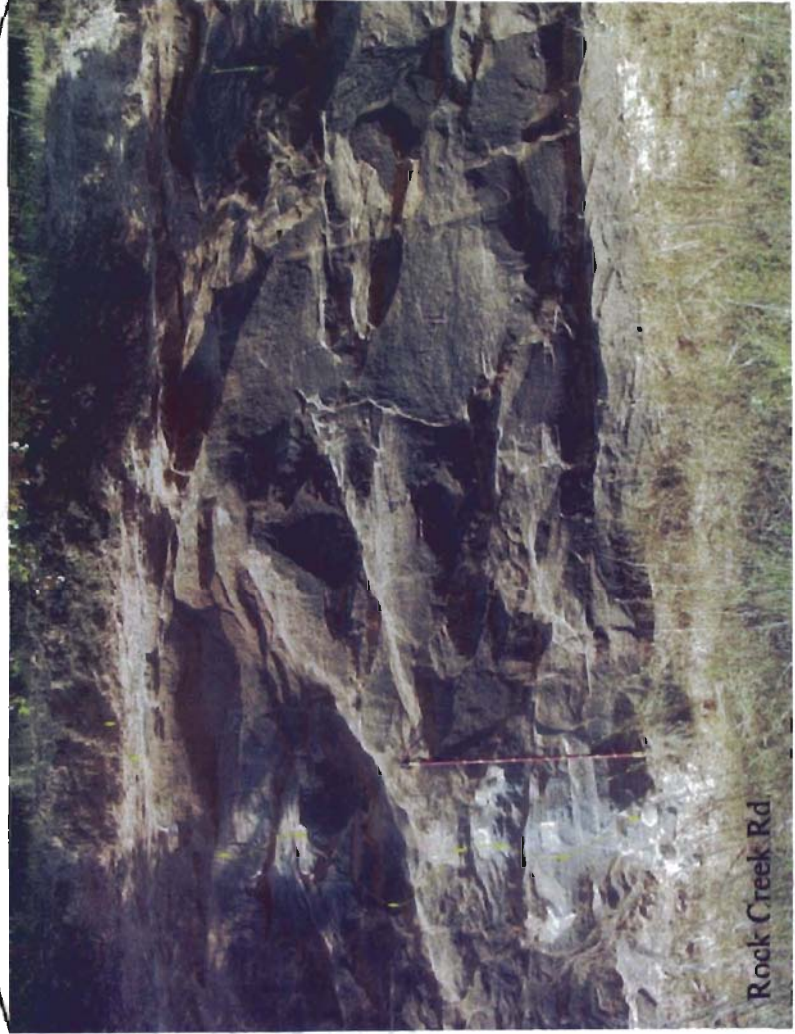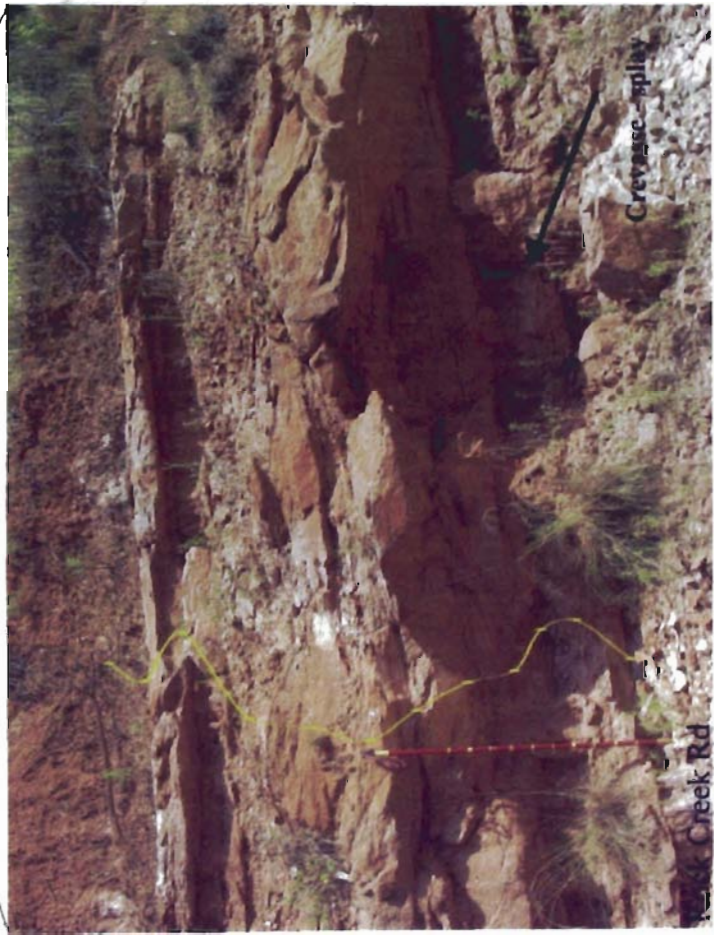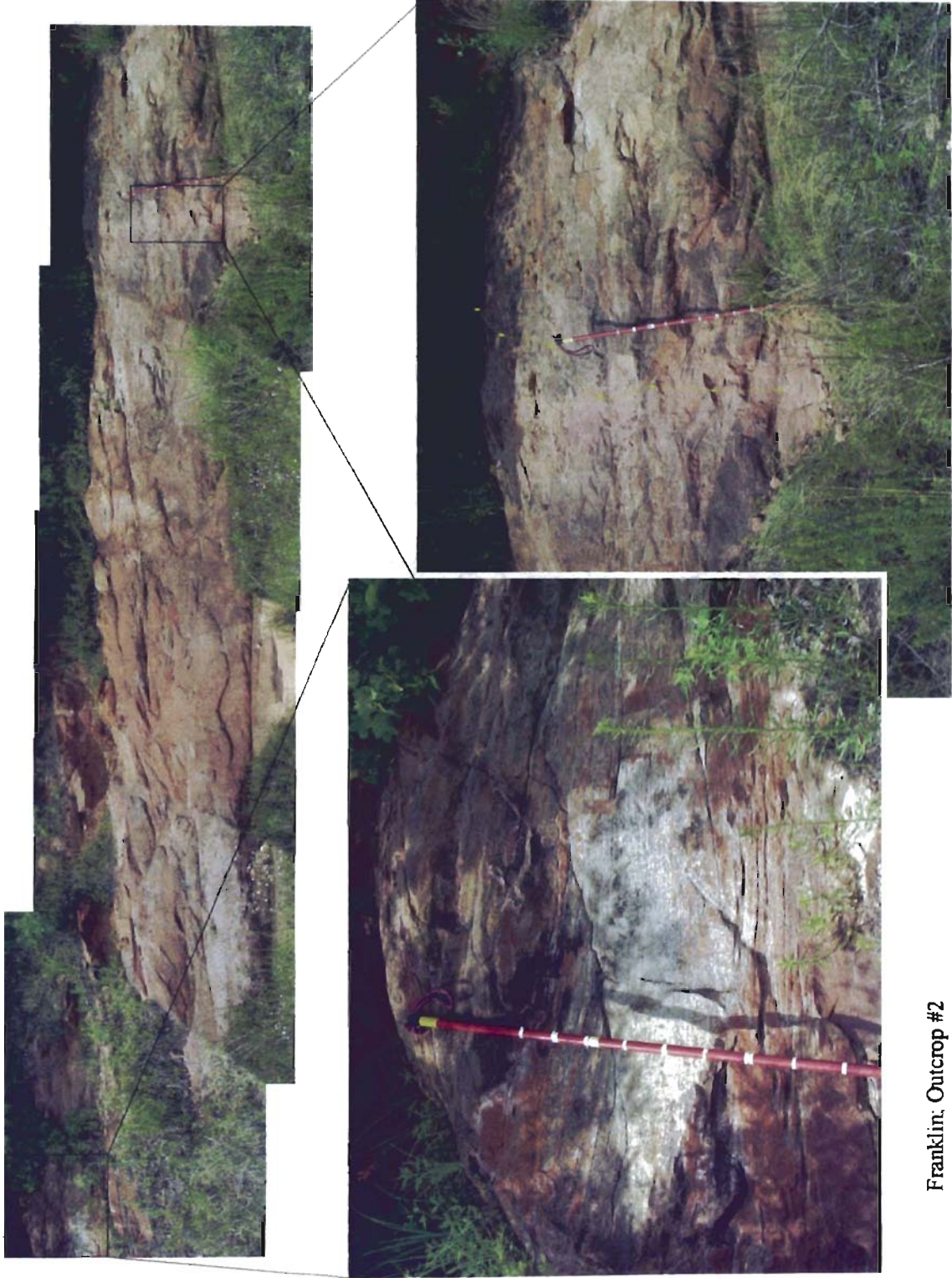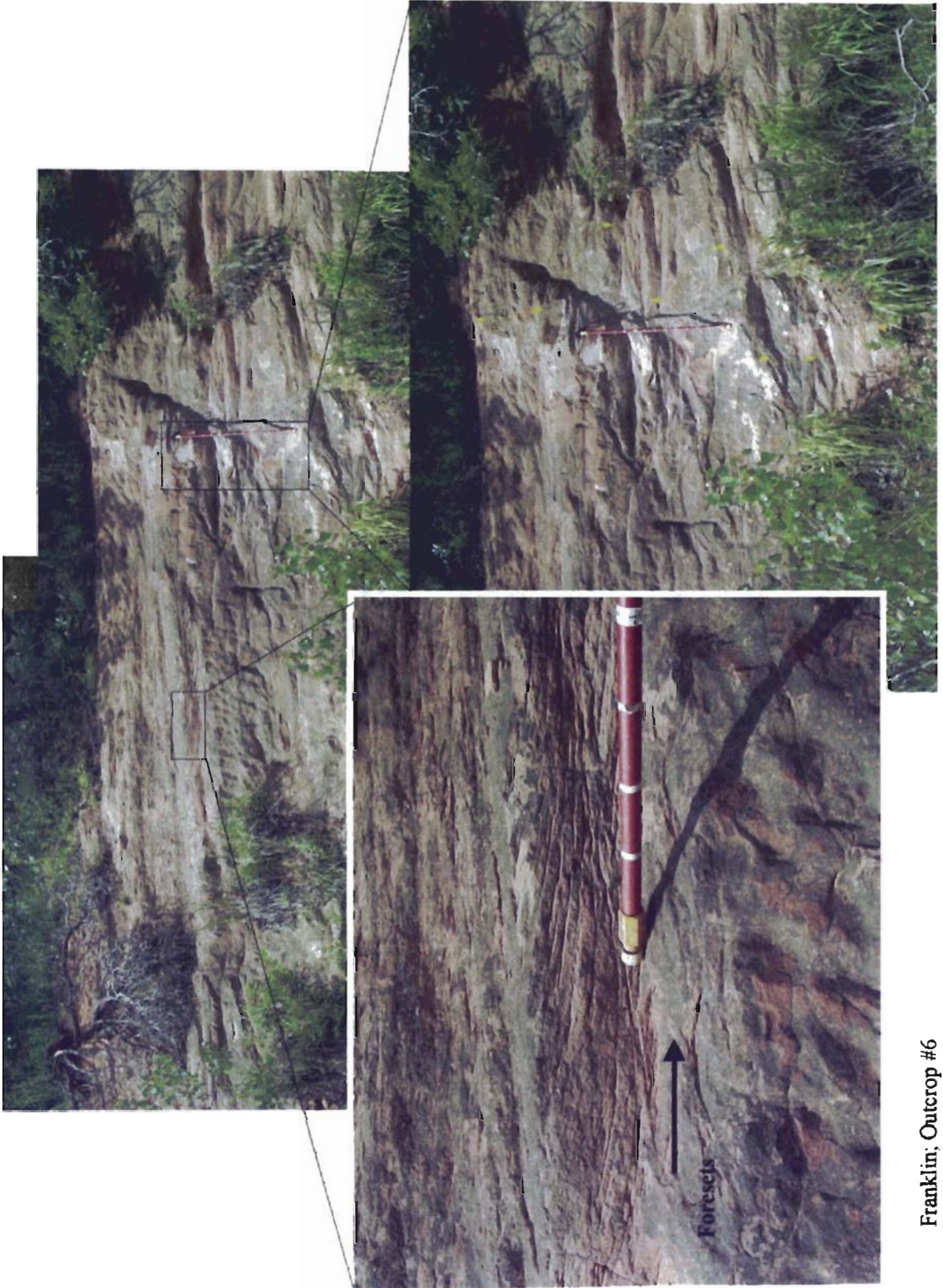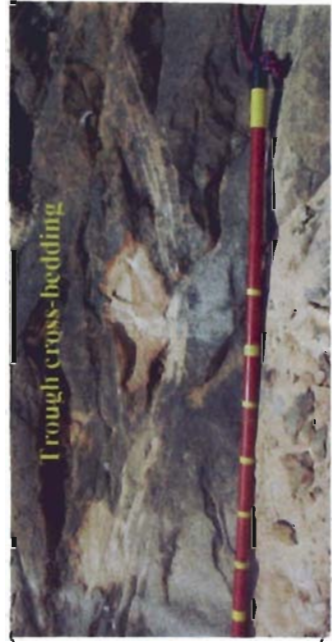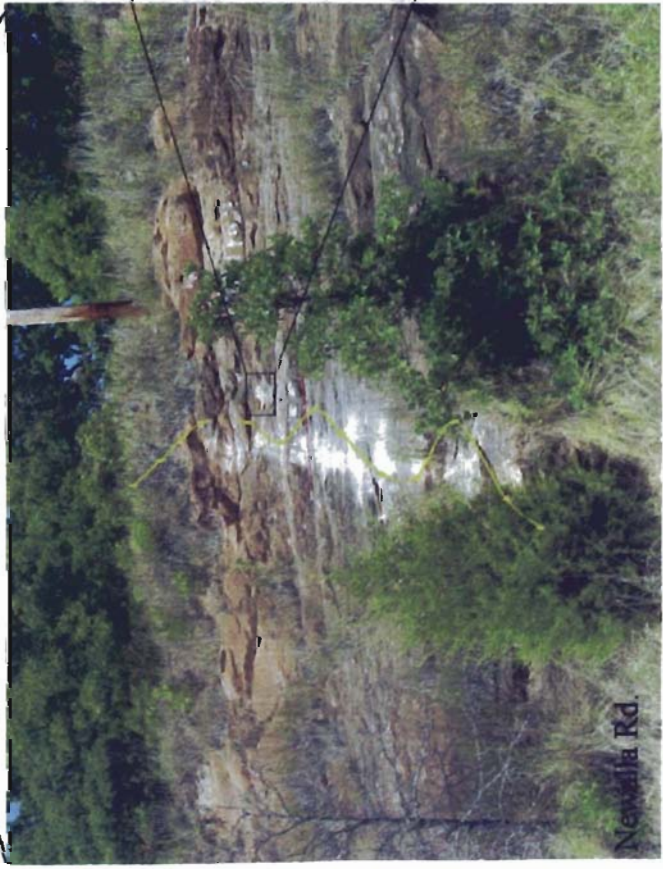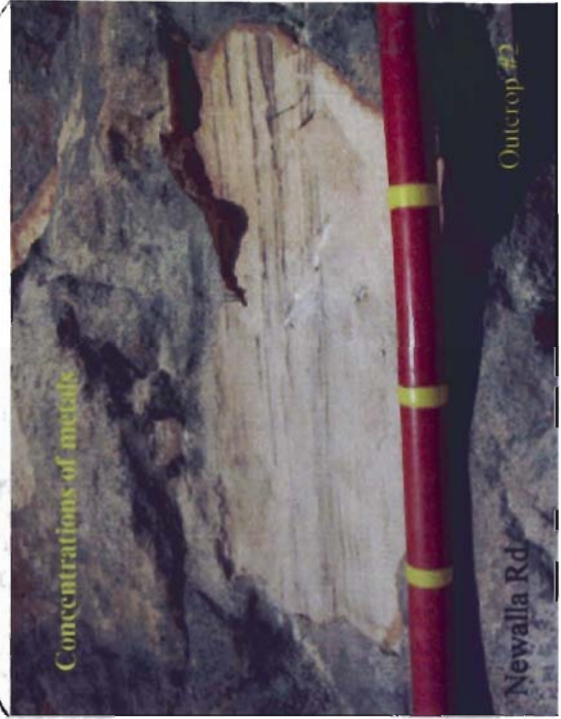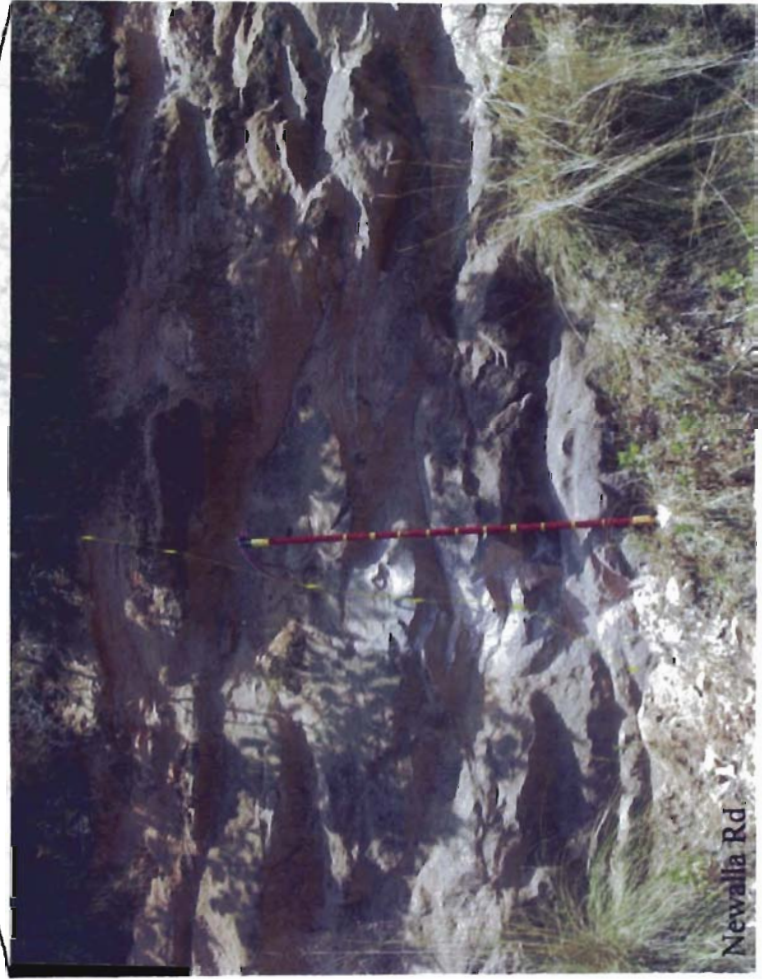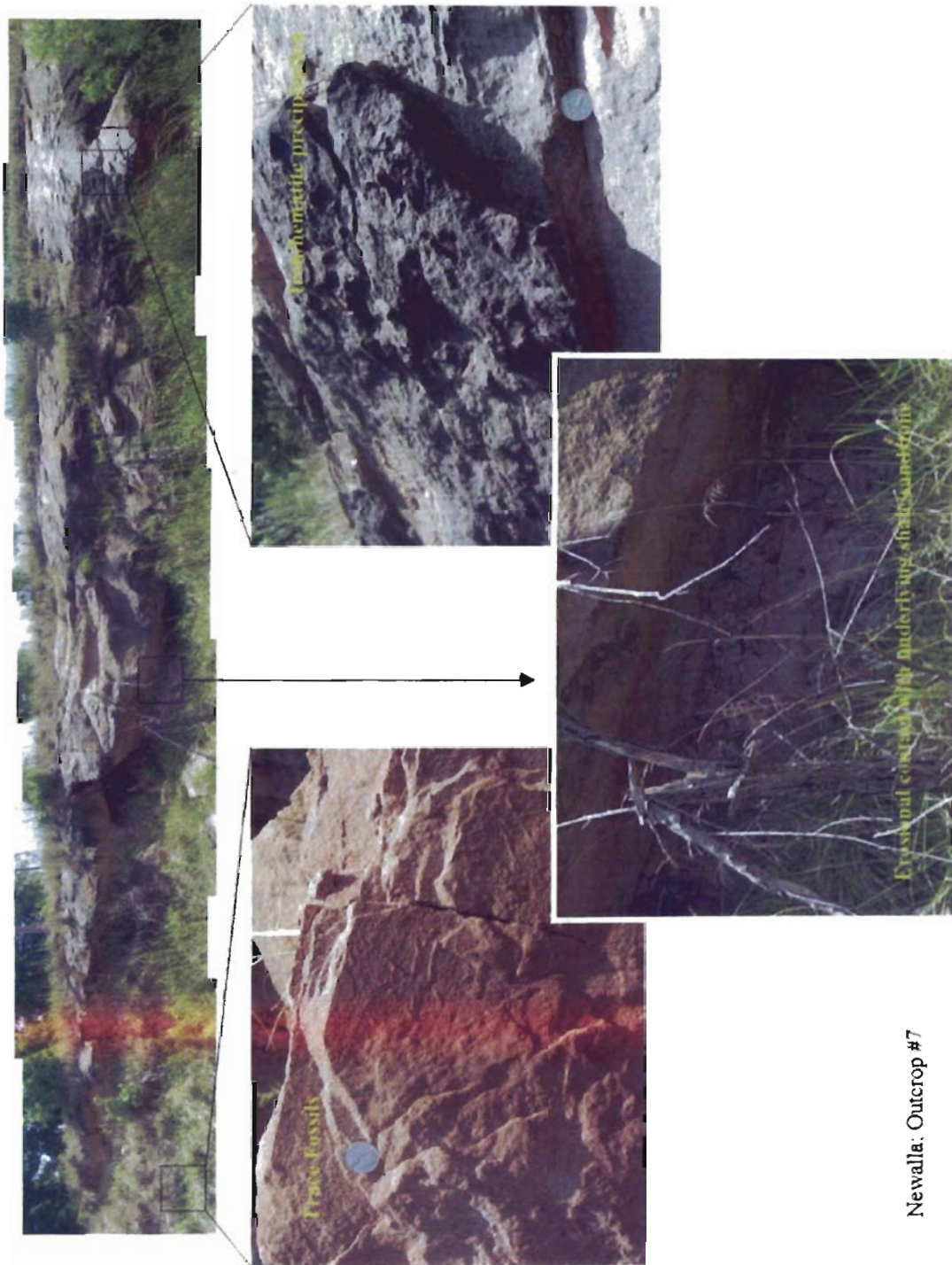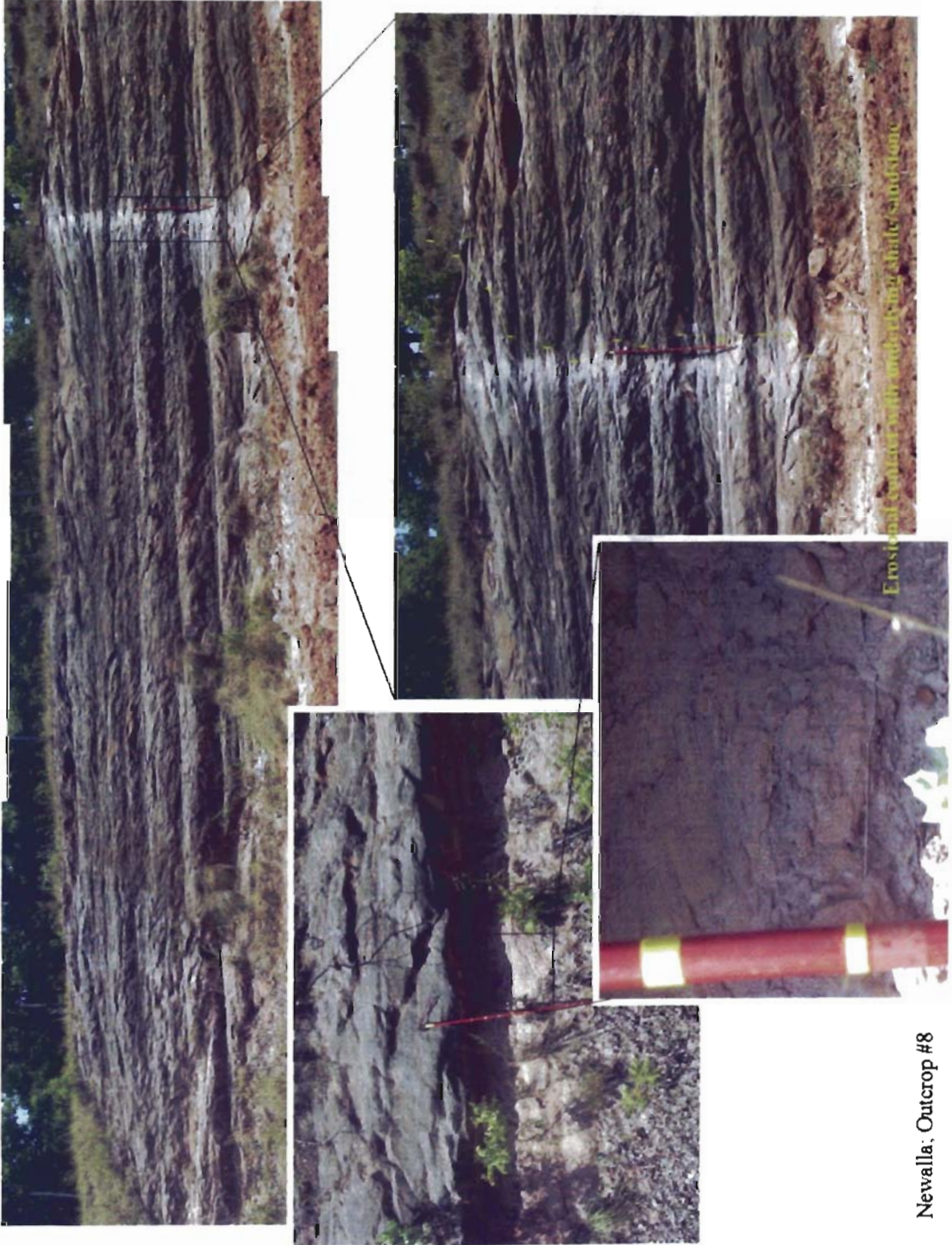
Peebly; Outcrop #2

Peebly, Outcrop #3

Peebly; Outcrop #6A

189

Ripple laminae

Erosional contact with underlying shale/sandtone
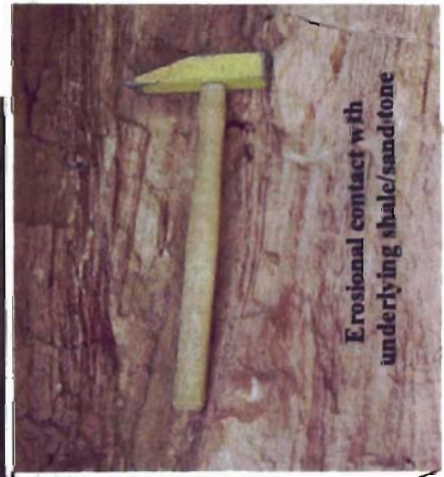
Peebly, Outcrop #6A

Peebly; Outcrop #6B

Foresets
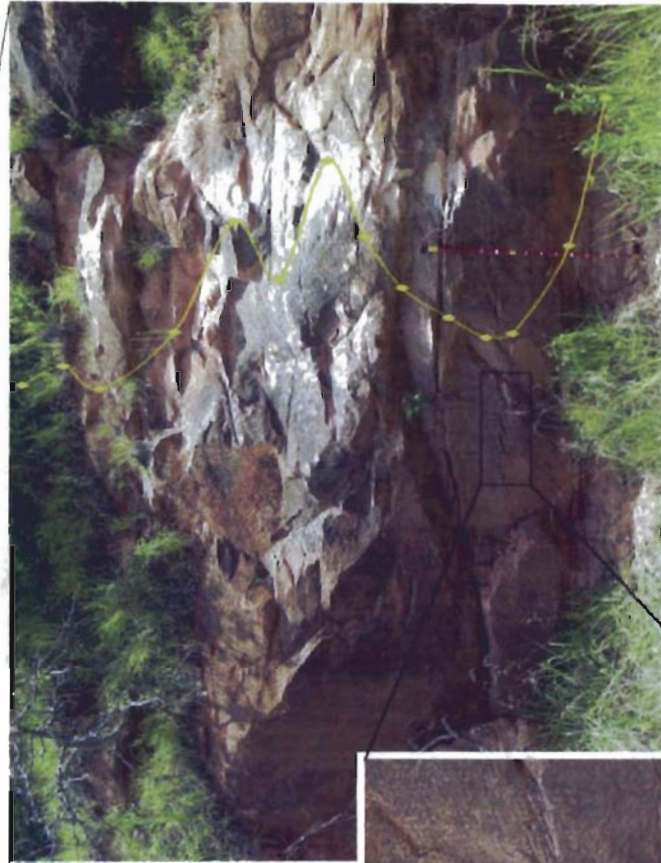
180th Ave: Outcrop #2

APPENDIX B

Group #2~ Sandstone with Erosional Base, but no Internal Sedimentary Structure

Outcrop #1

180th Ave.

Outcrop #3

195

180th Ave.

Chemical reduction

Outcrop #4

Outcrop #1A

Hematite rich
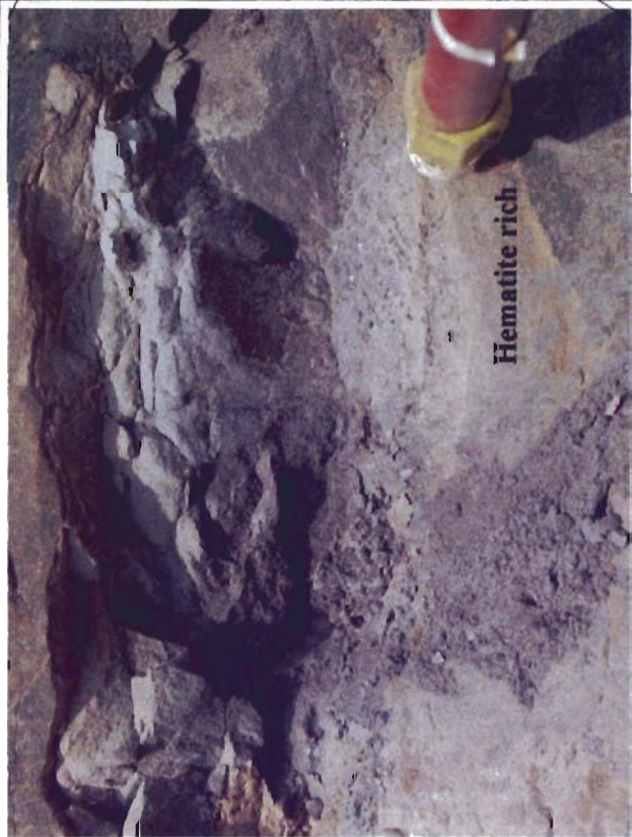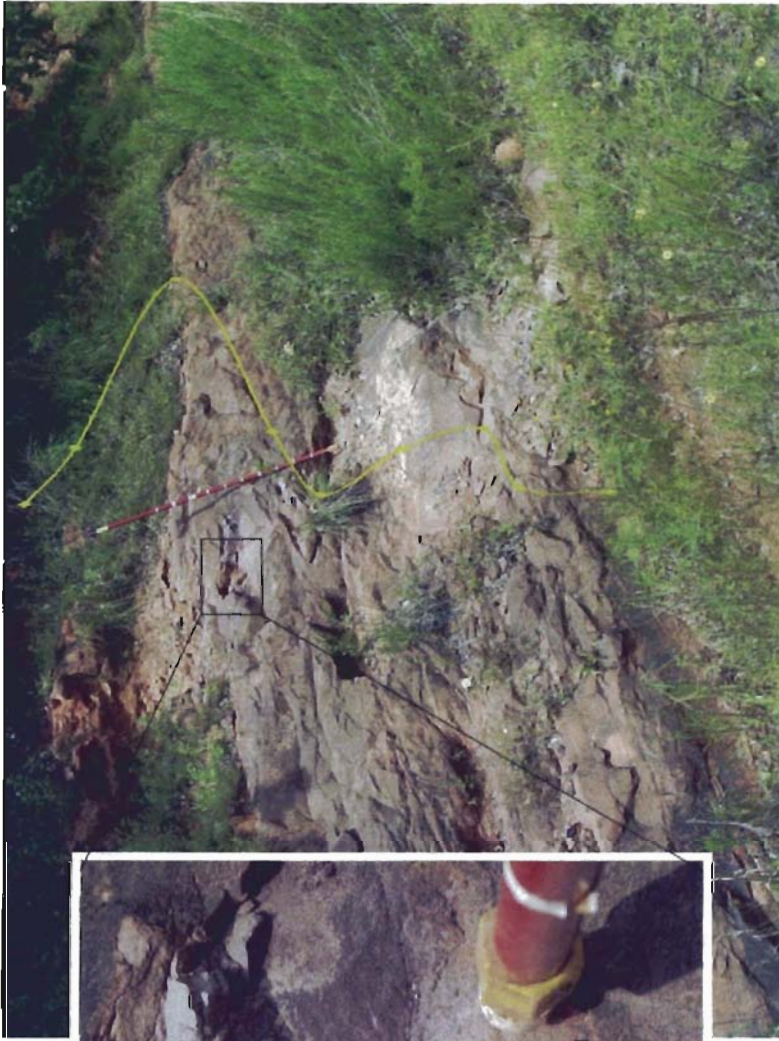
Franklin; Outcrop #1B

198

Outcrop #5

Outcrop #8

Alameda St.

Outcrop #3

APPENDIX B

Group #3~ Block Cross-Bedded Sandstone with Mud-Rip-Up Clasts

Rock Creek Rd.

Outcrop #3

Outcrop #3

Alameda St.

Foresets

APPENDIX B

Group #4~ Horizontal to Low-Angle Planar Laminations

Franklin; Outcrop #5

206
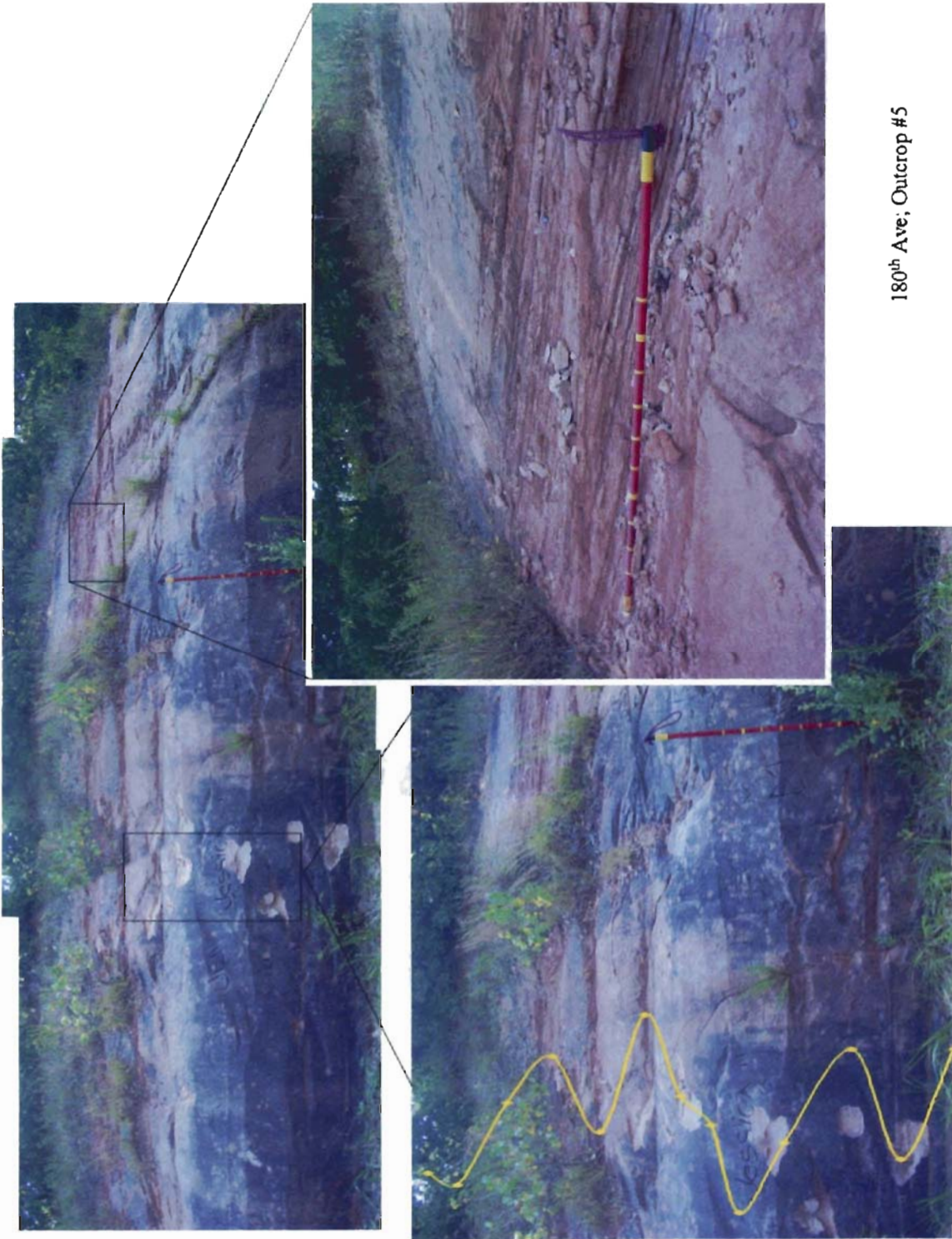
180th Ave; Outcrop #5

Alameda; Outcrop #5

Horizontal Laminae

208

Ripples Marks
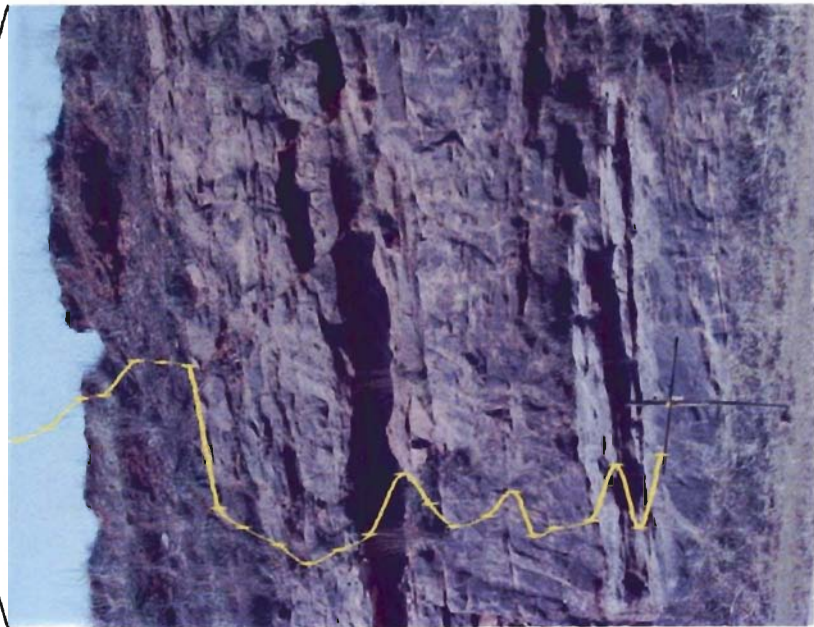
Alameda; Outcrop #1B

209

Alameda; Outcrop #1A

Metal zoning
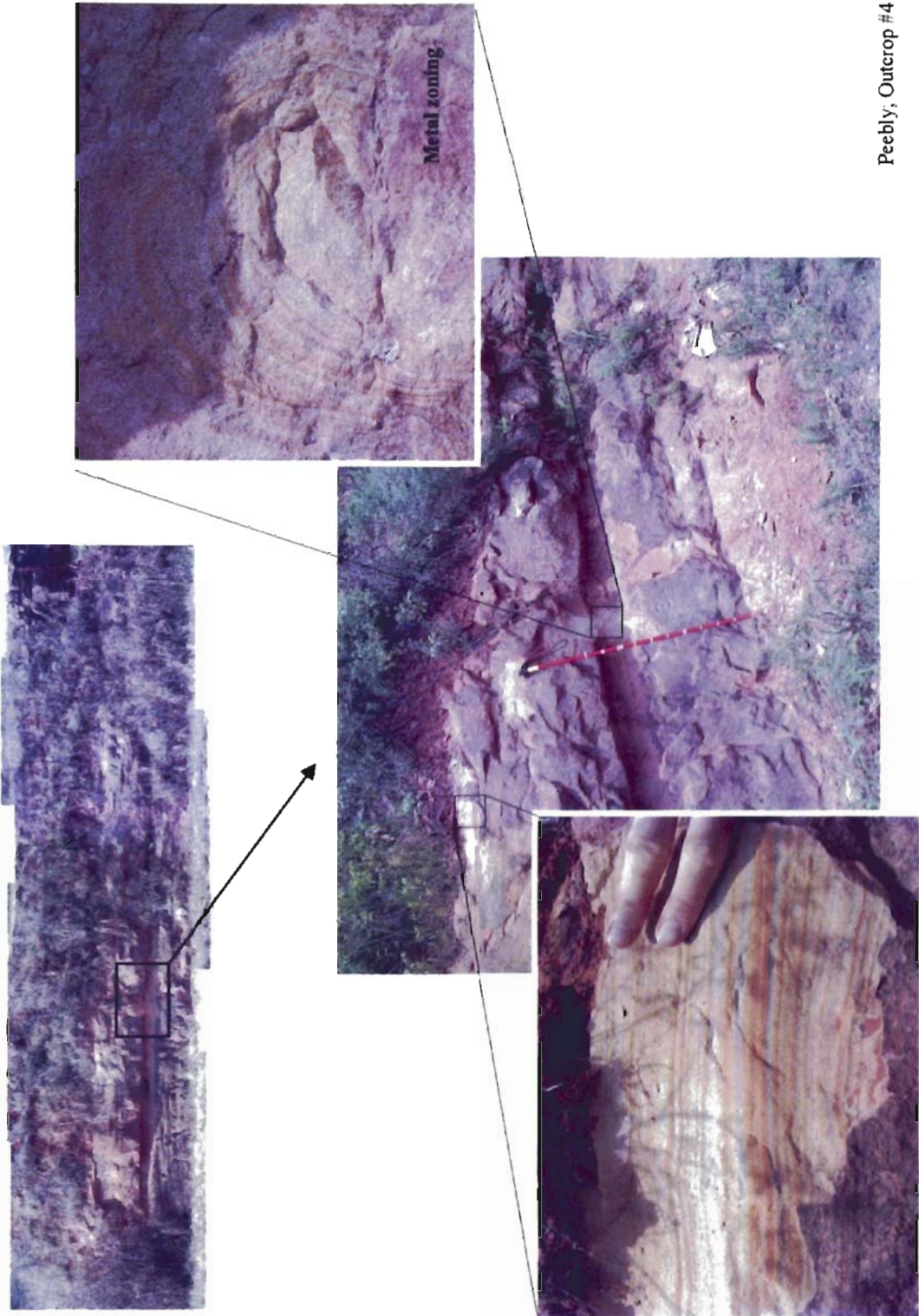
APPENDIX C

ELECTRON MICROPROBE TRANSECT DATA #1

Label	No	X		Y	W%(Mg)	W%(As)
Beam Current :	20					
Acc. Voltage :	20					
Take Off Angle :	40					
Tilt Angle :	0					
Azimut Angle :	0					
Label	No	X		Y	W%(Mg)	W%(As)
1	1	11561	0	29964	0.1391	0.0001
arsenicline_1	2	11561	21	29964	0.1369	0.0001
arsenicline_2	3	11540	41	29964	0.1011	0.0001
arsenicline_3	4	11520	62	29964	0.0005	0.0001
arsenicline_4	5	11499	82	29964	0.0831	0.0001
arsenicline_5	6	11479	103	29964	0.0015	0.0001
arsenicline_6	7	11458	124	29964	0.0027	0.0001
arsenicline_7	8	11437	144	29964	0.0027	0.0001
arsenicline_8	9	11417	165	29964	0.6111	0.0001
arsenicline_9	10	11396	185	29964	0.6283	0.0001
arsenicline_10	11	11376	206	29964	0.4032	0.0001
arsenicline_11	12	11355	227	29964	0.0035	0.0001
arsenicline_12	13	11334	247	29964	0.0065	0.0001
arsenicline_13	14	11314	268	29964	0.0035	0.0001
arsenicline_14	15	11293	288	29964	0.0001	0.0001
arsenicline_15	16	11273	309	29964	0.8149	0.0001
arsenicline_16	17	11252	329	29964	0.0207	0.0001
arsenicline_17	18	11232	350	29964	0.0057	0.0001
arsenicline_18	19	11211	371	29964	0.3047	0.0001
arsenicline_19	20	11190	391	29964	0.1622	0.0001
arsenicline_20	21	11170	412	29964	1.0853	0.0001
arsenicline_21	22	11149	432	29964	0.7612	0.0001
arsenicline_22	23	11129	453	29964	0.6516	0.0001
arsenicline_23	24	11108	474	29964	0.2556	0.0001
arsenicline_24	25	11087	494	29964	0.2495	0.0001
arsenicline_25	26	11067	515	29964	0.9995	0.0001
arsenicline_26	27	11046	535	29964	0.4371	0.0001
arsenicline_27	28	11026	556	29964	0.003	0.0001
arsenicline_28	29	11005	577	29964	0.0168	0.0001
arsenicline_29	30	10984	597	29964	0.467	0.0001
arsenicline_30	31	10964	618	29964	0.0331	0.0001
arsenicline_31	32	10943	638	29964	0.5409	0.0001
arsenicline_32	33	10923	659	29964	0.2538	0.0001
arsenicline_33	34	10902	680	29964	0.8101	0.0001
arsenicline_34	35	10881	700	29964	0.3725	0.0001
arsenicline_35	36	10861	721	29964	1.0475	0.0001
arsenicline_36	37	10840	741	29964	0.7713	0.0001
arsenicline_37	38	10820	762	29964	0.878	0.0001
arsenicline_38	39	10799	783	29964	0.6231	0.0001
arsenicline_39	40	10778	803	29964	0.0001	0.0001
arsenicline_40	41	10758	824	29964	0.0083	0.0001
arsenicline_41	42	10737	844	29964	1.0176	0.0001
arsenicline_42	43	10717	865	29964	0.4501	0.0001
arsenicline_43	44	10696	885	29964	0.1401	0.0001
arsenicline_44	45	10676	906	29964	0.4395	0.0001

arsenicline_45	46	10655	927	29964	0.237	0.0001
arsenicline_46	47	10634	947	29964	0.0371	0.0001
arsenicline_47	48	10614	968	29964	0.1635	0.0001
arsenicline_48	49	10593	988	29964	0.0128	0.0001
arsenicline_49	50	10573	1009	29964	0.3379	0.0001
arsenicline_50	51	10552	1030	29964	0.0005	0.0001
arsenicline_51	52	10531	1050	29964	0.0094	0.0001
arsenicline_52	53	10511	1071	29964	0.0915	0.0001
arsenicline_53	54	10490	1091	29964	0.1167	0.0001
arsenicline_54	55	10470	1112	29964	0.5383	0.0001
arsenicline_55	56	10449	1133	29964	0.6235	0.0001
arsenicline_56	57	10428	1153	29964	0.0138	0.0001
arsenicline_57	58	10408	1174	29964	0.0151	0.0001
arsenicline_58	59	10387	1194	29964	0.0035	0.0001
arsenicline_59	60	10367	1215	29964	0.0001	0.0001
arsenicline_60	61	10346	1236	29964	0.0005	0.0001
arsenicline_61	62	10325	1256	29964	0.0579	0.0001
arsenicline_62	63	10305	1277	29964	0.1078	0.0001
arsenicline_63	64	10284	1297	29964	0.2769	0.0001
arsenicline_64	65	10264	1318	29964	0.1442	0.0001
arsenicline_65	66	10243	1339	29964	0.4406	0.0001
arsenicline_66	67	10222	1359	29964	0.0001	0.0001
arsenicline_67	68	10202	1380	29964	0.3492	0.0001
arsenicline_68	69	10181	1400	29964	1.0779	0.0001
arsenicline_69	70	10161	1421	29964	1.1044	0.0001
arsenicline_70	71	10140	1442	29964	0.0251	0.0001
arsenicline_71	72	10119	1462	29964	0.5547	0.0001
arsenicline_72	73	10099	1483	29964	1.2185	0.0001
arsenicline_73	74	10078	1503	29964	0.1343	0.0001
arsenicline_74	75	10058	1524	29964	0.3384	0.0001
arsenicline_75	76	10037	1544	29964	0.4777	0.0001
arsenicline_76	77	10017	1565	29964	0.1801	0.0001
arsenicline_77	78	9996	1586	29964	0.1167	0.0001
arsenicline_78	79	9975	1606	29964	0.0001	0.0001
arsenicline_79	80	9955	1627	29964	0.1253	0.0001
arsenicline_80	81	9934	1647	29964	1.1795	0.0001
arsenicline_81	82	9914	1668	29964	0.3436	0.0001
arsenicline_82	83	9893	1689	29964	0.9149	0.0001
arsenicline_83	84	9872	1709	29964	0.7789	0.0001
arsenicline_84	85	9852	1730	29964	0.2926	0.0001
arsenicline_85	86	9831	1750	29964	0.323	0.0001
arsenicline_86	87	9811	1771	29964	0.3519	0.0001
arsenicline_87	88	9790	1792	29964	0.3749	0.0001
arsenicline_88	89	9769	1812	29964	0.3503	0.0001
arsenicline_89	90	9749	1833	29964	0.2189	0.0001
arsenicline_90	91	9728	1853	29964	0.2978	0.0001
arsenicline_91	92	9708	1874	29964	0.2953	0.0001
arsenicline_92	93	9687	1895	29964	0.2663	0.0001
arsenicline_93	94	9666	1915	29964	0.3584	0.0001
arsenicline_94	95	9646	1936	29964	0.1985	0.0001
arsenicline_95	96	9625	1956	29964	0.4319	0.0001

arsenicline_96	97	9605	1977	29964	0.5045	0.0001
arsenicline_97	98	9584	1998	29964	0.1757	0.0001
arsenicline_98	99	9563	2018	29964	0.8987	0.0001
arsenicline_99	100	9543	2039	29964	0.4028	0.0001
arsenicline_100	101	9522	2059	29964	0.9523	0.0001
arsenicline_101	102	9502	2080	29963	1.0034	0.0001
arsenicline_102	103	9481	2100	29963	1.6182	0.0001
arsenicline_103	104	9461	2121	29963	0.6723	0.0001
arsenicline_104	105	9440	2142	29963	0.0708	0.0001
arsenicline_105	106	9419	2162	29963	0.0938	0.0001
arsenicline_106	107	9399	2183	29963	0.3529	0.0001
arsenicline_107	108	9378	2203	29963	0.902	0.0001
arsenicline_108	109	9358	2224	29963	0.7762	0.0001
arsenicline_109	110	9337	2245	29963	0.1268	0.0001
arsenicline_110	111	9316	2265	29963	0.03	0.0001
arsenicline_111	112	9296	2286	29963	0.3941	0.0001
arsenicline_112	113	9275	2306	29963	1.1956	0.0001
arsenicline_113	114	9255	2327	29963	0.4475	0.0001
arsenicline_114	115	9234	2348	29963	0.0431	0.0001
arsenicline_115	116	9213	2368	29963	0.9577	0.0001
arsenicline_116	117	9193	2389	29963	1.038	0.0001
arsenicline_117	118	9172	2409	29963	0.4156	0.0001
arsenicline_118	119	9152	2430	29963	0.3675	0.0001
arsenicline_119	120	9131	2451	29963	0.2754	0.0001
arsenicline_120	121	9110	2471	29963	0.0612	0.0001
arsenicline_121	122	9090	2492	29963	0.9052	0.0001
arsenicline_122	123	9069	2512	29963	0.4454	0.0001
arsenicline_123	124	9049	2533	29963	0.3272	0.0001
arsenicline_124	125	9028	2554	29963	0.0001	0.0001
arsenicline_125	126	9007	2574	29963	0.2698	0.0001
arsenicline_126	127	8987	2595	29963	0.4633	0.0001
arsenicline_127	128	8966	2615	29963	0.2429	0.0001
arsenicline_128	129	8946	2636	29963	1.2459	0.0001
arsenicline_129	130	8925	2656	29963	0.7212	0.0001
arsenicline_130	131	8905	2677	29963	0.3162	0.0001
arsenicline_131	132	8884	2698	29963	0.3852	0.0001
arsenicline_132	133	8863	2718	29963	0.4528	0.0001
arsenicline_133	134	8843	2739	29963	0.8732	0.0001
arsenicline_134	135	8822	2759	29963	0.45	0.0001
arsenicline_135	136	8802	2780	29963	0.3414	0.0001
arsenicline_136	137	8781	2801	29963	0.2573	0.0001
arsenicline_137	138	8760	2821	29963	0.1138	0.0001
arsenicline_138	139	8740	2842	29963	1.0453	0.0001
arsenicline_139	140	8719	2862	29963	0.8189	0.0001
arsenicline_140	141	8699	2883	29963	0.0551	0.0001
arsenicline_141	142	8678	2904	29963	0.1538	0.0001
arsenicline_142	143	8657	2924	29963	1.5362	0.0001
arsenicline_143	144	8637	2945	29963	0.7901	0.0001
arsenicline_144	145	8616	2965	29963	0.8703	0.0001
arsenicline_145	146	8596	2986	29963	0.7521	0.0001
arsenicline_146	147	8575	3007	29963	0.2358	0.0001

arsenicline_147	148	8554	3027	29963	0.0389	0.0001
arsenicline_148	149	8534	3048	29963	0.0094	0.0001
arsenicline_149	150	8513	3068	29963	0.0595	0.0001
arsenicline_150	151	8493	3089	29963	0.4789	0.0001
arsenicline_151	152	8472	3110	29963	1.1846	0.0001
arsenicline_152	153	8451	3130	29963	0.5775	0.0001
arsenicline_153	154	8431	3151	29963	0.3753	0.0001
arsenicline_154	155	8410	3171	29963	0.1847	0.0001
arsenicline_155	156	8390	3192	29963	0.3131	0.0001
arsenicline_156	157	8369	3213	29963	0.27	0.0001
arsenicline_157	158	8348	3233	29963	0.3908	0.0001
arsenicline_158	159	8328	3254	29963	0.3603	0.0001
arsenicline_159	160	8307	3274	29963	0.0639	0.0001
arsenicline_160	161	8287	3295	29963	0.732	0.0001
arsenicline_161	162	8266	3315	29963	0.1201	0.0001
arsenicline_162	163	8246	3336	29963	0.0804	0.0001
arsenicline_163	164	8225	3357	29963	0.0963	0.0001
arsenicline_164	165	8204	3377	29963	0.2038	0.0001
arsenicline_165	166	8184	3398	29963	0.1428	0.0001
arsenicline_166	167	8163	3418	29963	0.5074	0.0001
arsenicline_167	168	8143	3439	29963	0.5396	0.0001
arsenicline_168	169	8122	3460	29963	0.7359	0.0001
arsenicline_169	170	8101	3480	29963	0.3976	0.0001
arsenicline_170	171	8081	3501	29963	0.3393	0.0001
arsenicline_171	172	8060	3521	29963	0.5905	0.0001
arsenicline_172	173	8040	3542	29963	0.7221	0.0001
arsenicline_173	174	8019	3563	29963	0.3242	0.0001
arsenicline_174	175	7998	3583	29963	0.0426	0.0001
arsenicline_175	176	7978	3604	29963	0.57	0.0001
arsenicline_176	177	7957	3624	29963	0.0175	0.0001
arsenicline_177	178	7937	3645	29963	0.363	0.0001
arsenicline_178	179	7916	3666	29963	0.3041	0.0001
arsenicline_179	180	7895	3686	29963	1.0332	0.0001
arsenicline_180	181	7875	3707	29963	0.2576	0.0001
arsenicline_181	182	7854	3727	29963	0.0924	0.0001
arsenicline_182	183	7834	3748	29963	0.8778	0.0001
arsenicline_183	184	7813	3769	29963	0.4191	0.0001
arsenicline_184	185	7792	3789	29963	0.0632	0.0001
arsenicline_185	186	7772	3810	29963	1.1262	0.0001
arsenicline_186	187	7751	3830	29963	0.6399	0.0001
arsenicline_187	188	7731	3851	29963	0.8533	0.0001
arsenicline_188	189	7710	3871	29963	0.9139	0.0001
arsenicline_189	190	7690	3892	29963	0.8778	0.0001
arsenicline_190	191	7669	3913	29963	0.8523	0.0001
arsenicline_191	192	7648	3933	29963	1.1847	0.0001
arsenicline_192	193	7628	3954	29963	0.9202	0.0001
arsenicline_193	194	7607	3974	29963	0.37	0.0001
arsenicline_194	195	7587	3995	29963	0.3566	0.0001
arsenicline_195	196	7566	4016	29963	0.0303	0.0001
arsenicline_196	197	7545	4036	29963	0.0124	0.0001
arsenicline_197	198	7525	4057	29963	1.0511	0.0001

arsenicline_198	199	7504	4077	29963	0.9388	0.0001
arsenicline_199	200	7484	4098	29963	0.9505	0.0001
arsenicline_200	201	7463		29963	1.1904	0.0001

APPENDIX D

ELECTRON MICROPROBE TRANSECT DATA #2

Label	crud_01	crud_02	line3_1	line3_2	line3_3	line3_4	line3_5
No	8	9	11	12	13	14	15
X	10099	10240	13269	13249	13229	13209	13189
Y	18334	18210	24290	24284	24278	24271	24265
MgO	0.02	0.00	0.00	0.02	0.00	0.02	0.01
Al2O3	0.01	0.04	0.16	0.10	0.02	0.00	0.02
Cr2O3	0.02	0.06	0.13	0.05	0.00	0.06	0.12
Fe2O3	83.2	77.5	85.1	80.9	81.4	80.9	79.7
As2O10	0.00	0.00	0.00	0.00	0.00	0.00	0.00
Total	83.3	77.6	85.4	81.1	81.5	81.0	79.8
Mg	0.0	0.0	0.0	0.0	0.0	0.0	0.0
Al	0.0	0.0	0.0	0.0	0.0	0.0	0.0
Cr	0.0	0.0	0.0	0.0	0.0	0.0	0.0
Fe	16.0	16.0	15.9	16.0	16.0	16.0	16.0
As	0.0	0.0	0.0	0.0	0.0	0.0	0.0
Total	16.0	16.0	16.0	16.0	16.0	16.0	16.0

Label	line3_6	line3_7	line4_1	line4_2	line4_3	line4_4	line4_5
No	16	17	18	19	20	21	22
X	13170	13150	13130	13108	13085	13063	13041
Y	24259	24253	24246	24239	24232	24225	24218
MgO	0.00	0.00	0.03	0.03	0.00	0.00	0.01
Al2O3	0.00	0.06	0.06	0.04	0.03	0.06	0.00
Cr2O3	0.03	0.00	0.00	0.02	0.00	0.11	0.00
Fe2O3	78.5	81.2	77.6	80.7	74.9	99.3	80.6
As2O10	0.00	0.00	0.00	0.00	0.00	0.00	0.00
Total	78.5	81.2	77.7	80.8	74.9	99.4	80.6
Mg	0.0	0.0	0.0	0.0	0.0	0.0	0.0
Al	0.0	0.0	0.0	0.0	0.0	0.0	0.0
Cr	0.0	0.0	0.0	0.0	0.0	0.0	0.0
Fe	16.0	16.0	16.0	16.0	16.0	16.0	16.0
As	0.0	0.0	0.0	0.0	0.0	0.0	0.0
Total	16.0	16.0	16.0	16.0	16.0	16.0	16.0

Label	line4_6	line4_7	line4_8	line4_9	line4_10	line4_11	line5_1
No	23	24	25	26	27	28	29
X	13018	12996	12974	12951	12929	12907	12884
Y	24211	24204	24197	24190	24183	24176	24169
MgO	0.00	0.00	0.00	0.04	0.00	0.00	0.01
Al2O3	0.07	0.03	0.13	0.03	0.00	0.51	0.22
Cr2O3	0.04	0.07	0.09	0.00	0.00	0.30	0.00
Fe2O3	83.4	80.6	80.6	75.4	82.3	61.7	82.5
As2O10	0.00	0.00	0.00	0.00	0.00	0.00	0.00
Total	83.6	80.7	80.8	75.5	82.3	62.5	82.7
Mg	0.0	0.0	0.0	0.0	0.0	0.0	0.0
Al	0.0	0.0	0.0	0.0	0.0	0.2	0.1
Cr	0.0	0.0	0.0	0.0	0.0	0.1	0.0
Fe	16.0	16.0	15.9	16.0	16.0	15.7	15.9
As	0.0	0.0	0.0	0.0	0.0	0.0	0.0
Total	16.0	16.0	16.0	16.0	16.0	16.0	16.0

Label	line5_2	line5_3	line5_4	line5_5	line5_6	line5_7	line5_8
No	30	31	32	33	34	35	36
X	12862	12839	12817	12795	12772	12750	12728
Y	24162	24155	24148	24141	24134	24127	24120
MgO	0.00	0.00	0.02	0.00	0.00	0.07	0.00
Al2O3	0.25	0.16	0.00	0.17	0.02	0.02	0.00
Cr2O3	0.03	0.10	0.00	0.14	0.02	0.00	0.02
Fe2O3	75.9	78.4	88.8	77.7	87.6	88.3	87.0
As2O10	0.00	0.00	0.00	0.00	0.00	0.00	0.00
Total	76.2	78.7	88.9	78.1	87.6	88.3	87.1
Mg	0.0	0.0	0.0	0.0	0.0	0.0	0.0
Al	0.1	0.1	0.0	0.1	0.0	0.0	0.0
Cr	0.0	0.0	0.0	0.0	0.0	0.0	0.0
Fe	15.9	15.9	16.0	15.9	16.0	16.0	16.0
As	0.0	0.0	0.0	0.0	0.0	0.0	0.0
Total	16.0	16.0	16.0	16.0	16.0	16.0	16.0

Label	line5_9	line5_10	line5_11	line5_12	line6_1	line6_2	line6_3
No	37	38	39	40	41	42	43
X	12705	12683	12661	12638	12616	12594	12571
Y	24113	24106	24099	24092	24085	24078	24071
MgO	0.00	0.01	0.00	0.01	0.04	0.02	0.00
Al2O3	0.00	0.01	0.04	0.10	0.03	0.00	0.01
Cr2O3	0.02	0.02	0.00	0.07	0.00	0.04	0.05
Fe2O3	85.0	78.8	85.8	82.4	79.7	85.1	85.1
As2O10	0.00	0.00	0.00	0.00	0.00	0.00	0.00
Total	85.0	78.8	85.9	82.5	79.8	85.1	85.1
Mg	0.0	0.0	0.0	0.0	0.0	0.0	0.0
Al	0.0	0.0	0.0	0.0	0.0	0.0	0.0
Cr	0.0	0.0	0.0	0.0	0.0	0.0	0.0
Fe	16.0	16.0	16.0	16.0	16.0	16.0	16.0
As	0.0	0.0	0.0	0.0	0.0	0.0	0.0
Total	16.0	16.0	16.0	16.0	16.0	16.0	16.0

Label	line6_4	line6_5	line6_6	line6_7	line6_8	line6_9	line6_10
No	44	45	46	47	48	49	50
X	12549	12527	12504	12482	12460	12437	12415
Y	24064	24057	24050	24043	24036	24029	24022
MgO	0.00	0.00	0.01	0.00	0.00	0.02	0.00
Al2O3	0.00	0.00	0.03	0.21	0.01	0.00	0.13
Cr2O3	0.00	0.07	0.00	0.14	0.01	0.07	0.17
Fe2O3	81.9	87.5	80.9	80.3	82.7	78.4	84.1
As2O10	0.00	0.00	0.00	0.00	0.00	0.00	0.00
Total	81.9	87.5	80.9	80.7	82.7	78.5	84.4
Mg	0.0	0.0	0.0	0.0	0.0	0.0	0.0
Al	0.0	0.0	0.0	0.1	0.0	0.0	0.0
Cr	0.0	0.0	0.0	0.0	0.0	0.0	0.0
Fe	16.0	16.0	16.0	15.9	16.0	16.0	15.9
As	0.0	0.0	0.0	0.0	0.0	0.0	0.0
Total	16.0	16.0	16.0	16.0	16.0	16.0	16.0

Label	line6_11	line6_12	line6_13	line6_14	line6_15	line6_16	line6_17
No	51	52	53	54	55	56	57
X	12393	12370	12348	12326	12303	12281	12259
Y	24015	24008	24001	23994	23987	23981	23974
MgO	0.01	0.00	0.00	0.02	0.05	0.03	0.02
Al2O3	0.09	0.07	0.08	0.00	0.08	0.06	0.10
Cr2O3	0.12	0.00	0.08	0.00	0.03	0.05	0.05
Fe2O3	82.2	86.9	75.0	84.6	78.6	79.0	76.0
As2O10	0.00	0.00	0.00	0.00	0.00	0.00	0.00
Total	82.4	86.9	75.1	84.7	78.8	79.1	76.2
Mg	0.0	0.0	0.0	0.0	0.0	0.0	0.0
Al	0.0	0.0	0.0	0.0	0.0	0.0	0.0
Cr	0.0	0.0	0.0	0.0	0.0	0.0	0.0
Fe	15.9	16.0	16.0	16.0	16.0	16.0	16.0
As	0.0	0.0	0.0	0.0	0.0	0.0	0.0
Total	16.0	16.0	16.0	16.0	16.0	16.0	16.0

Label	line6_18	line6_19	line6_20	line6_21	line6_22	line6_23	line6_24
No	58	59	60	61	62	63	64
X	12237	12214	12192	12170	12147	12125	12103
Y	23967	23960	23953	23946	23939	23932	23925
MgO	0.01	0.00	0.00	0.00	0.00	0.02	0.00
Al2O3	0.15	0.18	0.00	0.11	0.09	0.05	0.00
Cr2O3	0.04	0.00	0.00	0.17	0.02	0.01	0.07
Fe2O3	77.9	81.4	88.5	77.6	77.8	86.4	83.0
As2O10	0.00	0.00	0.00	0.00	0.00	0.00	0.00
Total	78.1	81.6	88.5	77.9	77.9	86.4	83.1
Mg	0.0	0.0	0.0	0.0	0.0	0.0	0.0
Al	0.0	0.1	0.0	0.0	0.0	0.0	0.0
Cr	0.0	0.0	0.0	0.0	0.0	0.0	0.0
Fe	15.9	15.9	16.0	15.9	16.0	16.0	16.0
As	0.0	0.0	0.0	0.0	0.0	0.0	0.0
Total	16.0	16.0	16.0	16.0	16.0	16.0	16.0

Label	line6_25	line6_26	line6_27	line6_28	line6_29	line6_30	line6_31
No	65	66	67	68	69	70	71
X	12080	12058	12036	12013	11991	11969	11946
Y	23918	23911	23904	23897	23890	23883	23876
MgO	0.00	0.03	0.01	0.00	0.00	0.03	0.02
Al2O3	0.07	0.00	0.11	0.01	0.02	0.03	0.00
Cr2O3	0.03	0.09	0.13	0.00	0.06	0.01	0.00
Fe2O3	80.8	88.7	82.3	74.7	68.5	83.3	77.5
As2O10	0.00	0.00	0.00	0.00	0.00	0.00	0.00
Total	80.9	88.8	82.6	74.7	68.6	83.3	77.6
Mg	0.0	0.0	0.0	0.0	0.0	0.0	0.0
Al	0.0	0.0	0.0	0.0	0.0	0.0	0.0
Cr	0.0	0.0	0.0	0.0	0.0	0.0	0.0
Fe	16.0	16.0	15.9	16.0	16.0	16.0	16.0
As	0.0	0.0	0.0	0.0	0.0	0.0	0.0
Total	16.0	16.0	16.0	16.0	16.0	16.0	16.0

Label	line6_32	line6_33	line6_34	line6_35	line6_36	line6_37	line6_38
No	72	73	74	75	76	77	78
X	11924	11902	11879	11857	11835	11812	11790
Y	23869	23862	23855	23848	23841	23834	23827
MgO	0.02	0.00	0.00	0.00	0.00	0.04	0.00
Al2O3	0.02	0.00	0.05	0.00	0.00	0.01	0.04
Cr2O3	0.00	0.04	0.04	0.02	0.04	0.00	0.00
Fe2O3	85.8	85.4	78.4	75.3	77.9	59.9	68.2
As2O10	0.00	0.00	0.00	0.00	0.00	0.00	0.00
Total	85.9	85.5	78.5	75.3	77.9	60.0	68.3
Mg	0.0	0.0	0.0	0.0	0.0	0.0	0.0
Al	0.0	0.0	0.0	0.0	0.0	0.0	0.0
Cr	0.0	0.0	0.0	0.0	0.0	0.0	0.0
Fe	16.0	16.0	16.0	16.0	16.0	16.0	16.0
As	0.0	0.0	0.0	0.0	0.0	0.0	0.0
Total	16.0	16.0	16.0	16.0	16.0	16.0	16.0

Label	line6_39	line6_40	line6_41	line6_42	line6_43	line6_44	line6_45
No	79	80	81	82	83	84	85
X	11768	11745	11723	11701	11678	11656	11634
Y	23820	23813	23806	23799	23792	23785	23778
MgO	0.02	0.04	0.00	0.00	0.03	0.01	0.00
Al2O3	0.00	0.00	0.54	0.02	0.03	0.02	0.00
Cr2O3	0.00	0.06	0.38	0.02	0.00	0.04	0.00
Fe2O3	75.8	74.0	74.1	80.0	80.9	82.5	77.3
As2O10	0.00	0.00	0.00	0.00	0.00	0.00	0.00
Total	75.8	74.1	75.1	80.0	81.0	82.5	77.3
Mg	0.0	0.0	0.0	0.0	0.0	0.0	0.0
Al	0.0	0.0	0.2	0.0	0.0	0.0	0.0
Cr	0.0	0.0	0.1	0.0	0.0	0.0	0.0
Fe	16.0	16.0	15.7	16.0	16.0	16.0	16.0
As	0.0	0.0	0.0	0.0	0.0	0.0	0.0
Total	16.0	16.0	16.0	16.0	16.0	16.0	16.0

Label	line6_46	line6_47	line6_48	line6_49	line6_50	line6_51	line6_52
No	86	87	88	89	90	91	92
X	11612	11589	11567	11545	11522	11500	11478
Y	23772	23765	23758	23751	23744	23737	23730
MgO	0.02	0.00	0.27	0.01	0.00	0.00	0.03
Al2O3	0.10	0.01	0.02	0.03	0.01	0.07	0.06
Cr2O3	0.04	0.00	0.02	0.02	0.00	0.15	0.06
Fe2O3	81.1	87.0	61.1	18.0	85.1	85.9	87.8
As2O10	0.00	0.00	0.00	0.00	0.00	0.00	0.00
Total	81.2	87.0	61.4	18.1	85.1	86.1	88.0
Mg	0.0	0.0	0.1	0.0	0.0	0.0	0.0
Al	0.0	0.0	0.0	0.0	0.0	0.0	0.0
Cr	0.0	0.0	0.0	0.0	0.0	0.0	0.0
Fe	16.0	16.0	15.9	15.9	16.0	15.9	16.0
As	0.0	0.0	0.0	0.0	0.0	0.0	0.0
Total	16.0	16.0	16.0	16.0	16.0	16.0	16.0

Label	line6_53	line6_54	line6_55	line6_56	line6_57	line6_58	line6_59
No	93	94	95	96	97	98	99
X	11455	11433	11411	11388	11366	11344	11321
Y	23723	23716	23709	23702	23695	23688	23681
MgO	0.00	0.00	0.00	0.00	0.00	0.00	0.00
Al2O3	0.02	0.00	0.00	0.00	0.02	0.00	0.03
Cr2O3	0.05	0.01	0.00	0.02	0.07	0.00	0.04
Fe2O3	87.4	88.5	88.2	87.3	82.8	90.9	86.2
As2O10	0.00	0.00	0.00	0.00	0.00	0.00	0.00
Total	87.5	88.5	88.2	87.3	82.9	90.9	86.3
Mg	0.0	0.0	0.0	0.0	0.0	0.0	0.0
Al	0.0	0.0	0.0	0.0	0.0	0.0	0.0
Cr	0.0	0.0	0.0	0.0	0.0	0.0	0.0
Fe	16.0	16.0	16.0	16.0	16.0	16.0	16.0
As	0.0	0.0	0.0	0.0	0.0	0.0	0.0
Total	16.0	16.0	16.0	16.0	16.0	16.0	16.0

Label	line6_60
No	100
X	11299
Y	23674
MgO	0.00
Al2O3	0.02
Cr2O3	0.01
Fe2O3	86.2
As2O10	0.00
Total	86.2
Mg	0.0
Al	0.0
Cr	0.0
Fe	16.0
As	0.0
Total	16.0

VITA

Gregory A Gromadzki

Candidate for the Degree of

Master of Science

Thesis: OUTCROP-BASED GAMMA-RAY CHARACTERIZATION OF ARSENIC-BEARING LITHOFACIES IN THE GARBER-WELLINGTON FORMATION, CENTRAL OKLAHOMA AQUIFER (COA), CLEVELAND COUNTY, OKLAHOMA

Major Field: Geology

Biographical:

     Personal Data: Born in Kendzierzyn-Kozle, Poland on November 01, 1979, the son of Ryszard and Grazyna Gromadzki

     Education: Graduated from Piscataway High School, Piscataway, New Jersey in June 1998; received Bachelor of Science degree in Geological Sciences from University of Maine, Orono, Maine in May, 2002. Completed the requirements for the Master of Science degree with a major in Geology at Oklahoma State University in May, 2004.

     Experience: Worked as a teaching assistant for the School of Geology at Oklahoma State University from August 2002 to December 2003; worked as a research assistant for Dr. Paxton from August 2003 to May 2004.

     Professional Memberships: Geological Society of America
                                     American Association of Petroleum Geologists